BRNO UNIVERSITY OF TECHNOLOGY

VYSOKÉ UČENÍ TECHNICKÉ V BRNĚ

FACULTY OF MECHANICAL ENGINEERING

FAKULTA STROJNÍHO INŽENÝRSTVÍ

INSTITUTE OF PROCESS ENGINEERING

ÚSTAV PROCESNÍHO INŽENÝRSTVÍ

TOTAL SITE INTEGRATION METHODOLOGY FOR ENERGY AND MATERIAL CIRCULAR ECONOMY

METODIKA PRO CELKOVOU INTEGRACI ENERGIE A MATERIÁLU V OBĚHOVÉM HOSPODÁŘSTVÍ

DOCTORAL THESIS

DIZERTAČNÍ PRÁCE

AUTHOR Limei GAI, MEng.

AUTOR PRÁCE

SUPERVISOR: Assoc. Prof. Dr-Hab. Ing. Petar Sabev VARBANOV, PhD

ŠKOLITEL

CO-SUPERVISORS:

Prof. Dr-Hab. Ing. Jiří Jaromír KLEMEŠ, DSc., dr. h. c. (mult)

Dr. Yee Van FAN, MPhil

BRNO 2021

KEYWORDS:

Process Integration, Total Site Integration, Circular Economy, Heat Integration, Mass Integration, Waste Recovery

KLÍČOVÁ SLOVA

Integrace procesů, Celková integrace komplexů, Oběhové hospodářství, Integrace tepela, Integrace materiálu, Znovuvyužití odpadů

CITATION

Limei Gai. Total Site Integration Methodology for Energy and Material Circular Economy. PhD thesis, Brno University of Technology, Faculty of Mechanical Engineering, Institute of Process Engineering, 2021. Supervisor: Petar Sabev Varbanov. Co-Supervisors: Jiří Jaromír Klemeš, Yee Van Fan.

Declaration

I declare that I am the author of this doctoral thesis. It has been prepared under the guidance of my supervisors. The reported results are original research which that has been developed based on my knowledge gained during my PhD study and consultation with experts. I have quoted all the sources, including my own publications. The related references are provided at the end of this thesis.

Brno: 2021 Limei Gai

Abstract

This thesis presents a methodology that has been developed to minimise resource (energy and mass) consumption and reduce waste discharge by combining Circular Economy (CE) and Process Integration (PI). PI can provide design tools for the implementation of the CE pattern, which is essential for resource conservation and contributing to sustainability. It addresses challenges that previously prevented practical implementation. Four methods are proposed based on the Circular Integration concept, the extension of Pinch Analysis (PA), and the Onion Model. The applicability of these methods is demonstrated by four case studies focused on minimising resource consumption and waste discharge. My contributions to the field include:

(i) The performance and integration of heat pumps with various industrial processes are studied by PA for low-grade heat recovery at the Total Site level.

(ii) A method combining PA and waste recovery technology is proposed. The multiple-level fresh resources PA (PA-MLFR) is extended to the level of Total Site Mass Integration. Waste material regeneration is optimised with a techno-economic objective.

(iii) A hierarchical targeting method combines the Onion Model and PA, considering both mass and heat integration.

(iv) A concept map and a model of multi-resource integration are proposed by tracing the processing paths of the secondary raw materials to useful products and services. The three-way trade-off between the degree of circularity, exergy and cost is assessed.

The proposed methods are represented graphically, with the support of a set of comprehensive underlying equations. The resource conservation and sustainability problems are transformed into an easily understandable format, from which arise robust solutions with low resource consumption and waste discharge. As case studies, the analysis run by the novel graphical-based methods for dealing with Total Site Energy and Mass Integration resulted in an overall 15 %-87 % reduction of minimum resource (e.g. heat/cold utility: 15 %-87 %, hydrogen 17 %-25 %) consumption and 36 %-75 % reduction of waste discharge. The presented methodology makes a significant contribution to resource conservation and offers significant economic benefits by transforming waste into useful secondary raw material. For future study, the interactions and synergetic relationship of the energy and material flows could be further explored to extend Total Site Mass and Energy (including heat, power and work) Integration.

Abstrakt

Predkladana práce představuje metodologii, která byla vyvinuta za účelem minimalizace spotřeby zdrojů (energie a hmoty/materiálu) a snížení vypouštění odpadu kombinací oběhového hospodářství (CE) a procesní integrace (PI). PI může poskytnout návrhové nástroje pro implementaci CE, která je nezbytná pro zachování zdrojů a přispívá k udržitelnosti. Řešil výzvy, které dříve bránily praktické implementaci. Jsou navrženy čtyři metody, které jsou založeny na konceptu kruhové integrace a rozšíření rámců Pinch Analysis (PA) a Onion Model. Použitelnost těchto metod dokládají čtyři případové studie zaměřené na minimalizaci spotřeby zdrojů a vypouštění odpadu. Moje příspěvky v této oblasti zahrnují:

(i) Výkon a integrace tepelných čerpadel s různými průmyslovými procesy studuje PA pro rekuperaci tepla nízkého stupně na úrovni Total Site.

(ii) Je navržena metoda kombinující PA a technologii využití odpadu. Víceúrovňový zdroj PA (PA-MLR) je rozšířen na úroveň Total Site Mass Integration. Regenerace odpadního materiálu je optimalizována s technicko-ekonomickým cílem.

(iii) Hierarchická metoda cílení kombinující cibulový model a PA s ohledem na hmotnostní a tepelnou integraci.

(iv) Koncepční mapa a model integrace více zdrojů jsou navrženy trasováním zpracovatelských cest druhotných surovin k užitečným výrobkům a službám. Hodnotí se třícestný kompromis mezi mírou oběhovosti, exergie a náklady.

Navrhované metody jsou znázorněny graficky s podporou sady komplexních základních rovnic. Problémy s ochranou zdrojů a udržitelností jsou transformovány do snadno srozumitelného formátu, ze kterého vyplývají robustní řešení s nízkou spotřebou zdrojů a vypouštěním odpadu. Jako případové studie vedla analýza provedená novými grafickými metodami pro řešení celkové energetické a hmotové integrace webu k celkovému snížení minimálního zdroje o 15 %-87 % (např. Teplá/studená energie: 15 %-87 %, vodík 17 %-25 %) spotřeba a 36 %-75 %snížení vypouštění odpadu. Předložená metodika významně přispívá k ochraně zdrojů a nabízí významné ekonomické výhody transformací odpadu na užitečnou druhotnou surovinu. Pro budoucí studii by bylo možné dále prozkoumat interakce a synergický vztah toků energie a materiálu, aby se prodloužila integrace celkové lokality a energie (včetně tepla, energie a práce).

Acknowledgement

Time flies. I still remember the first time I came to Brno, Czech Republic, and became a member of SPIL. In completion of my PhD thesis, it is most appropriate to reflect and recognise those individuals who have got me to where I am and express my heartfelt thanks.

First of all, I would like to give sincere thanks to my supervisors: Prof Jiří Jaromír Klemeš, Dr Petar Sabev Varbanov, and Dr Yee Van Fan. This thesis would not have been possible without the support and guidance of my supervisors. I sincerely appreciate Prof Jiří Jaromír Klemeš employing me as a member of the SPIL family and for the guidance on my doctoral study and research. I have been inspired by his profound knowledge, active enterprising and approachable personality charm. I also thank a lot to Dr Petar Sabev Varbanov for his patience, encouragement and support in my research and paper writing. And also, thanks very much to Dr Yee Van Fan for her guidance, advice and help in contributing to the development of my work. I would also like to give sincere thanks to my co-authors Dr Timothy Walmsley, Prof Sandro Nižetić, Prof Sharifah Rafidah Wan Alwi, and Prof Sergey Vladimirovich Romanenko, for their valuable suggestions on my journal papers. Their inspiring discussions inspired me to think from a different perspective. It has made a significant contribution to the development of my research.

I am grateful to my colleagues of the SPIL family for the discussion and support to improve my work, as well as for their help and companionship in life. Also grateful to Dr Šárka Zemanová and Prof Stehlík with all the communication, supporting administrative work and helping in many ways. I would also like to thank my master's supervisor, Dr Li Sun, without whom I might not had the chance to meet Prof Klemeš.

I would also gratefully appreciate and recognise the financial support granted by the EU supported project Sustainable Process Integration Laboratory – SPIL, project No. CZ.02.1.01/0.0/0.0/15_003/0000456 funded by EU "CZ Operational Programme Research, Development and Education", Priority 1: Strengthening capacity for quality research.

Last but not least, to my beloved family. Home is a haven from the wind. Their endless tolerance, unselfish love and support are always behind me, which are my motivation. Thanks to friends in Brno for all the together time and helping. Grateful to my master's co-supervisor, Prof Gaohong He, as well as my seniors of HE family during my master study, for their presence and attention. In summary, a big thanks to all the people who helped and cared for me.

Contributing Research Work Presented in Peer-Reviewed Publications

This thesis has been based on the author's publication in several highly recognised international journals. The developed method and work in **Chapter 3** are published in Energies (IF=3.004, CiteScore = 4.7) [3] and Chemical Engineering Transactions (CiteScore = 1.5) [8]. One publication closely related to the work in **Chapter 4** is published in the International Journal of Hydrogen Energy (IF=5.816, CiteScore = 9.0) [1]. The results in **Chapter 5** is based on the works published in Chemical Engineering Transactions (CiteScore = 1.5) [7]. The developed methodology and work in **Chapter 6** are published in Resources, Conservation and Recycling (IF=10.204, CiteScore = 14.7) [2], and Computer Aided Chemical Engineering (CiteScore = 1.1) [6]. The other review studies and assessments that make up the thesis or developed the results in Chapters 3 – 6 are published in Energy (IF = 7.147, CiteScore = 11.5), Journal of Environmental Management (IF = 6.789, CiteScore = 9.8) and conference proceedings of various international conferences such as IEEE (Scopus Index). The complete list of publications is presented in this chapter as follows. I have presented the research underpinning this thesis at 7 international conferences. A complete list of the conferences and presentations is provided in this chapter as follows.

Journal Articles - Publications with Impact Factors

1. **Gai, L.***, Varbanov, P.S., Fan, Y.V., Klemeš, J.J., Nižetić, S., 2021. Total Site Hydrogen Integration with Fresh Hydrogen of Multiple Quality and Waste Hydrogen Recovery in Refineries. International Journal of Hydrogen Energy. **[IF=5.816] [CiteScore = 9.0] (Q1)**
2. **Gai, L.**, Varbanov, P.S.*, Fan, Y.V., Klemeš, J.J., Romanenko, S.V., 2021. Trade-offs between the Recovery, Exergy Demand and Economy in the Recycling of Multiple Resources. Resources, Conservation and Recycling, 167, 105428. **[IF=10.204] [CiteScore = 14.7] (Q1)**
3. **Gai, L.***, Varbanov, P.S., Walmsley, T.G., Klemeš, J.J., 2020. Critical Analysis of Process Integration Options for Joule-Cycle and Conventional Heat Pumps. Energies, 13(3), 635. **[IF=3.004] [CiteScore = 4.7] (Q2)**
4. Fan Y.V.*, Romanenko, S., **Gai, L.**, Kupressova, E., Varbanov, P.S., Klemeš, J.J., 2021. Biomass integration for energy recovery and efficient use of resources: Tomsk Region. Energy, 235, 121378. **[IF = 7.147] [CiteScore = 11.5], (Q1)**

5. Wang, B.*, Klemeš, J.J., **Gai, L.**, Varbanov, P.S., Liang, Y., 2021. A Heat and Power Pinch for Process Integration targeting in hybrid energy systems, Journal of Environmental Management, 287, 112305. **[IF = 6.789] [CiteScore = 9.8] (Q1)**

Journal Articles - Publications with CiteScore

6. **Gai, L.**, Varbanov, P.S. *, Chin, H.H., Klemeš, J.J., Nižetić, S., 2021. Targeting and Optimisation of Industrial and Urban Symbiosis for Circular Economy. Computer Aided Chemical Engineering, 50, 1659-1664. **[CiteScore = 1.1] (Q4)**

7. **Gai, L.***, Varbanov, P.S., Klemeš, J.J., Sun, L., 2020. Hierarchical Targeting of Hydrogen Network System and Heat Integration in a Refinery. Chemical Engineering Transactions, 81, 217-222. **[CiteScore = 1.5] (Q3)**

8. **Gai, L.***, Varbanov, P.S., Walmsley, T.G., Klemeš, J.J., 2019. Process Integration Using a Joule Cycle Heat Pump. Chemical Engineering Transactions, 76, 415-420. **[CiteScore = 1.5] (Q3)**

9. Varbanov, P.S.*, **Gai, L.**, Fan, Y.V., Klemeš, J.J., Wan Alwi, S.R., 2020. Regional Power Plan Targeting for Minimisation of Environmental Footprints. Chemical Engineering Transactions, 81, 1159-1164. **[CiteScore = 1.5] (Q3)**

10. **Gai, L.**, Varbanov, P.S., Fan, Y.V., Klemeš, J.J., 2021. Membrane Separation for Light Hydrocarbons Recovery in the Petrochemical Industry. IEEE. (Accepted)

Conference Presentations

1. **Gai, L.**, Varbanov, P.S., Fan, Y.V., Klemeš, J.J., Membrane Separation for Light Hydrocarbons Recovery in the Petrochemical Industry. 6th International Conference on Smart and Sustainable Technologies (SpliTech 2021), Split and Bol, Croatia, September 8-11, 2021, SpliTech21.172(1570732662) (Hybrid)

2. **Gai, L.**, Varbanov, P.S., Fan, Y.V., Klemeš, J.J., Total Site Hydrogen Integration and Waste Hydrogen Purification for Minimising the Fresh Hydrogen Consumption. 3rd International Scientific Conference on "Sustainable and Efficient Use of Energy, Water and Natural Resources", St-Petersburg, Russia, 19-24 April 2021, SEWAN2021.137. (Online) **(Best Presentation Award)**

3. **Gai, L.**, Chin H.H., Varbanov, P.S., Klemeš, J.J., Application of circular economy principles in organic exhaust recovery in the petrochemical industry. The 5th

International Scientific and Technical Conference "Modern Power Systems and Units", 19-21 May 2021, MPSU21.1B.1535. (Online)

4. **Gai, L.**, Varbanov, P.S., Fan, Y.V., Klemeš, J.J., Pinch Analysis of Hydrogen Network and Waste Hydrogen Recovery in a Refinery. The 4th Sustainable Process Integration Laboratory Scientific Conference, 18-20 November 2020, SPIL20.0018. (Online)

5. **Gai, L.**, Varbanov, P.S., Fan, Y.V., Klemeš, J.J., Nižetić, S., A Hierarchical Targeting Method of Hydrogen and Heat Exchange Network Synthesis. The 3rd International Conference on Technologies & Business Models for Circular Economy (TBMCE), 15 December 2020, TBMCE20.0190. (Online)

6. **Gai, L.**, Varbanov, P.S., Klemeš, J.J., Sun, L., Hierarchical Targeting of Hydrogen Network System and Heat Integration in a Refinery. The 23rd Conference on Process Integration, Modelling and Optimisation for Energy Saving and Pollution Reduction (PRES2020), Xi'an, China, 17-21 August 2020, PRES20.0251. (Online)

7. **Gai, L.**, Varbanov, P.S., Klemeš, J.J., Mass Integration with Circular Economy of Hydrogen Network in Refinery. 4th SEE SDEWES Conference Sarajevo 2020, Sarajevo, Bosnia and Herzegovina, 28 June - 2 July 2020, SEE.SDEWES2020.0145. (Online)

8. **Gai, L.**, Varbanov, P.S., Walmsley, T.G., Klemeš, J.J., Process Integration Using a Joule Cycle Heat Pump. The 22nd Conference on Process Integration, Modelling and Optimisation for Energy Saving and Pollution Reduction (PRES2019), Agios Nikolaos, Crete, Greece, 20-23 October 2019, PRES19.0478.

9. Klemeš, J.J., Varbanov, P.S., **Gai, L.**, Potential of Fuel Cells Heat Integration with other Fuel Conversion Processes. 1st International Conference of PEM Fuel Cell Science and Technology, Invited Plenary Lecture, Xi'an, China, November 2019.

Table of Contents

KEYWORDS: II

KLÍČOVÁ SLOVA II

CITATION II

Declaration I

Abstract III

Abstrakt IV

Acknowledgement V

Contributing Research Work Presented in Peer-Reviewed Publications VI

Table of Contents I

CHAPTER 1 INTRODUCTION 1

1.1 General Introduction 1

1.2 Thesis Aim and Scope 6

1.3 Thesis Outline 9

CHAPTER 2 LITERATURE REVIEW 11

2.1 Introduction 11

2.2 Circular Economy 11

2.3 Energy Integration and Heat Recovery 14

2.4 Mass/Material Integration and Conservation 22

2.4.1 Total Site Mass Integration with Multiple-level Fresh Resources 24

2.4.2 Total Site Mass Integration with Intermediate Purity Headers 26

2.4.3 Optimisation of Waste Purification and Regeneration Process 27

2.5 Combined Heat and Mass Integration 29

CHAPTER 3 LOW-GRADE WASTE HEAT RECOVERY OF HEAT INTEGRATION 32

3.1 Introduction 32

3.2 Method 34

3.2.1 Step 1: Process Integration with Pinch Analysis 35

3.2.2 Step 2: Build and Simulate Different Heat Pumps 35
3.2.3 Step 3: Optimise the Heat Pumps 37
3.2.4 Step 4: Process Integrate with Heat Pump 38
3.2.5 Step 5: Evaluation of Heat Pump Suitability to Different Process GCC Profiles ..39
3.2.6 Step 6: Discuss and Analyse the Results 41
3.3 Simulation and Optimisation of Heat Pumps 41
3.4 Case Studies 45
3.4.1 Formulation and Development: Process Integration Using JCHP, VCHP and TCHP 45
3.4.2 Evaluation 55
3.5 Conclusions 57
CHAPTER 4 TOTAL SITE MASS INTEGRATION WITH MULTIPLE-LEVEL FRESH RESOURCES AND INTERMEDIATE PURITY HEADERS 59
4.1 Introduction 59
4.2 An Introduced Novel Methods 61
4.2.1 Overall Integration Procedure of Total Site Mass Integration 62
4.2.2 Multiple-level Fresh Resources Pinch Analysis (PA-MLFR) 64
4.2.3 Optimisation of Waste Purification and Regeneration Process 72
4.2.4 Multiple-level Fresh Resources Pinch Analysis with Intermediate Headers (PA-MLFR-IH) 76
4.3 Case Studies 82
4.3.1 Multiple-level Fresh Resources Pinch Analysis (PA-MLFR) of Mass Integration 82
4.3.2 Optimisation of Waste Hydrogen Regeneration 89
4.3.3 Multiple-level Fresh Resources Pinch Analysis with Intermediate Headers (PA-MLFR-IH) in Mass Integration 94
4.4 Conclusions 104
CHAPTER 5 HIERARCHICAL TARGETING OF HEAT AND MASS INTEGRATION..... 107

5.1 Introduction 107
5.2 Method 108
5.3 Case Study 110
5.4 Conclusions 114
CHAPTER 6 MASS AND ENERGY TRADE-OFFS 115
6.1 Introduction 115
6.2 Method 117
6.2.1 Multi-resource integration map 118
6.2.2 Degree of circularity 120
6.2.3 Main criteria, trade-offs and degrees of freedom 123
6.2.4 Model formulation 123
6.3 Case Study - integration of waste resources recovery 129
6.3.1 Variation of exergy input with circularity 132
6.3.2 Trade-off between economy and circularity 138
6.3.3 Comparison of exergy and cost optima 142
6.4 Conclusions 142
CHAPTER 7 CONCLUSIONS AND RECOMMENDATIONS FOR FUTURE RESEARCH 145
Nomenclature 148
REFERENCES 153
APPENDIX: Tables 171
APPENDIX: List of Figures 174
APPENDIX: List of Tables 177

CHAPTER 1 INTRODUCTION

1.1 General Introduction

With the rapid industrialisation, severe population problems and growing demands for goods and services, global problems are becoming increasingly severe ("OECD environmental outlook to 2050," 2012). These include resource (energy and material) depletion, environmental pollution and ecological crisis, and they prevent the sustainable development of the world. Various methods for resource recovery and reuse have been developed (Klemeš, 2015) for minimising resource depletion and environmental pollution. The most prominent paradigms for resource conservation contributing to sustainability include Circular Economy (Hartley et al., 2020), Industrial Symbiosis (Domenech et al., 2019), and Process Integration (Klemeš, 2013).

The conservation of energy and materials is one of the most effective methods for contributing to sustainability. Circular Economy (CE) aims at reducing the consumption of original resources and primary energy as far as possible by maximising the recovery of materials and energy. The Circular Economy has attracted considerable attention from scholars and practitioners. In 2020, the European Commission adopted a new Circular Economy Action Plan (European Commission, 2020). This is one of the main blocks of the European Green Deal (European Commission, 2019) and a new agenda for sustainable development of the European Union (EU). A series of policy recommendations (Hartley et al., 2020) from the Life Cycle perspective and a set of new targets (Morseletto, 2020) was proposed to facilitate the transition to a CE. The concept (Eiroa et al., 2019), conceptual deadlock (Kirchherr et al., 2017), and assessment tools (e.g. circularity indicators) (Saidani et al., 2019) of CE are reviewed and discussed. Circular Economy is a systematic framework confined to recycling as well as accounting for the efficiency and the economy. Implementing a Circular Economy arrangement requires technology development, investment, and operating cost. A Circular Economy is expected to bring economic benefits along with pollution reduction to ensure sustainable development. A higher circularity generally means that more secondary products substitute the use of fresh resources (utilities). Recycling affects both energy consumption and investment, as shown in Figure 1. The optimal performance of the multi-resource system cannot be fully reflected by the degree of circularity alone. Balancing and optimising the trade-offs between circularity, energy consumption, and economic benefit is challenged and critical to achieving sustainable system design and operation (Gai et al., 2021b).

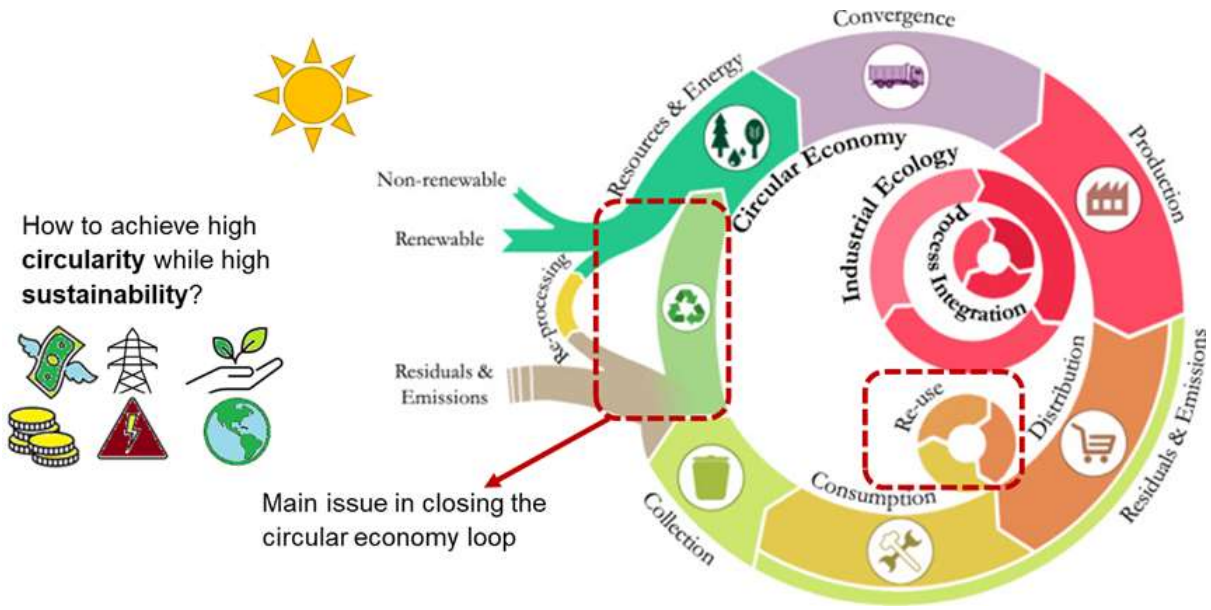

Figure 1. Trade-offs between circularity, energy consumption, and economic benefit in Circular Economy (Gai et al., 2021b)

Although the concept of CE is intuitively easy to understand, implementing it in practice is challenging (Kirchherr et al., 2017a) as the effectiveness of basic technical solutions is hampered (Kirchherr et al., 2018). Process Integration (PI) is a holistic engineering methodology aimed at minimising resource consumption in line with the goals of CE. It can provide some of the necessary design tools for the implementation of CE. The common Process Integration methods include Heat Integration (Linnhoff et al., 1994), Mass Integration (El - Halwagi and Manousiouthakis, 1989), Water Integration (Wang and Smith, 1994), Hydrogen Integration (Towler et al., 1996), the use of exergy in Combined Heat and Power Integration (Dhole and Linnhoff, 1993), emergy (Bandyopadhyay et al., 2010). The recently available PI methods (Klemeš et al., 2018b) – especially Total Site Integration (Klemeš et al., 1997), Power Pinch (Mohammad Rozali et al., 2013) and combined integration of different types of resources, provide a significant tool base for designing resource conservation networks. Pinch Analysis (PA) and Mathematical Programming (MP) are the most popular methods of PI. PA (Klemeš et al., 2018b) has good insights. However, it is complex or difficult for multiple constraints or contaminants problems (Gai et al., 2021a). Mathematical Programming (MP) can be used for problems with complex constraints (Chin et al., 2020) or multiple objectives (Afshari et al., 2020). However, directly applying MP provides poor insights and may not guarantee a global optimal solution (Liew et al., 2017). The consideration of multiple constraints in PI is still an issue that requires further effort. Combining different methods is one possible direction for the

future.

Industrial processes typically involve exchanges of mass and energy from reaction to separation and recycle, linked to the heat exchanger networks, utility systems and waste treatment systems. The reduction of mass and energy demands in the process industry is one of the most effective means of achieving sustainable operation. As energy prices continue to rise and governments enact more regulations, there is growing pressure to reduce operating costs and emissions of pollutants. Approximately 26 % of the final energy consumption is due to industrial activities based on the estimated U.S. energy consumption in 2019, see Figure 2 (LLNL Flow Charts, 2019). A key feature of the energy structure of the US economy is the 2/3 share of losses from all energy sourced. The energy integration optimisation of industrial processes can reduce energy consumption, resulting in substantial cost savings.

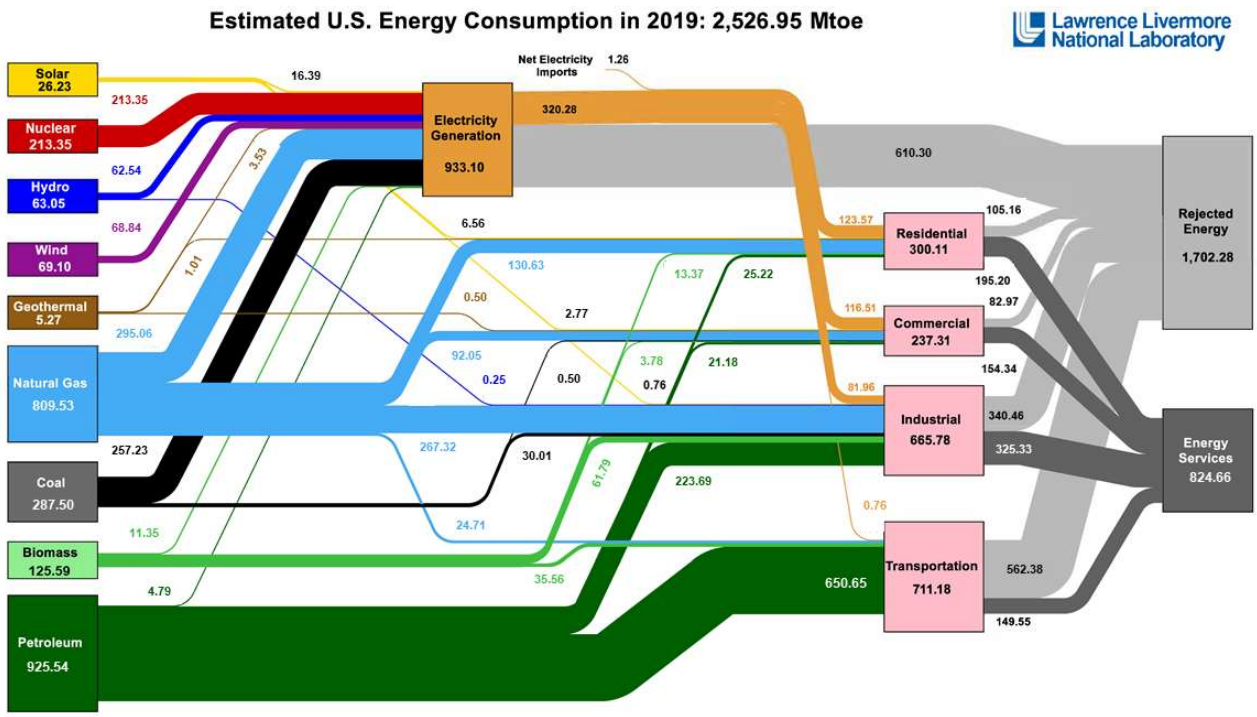

Figure 2. Estimated US energy consumption in 2019 (LLNL Flow Charts, 2019)

Process Integration (PI) has been originally developed to improve heat recovery in industries, that is, Heat Integration (Linhhoff et al., 1994). Heat Integration has been extended from a single process to multiple processes on a Total Site level. Total Site Integration (TSI) is widely used for integration between different processes, plants, or industries. Afterwards, TSHI is extended to including process units beyond the processing industry – such as residential or

commercial buildings, hotels, farms. The supply side also is discussed, where renewables are integrated to reduce the carbon footprint of the Locally Integrated Energy Sectors (Perry et al., 2008). TSHI was further extended by introducing a set of time slices to meet the changes in energy supply and demand (Liew et al., 2018). The waste heat recovery mainly adopts conventional heat pump technology (Gai et al., 2020a). However, there are limited studies on the TSHI of new heat pump technologies and industrial processes. The low-grade waste heat recovery in Total Site Heat Integration could be further considered, see Figure 3.

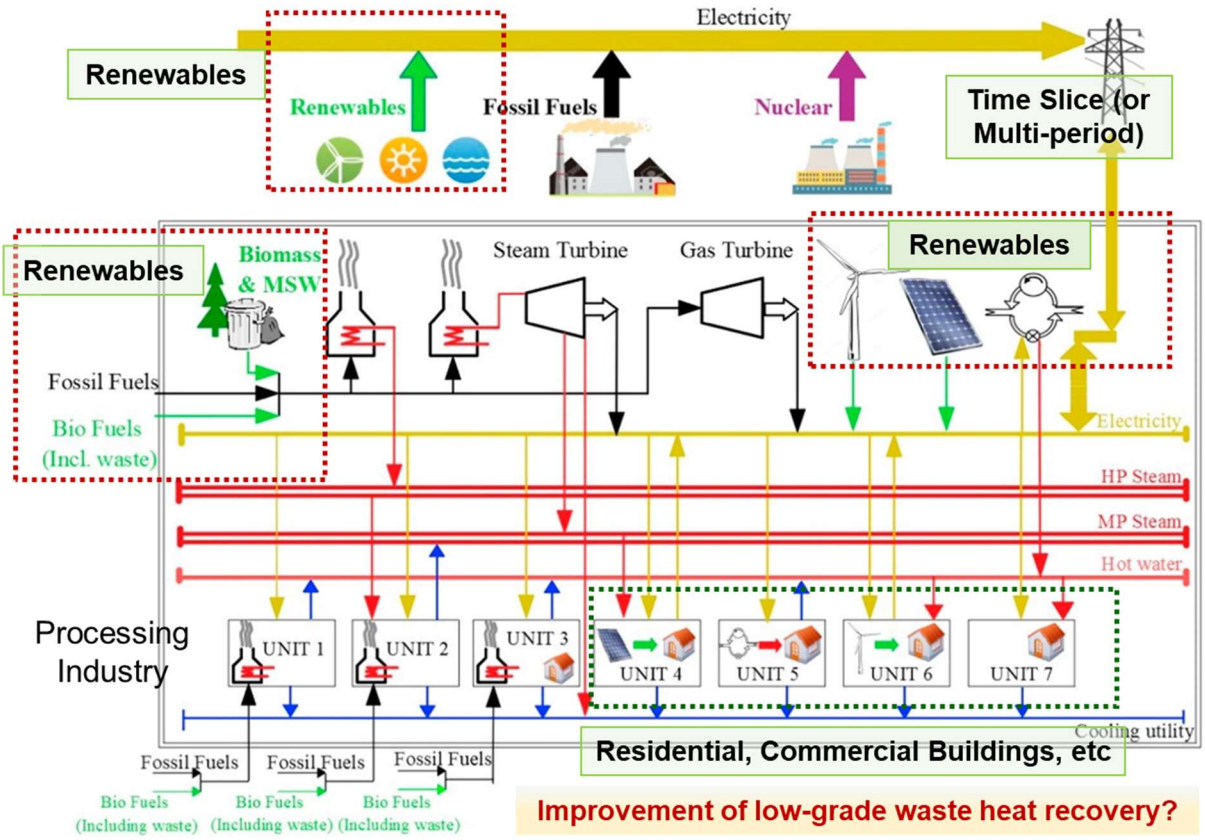

Figure 3. Total Site Heat Integration of Locally Integrated Energy Sectors, amended from (Klemeš et al., 2018b)

Inspired by the energy integration method, mass integration is developed. It aims to minimise fresh resource consumption and waste discharge. It is also divided into intra-plant Mass Integration and Total Site Mass/Material Integration (i.e. inter-plant Mass Integration) (Lou et al., 2019). Most current Pinch Analysis for Mass Integration only considered fresh resources with single quality, not multiple-level quality. A lower-cost fresh resource with low purity should be preferred for a process requiring a low-purity resource. However, few studies

extend the Pinch Analysis for Total Site Mass Integration with multiple-level fresh resources (Gai et al., 2021a); see Figure 4. Intermediate headers (Chin et al., 2021c) also could be considered to simplify the configuration and improve the expandability and flexibility of the mass exchange network. Moreover, With the increasingly serious environmental problems, industries pay more and more attention to waste recovery and regeneration. However, in most current studies, various purification options (Ruan et al., 2020) and their capabilities are not considered in Mass Integration with waste regeneration. The changes in technical performance and economy of waste purification process have not been fully considered in Total Site Mass Integration with multiple-level fresh resources and/or intermediate purity headers.

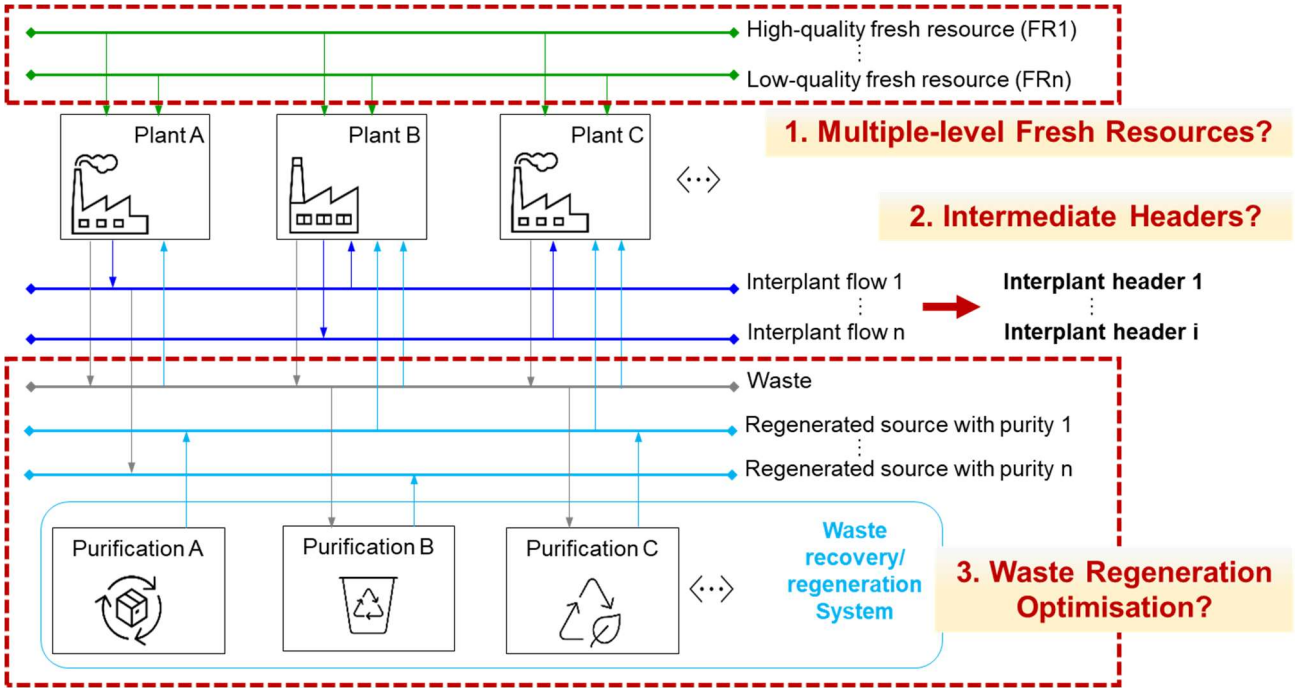

Figure 4. Total Site Mass Integration with multiple-level fresh resources and intermediate purity headers (Gai et al., 2021a)

The resources include energy and mass (or material). Integration of mass and energy exchange networks into combined energy and Mass Exchange Networks synthesis is beneficial (Wissocq et al., 2019) because mass transfer processes are affected by operating temperature. However, due to its complex nature, combining energy and mass integration is challenging. The aim of the combined energy and mass integration methods is to simultaneously reduce external energy requirements and material consumption in the industrial process by increasing heat and mass recovery and reuse. The synthesis problems of water and heat exchange networks

(WAHENs) represent special cases of MEN and HEN synthesis problems. Some methods of WAHENs synthesis have been developed, including Mathematical Programming (Ibrić et al., 2021), Pinch Analysis (Kamat and Bandyopadhyay, 2021a), hybrid approach (Kamat and Bandyopadhyay, 2021b). WAHENs synthesis can lead to more profitable and sustainable solutions to reduce the demand for water and other utilities. An optimal solution for WAHENs design was obtained (Ahmetović and Kravanja, 2013) by mathematical programming, where the objective function of the model was to minimise the Total Annual Cost (TAC). That work achieved a significant decrease in hot (3,780 vs. 27,772.5 kW) and cold (0 vs. 23,047.5 kW) utility consumption, freshwater usage (90 vs. 112.5 kg/s), and TAC (2,652,959 vs. 16,346,735 $/y) compared to the non-integrated WAHENs. It can be seen that both energy and water consumption are significant. It demonstrates the importance of mass and energy integration for resource-saving and pollution reduction (Klemeš et al., 2018a). They show that to achieve a more sustainable development path in any economic sector, and it is necessary to optimise the material and energy flows of process systems together (Yoro et al., 2019) because they feature quantitatively significant interactions, which cannot be neglected. It is important to establish and develop a multi-level, multi-structure, multi-function industrial production system that can turn industrial waste into a resource, realise circular production and intensive resource management by applying modern science and technology.

The method of Total Site Integration considering both mass and energy usually is mathematical programming. Existing graphical-based methods of Combined Heat and Mass Integration mainly focus on process-wide level, not Total Site level with multiple-level fresh resources, intermediate purity headers and waste recovery. The graphical-based methods still need to be further improved.

1.2 Thesis Aim and Scope

The overall research aim is to extend the Total Site Integration decision support tools to aid in minimising resource (energy and material) consumption and waste discharge in a multi-resource system for enabling more efficient implementations of sustainable Circular Economy. The research in this thesis fills the following research gaps:

I. Waste heat recovery with heat pumps mainly adopts conventional technology. There are limited studies on the Heat Integration of new heat pump technologies and industrial processes. The low-grade waste heat recovery of Heat Integration should be further considered.

II. There are lacking studies considering Pinch-based Analysis for Total Site Mass Integration with multiple-level fresh resources and intermediate headers. Furthermore, the purity of the waste material after regeneration in Mass Integration with waste recycle/reuse is assumed without considering various purification options and its purification capabilities. The fresh resource with various quality levels (multiple-level fresh resources) and waste material regeneration in Total Site Mass Integration should also be further considered.

III. The method of Total Site Integration considering both mass and energy is usually Mathematical Programming. The graphical-based method still needs to be further improved. Up to now, the graph-based method only considered the matching of heat grade, and the mass integration is limited to the mass balance, lacking the matching of grade considering the mass.

IV. The Circular Economy concept currently still lacks engineering design methods and quantification in the field of multi-resource systems integrating both materials and energy. The trade-off between circularity, energy consumption, and cost for obtaining a more sustainable system is a challenge.

Industries and sectors that consume energy and materials are target sectors. Case studies have been presented related to these sectors to demonstrate the developed methodology. Four novel methods are developed and applied to four case studies. The scope of the study is divided into the following main sections:

I. Pinch Analysis of Processes Integrated New Joule-Cycle Heat Pump

The performance and integration of an emerging Joule-Cycle heat pump for various industrial processes has been studied through Pinch Methodology for low-grade heat recovery.

Case Study: Critical Analysis of Process Integrated with Joule-Cycle and Conventional Heat Pumps

The performance and integration of different types of heat pumps with various processes have been investigated through extended Pinch Analysis to address these questions. The heat pumps are simulated by applying the Petro-SIM process simulator. Four different industrial processes (i.e. milk spray drying process, dairy product process, candy processing and packaging, methanol distillation) integrated with heat pumps have been studied by extended Pinch Analysis for low-grade waste heat recovery. For

the different scenarios of process Heat Integration with heat pumps, this study can provide guidance and suggestion for the selection of heat pumps.

II. Multiple-level fresh resources Pinch Analysis of Total Site Mass Integration

A method combining Pinch Methodology and waste recovery technology is proposed, resulting in Total Site Mass Integration to minimise fresh resource consumption and waste discharge. Multiple-level fresh resources Pinch Analysis is extended to the level of Total Site Mass Integration by considering multiple-level fresh resources and intermediate headers. Waste material regeneration is optimised with a techno-economic objective to further reduce fresh resource consumption.

Case Study: Hydrogen Integration of Inter-plant Hydrogen Networks

Total Site Hydrogen Integration in refineries of a petrochemical industrial park is selected as a case study in demonstrating the proposed method. It is of high importance for refineries to reduce hydrogen consumption, waste hydrogen discharge and production cost to integrate and optimise inter-plant hydrogen networks.

III. Hierarchical targeting of heat and mass integration

A graphics-based method of Total Site Integration, considering both mass and energy quality, is extended. The hierarchical targeting method, which combines the Onion Model and Pinch Analysis, is simple to use and has the advantages of graphic visualisation. The interactions between mass and energy exchange networks are explored.

Case Study: Heat and Hydrogen Integration in Refineries

Combined hydrogen and heat Integration for oil refineries is studied to reduce hydrogen utility demands and waste hydrogen emissions.

IV. Trade-offs between the recovery, exergy demand and economy

A concept map and an evaluation model for multi-resource Total Site Integration is developed. This concept map is a visual representation of multi-resource system integration tracing the processing paths of the secondary raw materials to useful products and services. Following the concept map, a Total Site Circular Integration method for multi-resource is extended by combining the tools and methods of Circular Economy and Process Integration.

Case Study: Waste Resources Recovery and Integration in Waste Management

The integration of waste resources from different sectors –residential communities and wood processing plants- is studied and evaluated. The visual multi-resource integration representation clearly outlines the key trade-off of recycling systems – between the resources dedicated to the recycling processes and the resources dedicated to the supply of fresh resources. The evaluation model links the degree of circularity to the cost and to the exergy input, evaluating the trade-off. It provides guidance for the integration of multi-resource recycling systems, allowing the decision-makers to estimate the economic and exergy performance of the proposed Circular Economy solutions, aiding in improving the sustainability contributions of industrial and urban systems.

1.3 Thesis Outline

Chapter 2 presents the concept of integration of a new Joule cycle heat pump with various industrial processes for low-grade waste heat recovery in Heat Integration. The study has been published in Energies (Gai et al., 2020a) and Chemical Engineering Transactions (Gai et al., 2019). **Chapter 3** develops an extended multiple-level fresh resources Pinch Analysis in Total Site Mass Integration by considering fresh resources with various quality levels to minimise fresh resource consumption and waste discharge. The study has been published in the International Journal of Hydrogen Energy (Gai et al., 2021a). **Chapter 4** describes the idea of the methodology for mass and energy Integration, where a hierarchical targeting method of energy and mass (H_2) for refineries is proposed. The study has been published in Chemical Engineering Transactions (Gai et al., 2020b). **Chapter 5** proposes a novel model, linking the quantities of reused materials and energy with the use of additional resources enabling that reuse, as well as the use of resources in a linear (non-circular) way and the cost of running the system. The study has been published in Resources, Conservation and Recycling (Gai et al., 2021b). All these decision-making tools share a common aim, to reduce resource (materials or energy) consumption and waste discharge in a circular economy. **Chapter 6** overviews the contribution of this thesis with a recommendation for future work, followed by references and the appendix. The publications which each chapter presents are as follows.

Chapter 2: Low-Grade Waste Heat Recovery of Heat Integration

- **Gai, L.***, Varbanov, P.S., Walmsley, T.G., Klemeš, J.J., 2020. Critical Analysis of Process Integration Options for Joule-Cycle and Conventional Heat Pumps. Energies, 13(3), 635. **[IF=3.004] [CiteScore = 4.7] (Q2)**

- **Gai, L.***, Varbanov, P.S., Walmsley, T.G., Klemeš, J.J., 2019. Process Integration Using a Joule Cycle Heat Pump. Chemical Engineering Transactions, 76, 415-420. **[CiteScore = 1.5] (Q3)**

Chapter 3: Total Site Mass Integration with Multiple-Level Fresh Resources and Intermediate Purity Headers

- **Gai, L.***, Varbanov, P.S., Fan, Y.V., Klemeš, J.J., Nižetić, S., 2021. Total Site Hydrogen Integration with Fresh Hydrogen of Multiple Quality and Waste Hydrogen Recovery in Refineries. International Journal of Hydrogen Energy. **[IF=5.816] [CiteScore = 9.0] (Q1)**
- **Gai, L.**, Varbanov, P.S., Fan, Y.V., Klemeš, J.J., 2021. Membrane Separation for Light Hydrocarbons Recovery in the Petrochemical Industry. IEEE. (Accepted)

Chapter 4: Hierarchical Targeting of Heat and Mass Integration

- **Gai, L.***, Varbanov, P.S., Klemeš, J.J., Sun, L., 2020. Hierarchical Targeting of Hydrogen Network System and Heat Integration in a Refinery. Chemical Engineering Transactions, 81, 217-222. **[CiteScore = 1.5] (Q3)**

Chapter 5: Mass and Energy Trade-Offs

- **Gai, L.**, Varbanov, P.S.*, Fan, Y.V., Klemeš, J.J., Romanenko, S.V., 2021. Trade-offs between the Recovery, Exergy Demand and Economy in the Recycling of Multiple Resources. Resources, Conservation and Recycling, 167, 105428. **[IF=10.204] [CiteScore = 14.7] (Q1)**
- **Gai, L.**, Varbanov, P.S.*, Chin, H.H., Klemeš, J.J., Nižetić, S., 2021. Targeting and Optimisation of Industrial and Urban Symbiosis for Circular Economy. Computer Aided Chemical Engineering, 50, 1659-1664. **[CiteScore = 1.1] (Q4)**

CHAPTER 2 LITERATURE REVIEW

2.1 Introduction

This chapter summarises the literature relevant to the aim and scope of the thesis. Section 2.2 reviews Circular Economy arises from the critical role in resource conservation and sustainability and discusses the challenge of practical implementation. Section 2.3 to Section 2.5 presents the state-of-the-art review for Process Integration for minimising resource consumption in line with the goal of Circular Economy, including energy integration and mass integration. Section 2.3 mainly introduces the literature review of energy integration, especially Heat Integration (including Combined Heat and Power, Total Site Heat Integration) to minimise industrial energy consumption. Section 2.4 reviews the mass/material integration driven by the waste minimisation initiative, which is divided into three subsections mainly focusing on multiple-level fresh resources (Section 2.4.1), intermediate headers (Section 2.4.2), waste purification and regeneration (Section 2.4.3). Section 2.5 discusses the synthesis of heat and mass exchange networks, i.e. combined Heat and Mass Integration. The research gaps and their potentials in achieving the thesis aim are highlighted.

2.2 Circular Economy

The conservation of energy and materials (Klemeš, 2013) is one of the most effective methods for contributing to sustainability. For a successful application, it requires an adequate set of indicators of the environmental impact and cost (Klemeš, 2015). The concept of CE has attracted considerable attention from scholars and practitioners. Kirchherr et al. (2017) reviewed 114 definitions of CE and pointed out that different understandings of the Circular Economy concept may lead to conceptual deadlock. Suárez-Eiroa et al. (2019) reviewed the sources related to CE. They proposed the principle of combining the CE theoretical goal within the framework of sustainable development with the practical implementation strategy. Fan et al. (2019) provided an overview of various methods for energy saving and pollution reduction. They pointed out that the methods for CE, resource and utility management and waste management can be used in synergy to achieve environmental sustainability at an acceptable cost. In 2020, the European Commission adopted a new Circular Economy Action Plan (European Commission, 2020). This is one of the main blocks of the European Green Deal (European Commission, 2019) and a new agenda for sustainable development of the European Union (EU). A series of policy recommendations (Hartley et al., 2020) from the Life Cycle perspective and a set of new targets (Morseletto, 2020) was proposed to facilitate the transition

to a CE.

CE requires appropriate assessment tools to make progress. Many circularity indicators are available to evaluate the usefulness of circular arrangements. The review by Saidani et al. (2019) revealed 55 circular indicator sets. They can be applied to a multitude of contexts, ranging from multiple chemical species evaluation and up to regional or global system boundaries. Examples can be given with the National Circular Economy Indicator System (NCEIS) (Geng et al., 2012), the Sustainable Circular Index (SCI) (Azevedo et al., 2017), the Circular Economic Value (CEV) (Fogarassy et al., 2017), the Circularity Index (CI) (Cullen, 2017). A comparison of the indicators proposed in the last decade is given in the Appendix (Table S1). Some variations can be selected based on the specifics of the considered system and the type of problem solved. Some of the indicators focus on the recovery of materials, others on energy or combine both. There are also several indicators evaluating the monetary equivalents of the mass or energy flows or their ratios.

One possible metric for characterisation of reuse and recycle of materials is the "Circular Material Use Rate", officially employed by Eurostat (2018). They define it as the ratio of the materials reused in a circular manner over the overall material use. This is a very useful indicator for characterising material cycles. However, by the nature of its definition, it misses the other crucial component of the overall set of human activities – the energy flows. The circularity of energy (Zore et al., 2018) was proposed based on the circularity of raw materials to measure the energy reuse in a system. Some systems have both material and energy recovery. Angioletti et al. (2017) extended the concept of Circularity Product Indicator (CPI). They defined it as a geometric combination of circularity indicators – for Material Circularity Indicator (MCI), Energy Circularity Indicator (ECI) and auxiliary Resource Circularity Indicator (RCI). However, for the ECI, only the quantity of energy is considered, and the quality of energy is ignored.

The concept of CE is intuitively easy to understand but implementing it in practice is a complicated task. Industrial symbiosis is considered as a solution to enhance environmental sustainability and gain economic benefits at the same time. It is one of the practical ways to integrate CE into manufacturing activities. Industrial Symbiosis assumes a complete industrial ecosystem in which symbionts are formed among enterprises. That is achieved by sharing the same kind of resources or the complementation of different types of resources (e.g. materials, energy, water, capacity, expertise, assets) (Domenech et al., 2019). The symbiont promotes the

improvement of resource allocation efficiency and exchange. This increases the enterprise benefit and promotes overall industrial development. A good example is the application of the urban and industrial symbiosis method used for formulating a cross-industry network of multiple supply chains (Tseng et al., 2018).

In assessing the energy inputs and the energy efficiency of the considered processes, it is necessary to account for the different forms of energy – mainly heat and power, and the entropy generation by the various unit operations, especially mixing. This consideration leads to the use of exergy as the unifying criterion. Exergy has been used as a criterion to evaluate the efficiency of recovery for the reuse of metals and other components from Cd-Te photovoltaic modules (Abadías Llamas et al., 2020). That work assessed the exergy efficiency and CO_2 emissions of selected flowsheets, providing a detailed explanation and justification of all the steps. The trade-off between the use of recycled and fresh resources is not considered, however. A similar approach has been taken by Vilardi et al. (2020) to evaluate the exergy efficiency, loss and destruction of biogas upgrading processes. Another step in the right direction has been the evaluation of the embodied exergy in various parts of a product (Almeida et al., 2017). The authors showed the importance of using the embodied exergy and the linked embodied emissions instead of simple mass-based criteria.

Some of the reviewed works, representative of the state-of-the-art, deal with issues relevant to the use of secondary resources via CE – emphasising the degree of circularity itself. Others model the resource recovery in terms of waste heat, wastewater, or combinations of those, as well as exergy efficiency. The Circular Integration (Walmsley et al., 2019a), extended by (Fan et al., 2019) and more recently including the widely discussed plastics by (Klemeš et al., 2020), sets the thinking towards the need to consider mass and energy flow integration jointly, on the example of organic materials reuse. The main counterparts in the trade-off are the use of fresh resources on the one hand and the supply of secondary resources via waste stream interception and treatment on the other hand. It has been shown in (Varbanov et al., 2020a) that material and energy flows follow different patterns, which sets them as two interacting dimensions in process efficiency evaluation. This observation indicates that the consideration of the mass and energy flows together still needs to be further improved to evaluate their interaction clearly, also accounting for the economic cost.

In the recycling and reuse of waste streams as secondary resources, the trade-offs between the recycling and the supply of fresh resources determine the overall resource use and

environmental impact of each process. A higher circularity generally means that more secondary products substitute the use of fresh resources (utilities). However, recycling affects both energy consumption and investment. Both the recycling and the linear production processes consume resources and release emissions. The implementation of circularity measures also requires investment and some operating resources. For multi-resource systems, even with fixed circularity, the primary (virgin) and secondary (waste) resource supplies can be processed via different processing paths. This provides additional degrees of freedom, where energy consumption and investment may differ amongst the paths. Most of the previous research deals with circularity or economic benefits alone. The trade-off between the degree of circularity in industrial and urban processes and the spent resources in terms of energy and funds poses a challenging task.

To summarise, (i) The Circular Economy concept currently still needs more extended engineering design methods and quantification in the field of multi-resource systems integrating both materials and energy. (ii) The optimal performance of a multi-resource system cannot be fully modelled by the degree of circularity alone. Balancing and optimising the trade-offs between circularity rate, energy use, and the cost is critical for obtaining a more sustainable system design and operation.

2.3 Energy Integration and Heat Recovery

Process Integration (PI) is an engineering methodology for minimising resource consumption in line with the goals of CE. It can provide some of the necessary design tools for the implementation of CE. Key methods constituting the area include Heat Integration (Linnhoff et al., 1994), Mass Integration (El‐Halwagi and Manousiouthakis, 1989), Water Integration (Wang and Smith, 1994), Hydrogen Integration (Towler et al., 1996), the use of exergy in CHP Integration (Dhole and Linnhoff, 1993), emergy (Bandyopadhyay et al., 2010). The recently available PI method (Klemeš et al., 2018b)– especially Total Site (Klemeš et al., 1997) and Power Pinch (Mohammad Rozali et al., 2013) concepts, provide a significant tool base for designing reuse networks of single types of resources. The concept of Circular Integration was overviewed by (Walmsley et al., 2019a). It is a step towards bridging CE and PI to minimise resource consumption. However, the research of PI in multi-resource integration and recycling needs to be improved.

Process Integration (PI) has been originally developed to improve heat recovery in the industry. Heat Integration (HI) was the earliest PI approach and energy integration. In the

energy crisis of the 1970s, HI was introduced for the optimal synthesis of Heat Exchanger Networks (HENs) to minimise industrial energy consumption (Linnhoff and Flower, 1978a), based on the initial idea of plotting temperature-enthalpy profiles of the considered processes (Hohmann E.C., 1971). The HEN design was followed by the efficient design of various energy-intensive processes, e.g., distillation and utility systems. With the extensive development of Heat Integration techniques in the 1980s and 1990s, this trend has reached a mature stage in recent years. It has been further expanded with an important implementation in reducing greenhouse gas emissions and addressing environmental and sustainability issues (Klemeš et al., 2011). Heat transfer enhancement and heat integration in heat exchanger network retrofit and operation (Klemeš et al., 2020), the modelling and optimisation of utility systems were both reviewed (Varbanov et al., 2020c). Pinch Analysis and Mathematical Programming are the most popular methods of Process Integration (Klemeš et al., 2013).

Pinch Analysis (Klemeš et al., 2018b) is one of the bases of Heat Integration (HI) development. It is a method of targeting and prioritising the integration of process energy systems. Pinch Analysis (Klemeš, 2013) is a graphical technique based on thermodynamics to analyse energy distribution along with temperature in the process to find the "bottleneck" of an energy system and account for that in the design, operation and retrofit of heat recovery networks. Pinch Analysis (PA) was pioneered by Linnhoff and Flower (1978b) to improve industrial energy efficiency through Heat Integration. The thermodynamic principles and the temperature-enthalpy diagram (also known as the Composite Curves) were used by Linhhoff et al. (1994) to map the total heating and cooling requirements of a process. After decades of development, Heat Integration of a single process has become a recognised concept in the industry. Kemp (2007) compiled an updated edition of Linnhoff's "User Guide", adding several chapters on the Heat Integration of batch processes, as well as additional case studies.

Heat Integration using PA has been extended from a single process to multiple processes on a Total Site. Total Site Integration (TSI) is widely used for integration between different processes, plants, or industries. Dhole and Linnhoff (1993) first proposed Total Site targets for a utility system of different factories based on the idea of Site Heat Sources and Sinks. Klemeš et al. (1997) proved the success of Total Site Heat Integration (TSHI) by adding the power co-generation targeting. The first introduction of TSHI is aimed at maximising energy savings by integrating industrial processes. The Site Utility System is used as a heat transfer intermediary to recover thermal energy between processes. Heat excess from a process can be transferred to a utility system for generating or heating utilities. The utility stream

generated can be further used by another process to satisfy energy demands. Perry et al. (2008) extended Total Site Integration (TSI) to including process units beyond the processing industry – such as residential or commercial buildings, hotels, farms. The authors also discussed the supply side, where renewables can be integrated to reduce the carbon footprint of the Locally Integrated Energy Sectors (LIES) – already shown in Figure 3. Energy availability and storage systems (Suresh and Saini, 2020) are key elements in integrating urban and renewable energy into industrial energy systems. For the utilisation of renewables, their availability and extraction potential become the focus of this system (Nemet et al., 2012).

TSI was further extended (Varbanov and Klemeš, 2010) by introducing a set of time slices to meet the changes in energy supply and demand. Liew et al. (2012) proposed a numerical method concerning Total Site sensitivity to assess the impact of plant shutdowns or production changes on cogeneration systems over a Total Site.

For all the processes on a site, a unified minimum temperature difference (ΔT_{min}) is not always appropriate. Varbanov et al. (2012) modified the approach of setting a single uniform ΔT_{min}. More realistic heat recovery targets are obtained by TSHI with process-specific ΔT_{min}. A trade-off between heat recovery and distance-related costs (Wang et al., 2014) was considered to ensure the cost-effectiveness of TSHI. Chew et al. (2015) extended the TS targeting method to take into account the pressure drop in the steam network. A design method of hot oil cycle (Ataei et al., 2014) for industrial processes was introduced to reduce utility use and low-grade waste heat. A TSHI for the design of integrated evaporation systems, including vapour recompression (Walmsley, 2016), was proposed. The Plus–Minus principle was adopted (Liew et al., 2014) in the retrofit framework to ensure that individual processes and utility system retrofit can directly save energy at the TS level. A Retrofit Tracing Grid Diagram was introduced (Nemet et al., 2015) to represent all streams and heat exchangers on a temperature scale. This tool can help visualise the current state of the heat exchanger network. Tarighaleslami et al. (2017) combined three optimisation criteria of utility cost, exergy destruction and Total Annualised Cost into a derivative-based optimisation procedure and proposed a new TSHI method for optimising both non-isothermal and isothermal utilities. The textbook by Klemeš et al. (2018a) summarised the Process Integration methods and discussed TSI for co-generation as part of the material. To consider long-term and short-term thermal energy supply and demand changes, Liew et al. (2018) extended the cascade energy target approach of TSHI, i.e. Seasonal Total Site Heat Storage Cascade (Seasonal TS-HSC). Pirmohamadi et al. (2019) improved the optimal design of the Total Site co-generation system

by exergy analysis. To optimise the cooling, heating and power utilities in a trigeneration system, Jamaluddin et al. (2019) presented a new TSI method of Trigeneration System Cascade Analysis (TriGenSCA) using a numerical Pinch Analysis.

The development of TSHI has been reviewed by Liew et al. (2017). TSHI has been applied to different types of industrial processes to reduce energy consumption, e.g. heavy chemical complexes (Matsuda, 2016), industrial clusters (Hackl et al., 2011), petro-chemical plants (Liew et al., 2014), steel plants (Matsuda et al., 2012), dairy plants (Walmsley et al., 2019b) and bromine plants (Boldyryev and Varbanov, 2015).

Graphical methods have proven useful practical in solving single constraint (or contaminant) problems (Zhang et al., 2016). The progressive development of PA in various resource networks demonstrates that this methodology has gained public recognition for its simple and insightful approach to using graphical or digital techniques. In addition to PA, Mathematical Programming (MP) is another method widely used in Heat Integration and TSHI. The applied methods mainly include Mixed-Integer Linear Programming (MILP), Mixed-Integer Nonlinear Programming (MINLP), based on multiperiod models for process loads varying over time, and often employing multiple objective functions, as follows. A MILP was proposed to optimise the structure and parameters of a utility system under fixed demands (Papoulias and Grossmann, 1983). A MILP was proposed with improved models of utility equipment components (Varbanov et al., 2004) for cost-effective de-carbonisation of utility systems (Varbanov et al., 2005). A MILP model which combined TSHI and exergy analysis was presented (Farhat et al., 2015) to obtain energy savings between multiple processes or plants. An MINLP based on a transhipment model with exergo-economic analysis was introduced to minimise the cost caused by exergy destruction in utility systems (Shamsi and Omidkhah, 2012). An MINLP was decomposed (Zhao et al., 2015) into MILP and NLP models to optimise the refinery production system and utility system, which improved the solution quality and time. An MINLP of indirect TSHI by hot water circuit was developed (Chang et al., 2015), with the lowest annual total cost considering pipeline investment, pumping cost and heat loss. An MINLP was developed (Beangstrom and Majozi, 2016) to synthesise steam systems with hot liquid reuse. An MINLP model was proposed for the simultaneous synthesis of the utility system and HEN by recovery heat from steam condensate and boiler feedwater preheating (Luo et al., 2016). An MINLP based superstructure was formulated to design utility plants with local integration of renewable resources (Pérez-Uresti et al., 2019).

A multi-period MINLP model was proposed (Papalexandri et al., 1996) for the optimisation of steam network with variable demands, and the process uncertainty was solved by data reconciliation. A multi-period MILP was formulated (Marechal and Kalitventzeff, 2003) to integrate utility systems, and the operating periods were identified by using A Genetic Algorithm (GA). A multi-period MILP base on a transhipment model was developed (Shang and Kokossis, 2004) to optimise steam levels of total site utility systems. A multi-period MILP model was proposed (Cheung and Hui, 2004) for plant maintenance and production of total site schedules. An improved multi-period MILP model was presented (Zhang and Hua, 2007) to integrate the utility system more effectively with the processing system in a refinery. A multi-period MILP model was improved (Luo et al., 2012) to optimise multiple interconnected steam power plants (SPPS) while minimising environmental costs and impacts. A MILP model with a multi-period item and a recourse item were formulated (Sun et al., 2017) to minimise the total cost to compensate for uncertainties in a utility system design. The cogeneration potential of Total Site utility systems was targeted by the Aspen Plus simulator (Ren et al., 2018). A MILP model with multiple periods was developed for retrofitting the heat exchange network with long-term investment and maintenance planning (Chin et al., 2020). A multi-objective MILP model considering the conflict of economic, environmental and social objectives was proposed (Afshari et al., 2020) for the optimal design of industrial energy symbiosis networks. This model t considered the key sustainability pillars and seasonal fluctuations in energy demands. A multi-objective MINLP with economic and environmental objectives was proposed (Liu et al., 2020) to extend the integration of interplant heat exchange networks (HENs) and utility systems. The HENs were integrated by producing steam through process streams and using steams as intermediate fluids for interplant heat recovery.

There are also other mathematical models. A Simulated Annealing model (Maia and Qassim, 1997) was applied to optimise utility system configuration to adapt to variable demands in different seasons. A cogeneration system was integrated with a process using dynamic modelling (Moita et al., 2005), considering the sensitivity of multiple operational scenarios and atmospheric conditions changes to Process Integration performance. A fuzzy-random interval programming model was used to deal with energy management systems under various uncertainties (Cai et al., 2009). Lagrangian relaxation (Sashirekha et al., 2013), Benders decomposition (Abdolmohammadi and Kazemi, 2013), and real coded genetic algorithm with improved Mühlenbein mutation (Haghrah et al., 2016) were introduced to deal with combined heat and power problem. A two-stage method combining MILP and particle

swarm optimisation (PSO) algorithm was proposed based on a shifted retrofit thermodynamic grid diagram in Heat exchanger network retrofit (Wang et al., 2020).

In the 21st century, energy crises, global warming and environmental pollution are becoming more and more serious. It is urgent to improve energy efficiency, save energy and reduce emissions. One of the critical issues is to valorise low potential waste heat instead of rejecting it. Appropriate integration of heat pumps has the characteristics of efficient recovery of low-temperature heat energy, hot utility energy-saving and potentially environmental protection. Heat pumps (HP) continue to receive considerable attention and development and are becoming a critical sustainable energy technology.

Sadi Carnot (Carnot, 1986), a French scientist in the early 19th century, first proposed the “Carnot Cycle” theory in his paper in 1824, which became the origin of HP technology. In 1912, the world's first set of HP equipment was successfully installed in Zurich, Switzerland, with river water as the low heat source for heating. HPs entered the early stage of development from the 1940s to the early 1950s. HPs used in household and industrial buildings began to enter the market. Since the 1970s, the HP industry has advanced rapidly, and all countries have attached great importance to HP research. Large HP development plans have been instituted by countries and organisations such as the European Community and the International Energy Agency. At present, Europe, America and Japan are competing to develop new types of HPs.

Traditional HP technologies include the vapour compression heat pump (VCHP) (Radermacher and Hwang, 2005), absorption heat pump (Herold et al., 2016), and transcritical heat pump (Lorentzen, 1990). Pavlas et al. (2010) developed a Process Integration methodology for an HP integrated with a biomass gasification process of a wood processing plant. Liew and Walmsley (2016) adopted a Total Site targeting method to integrate open cycle VCHP for enhancing overall site energy efficiency. Walmsley (2016) presented a Total Site Heat Integration (TSHI) method for integrated evaporation systems using an HP (vapour recompression) effectively with application to milk concentrating. (Walmsley and Varbanov (2017) performed a Pinch Analysis of the hybrid compression–absorption HP process for convective dryers by employing simulation and optimisation tools. Stampfli et al. (2018) adapted Pinch Analysis to integrating VCHP for HPs in batch processes. A hybrid method (Stampfli et al., 2019) that unifies the insight-based and mathematical programming approaches have been proposed for industrial HP integration in batch processes to avoid long computation times. Another criterion, EPC (i.e., the coefficient of performance in exergy per

total annual cost), was proposed (Wang et al., 2018) for selecting HPs, modelling diverse types of HPs for operating conditions. This criterion can both evaluate the thermodynamic and economic performances of HPs.

Urbanucci et al. (2019) proposed a two-level optimisation algorithm for the high-temperature HP integration in a trigeneration system. The proposed model allowed them to analyse the HP performance for various working fluids and operating conditions. Schlosser et al. (2019) developed a model for evaluation of the efficiency gains of combining HP storage and intelligent system control for integrating multiple heat sources and sinks, reporting a significant reduction in energy demand. To integrate heat-upgrading technologies in process sites, Oluleye et al. (2016) developed a systems-oriented criterion for conceptual screening and selection of HPs. A Mixed Integer Linear Programming (MILP) framework has been developed (Oluleye et al., 2017). The screening criterion measured the exergy degradation of technology options. However, the techniques presented in that work are only applicable to conceptual system design. Goumba et al. (2017) considered the different waste heat sources and proposed the "Recov'Heat" tool for minimising the utility demands, which makes the heat pumping task easier.

The above studies only use known models to consider the integration of VCHP and processes. Some of the older HP types used Freon as a working fluid. However, Freon is no longer used because of its negative impact on the Earth's atmospheric ozone (Sarbu, 2014). In addition to the improvement of the Coefficient of Performance (COP) of HPs and effective utilisation of the energy input, to further improve the environmental protection, engineers are committed to the development of new working fluids and HP technologies. HP applications are also in continuous development, is widely used in air conditioning and industrial fields and playing a significant role in terms of energy-saving and environmental protection.

Another type of HP with a commercial application is the TCHP, which uses CO_2 as a working fluid. CO_2 is a natural refrigerant, commonly known under the label "R744". It has a relatively low global warming potential (GWP) value of only 1 and does not cause damage to the ozone layer. It is non-toxic, non-flammable, low-cost and easy to obtain. At present, hot water systems with CO_2 HPs usually adopt a transcritical cycle. In the early 1990s, Lorentzen (1990) proposed a transcritical CO_2 cycle based on the specific physical properties of CO_2, which significantly promoted the development of CO_2 systems in the field of refrigeration. Over the past twenty years, research institutions and enterprises in many countries around the

world have done a lot of research on TCHP, which has become a research hotspot in the field of refrigeration. The exothermic process of significant temperature change (~80–100 °C) on the high-pressure side of the transcritical CO_2 system is very suitable for hot water heating. As a result, research on transcritical CO_2 HPs (TCHP) started as a hot water heater. Nekså et al. (1998) built a test device for a hot water HP system. The first demonstration TCHP water heater (Nekså, 2002) was established for industrial use. Kim et al. (2008) used a combined scroll expander–compressor unit in a two-stage compression CO_2 transcritical cycle to improve the cycle COP. van de Bor et al. (2015) compared several heat recovery technologies based on HPs and heat engines. Integration schemes with processes are not considered.

In VCHP and TCHP, the working fluid undergoes a phase change in at least one of the constituent processes, during which it absorbs or releases heat from the heat source to the heat exchanger (HX). This dependence on latent heat transfer may be a problem in some applications where average temperature variation is significant, exergy transfer efficiency is low, and COP is low. Fu and Gundersen (2016) developed an HP for industrial applications based on the Joule cycle (which they called a reversed Brayton cycle). The operating parameters are investigated by thermodynamic and mathematical models, applying Pinch Analysis and Appropriate Placement rules. The provided case studies also illustrate the Hest Exchanger Network (HEN) synthesis conforming to the Heat Integration targets.

ECOP (Ecop Technologies GmbH) (Adler and Mauthner, 2017) applied an HP process based on a reverse Joule cycle (also known as Joule–Brayton or Brayton cycle) with the rotation HP implementation. Compared with the traditional HP, the Joule cycle heat pump (JCHP) features sensible heat exchange between the working fluid and process heat source/sink, which is an advantage when the process streams do not condense or evaporate or have smaller Specific Heat Capacity (CP). This provides more flexibility in accommodating process streams and achieving a higher temperature lift.

A recent work (Wallerand et al., 2018a) has presented a system synthesis method for HP integration in the industry. The method uses a superstructure-based mathematical model, resulting in a Mixed Integer Nonlinear Programming (MINLP) formulation, achieving performance improvements over similar previous methods of up to 30 %. The model considers phase-change based HPs (mainly VCHP). As is shown in this work, the correct choice of HP type bears the significance of an order of magnitude higher than such improvements.

In summary, there are limited studies on the Heat Integration of new heat pump

technologies and industrial processes. The low-grade waste heat recovery in energy integration should be further considered. The waste heat recovery mainly adopts conventional heat pump technology. An emerging Joule-Cycle heat pump is more likely to obtain higher COP than a traditional heat pump (HP) under certain circumstances. There is also a gap in the literature for a comparative analysis of different HP types.

2.4 Mass/Material Integration and Conservation

Mass Integration (El‐Halwagi and Manousiouthakis, 1989) was developed in the late 1980s for the synthesis of a mass exchange network following the analogy between heat and mass transfer. It aims to minimise fresh resources consumption and waste discharge (Gai et al., 2021b). It has been widely used to design and obtain optimal targets for various resource conservation networks (RCNs) (Foo, 2012), including water minimisation (Wang and Smith, 1994), refinery hydrogen network problems (Towler et al., 1996), Carbon Emissions Capture and Storage (CeCS) planning (Ooi et al., 2013), etc. RCN synthesis (Foo, 2012) addresses the optimum use of various material resources, e.g. water (Chin et al., 2021a), utility gases (e.g., hydrogen and nitrogen) (Gai et al., 2021a), solvent, solids (Kazantzi and El-Halwagi, 2005), plastic waste (Gai et al., 2021b).

Types of RCNs include intra-plant RCNs and inter-plant RCNs (Chew et al., 2010a). Various reuse/recycle (Wang and Smith, 1994) and regeneration (Kuo and Smith, 1998) strategies can be implemented for individual RCNs (intra-plant RCNs). Upon the exhaustion of intra-plant material recovery potential, the material recovery of inter-plant RCNs (across different RCNs) could be explored (Chew et al., 2010b), which is Total Site Mass/Material Integration. There are also batch process modes (Gouws et al., 2010) in addition to the various RCNs that are operated in continuous mode. The time dimension when integrating batch material networks (BMN) (Foo, 2010) is an important consideration.

Various RCNs synthesis methods have been developed, mainly including insight-based Pinch Analysis and Mathematical Programming approaches (Foo, 2012). The insight-based techniques mainly include graphical targeting techniques, i.e. Material Recovery Pinch Diagram (MRPD) developed by EI-Halwagi et al. (2003), and algebraic targeting techniques, i.e. Material Cascade Analysis (MCA), Surplus Diagram (Alves, 1999), Average Pressure Profiles (Ding et al., 2011) and Material Surplus Composite Curve (Saw et al., 2011). Some review articles (Foo, 2009) and textbooks (Klemeš, 2013) reviewed the progress (El-Halwagi, 2017) and the latest development of PA and prospected the possible direction of future

development (Klemeš et al., 2018b). Widespread studies have also been conducted on the topic of mathematical programming targeting (Mughees and Al-Ahmad, 2015).

The most common mass integrations are water integration and hydrogen integration, which the State-of-the-Art Analysis is discussed in detail next. Fresh water is a globally valuable resource, which has driven water integration for minimising freshwater consumption and wastewater discharge by optimisation of water systems. Similarly, petroleum resources, as the most important raw material for modern industry, have very limited reserves. The effective utilisation of petroleum resources is necessary for socially sustainable development and attracts increasing attention. Hydrocracking of heavy oil fractions has become an established practice, aiming at the improvement of the utilisation rate of crude oil. The hydrogenation process has been widely used in the petrochemical industry. As a result, hydrogen demand in refineries keeps increasing rapidly (Alves and Towler, 2002). Refiners are highly interested in controlling the hydrogen cost to increase revenue. Hydrogen network optimisation and rational utilisation of hydrogen resources are important to reduce hydrogen consumption and the production cost of oil refineries. The goal of hydrogen network optimisation is to reduce fresh hydrogen consumption and waste hydrogen discharge (Simpson, 1984).

In 1994, Wang and Smith (1994) proposed the concept of Water Pinch, along with many other important concepts, including a limiting composite curve and a water supply line. Tan et al. (2007) developed a new systematic technique for the retrofit of the water network with regeneration based on Water Pinch Analysis (WPA). Foo (2009) investigated intra-plant water network synthesis featuring freshwater of multiple quality levels. Two targeting methods (Pinch Analysis and problem table) for multiple-level fresh resources were proposed. Water footprint and WPA were combined (Tan et al., 2009). Jia et al. (2015) extended the Water Footprint Pinch analysis technique, which was based on the decomposition of total water footprint into external and internal footprint components. Several studies have considered the combination of different methods. An extended Pinch Analysis (Chin et al., 2021e) and an enhanced cascade table analysis method (Chin et al., 2021b) were proposed to target a multiple-contaminant water network. WPA has been successfully applied to optimise the water systems in various industries, including the steel industry (Tian et al., 2008), chemical industry (Liu et al., 2019), refineries (Nabi Bidhendi and Shafikhani, 2018), and others (Skouteris et al., 2018).

The development of Hydrogen Pinch Analysis (Klemeš, 2013) provides an important theoretical and practical basis for hydrogen network optimisation. Hydrogen Pinch Analysis

has been widely applied in the integration of the intra-plant hydrogen network in refineries. In the late 1990s, Alves (1999) proposed the concept of Hydrogen Pinch and the corresponding hydrogen network optimisation method. El-Halwagi et al. (2003) presented a rigorous graphical targeting method for mass exchange networks with a single contaminant. Almutlaq et al. (2005) added a simple algebraic method into the rigorous graphical targeting to convert the graph into algebraic methods. Zhao et al. (2006) proposed the hydrogen load-flowrate diagram, which is not restricted by fresh hydrogen concentration. A multiple-contaminant deficit diagram for hydrogen network targeting (Zhao et al., 2007) is presented, which improves Alves's method (Alves, 1999). This method needs to be computed iteratively. A graphical method based on an improved ternary diagram was developed to optimise hydrogen networks with multiple contaminants (Wang et al., 2012). The disadvantage is that one hydrogen sink can only match three hydrogen sources. Chin et al. (2021b) proposed an extended Pinch Analysis to target multiple-contaminant water networks, which is analogous to the hydrogen networks.

In addition to Pinch Analysis, Mathematical Programming is another method widely used in mass exchange network optimisation. Hallale and Liu (2001) proposed a superstructure-based Mixed-Integer Linear Programming (MILP) model to optimise hydrogen networks considering hydrogen pressure constraints and waste hydrogen regeneration. Pressure Swing Adsorption (PSA) was used for waste hydrogen purification. However, the hydrogen recovery ratio and regenerated hydrogen purity were fixed. Another Mathematical Programming model was later proposed for hydrogen network optimisation, having a hydrogen header (Deng et al., 2014), to reduce the number of connections between hydrogen sources and sinks. Mughees and Al-Ahmad (2015) applied the WPA in water minimisation by combing graphical and mathematical methods (LINGO programming), and their results showed that this approach is easy to apply and can provide more precise results than other techniques. Skouteris et al. (2018) proposed an algebraic technique and utilised the approach for the targeting of water regeneration, where an interception unit is used to partially purify the water sources for further re-use/recycle. A hydrogen network superstructure with hydrogen turbines (Liu et al., 2020) is presented, considering the pressure of the hydrogen streams.

2.4.1 Total Site Mass Integration with Multiple-level Fresh Resources

The above studies all focus on the intra-plant level for Mass Integration. The research on Total Site Integration of inter-plant mass exchange networks has also attracted attention.

Total Site Integration based on Pinch Analysis and Problem Table is proposed for Inter-plant Resource Conservation Network (Foo, 2012). It is divided into unassisted (Chew et al., 2010a) and assisted (Chew et al., 2010b) integration schemes taking the water network as a case study. However, multiple-level fresh resources and waste regeneration were not considered. A non-convex Mixed-Integer Nonlinear Programming (MINLP) is developed for interplant hydrogen network, and a special outer-approximation algorithm is explored (Jagannath et al., 2012). Liu et al. (2016) presented a MINLP for the inter-plant water allocation problem to minimise freshwater consumption and total annualised cost. Shehata (2016) presented an extended automated targeting approach for inter-plant hydrogen networks with purification units. Two purification techniques of PSA and membrane separation were considered. However, the hydrogen recovery ratio and the regenerated hydrogen purity of the purification unit are fixed. Deng et al. (2017) proposed MINLP to optimise inter-plant hydrogen network with PSA for waste hydrogen regeneration. The superstructure-based mathematical programming is presented to optimise inter-plant hydrogen network considering intermediate headers of purity and pressure (Kang et al., 2018). A two-step strategy is adopted to solve the problem aiming at minimising total annual cost. A MILP applying the transhipment model (Lou et al., 2019) is improved for the same problem. However, the recovery ratio and regenerated hydrogen purity of PSA are assumed. The effect of design conditions on PSA performance is not considered. A simultaneous optimisation method is proposed for inter-plant hydrogen networks with operating conditions fluctuation (Han et al., 2020). This multi-period optimisation problem aims to minimise cost.

A Mathematical Programming method can be used for mass exchange networks with complex constraints or multiple objectives. However, mathematical programming is not as intuitive and clear in physical meaning as Pinch Analysis and may not guarantee a globally optimal solution (Klemeš and Kravanja, 2013). The Pinch Analysis method has clear physical meaning, visual, easy to understand and simple operation compared with the mathematical programming method. Most current Mass Pinch Analysis only considered fresh resources with single quality, not multiple quality levels. Some processes in industrials require high-purity fresh resources (Yang et al., 2019), while others are less critical of fresh resource purity. For generating higher-purity fresh resource streams, the production process is more complex, resulting in a higher price of the fresh resource (Li et al., 2017). A lower-cost fresh resource with a low concentration should be preferred for a process requiring a low-purity fresh resource. High purity fresh resource is used only in processes that require high concentration fresh

resources. It is necessary to consider the fresh resource of multiple quality levels (multiple-level fresh resources) in the mass exchange networks synthesis. However, few studies extend the targeting method of Pinch Analysis for Total Site Integration of inter-plant mass exchange networks with a multiple-level fresh resources.

2.4.2 Total Site Mass Integration with Intermediate Purity Headers

The sources were directly connected to the sinks for reuse in the earlier works of intra-plant mass integration. The resulting network may be relatively complex. The changes of flowrate and purity in the sources (upstream) will affect the sinks (downstream).

In order to simplify the network configuration and enhance the controllability of the mass exchange network, intermediate headers can be used in the analogy of a heat exchange network. In Heat Integration (Klemeš, 2013), it is common to set steam mains (Varbanov et al., 2020c) at different pressure levels to maximise heat recovery (Liew et al., 2018) or minimise total annual cost (Pérez-Uresti et al., 2019). Similar studies have been developed on water networks to improve the operation and control of water networks in large processing plants. Feng and Seider (Feng and Seider, 2001) proposed a Pinch Analysis method for a single-contaminant water network with intermediate headers. Wang et al. presented (Wang et al., 2003) a design method of a multiple-contaminant water network with a single intermediate header. The water-saving factor is introduced, and the non-linear model is converted into a linear model in this method. The regeneration water main/header (Cao et al., 2004) is designed by optimising the water quality. A method using superstructure and Mixed-Integer Non-Linear Programming (MINLP) is proposed for a multiple-contaminant water network with one or two intermediate headers (Zheng et al., 2006). However, the MINLP model cannot guarantee the optimal global solution. In order to improve the local optimum, a method based on heuristic rules and mathematical programming is developed (Ma et al., 2007). For a single-contaminant hydrogen network with the single intermediate header, an improved Problem Table is used for flowrate targeting (Deng et al., 2015), and the nearest neighbours algorithm and pressure-impurity diagram are applied to minimise the compressor work (Deng et al., 2017b). Deng et al. (2014) presented a superstructure-based mathematical programming model for the integration of single-contaminant hydrogen networks with one or two intermediate headers.

Some studies have extended the scope to the Total Site Mass Integration for inter-plant mass exchange network. A Mixed-Integer Non-Linear Programming (MINLP) based on the superstructure is presented in an inter-plant water network considering multiple-contaminant

and water headers (both central and decentralised) (Chen et al., 2010). Fadzil et al. proposed the concepts of one-way centralised water header (Fadzil et al., 2018) and two-way centralised water header (Ahmad Fadzil et al., 2018) for Total Site Water Integration in the inter-plant water network. Total Site Centralised Water Cascade Table (TSC-WCT) is developed to minimise freshwater consumption and wastewater discharge. However, the intermediate headers are fixed to two in this method. Jia et al. (Jia et al., 2020) applied Pinch Analysis for Total Site Water Integration with central water header. The intermediate headers of intra-plant were not considered. Chin et al. (2021b) proposed an extended Material Recovery Pinch Diagram to targeting the material headers with minimum fresh resource consumption for the Total Site Material Recycling Network. However, in this study, an only single quality fresh resource is considered.

However, in most of the current studies, the number and purity of intermediate headers are usually fixed at one or two without optimisation in a mass exchange network. The purity location (number and connection) and purity of intermediate headers need to be further considered and optimised. A mathematical programming model based on a superstructure is proposed (Kang et al., 2018) in an inter-plant hydrogen network with single-contaminant and intermediate headers. The purity and pressure of the intermediate headers (both centralised and decentralised) are optimised to minimise the total annual cost. The Mathematical Programming method can be used for problems with complex constraints or multiple objectives. However, Mathematical Programming is not as intuitive and clear in physical meaning as Pinch Analysis and may not guarantee a globally optimal solution. An extension of Pinch Analysis is needed to optimise the intermediate headers of the mass exchange network.

2.4.3 Optimisation of Waste Purification and Regeneration Process

Hydrogen Integration realises hydrogen cascade utilisation to reduce hydrogen consumption by analysing the bottleneck of a hydrogen network. However, there is still a large amount of waste hydrogen in refineries, which is mostly burned as fuel (Jia and Zhang, 2011). According to statistics, about 40 % of hydrogen in refinery gas is burned every year. The hydrogen concentration of waste hydrogen discharge is still high varying from 30 % (Zhang et al., 2016) to 70 % (Jia and Zhang, 2011). Directly burning those waste hydrogen streams causes the waste of resources. With the increasingly serious environmental problems, refineries pay more and more attention to the recovery and regeneration of waste hydrogen. It helps achieve hydrogen balance and reduce fresh hydrogen consumption. Hydrogen Integration considering

waste hydrogen purification has been proposed, including graphical-based (Zhang et al., 2016) and mathematical programming (Lou et al., 2019) methods. Zhang et al. (2011) proposed a triangle rule for optimisation of waste hydrogen purification in a hydrogen network. An optimisation method of hydrogen network purification considering purification energy demand is explored (Zhang et al., 2016). The optimal and critical purification flow was determined by Pinch Analysis. A graphical method was proposed to optimise purification feed and fresh hydrogen sources, considering the interaction between feed purity and feed flowrate through waste hydrogen purification units (Dai et al., 2017). However, these studies assume the regenerated hydrogen purity after purification. The changes in the technical performance and economy of the purification unit were not considered. It is difficult to know whether the purification unit can achieve the assumed purity requirements.

The common purification technologies for waste hydrogen include cryogenic (Song et al., 2019), PSA (Yáñez et al., 2020), and membrane separation (Adhikari and Fernando, 2006). These purification technologies have their own advantages and application scope. It is necessary to select and design the optimal purification process according to the operating conditions of waste hydrogen. A kriging-based PSA model is formulated (Li et al., 2020) to simulate and optimise the waste hydrogen regeneration of hydrogen networks. A case study shows that the model has high accuracy. A PSA/membrane hybrid process (Li et al., 2016) with a high recovery ratio is presented for waste hydrogen purification. Ruan et al. (2019) proposed a graphic method with multi-technique integration separation sequences for multi-input refinery gases. This method can quickly and appropriately select the recovery process without tedious screening to a large number of sequences. However, this method focused on the optimisation of waste hydrogen purification processes, not considering the integration of hydrogen networks at the Total Site level.

The optimisation of waste purification should conform to the principle of Circular Economy (Fan et al., 2019). Circular Economy (Walmsley et al., 2018) is a systematic framework confined to recycling as well as accounting for the efficiency and the economy. Implementing a Circular Economy arrangement requires technology development, investment, and operating cost (Gai et al., 2021). This practice should bring economic benefits along with pollution reduction to ensure sustainable development. Techno-economic analysis (Martínez et al., 2020) is needed for the waste hydrogen purification process. Output has to be higher than the input to be valuable.

To summarise,

i. Most current Pinch Analysis for Mass Integration only considered fresh resources with single quality, not multiple quality. A lower-cost fresh resource with low purity should be preferred for a process requiring low-purity resources. However, few studies extend the Pinch Analysis for Total Site Mass Integration with multiple-level fresh resources.
ii. Furthermore, intermediate headers also could be considered to simplify the configuration and improve the expandability and flexibility of the mass exchange network.
iii. Moreover, with the increasingly serious environmental problems, industries pay more and more attention to waste recovery and regeneration. However, in most current studies, various purification options and their capabilities are not considered in Mass Integration with waste regeneration. The changes in technical performance and economy of the waste purification process are ignored.

2.5 Combined Heat and Mass Integration

Energy and Mass Conservation in process industries is one of the most effective sustainable design methods. The synthesis of Heat Exchanger Networks (HENs) and Mass Exchanger Networks (MENs) have become two major research topics in the fields of process systems and sustainability. The aim is to reduce the external use of energy and mass and to reduce emissions. Many methods of individual Heat Integration for HEN and individual Mass Integration for MEN have been summarised in the above literature review. In addition, some attempts have been made at developing combined heat and mass exchange networks (HAMENs) (Silva Ortiz et al., 2019) synthesis methods since the mass transfer and reaction processes are affected by the operating temperature and pressure.

The synthesis problems of water and heat exchanger networks (WAHENs) represent special cases of HAMENs. The research progress was reviewed (Ahmetović et al., 2015). Some methods have been developed, including Mathematical Programming (Ibrić et al., 2021), Pinch Analysis (Kamat and Bandyopadhyay, 2021a), hybrid approach (Kamat and Bandyopadhyay, 2021b). WAHENs synthesis is successfully applied to optimise the water and energy consumption in various industries, e.g. the production of vinyl acetate monomer (Tan et al., 2013) and vinyl chloride monomer (Chen et al., 2014), as well as vinyl chloride polymerisation (Liao et al., 2011).

The combined hydrogen and heat exchange networks is another important example to

consider, except for WAHENs. Hydrogen as an important raw material in refineries has been paid more and more attention. The hydrogen demand for refineries keeps increasing rapidly, and the cost of hydrogen is rising too. The problem of hydrogen supply shortage is becoming increasingly prominent (Lou et al., 2019). How to use hydrogen reasonably and make the best use of everything has become a new problem faced by refineries. It is necessary to analyse, optimise and control hydrogen networks to reduce production cost and improve hydrogen utilisation. It has great significance to improve the economic benefit of the refinery. Some methods have been developed; among them, Mathematical Programming (Liu et al., 2020) and graphical (Gai et al., 2021a) methods are two main methods. Mathematical Programming can effectively deal with problems involving more complexity and more rigorous multi-objectives. However, it is like a black box that automatically generates results after data is entered. It is useless to provide engineers with the controllability of the solution space and insight into networks design.

Graphical methods are often easier to understand and more important as visual tools for Hydrogen Integration. Hydrogen Pinch is an extension of Pinch Analysis for Heat Integration. Hydrogen Pinch analysis is an important method for hydrogen network optimisation. Since it was put forward in the late 1990s (Alves, 1999), it has made a mature and steady development (Elsherif et al., 2015) in solving the bottleneck of hydrogen networks. It has the advantages of being simple and intuitive, efficient and easy to understand. A variety of Hydrogen Pinch Analysis tools have been proposed, such as the Hydrogen Surplus Diagram (Alves, 1999), Material Recycle Pinch Diagram - MRPD (El-Halwagi et al., 2003), Average Pressure Profiles (Ding et al., 2011), Material Surplus Composite Curve (Saw et al., 2011) and hydrogen network purification targeting (Zhang et al., 2016). However, existing graphical-based methods of Hydrogen Integration mainly focus on process-wide level, not Total Site Integration. The Hydrogen Integration needs to extend from a single process to a site level and higher. A visualisation method (Ong et al., 2017) combining Pinch Analysis and P-graph was developed to Total Site mass, heat and power integration. However, this method only considered the matching of heat grade, and the mass integration was limited to the mass balance, lacking the matching of grade considering the mass.

Following the foundational work on Total Site Heat Integration (Klemeš et al., 1997), there have been other studies, including algorithmic targeting (Liew et al., 2017) and extensions to trigeneration (Jamaluddin et al., 2019). Hydrogen Integration (Lou et al., 2019) is still considered separately. Few studies have considered both Heat Integration and hydrogen

optimisation in refineries. However, Heat Exchange Networks and Hydrogen Networks is coexistence and interaction in most cases. Petroleum refineries are big consumers of both energy and hydrogen. The Total Site Integration of Heat Exchange Networks and Hydrogen Networks, although seen as an area of great potential, has received much less attention. It is necessary to consider both the Total Site Integration of heat and hydrogen simultaneously in refineries to minimise resource consumption and emissions.

To summarise: (i) The method of Total Site Integration considering both mass and energy is usually Mathematical Programming. The graphical-based method still needs to be further improved. (ii) Few studies have considered both Heat Integration and hydrogen optimisation in refineries. A hierarchical targeting method based on graphics of Total Site Integration that considering both hydrogen and heat is necessary to extend for minimising hydrogen consumption.

CHAPTER 3 LOW-GRADE WASTE HEAT RECOVERY OF HEAT INTEGRATION

The work presented in this chapter is based on the author's publication in Energies entitled "Critical Analysis of Process Integration Options for Joule-Cycle and Conventional Heat Pumps", as clarified on Page VI (Contributing publications). The author of this thesis is the first and corresponding author of this publication. The other co-authors who contributed to this publication are the supervisor (Varbanov, P.S.), co-supervisor (Klemeš, J.J.) and collaborator (Walmsley, T.G.). My original contributions are listed in the introduction.

3.1 Introduction

To date, research on heat pumps (HP) has mainly focused on vapour compression heat pumps (VCHP) (Wallerand et al., 2018a), transcritical heat pumps (TCHP) (van de Bor et al., 2015), absorption heat pumps (Herold et al., 2016), and their heat integration with processes. A recent work (Wallerand et al., 2018a) has presented a system synthesis method for HP integration in the industry. The method uses a superstructure-based mathematical model, resulting in a Mixed Integer Nonlinear Programming (MINLP) formulation, achieving performance improvements over similar previous methods of up to 30 %. The model considers phase-change based HPs (mainly VCHP). As is shown in this work, the correct choice of HP type bears the significance of an order of magnitude higher than such improvements.

ECOP (Ecop Technologies GmbH) (Adler and Mauthner, 2017) applied an HP process based on a reverse Joule cycle (also known as Joule–Brayton or Brayton cycle) with the rotation HP implementation. Compared with the traditional HP, the Joule cycle heat pump (JCHP) features sensible heat exchange between the working fluid and process heat source/sink, which is an advantage when the process streams do not condense or evaporate or have smaller Specific Heat Capacity (CP). This provides more flexibility in accommodating process streams and achieving a higher temperature lift. Few studies have considered the Joule cycle heat pump (JCHP), which raises several questions. What are the characteristics and specifics of these different heat pumps? How are they different when they integrate with the processes? For different processes, which heat pump is more appropriate?

Many processes need heat transfer in industrial processing and power generation. Some need heating, and some need cooling or condensation. If the heat exchange network can be appropriately designed, the utility can be minimised, and the capital investment can be reduced to achieve energy saving. Pinch Analysis, pioneered by Linnhoff and Hindmarsh (1983), has

become a widely used method for the comprehensive design of heat exchange networks. The heat exchange network with minimum energy consumption can be obtained by optimising the heat recovery system, energy supply and process operation. Energy targeting is a powerful aid to process design and integration. Stampfli et al. (2018) suggested the COP equation/curve for Process Integration with VCHP. According to the COP equation, when the condensation duty provided by the process sink is known, the evaporative duty of the HP can be obtained, and the COP curve can be drawn in Grand Composite Curve (GCC). The condensation duty can also be obtained when the process is used as a source. Gai et al. (2019) extended the COP curve when the process was integrated with the JCHP. However, the COP curve for the Process Integration with an HP is derived under some assumptions or ideal conditions. Also, in the TCHP, the working fluid CO_2 is a transcritical cycle and the physical property changes substantially, so it is difficult to express the COP curve with an equation accurately.

An emerging JCHP is more likely to obtain a higher COP than a traditional HP under certain circumstances. However, there have been so far just a few studies on the use of JCHP and industrial processes. There is also a gap in the literature for a comparative analysis of different HP types, including the emerging JCHP. The COP equations of HP have some ideal assumptions. These results deviate from the actual performance of the HP, which cannot well represent the real performance of the HP. The performance and integration of different types of heat pumps with various processes have been studied through Pinch Methodology to address these questions. The novel contributions of this chapter include:

i. This study simulates and optimises the operation of the main classes of HPs in a process simulation software—Petro-SIM (KBC, 2016)—to evaluate the performance of the HP as close to reality as possible. These classes include the VCHP, TCHP and the JCHP. The setting of various parameters considers possible process configurations.
ii. All COP curves and heat duties in the GCC for process and HP integration will be plotted against the actual data calculated in Petro-SIM.
iii. The choice of HP type should be performed based on the temperature–enthalpy profile of the considered industrial process for obtaining optimal performance. The performance and application scope of three different HP systems— JCHP, VCHP, and TCHP—are discussed and compared to understand the energy-saving potential of applying HP.

Section 3.2 introduces the simulation and optimisation of the considered HP types and

the method of integration with the process for achieving heat recovery. In Section 3.3, the suitability of the HP types to different temperature–enthalpy (T–H) profiles are evaluated, aiming at the minimisation of power consumption. The optimal COP of each integration case was obtained by optimising the operating parameters of the HP when given source and sink at different temperatures. In Section 3.4, the model is further applied to the integration of HP and different industrial process cases using Pinch Analysis, and the energy-saving potential of different types of HP is evaluated using the GCC (Klemeš et al., 2018a).

3.2 Method

The main goal of heat pumping is to serve, simultaneously, part (or all) of the process heating and cooling demands via heat upgrading from lower to higher temperatures. In Process Integration terms (Klemeš et al., 2018a), this means taking heat from below the Pinch and returning it to the process above the Pinch.

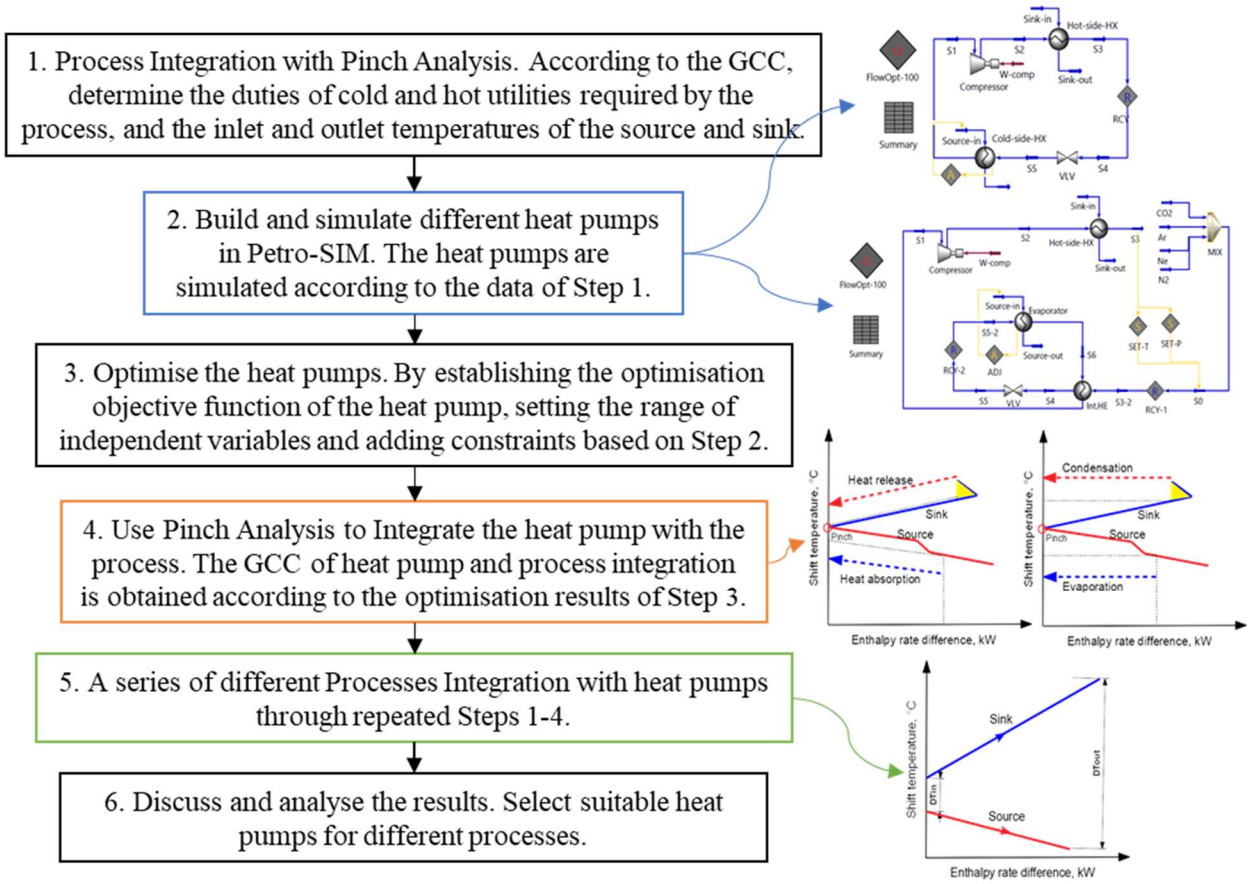

Figure 5. The method procedure of heat pump and process heat integration

The current method has to assist engineers in the selection of the best HP type for a given process configuration. COP is the criterion indicating the quality of the solution because higher COP means serving the process at the expense of lower external energy input. The method follows the algorithm shown in Figure 5.

3.2.1 Step 1: Process Integration with Pinch Analysis

Pinch Methodology (Klemeš et al., 2018b) is a method to calculate thermodynamically feasible energy targets based on thermodynamic principles and analysis. The GCC illustrates the difference between the heat available from hot streams and the heat required by cold streams at every temperature level, identifying the residual heating and cooling demands of the process to be covered by external utilities. A key property of these targets is that both loads and temperatures of the utility targets are identified. In this study, the process is firstly analysed by Pinch Analysis. The target duties of cold and hot utilities required by the process are determined, and the inlet and outlet temperatures of the heat source and heat sink for heat pumping are selected using the GCC.

3.2.2 Step 2: Build and Simulate Different Heat Pumps

The HPs are simulated according to the data of the heat source and heat sink of Step 1. It takes the temperatures and the required heating or cooling duty of the process. In this work, JCHP, VCHP, and TCHP have been simulated by Petro-SIM (KBC, 2016), as shown in Figure 6. The use of Petro-SIM is similar to Aspen Hysys, as both are fork projects of the Hyprotech Hysys versions in the past. The main advantage of using Petro-SIM is that KBC has added dedicated modelling components for energy-related process units, such as boilers, turbines, compressors and HPs.

Fluid packages are based on the Peng-Robinson model (Lopez-Echeverry et al., 2017) in combination with the Lee–Kesler Equation of State as a standard package in Petro-SIM.

Referring to the cases in Figure 6, the similarities between the three different HP cycles are as follows.

1) The working fluid enters the compressor to increase the pressure and temperature.
2) The working fluid then heats the Process Heat Sink (the sink) in a heat exchanger (HX unit named “Hot-side-HX”) and is cooled down.
3) The pressure and temperature of the working fluid are reduced through the Expander or let-down valve (VLV).

4) At the next step, the working fluid absorbs heat from the Process Heat Source (the source) in a Cold-side-HX or Evaporator unit.
5) The working fluid finally returns to the Compressor to complete the cycle.

A critical difference is that the working fluid of a JCHP always maintains the working fluid in a gaseous state. After being cooled by the Sink, the working fluid, generates work through the Expander in the JCHP, as shown in Figure 6a, instead of using a let-down valve as in the other two cycles. In a VCHP, the working fluid has a phase change in both heat exchangers. In the Hot-side-HX, it is condensed from a gas to a liquid phase. In the Cold-side-HX, it is heated from the liquid phase to the gas phase, as shown in Figure 6b. In a TCHP, an intermediate heat exchanger is often added, and the working fluid follows a transcritical cycle, as shown in Figure 6c.

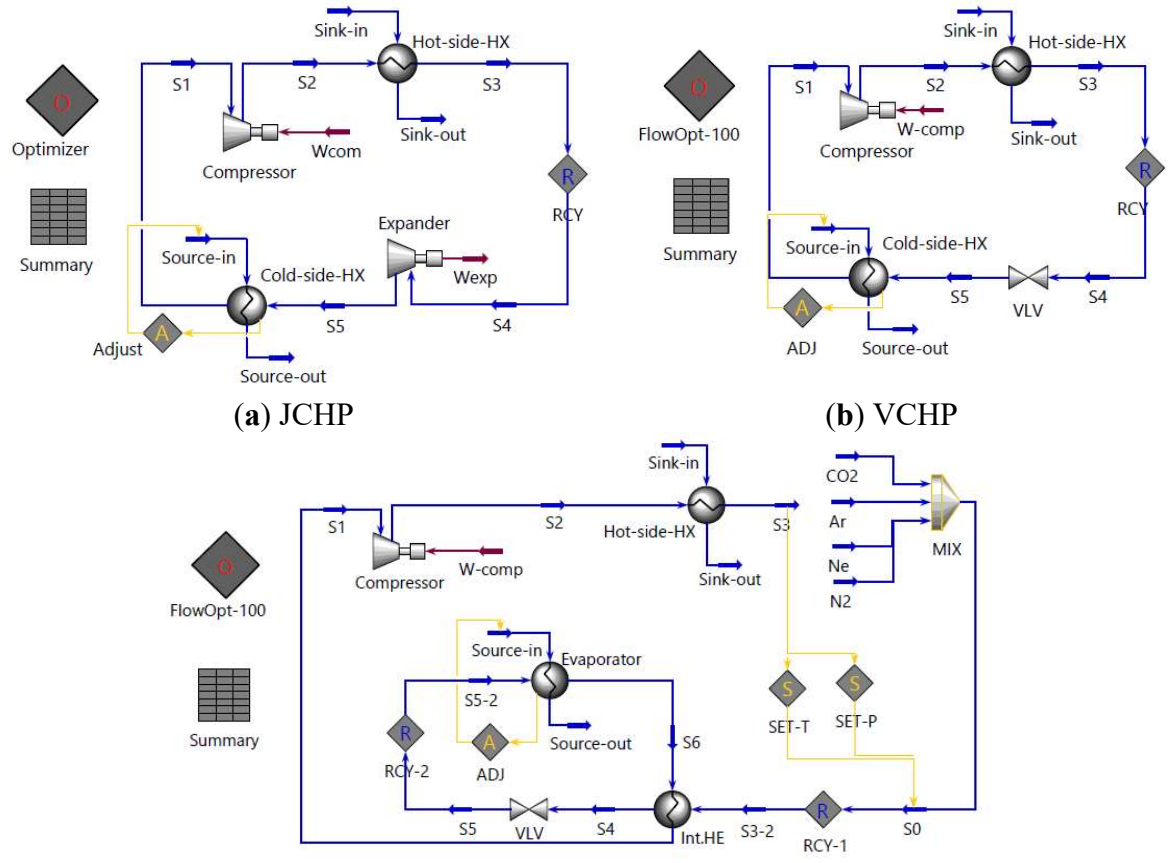

(**a**) JCHP (**b**) VCHP

(**c**) TCHP

Figure 6. Simulation flowsheet of the heat pump as output from Petro-SIM: (**a**) JCHP, (**b**) VCHP and (**c**) TCHP.

To make the simulated HP reflecting the performance of the real HP very closely, it is

necessary to specify reasonable values of the device parameters in the simulation case, matching as close as possible the HP cycle and its measured indicators—mainly temperatures, pressures of the working fluid, the minimum approach temperature (ΔTmin) of the heat exchangers and the isentropic efficiency of the compressor and expander. ECOP (Adler and Mauthner, 2017) has developed a special rotation HP with an embedded compressor/expander that achieves high entropy efficiency for a JCHP. In this study, the JCHP model adopts the performance characteristics of that specific compressor/expander (Adler and Mauthner, 2017). A common turbocompressor unit is used as the compressor of VCHP and TCHP, which is the most used type for industrial-scale HPs. A formula for the relationship between the isentropic efficiency and compression ratio of compressors was proposed by (Wang et al., 2018). It is assumed that the recoverable waste heat duty of process streams is known to recover waste heat of process in this study. This can be achieved by a "Adjust" unit (ADJ; Figure 6) to regulate the flow of the working fluid or source to fix the heat duty of the Cold-side-HX when the process stream is the source for an HP. When the process stream is the sink of an HP, this can be achieved by adjusting the flow of the working fluid or sink to fix the heat duty of the Hot-side-HX.

3.2.3 Step 3: Optimise the Heat Pumps

Based on Step 2, the HP operating variables are optimised, and the optimal performance result is obtained by establishing the objective function of the HP optimisation, setting the range of independent variables and adding constraint conditions of the equation in Petro-SIM. It is necessary to optimise the HP based on the simulation to obtain its best performance. Petro-SIM has a multivariable optimiser. The optimiser can be used to optimise selected independent variables within defined ranges when a simulation converges, to minimise or maximise the objective function. The optimisation functionality of Petro-SIM can manipulate multiple process variables. It can be used for constrained optimisation expression with some flexibility, such as solving the objective function to maximise profit or minimise utility consumption. The iterative calculation method of the Optimiser in Petro-SIM is based on the IPOPT solver (KBC, 2016). In this study, the HP system is optimised by adding an Optimiser unit in the Petro-SIM simulation. In the Optimiser, the independent variables, objective function and constraints are defined to perform the optimisation. In this study, the independent optimisation variables were set as the outlet pressure (or temperature) of the Compressor and the outlet pressure (or temperature) of the Expander/VLV. The constraints are set as the ΔT_{min} of the HXs. The optimisation objective function is COP of the HP. The performance of an HP is generally

evaluated by the COP. The COP of an HP is given in Eq. (1) (Cube and Steimle, 2013).

$$COP = \frac{Q_h}{W} \quad (1)$$

and

$$W = Q_h - Q_c \quad (2)$$

Where: Q_h—Heat output of heat pump, kW;

W—Electrical or power consumption of HP, kW.

The identification of the HP behaviour and best performance is performed by maximising the COP value of the HP under consideration, using the model set up in Petro-SIM (KBC, 2016). The specifications of the temperatures and duties are varied within ranges expected from the considered process type, and the behaviour of the system is investigated. The procedure then provides the best HP—process configuration with the optimal values of the pressures after the compressor and the expander of the selected HP.

3.2.4 Step 4: Process Integrate with Heat Pump

At the next step, Pinch Analysis is used to integrate the HP with the process. The placement of the HP is configured following the outcomes from the previous step. When an HP is integrated with a process, the choice of an HP system depends on the operating temperature and the heat loads below and above the Pinch. In this part, the calculation results of the HPs are plotted against the GCC of the considered process, and the optimal results are linked to the GCC profiles, including the required duties and temperatures. In this way, engineers applying the method can get a better understanding of the optimal results.

The GCC of an HP and an illustrative process is shown in Figure 7. The appropriate placement of an HP means that the heat must be recovered from below the Pinch and released above the Pinch. Improper placement on either side of the Pinch will result in lower energy efficiency. The figure has two lines representing each heat exchange between the HP and the process. The thick dashed lines represent the heat transfer taking place inside the HP block—absorbing and releasing heat. The thin dashed lines represent the heat exchange directly with the process. These form extra heat circuits for minimising the probability of contamination of the internal HP fluids. All other GCC figures in this study follow the same convention.

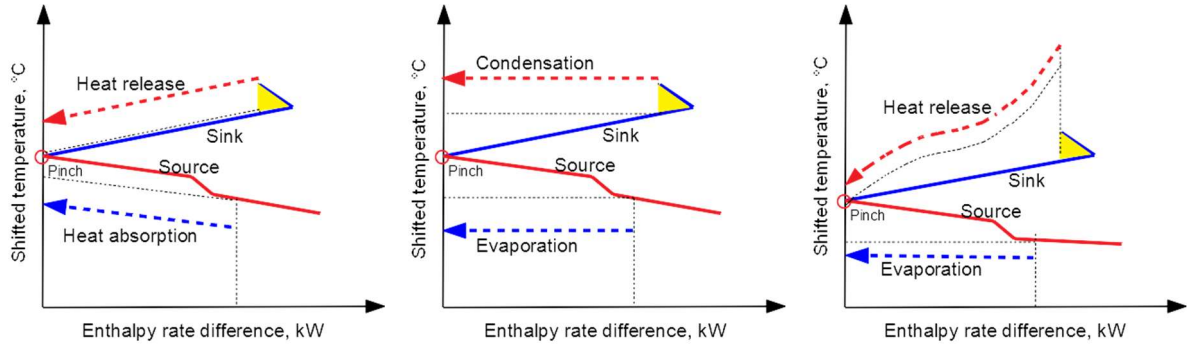

Figure 7. Grand Composite Curve (GCC) construction of a process with an integrated heat pump: (a) JCHP, (b) VCHP and (c) TCHP.

The example GCC of the JCHP is shown in Figure 7a. In the JCHP cycle, the working fluid remains in a gaseous state during the whole cycle of heat exchange with the process source and sink, as well as the compression and expansion. This results in certain variations of the JCHP working fluid temperature. The heat absorption curve (blue dashed line) and heat release curve (red dashed line) are both oblique straight lines, as shown in Figure 7a. The working fluid slope of a JCHP is relatively large in GCC.

The example GCC of the VCHP is presented in Figure 7b. The working fluid of a VCHP is evaporated during heat exchange with the source and is condensed during heat exchange with the sink, so the phase transition occurs. The temperature of the working fluid of VCHP is almost unchanged in the exchange of heat with the source or sink. The evaporation curve (blue dashed line) and condensation curve (red dashed line) are horizontal straight lines (i.e., minimal temperature change).

The GCC of the TCHP is shown in Figure 7c. The working fluid of TCHP is evaporated when the heat is absorbed from the process source. The heat release to the process sink takes place at supercritical conditions of the working fluid. This is why the working fluid temperature of TCHP remains constant during heat absorption from the source but changes significantly during the heat release to the sink. The evaporation curve (blue dashed line) is a horizontal straight line, whereas the heat release curve (red dashed line) is an oblique curve, as shown in Figure 7c.

3.2.5 Step 5: Evaluation of Heat Pump Suitability to Different Process GCC Profiles

The heat duties, inlet and outlet temperatures of the heat source and sink vary among different processes. Pinch Analysis with HP placement is used, performing Steps 1–4 for a set

of GCC profiles representing processes with different thermal properties. The T–H diagrams of different processes are shown in Figure 8. The configurations shown represent pairs of process heat sinks and sources of a gradual, steep and medium slope. Combinations of these are possible, but the three configurations in Figure 8. are the basic ones, which help to understand the major trends.

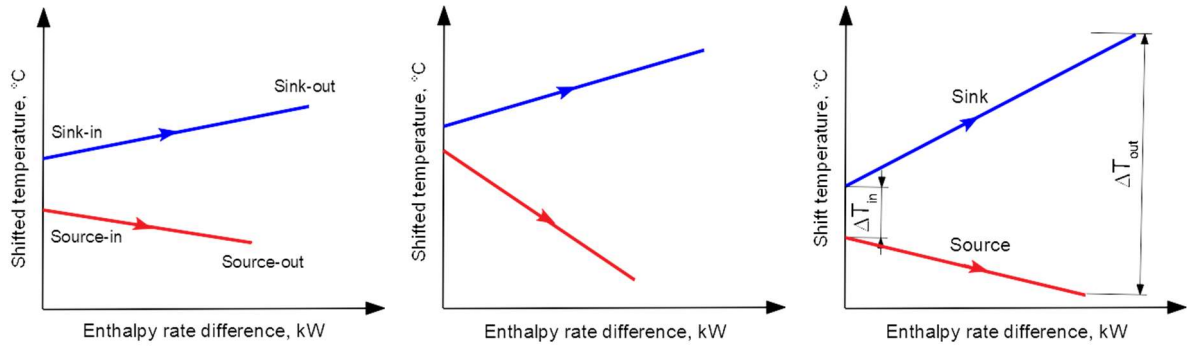

Figure 8. T–H diagrams of different source and sink configurations for heat pump application. (a). Gradual slope; (b). Steep slope; (c). Medium slope.

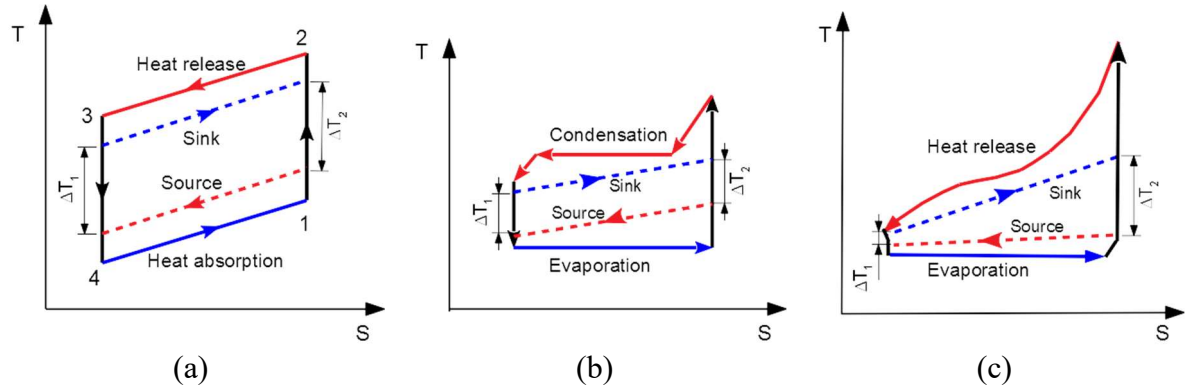

Figure 9. Ideal T–S diagram of the heat pumps (a) JCHP, (b) VCHP and (c) TCHP.

Each of these types of profiles implies a different degree of compatibility with the HP types considered in this work. The compatibility can be qualitatively assessed on the temperature–entropy (T–S) diagrams combining the process heat source/sink profiles with the HP profiles. Such plots are shown in Figure 9. The solid red lines represent the heat release or condensation of the working fluid in the HP, and the solid blue lines are the heat absorption or evaporation of the working fluid. The red dashed lines represent the heat release of the source, and the blue dashed lines represent the heat absorption of the sink. The performance of these three types of HPs (JCHP/ VCHP/ TCHP) is calculated by varying the inlet and the outlet

temperatures of the process heat source and sink and relating the results to the possible representations of temperature lifts ΔT_{in}, ΔT_{out}, or ΔT_1, ΔT_2 (e.g., Eqs. (3)-(6)).

$$\Delta T_{\text{in}} = T_{sink-in} - T_{source-in} \tag{3}$$

$$\Delta T_{out} = T_{sink-out} - T_{source-out} \tag{4}$$

$$\Delta T_1 = T_{sink-in} - T_{source-out} \tag{5}$$

$$\Delta T_2 = T_{sink-out} - T_{source-in} \tag{6}$$

Where, ΔT_{in}—The inlet temperature difference of the source and sink, °C. ΔT_{out}—The outlet temperature difference of the source and sink, °C. ΔT_1—The difference between the inlet temperature of the sink and the outlet temperature of the source, °C. ΔT_2—The difference between the outlet temperature of the sink and the inlet temperature of the source, °C.

3.2.6 Step 6: Discuss and Analyse the Results

To select the HP suitable for each of the possible processes, the solutions obtained during Steps 1–5 provide engineers with sufficient information and understanding of why the proposed measures are appropriate and efficient. The evaluation is performed by the combined use of Pinch Analysis and Petro-SIM to simulate and optimise the HPs. The actions include constructing the GCC of the process and combining it with the plots of the considered HPs. The combined plots are then used for explaining the solutions and relating them to the process specifications—i.e., the temperatures and heating/cooling duties of the main process, plus the HP properties—i.e., working fluid and operating pressures.

3.3 Simulation and Optimisation of Heat Pumps

A series of simulations and optimisations were performed by changing the inlet and outlet temperatures of the source and sink to study the performance of these different HP cycles in different scenarios. The settings of parameters and variables of the HP are shown in Table 1. ΔT_{min} denotes the specifications of the minimum allowed temperature differences of the heat exchangers. The pressure differences (ΔP) between the stream inlets and outlets of the heat exchangers in the HP are all 50 kPa. In the "Adjust" unit, the heat transfer duty of the heat exchanger Cold-side-HX is set to 10 MW by adjusting the flowrate of stream Source-in, which is the optimisation variable. The optimisation objective is to maximise the COP. Based on the simulation results, the application range of these three types of HPs is classified and can be

predicted, mapping their suitability for the various process heat source and sink scenarios.

Table 1. Settings of parameters and variables.

Settings		JCHP-Ar	JCHP-CO_2	VCHP	TCHP
Working fluid		Argon (Ar)	CO_2	NH_3	CO_2
Compressor/Expander efficiency		96%	96%	65%	65%
Variable Range	[1] P_2, MPa	3–8	2.5–7	1–7.5	7.5–20
	[2] P_5, MPa	0.5–5	1–4	0.2–1	2–5
constraints	ΔT_{min} of Hot-side-HX	5–30	5–30	5–30	5–30
	ΔT_{min} of Cold-side-HX	5–30	5–30	5–30	5–30

[1] P_2 -- The outlet pressure of the compressor in the HP cycle, MPa. [2] P_5—The outlet pressure of the expander or expansion valve in the HP cycle, MPa.

The simulation results of the considered scenarios are shown in Figure 10 and Figure 11. In Figure 10, the performance as a function of the temperature lifts (expressed as the inlet and outlet temperature differences) is evaluated. Figure 11 provides an evaluation of the COP as a function of the temperature lift expressed as ΔT_1 and ΔT_2.

Case 1: COP modelled as a function of the temperature lift represented by ΔT_{in} and ΔT_{out}

The variation of COP of different HPs with ΔT_{in} and ΔT_{out} is shown in Figure 10. As can be seen from Figure 10a, when 0 °C < ΔT_{in} < 30 °C and 30 °C < ΔT_{out} < 80 °C, the COP of JCHP-Ar decreased with the increase of ΔT_{in} but did not change much with ΔT_{out}. The COP of JCHP-CO_2 decreased with the increase of ΔT_{in} but did not change much with ΔT_{out}, as Figure 10b illustrates. This indicates that, when the inlet temperature difference (ΔT_{in}) between the heat source and sink is not significant, even if the outlet temperature difference (ΔT_{out}) between the two is very large (such as ΔT_{out} increasing to 80 °C), the COP of the actual JCHP is still very high. It can be seen that the JCHP is very suitable for processes where the ΔT_{out} is massive, and ΔT_{in} is small. The smaller ΔT_{in}, the higher is the COP of JCHP.

When 0 °C < ΔT_{in} < 30 °C and 30 °C < ΔT_{out} < 80 °C, the COP of the evaluated VCHP decreased with the increase of ΔT_{out}, but did not change much with ΔT_{in}, as can be detected from Figure 10c. Therefore, when ΔT_{out} between the source and sink is small, even if the ΔT_{in} between the two is significant (the maximum ΔT_{in} can only be equal to the ΔT_{out}), the COP of the actual VCHP is higher. The observations imply that VCHP is very suitable for processes where the temperature difference (ΔT) between the heat source and sink is not large. The smaller ΔT_{out}, the higher is the COP of VCHP.

The COP of the evaluated TCHP decreased with the increase of ΔT_{out} and ΔT_{in} when 0 °C < ΔT_{in} < 30 °C and 30 °C < ΔT_{out} < 80 °C, as can be detected from Figure 10d. The observations imply that the application scope of TCHP is relatively narrow. TCHP is very suitable for processes where the ΔT_{in} is small and ΔT_{out} < 40 °C.

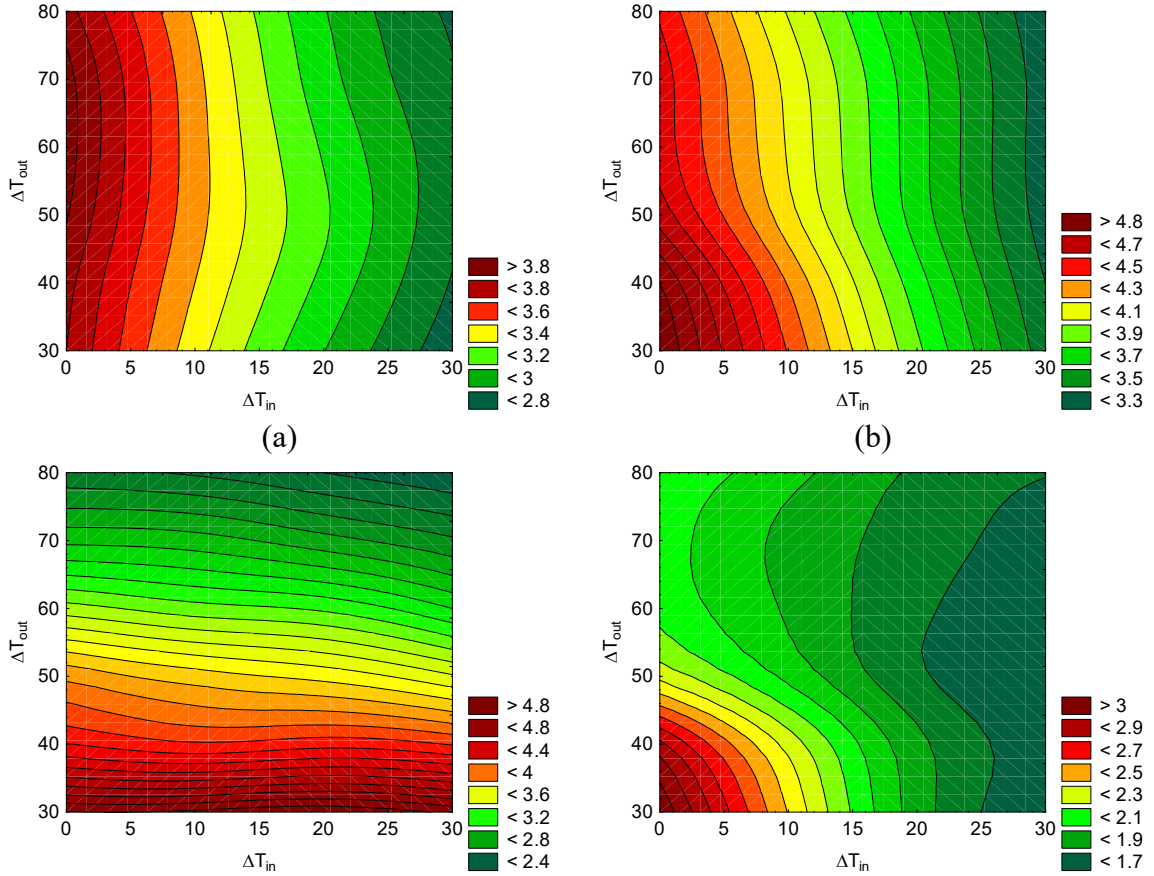

Figure 10. COP of different heat pumps varies with ΔT_{in} and ΔT_{out}: (a) JCHP-Ar, (b) JCHP-CO_2, (c) VCHP and (d) TCHP.

The variation trend of TCHP is not very regular, and the performance contours are less noticeable. This is because TCHP is a transcritical cycle, and the thermophysical properties of CO_2 in the supercritical state are nonlinear, as the substance does not behave like a gas or a liquid. This makes it necessary to model the HP behaviour also as a function of the other two temperature lift representations: ΔT_1 and ΔT_2, by analogy with heat exchanger temperature differences and the T–S diagrams of the HP cycles.

Case 2: COP modelled as a function of the temperature lift represented as ΔT_1 and ΔT_2

The change of COP of different HPs with ΔT_{in} and ΔT_{out} is studied by fixing the outlet

temperature of sink $T_{sink\text{-}out}$ to a certain level. In this study, the $T_{sink\text{-}out}$ is set as 50 °C. When $T_{sink\text{-}out}$ is 50 °C, the change of COP of the different HPs with ΔT_1 and ΔT_2 is shown in Figure 11. It can be seen that the COP of JCHP-Ar decreased with the increase of ΔT_1 and ΔT_2. The COP of JCHP-CO_2 first increased and then decreased with the increase of ΔT_1 and ΔT_2, featuring a maximum. The COP of VCHP and TCHP decreased with the increase of ΔT_1 but did not change much with ΔT_2.

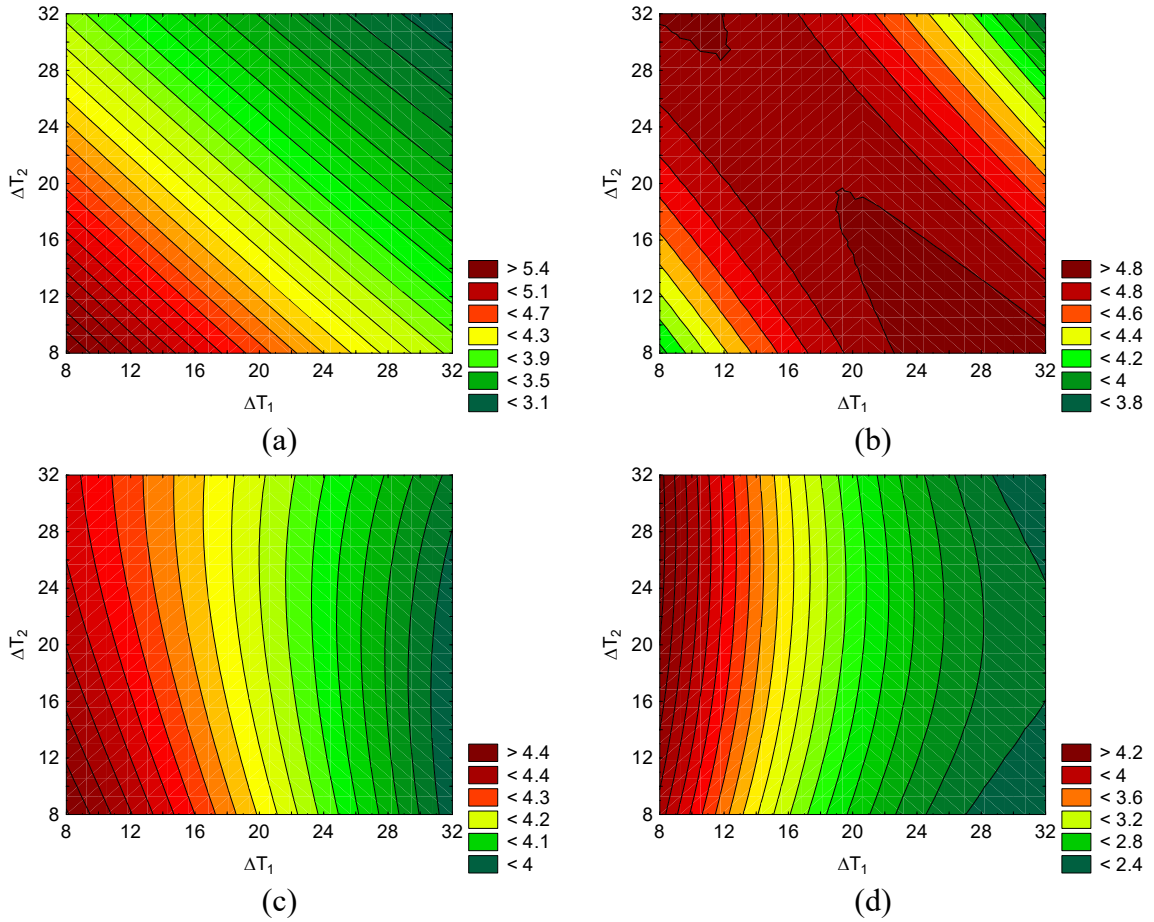

Figure 11. COP of different heat pumps varies with ΔT_1 and ΔT_2 (a) JCHP-Ar, (b) JCHP-CO_2, (c) VCHP and (d) TCHP.

It can be seen from Figure 11d that when the temperature difference ΔT_1 is small, even if the temperature difference ΔT_2 is large, the COP of the TCHP is higher. The TCHP is then very suitable for a small temperature rise ΔT_1 (preferably $\Delta T_1 \leqslant 10$ °C) combined with a large ΔT_2 process.

In conclusion, the observations imply from Figure 10 and Figure 11 that JCHP is very suitable for the process of steep T–H lines of the source and sink in GCC. VCHP is suitable for

selection when the slopes of the T–H lines of the source and sink have a relatively low gradient (closer to flat). TCHP is suitable for selection when the slope of the T–H line of the source has a relatively low gradient (closer to flat) and steep T–H line of the sink in GCC.

3.4 Case Studies

This section analyses the integration of the different types of HPs using industrial examples to assess the practicability of the conclusion of Section 3.3. The optimisation objective function is the COP of the HP.

3.4.1 Formulation and Development: Process Integration Using JCHP, VCHP and TCHP

Four different industrial processes have been studied. The first process is a spray drying process of milk powder in a dairy factory (Atkins et al., 2011), and its GCC is shown in Figure 12. The second process is also from dairy product processing (Wallerand et al., 2018b), which uses raw milk to produce concentrated milk, pasteurised milk, cream, yoghurt and dessert. The GCC for that is shown in Figure 13. The third example is from candy processing and packaging in a candy factory (Miah et al., 2015). The GCC is shown in Figure 14. The fourth process is a 4-column double-effect methanol distillation in a chemical plant (Cui et al., 2017). The GCC is shown in Figure 15. The ΔT_{min} between the heat source/sink and the working fluid in the HP cycle is 5 °C. The compressors and expanders of the JCHP adopt centrifugal force rotating system structure, and their isentropic efficiency can be as high as 96 %. The compressors of VCHP and TCHP are ordinary turbocompressors. In this study, isentropic efficiency is assumed to be 65 %.

I. Case 1: Milk Spray Drying Process

The spray drying process of the milk powder was integrated with the HP. The stream data were only adopted the spray drying process from (Atkins et al., 2011), as shown in Table 2. The ΔTmin of the process is 20 °C.

As can be seen from the GCC in Figure 12, the Pinch Temperature of this process is 65 °C. The hot utility required is 17.66 MW, and the cold utility required is 5.36 MW. It is assumed that all the source energy is used to heat the sink when the process is integrated with an HP. The heat duty of the heat exchanger at the source side for the HP is fixed at 5.36 MW. The allowed range of the independent variables and the optimisation results of a spray dryer with an integrated HP (maximising the COP) are shown in Table 3.

Table 2. The stream data from a spray drying process.

Steam Name	Type	T_s, °C	T_t, °C	CP, kW/°C
Milk Concentrate	Cold	54	65	37.6
Dryer Inlet Air	Cold	25	200	119.2
Fluid Bed A Inlet Air	Cold	25	50	10.2
Fluid Bed B Inlet Air	Cold	25	45	14.9
Fluid Bed C Inlet Air	Cold	25	32	11.2
Air Exhaust	Hot	75	20	174.7

For evaluation and interpretation, the GCC of the process integrated with different types of HPs is given, as shown in Figure 12. As can be seen from Table 3, the four HPs (JCHP-Ar, JCHP-CO_2, VCHP and TCHP) can save 47 %, 46 %, 66 % and 69 % of the hot utility by improving the waste heat quality of the process. The ranking of best COP of the HPs is JCHP-CO_2 > JCHP-Ar > VCHP > TCHP when integrating with this process. The reason can be seen in Figure 12, showing that the inlet temperature difference ΔT_{in} between source and sink is too small, while the outlet temperature difference ΔTout is too large. That is, the slopes of source and sink are both steep in the GCC.

Table 3. Variation settings and optimisation results of spray drying with an integrated heat pump.

Heat pump	Variation Ranges		Optimisation Results					
	[1] P_2, MPa	[2] P_5, MPa	COP, -	Q_{sink}, MW	W, MW	P_2, MPa	P_5, MPa	[3] R, -
JCHP-Ar	5-9	2-5	2.83	8.29	2.93	8.99	4.35	2.09
JCHP-CO_2	4-7	1-3	2.93	8.04	2.74	6.47	1.70	3.92
VCHP	2.5-9	0.2-1	1.85	11.66	6.30	8.01	0.51	17.40
TCHP	12-20	2-5	1.77	12.11	6.83	18.65	3.03	6.27

[1] P_2: The outlet pressure of the compressor in the HP cycle, MPa. [2] P_5: The outlet pressure of the expander or expansion valve in the HP cycle, MPa. [3] R: The compression ratio of the compressor, -.

In the HP cycle, the working fluid of the JCHP does not undergo a phase change and remains in the gas phase. As a result, the ΔT between the inlet and the outlet of the working fluid in the JCHP changes significantly in the heat exchange with the source or sink. The slope of the working fluid is relatively large in GCC, as shown in Figure 12a-b. The working fluid of VCHP is evaporated during heat exchange with the source and is condensed during heat exchange with the sink, so the phase transition occurs. Therefore, in the heat exchange with the source or sink, the ΔT between the inlet and the outlet of the working fluid in the VCHP

changes a little. The slope of the working fluid is small in GCC, as shown in Figure 12c. The reason for the temperature difference in the red dashed line in Figure 12c is that the working fluid becomes a superheated gas after increasing the pressure by the compressor. In the heat exchanger hot-side-HX, the working fluid is cooled to a saturated gas and then condensed to a liquid. Therefore, the red dashed line is tilted first and then becomes horizontal. However, when the working fluid is a gas that cools down from the superheated state to the saturated state, the CP is small, and the heat exchange efficiency is low. At the same time, the sink is a gas that the CP is small, and the sink slope is large during the heat exchange, so the oblique part of the red dashed line is longer.

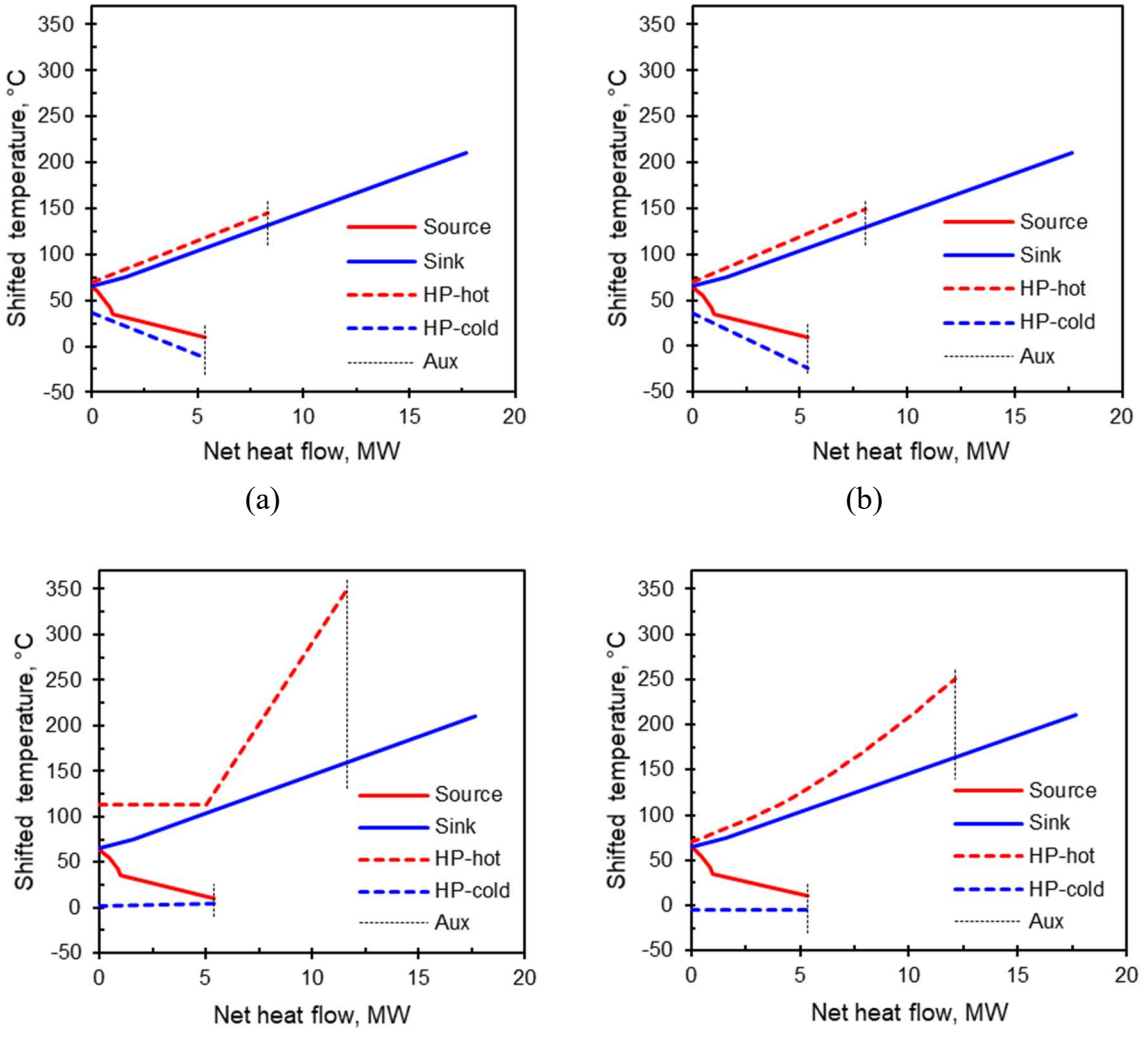

Figure 12. GCC of Case 1 and Process Integration using (a) JCHP-Ar, (b) JCHP-CO_2, (c) VCHP and (d) TCHP.

The working fluid of TCHP is evaporated during exchanging heat with the source, while is supercritical fluid during heat transfer with the sink. As the slope of the working fluid is small during the heat transfer with the source in the GCC, whereas the slope of the working fluid is significant in the heat exchange with sink in the GCC, as shown in Figure 12d. In this case, the average temperature between working fluid and source/sink in JCHP is small, so the energy loss of the heat exchangers is lower, the heat exchange efficiency is higher, and it affects the COP positively. The average temperature between the working fluid and the source/sink in VCHP and TCHP is large, so the energy loss is higher, the heat exchange efficiency is smaller, and it affects the COP negatively. The performance of VCHP and TCHP are both weak. In addition, the compression ratio of the compressor in VCHP is 17.40, too high for a single stage. This means that multiple stages of compression would be required, resulting in a substantial increase in the cost of the compressor and a higher cost for VCHP. The outlet pressure of the compressor in TCHP is very high (18.65 MPa). This means high-pressure requirements for equipment of TCHP, with very high equipment investment costs. The economy of the VCHP and TCHP are both weak, and this process is more suitable for Heat Integration with JCHP, which is consistent with the conclusion of Section 3.3. It can be seen that the method proposed in this study is feasible and effective.

II. Case 2: Raw Milk Processing into Dairy Products

The stream data are taken from (Wallerand et al., 2018b), as shown in the Appendix (Table S2). The ΔT_{min} of the process is 4 °C. As can be seen from the GCC in Figure 9, the Pinch Temperature of this process is 66.9 °C. The hot utility required is 2.34 MW, and the cold utility required is 0.94 MW. It is assumed that the heat duty of the heat exchanger at the source side is fixed at 0.71 MW. Both the process heat source and the sink undergo a phase transition. The source needs to be condensed, and the sink needs to be heated and evaporated. The pressure differences of the heat exchangers on the source side and sink sides are both set at 0 kPa. The setting range of independent variables and optimisation results of HP integration into a dairy product process are shown in Table 4.

The GCC of the dairy products process integrated with different types of HPs is shown in Figure 13. As can be seen from Table 4, the four HPs (JCHP-Ar, JCHP-CO_2, VCHP, and TCHP) can save 43 %, 39 %, 33 %, and 78 % of the hot utility by improving the waste heat quality of the process. The ranking of the HP COPs is VCHP > JCHP-CO_2 > JCHP-Ar > TCHP when integrating with the dairy products process.

Table 4. Variable settings and optimisation results of a dairy product with an integrated heat pump.

Heat pump	Variable Ranges		Optimisation Results					
	[1] P_2, MPa	[2] P_5, MPa	COP, -	Q_{sink}, MW	W, MW	P_2, MPa	P_5, MPa	[3] R, -
JCHP-Ar	5-9	3-5	3.89	1.00	0.26	6.97	4.87	1.45
JCHP-CO_2	4-8	1-4	4.52	0.92	0.20	4.37	2.56	1.74
VCHP	3.5-7	0.5-3	13.07	0.77	0.05	3.62	2.73	1.35
TCHP	14-20	2-5	1.68	1.81	1.08	17.54	3.03	5.89

[1] P_2: The outlet pressure of the compressor in the HP cycle, MPa. [2] P_5: The outlet pressure of the expander or expansion valve in the HP cycle, MPa. [3] R: The compression ratio of the compressor.

The reason can be seen in Figure 13. The ΔT_{in} and the ΔT_{out} between the source and the sink are both too small (1.5 °C). The slopes of both the source and sink in the GCC plot are too small (flat). As the working fluid of the JCHP remains a gas across the whole HP cycle, the ΔT between the inlet and the outlet of the working fluid in the JCHP varies significantly in the heat exchange with the source or sink. The slope of the working fluid is relatively large in the GCC, as shown in Figure 13a,b. As the working fluid of the VCHP is evaporated during heat exchange with the source and is condensed during heat exchange with the sink, the ΔT between inlet and outlet of the working fluid in the VCHP does not change in the heat exchange with the source or sink. The slope of the working fluid is small in the GCC, as shown in Figure 13c.

The working fluid of TCHP is evaporated during exchanging heat with the source, whereas it is a supercritical fluid during the heat transfer to the sink. Therefore, the slope of the working fluid is small in the heat exchange with the source in the GCC, while the slope of the working fluid is steep in the heat exchange with sink in GCC, as shown in Figure 13d. In this case, the average temperature between the working fluid and the source/sink in VCHP is small, so the energy loss of the heat exchangers is lower, the heat exchange efficiency is higher, and it affects COP positively. Although the average temperature between working fluid and source/sink in JCHP and TCHP is large, so the energy loss is higher, the heat exchange efficiency is smaller and affects the COP negatively. The performance of JCHP and TCHP are both weak. In addition, the outlet pressure of the compressor in TCHP is too high (17.54 MPa). This means high-pressure requirements for equipment of TCHP, with very high equipment investment costs. The TCHP economy is weak. This process is more suitable for Heat Integration with VCHP, which is consistent with the conclusion of Section 3.3. It can be seen that the method proposed in this study is feasible and effective.

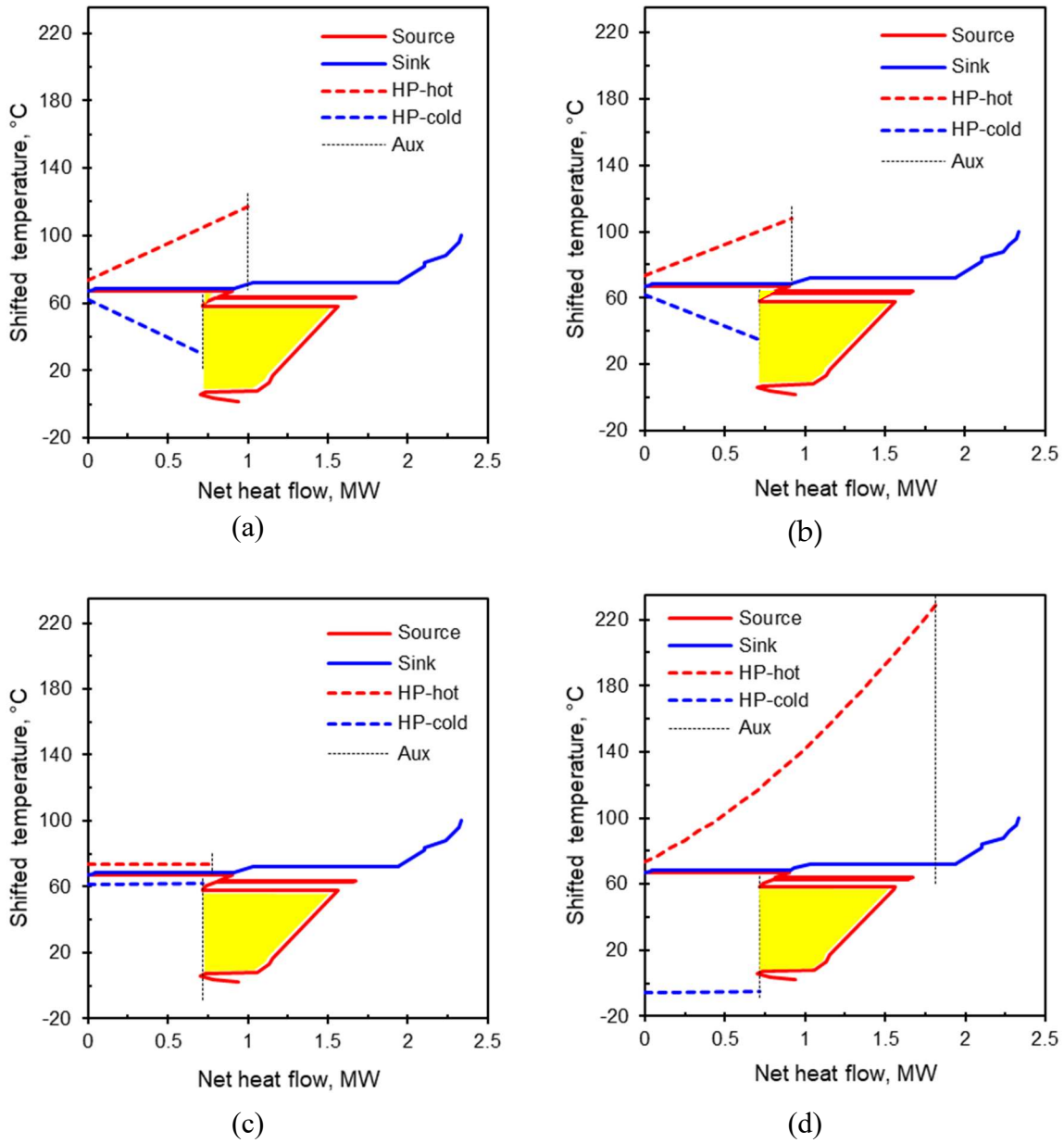

Figure 13. GCC of case 2 with integration options using (a) JCHP-Ar, (b) JCHP-CO_2, (c) VCHP and (d) TCHP.

III. Case 3: Candy Processing and Packaging

The process of candy processing and packaging was evaluated for HP integration. The stream data were taken from (Miah et al., 2015) and are listed in the Appendix (Table S3). The ΔT_{min} of the process is 5 °C. As can be seen from the GCC in Figure 14, the Pinch temperature of this process is 19.5 °C. The hot utility required is 1.82 MW, and the cold utility required is 0.33 MW. It is assumed that all the source energy is used to heat the sink when the process is integrated with an HP, fixing the source duty to 0.33 MW. The pressure differences of the heat

exchangers on the source side and sink sides are both 50 kPa. The setting ranges of the independent optimisation variables and optimisation results of a process of candy processing and packaging integration HP are shown in Table 5.

Table 5. Variable settings and optimisation results of a process of candy processing and packaging integration heat pump.

Heat pump	Variable Ranges		Optimisation Results					
	[1] P_2, MPa	[2] P_5, MPa	COP, -	Q_{sink}, MW	W, MW	P_2, MPa	P_5, MPa	[3] R, -
JCHP-Ar	5-9	3-5	2.81	0.53	0.19	7.05	3.75	1.90
JCHP-CO_2	4-7	1-4	3.55	0.46	0.13	6.13	2.65	2.36
VCHP	1.5-7	0.5-2	4.44	0.43	0.10	2.25	0.62	3.95
TCHP	9-15	2-5	1.85	0.67	0.36	10.75	3.03	3.61

[1] P_2 -- The outlet pressure of the compressor in the HP cycle, MPa. [2] P_5 -- The outlet pressure of the expander or expansion valve in the HP cycle, MPa. [3] R -- The compression ratio of the compressor, -.

For intuitive display of the results and analysis, the GCC of the process combined with the HPs is shown in Figure 14. As can be seen from Table 5, the four HPs (JCHP-Ar, JCHP-CO_2, VCHP and TCHP) can save 29 %, 25 %, 24 % and 37 % of the hot utility by improving the waste heat quality of the process. The ranking of the HP COPs is VCHP > JCHP-CO_2 > JCHP-Ar > TCHP when integrating with this process. The reason can be seen in Figure 14, stemming from the fact that the ΔT_{in} between the source and the sink is approximately the same as the ΔT_{out}. The slopes of source and sink are both small in the GCC. As the working fluid of the JCHP does not undergo a phase change remaining gas, the ΔT between inlet and outlet of the working fluid in JCHP changes significantly in the heat exchange with both the source and the sink. The slope of the working fluid is relatively large in the GCC (Figure 14a,b). Due to the phase changes of the working fluid of the VCHP, the ΔT between the inlet and outlet of the working fluid in the VCHP change very little. The slope of the working fluid is small in the GCC – see Figure 14c. For the TCHP, the slope of the working fluid is small in the heat exchange with the source in the GCC, whereas the slope of the working fluid is large in the heat exchange with sink in the GCC, see Figure 14d.

In this case, the average temperature between working fluid and source/sink in VCHP is small, so the energy loss of the heat exchangers is lower, the heat exchange efficiency is higher, and it affects the COP positively. Although the average temperature between working fluid and source/sink in JCHP and TCHP is large, and therefore the energy loss is higher, the

heat exchange efficiency is smaller and affects the COP negatively. The performance of JCHP and TCHP are both weak. This process is more suitable for heat integration with a VCHP, which is consistent with the conclusion of Section 3.3.

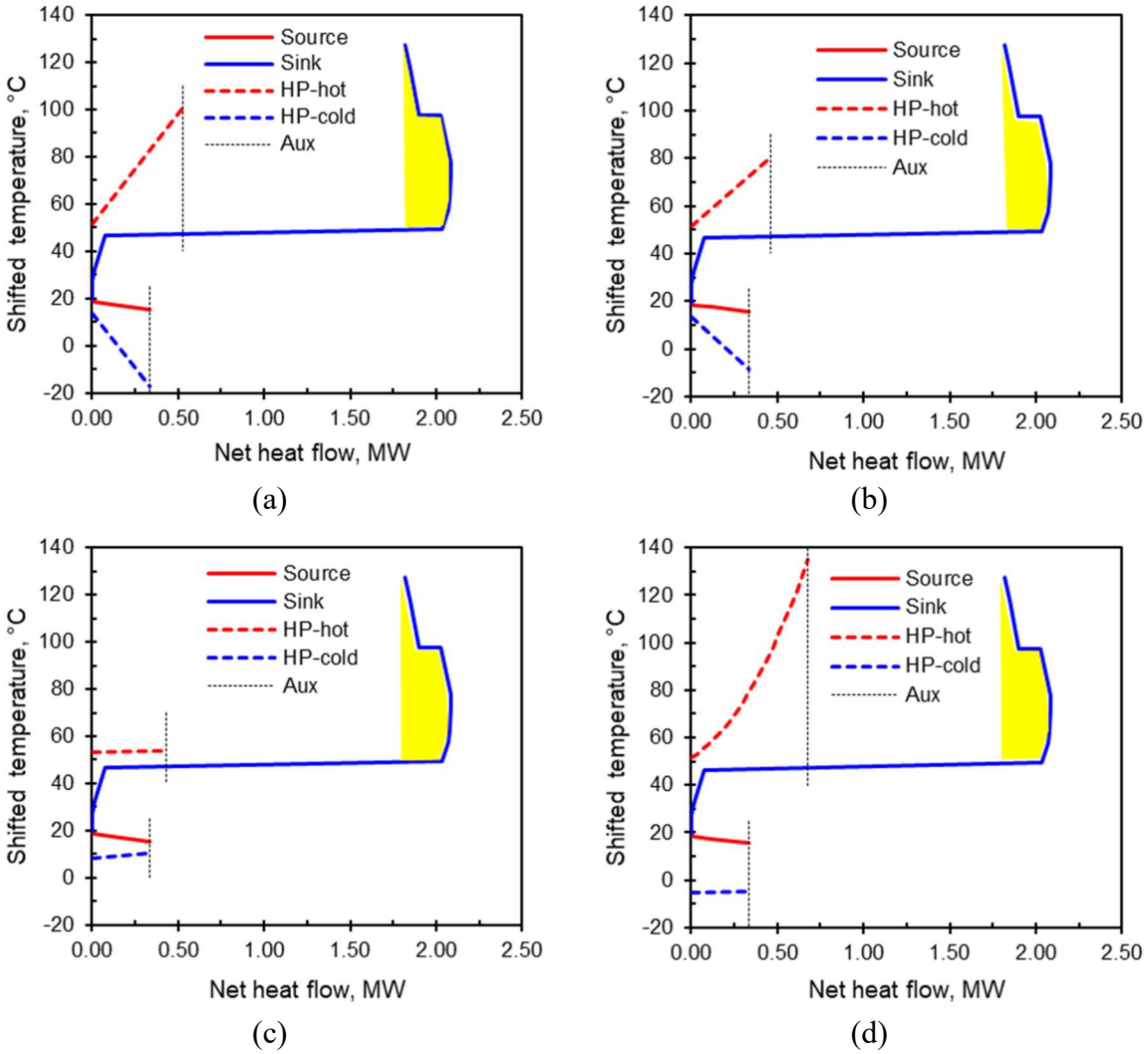

Figure 14. GCC of case 3 and integration options using (a) JCHP-Ar, (b) JCHP-CO2, (c) VCHP and (d) TCHP.

IV. Case 4: Methanol Distillation Process

The methanol distillation process was evaluated for HP integration based on the stream data from a 4-column double-effect methanol distillation process of a chemical plant (Cui et al., 2017). The data are given in the appendix Table S4. The ΔT_{min} of the process is 15 °C. As can be seen from the GCC in Figure 15, the Pinch Temperature of this process is 74.26 °C. The hot utility required is 138.48 MW, and the cold utility required is 139.90 MW. It is assumed

that the heat duty of the heat exchanger at the sink side is fixed at 20.86 MW. The pressure differences of the heat exchangers at the source side are set at 50 kPa, and at the sink, the side is set 0 kPa. The setting range of independent variables and optimisation results of a 4-column double-effect methanol distillation with an integrated HP are shown in Table 6. Finally, for a more intuitive display of the results, the GCC of a 4-column double-effect methanol distillation process integrated with different types of HPs is given, as shown in Figure 15. As can be seen from Table 6, the HPs can save 15 % of the hot utility by improving the waste heat quality of the process. The ranking of the HP COPs is VCHP > JCHP-CO_2 > JCHP-Ar > TCHP when integrating with this process. The reason can be seen in Figure 15 and is related to the observation that the ΔTin between source and sink is small, while the ΔTout is too significant. The slopes of source and sink are both steep in the GCC.

Table 6. Variable settings and optimisation results of a methanol distillation with an integrated heat pump.

	Variable Ranges			Optimisation Results					
	[1] P_2, MPa	[2] P_5, MPa	[3] T_5, °C	COP, -	Q_{source}, MW	W, MW	P_2, MPa	P_5, MPa	[4] R, -
JCHP-Ar	4-8	1-5	--	3.23	14.40	6.46	5.49	3.50	1.59
JCHP-CO_2	4-9	1-4	--	4.02	15.03	5.19	4.92	2.55	1.97
VCHP	2.5-8	0.2-3	--	5.67	17.18	3.64	5.28	2.40	2.24
TCHP	20-30	--	-10-25	1.50	7.09	13.92	25.71	6.07	4.27

[1] P2: The outlet pressure of the compressor in the HP cycle, MPa. [2] P5: The outlet pressure of the expander or expansion valve in the HP cycle, MPa. [3] T5: The outlet temperature of the expansion valve in the HP cycle, MPa. [4] R: The compression ratio of the compressor.

The ΔT between the inlet and outlet of the working fluid in JCHP changes significantly in the heat exchange with both the source and the sink. The slope of the working fluid is relatively large in the GCC, as shown in Figure 15a,b. For the VCHP, in the heat exchange with the source and the sink, the ΔT between the inlet and outlet of the working fluid in VCHP change very little. The slope of the working fluid is small in the GCC - see Figure 15c. The TCHP shows a different behaviour due to the transcritical nature of the heat release part. The slope of the working fluid is small in the heat exchange with the source in the GCC, while the slope of the working fluid is steep in the heat exchange with the sink in the GCC, as shown in Figure 15d.

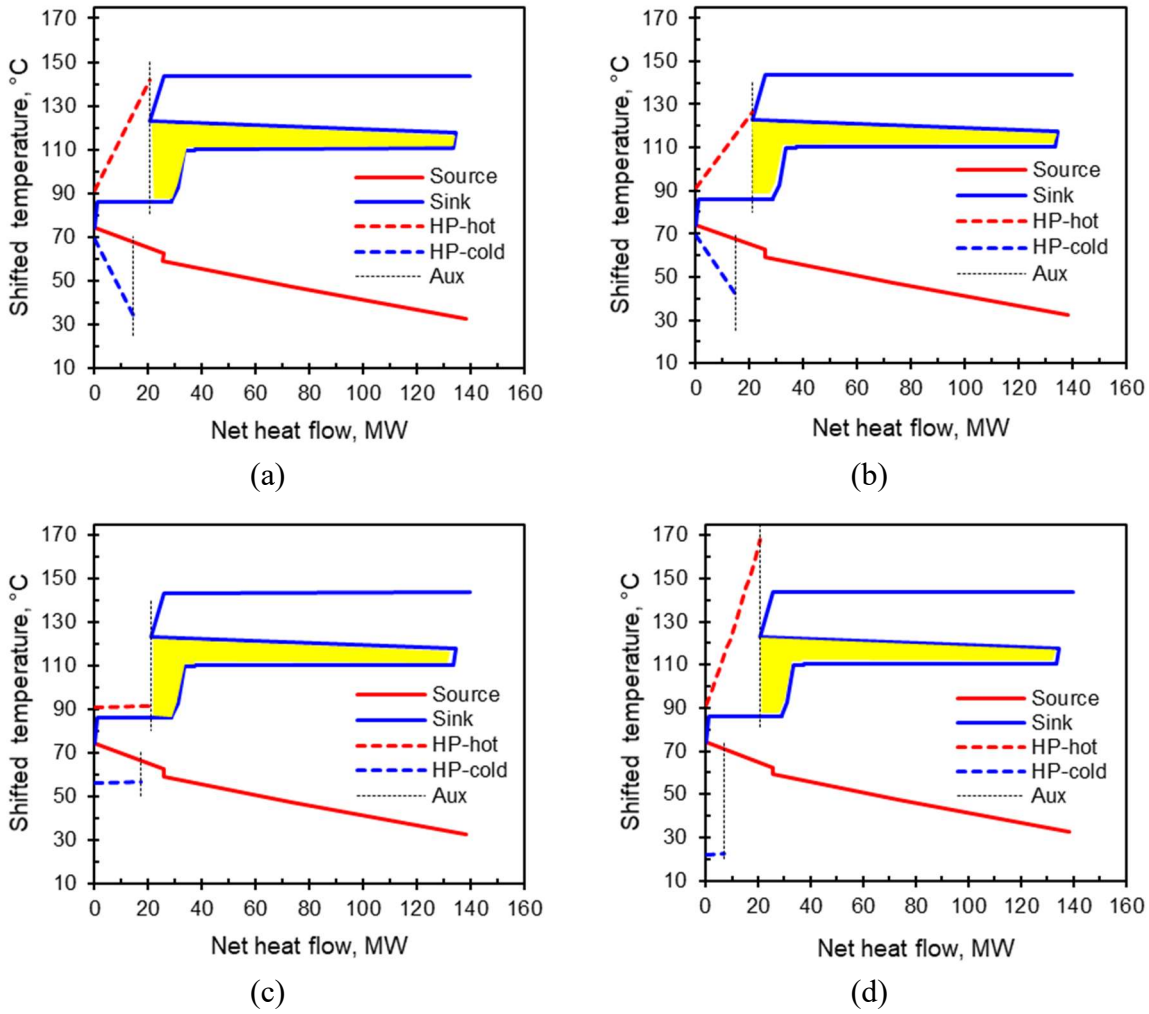

Figure 15. GCC of case 4 and integration options using (a) JCHP-Ar, (b) JCHP-CO2, (c) VCHP and (d) TCHP.

In this case, the average ΔT between working fluid and source/sink in VCHP is small, so the energy loss of the heat exchangers is lower, the heat exchange efficiency is higher, and COP is affected positively. Although the average ΔT between working fluid and source/sink in JCHP and TCHP is massive, and thus the energy loss is higher, the heat exchange efficiency is smaller, and this affects the COP negatively. The performance of the JCHP and the TCHP are both weak. In addition, the outlet pressure of the compressor in TCHP is too high (25.71 MPa). This means high-pressure requirements for equipment of TCHP, with high equipment investment cost. The TCHP economy is likely to be poor. This process is more suitable for heat integration with VCHP, which is consistent with the conclusion of Section 3.3.

For the optimal COP of JCHP, the reason for the large ΔT between the working fluid and the source/sink after heat exchange can be seen in Figure 16. The figure shows the

relationship between power consumption and COP of JCHP with compression ratio. In the JCHP, the heat load of the sink-side heat exchanger Q_h and the outlet pressure of the expander are fixed. By changing the outlet pressure of the compressor, a series of work required by the compressor, work produced by the expander and COP are obtained. It can be seen from Eq (1) that the COP is inversely proportional to the power consumption of the HP when Q_h is constant.

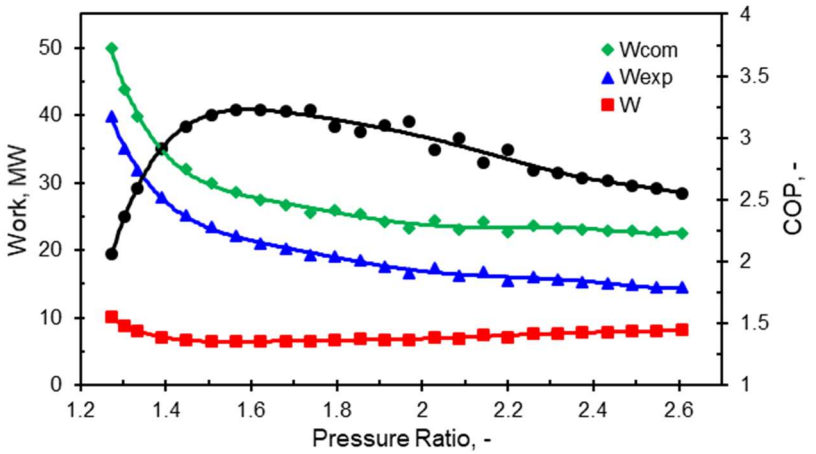

Figure 16. The relationship between power consumption and COP of JCHP with a compression ratio

As can be seen from Figure 16, with the increase of the compression ratio of the compressor (the increase of the outlet pressure of the compressor compared to inlet pressure), the power consumption of the JCHP first decreases and then increases. The COP of JCHP increases first and then decreases with the increase of compressor compression ratio. That is, there is an optimal pressure for the optimal COP of the JCHP. When the outlet pressure of the compressor is lower than the optimal pressure, although the outlet temperature of the compressor decreases (the inlet temperature of the working fluid exchanging heat with the source decreases and the temperature difference decreases), the COP of JCHP is not optimal. The same is true for the sink side.

3.4.2 Evaluation

The results of the Heat Integration of the four industrial processes with HPs are compared. They are summarised in Table 7.

For the processes with steep source and sink slopes, such as the spray drying process of the milk powder in a dairy factory in Case Study 1, the average ΔT of working fluid and source/sink in JCHP is small, resulting in a small energy loss and high heat exchange efficiency.

The COP of JCHP is large, so it is appropriate to choose the JCHP.

When the source and sink slope of the process is gentle or (nearly) flat, for example, as in the dairy product processing of Case Study 2 and the candy processing and packaging in Case Study 3, the VCHP is most suitable because the average temperature difference is small between the working fluid and source/sink, the energy loss is small resulting in high thermal efficiency and high COP values. In Case Study 2, the ΔT_{in} is as low as 1.5°C, and the COP of VCHP is as high as 13.07.

Table 7. Results of different industrial processes integrated with heat pumps.

Name		Unit	Case 1: Milk Spray Drying Process	Case 2: Dairy product process	Case 3: Candy processing and packaging	Case 4: Methanol distillation
GCC	T_{min}	°C	10	2	15.5	32.5
	T_{Pinch}	°C	65	66.9	19.5	74.26
	T_{max}	°C	210	100	127.5	143.68
	Utility-cold	MW	5.36	0.94	0.33	138.48
	Utility-hot	MW	17.66	2.34	1.82	139.90
Source	$T_{source-in}$	°C	40.7	66.9	19.5	74.26
	$T_{source-out}$	°C	10	66.9	15.5	67
Sink	$T_{sink-in}$	°C	65	68.4	46.5	86.1
	$T_{sink-out}$	°C	--	68.4	49.5	86.1
Duty	Q_{source}	MW	5.36	0.71	0.33	--
	Q_{sink}	MW	--	--	--	20.86
COP	JCHP-Ar	-	2.83	3.89	2.81	3.23
	JCHP-CO_2	-	2.93	4.52	3.55	4.02
	VCHP	-	1.85	13.07	4.44	5.67
	TCHP	-	1.77	1.68	1.85	1.50

From Case Study 2 to Case Study 3, the ΔT_{in} increased from 1.5 °C to 11.84 °C, and the COP of the VCHP decreased from 13.07 to 4.44. Therefore, the smaller the ΔT_{in} between source and sink is, the larger is the COP of the VCHP. The COP of the VCHP decreased rapidly with the increase of ΔT_{in} between source and sink. However, the COP of JCHP decreased less with the increase of ΔT_{in} between source and sink.

The application scope of the TCHP is limited. The TCHP is more appropriate for a process with a relatively gentle source slope and a relatively steep sink slope. The best process is one in which the inlet temperature of the source is less than or equal to 20 °C, and the ΔT_{in} between the source and sink is less than 10 °C.

3.5 Conclusions

Several main types of HPs have been critically analysed for obtaining rules and criteria on appropriate HP selection for various process configurations. In addition to the relatively recent JCHP, other HP types are in use and have been industrialised, including the VCHP and TCHP types. This chapter performs a comparative evaluation of the performance of the Heat Integration scenarios of different HP types (VCHP, TCHP and JCHP) and processes by applying the Petro-SIM process simulator and Pinch Analysis.

An answer is provided to the question of which type of HP is most suitable for a specific process. The results show that for processes with larger source and sink slopes on the T–H plot, the COP of JCHP is higher, and JCHP is more suitable. For processes with a relatively smaller and medium slope of the source and sink T–H profiles, the COP of VCHP is relatively large, and VCHP is more suitable. The scope of application of TCHP is small.

For processes with a relatively low source T-H slope and a relatively large sink T-H slope, the COP of TCHP is more substantial, and it is appropriate to select it. Because the critical temperature of CO_2 is 31.26 °C, the added constraint in this context is a process for which the source inlet temperature is lower than 20 °C, the sink temperature requires more than 40 °C, and the ΔT_{in} between the source and the sink is less than 10 °C.

By improving the waste heat quality of the process, the HPs can save 15 to 78 % of the hot utility. The smaller the ΔT_{in} between source and sink is, the larger is the COP of the VCHP. The ΔT_{in} increased from 1.5 °C to 11.84 °C, and the COP of the VCHP decreased from 13.07 to 4.44. The COP of the VCHP decreased rapidly with the increase of ΔT_{in} between source and sink. However, the COP of JCHP decreased less with the increase of ΔT_{in} between source and sink.

It is shown that if an inappropriate HP is selected to integrate with the process, the COP of the HP will decline, which may lead to an increase in investment and a decrease in the economy of the HP. In extreme cases, the differences between the most and the least suitable integration mappings can be of the order of 100 % and up to tenfold. This shows the importance of performing such an analysis and making the correct choice of an HP.

For the different scenarios of Heat Integration with HPs, this study can provide guidance and suggestions for the selection of HPs, enabling a quick selection of the appropriate HPs. A simplifying assumption for the current work is the use of the COP of the HP—process

combinations as the performance criterion, land considering the investment cost of HPs only qualitatively. The full analysis, relaxing this assumption and considering the investment and analysis of the economy is planned for future work. Future research will be targeted to find the balance between the COP and the economy of the HP application.

CHAPTER 4 TOTAL SITE MASS INTEGRATION WITH MULTIPLE-LEVEL FRESH RESOURCES AND INTERMEDIATE PURITY HEADERS

The work presented in this chapter is based on two papers by the author. One paper is published in International Journal of Hydrogen Energy entitled "Total Site Hydrogen Integration with fresh hydrogen of multiple quality and waste hydrogen recovery in refineries", as clarified on Page VI (Contributing publications). The author of this thesis is the first and corresponding author of this publication. The other contributing co-authors were the thesis supervisor (Varbanov, P.S.), co-supervisors (Klemeš, J.J. and Fan, Y.V.) and collaborator (Nižetić, S.). The other one is going to be published in Sustainable Production and Consumption entitled "Collaborative Total Site Mass Integration with Multiple-level Fresh Resources and Intermediate Purity Headers". The author of this thesis is the first and corresponding author of this publication. The other contributing co-authors were the thesis supervisor (Varbanov, P.S.), co-supervisors (Klemeš, J.J. and Fan, Y.V.) and collaborator (Wan Alwi, S.R.). My original contributions are listed in the introduction.

4.1 Introduction

Mass Integration (El-Halwagi and Manousiouthakis, 1989) has been widely used to design and obtain optimal targets for various resource conservation networks (Foo, 2012). Integration and optimisation of mass exchange networks are significant for reducing fresh resource consumption, waste discharge and production cost of industry (Gai et al., 2021b). The most common mass integrations are including water minimisation (Wang and Smith, 1994) and refinery hydrogen network problems (Towler et al., 1996).

The development of mass Pinch Analysis provides an important theoretical and practical basis for mass exchange network optimisation. It mainly includes the Material Recycle Pinch Diagram (MRPD) (El-Halwagi et al., 2003), Material Surplus Diagram (Alves and Towler, 2002), Average Pressure Profiles (Ding et al., 2011) and Material Surplus Composite Curve (Saw et al., 2011). Pinch Analysis has been widely applied in the integration of the intra-plant mass exchange network. The bottleneck of the mass exchange network is analysed starting from the utilisation of fresh resources. In addition to Pinch Analysis, mathematical programming is another method widely presented and used in mass exchange network optimisation, e.g. MILP considering gas pressure constraints (Hallale and Liu, 2001), superstructure models with intermediate purity headers (Deng et al., 2014) and hydrogen turbine (Liu et al., 2020).

Mass Integration has been extended from the intra-plant level to Total Site Integration of inter-plant mass exchange networks (Han et al., 2020), which has attracted more and more attention. There are multiple fresh resources with various quality levels (Yang et al., 2019), sometimes in Mass Integration. In order to reduce the consumption of expensive higher quality fresh resources, cheaper and lower quality fresh resources should be preferred (Li et al., 2017). A targeting method for multiple impure freshwater sources (Foo, 2009) is proposed in intra-plant water network synthesis. However, most current Pinch Analysis only considered fresh resources with single quality, not multiple quality levels.

Furthermore, intermediate headers can be used to simplify the network configuration and enhance the controllability of the mass exchange networks. Some studies have extended the scope to the Total Site Mass Integration for inter-plant mass exchange network. A Mixed-Integer Non-Linear Programming (MINLP) based on the superstructure is presented in an inter-plant water network considering multiple-contaminant and water headers (both central and decentralised) (Chen et al., 2010). Fadzil et al. proposed the concepts of one-way centralised water header (Fadzil et al., 2018) and two-way centralised water header (Ahmad Fadzil et al., 2018) for Total Site Water Integration in the inter-plant water network. However, the intermediate headers are fixed to two in this method. Chin et al. (2021b) proposed an extended Material Recovery Pinch Diagram to targeting the material headers with minimum fresh resource consumption for the Total Site Material Recycling Network. However, in this study, an only single quality fresh resource is considered.

Hydrogen Integration realises hydrogen cascade utilisation to reduce hydrogen consumption by analysing the bottleneck of a hydrogen network. However, there is still a large amount of waste hydrogen discharge in refineries, which is mostly burned as fuel (Jia and Zhang, 2011), leading to the waste of resources. Hydrogen Integration considering waste hydrogen purification has been proposed, including graphical-based (Zhang et al., 2016) and mathematical programming (Lou et al., 2019) methods. However, these studies assume the regenerated hydrogen purity after purification. The performance changes and techno-economy of the purification unit were not considered.

In summary, (i) few studies have proposed a Total Site Mass Integration method based on Pinch Analysis for inter-plant mass exchange network with a multiple-level fresh resources. (ii) In most of the current studies, the number and purity of intermediate headers are usually fixed at one or two without optimisation in a mass exchange network. The purity location

(number and connection) and purity of intermediate headers need to be further considered and optimised in Total Site Mass Integration with multiple-level fresh resources. (iii) Waste regeneration is optimised with a techno-economic objective to reduce fresh resource consumption of Total Site Mass Integration further, considering the comparison of various purification technologies.

This study aims to develop an extended Pinch Analysis for Total Site Mass Integration with multiple-level fresh resources and intermediate headers. Multiple-level fresh resources with various purity levels are considered to minimise the consumption of high-cost fresh resources at a higher quality. Intermediate headers are also considered for simplifying the configuration and enhance the expandability and flexibility of mass exchange networks. Waste materials after Total Site Integration is further regenerated. A novel method combining the extended Pinch Analysis and waste recovery is proposed. Various waste purification options are considered for the waste regeneration after Total Site Integration to further increase waste recovery. The technical feasibility and economy of the various purification approaches are considered. The presented method is demonstrated with case studies of the integration of the the hydrogen networks and the integration of water allocation networks. The novel contributions of this chapter include:

I. Consideration of several fresh resources of various quality levels instead of a single source of a fresh resource.
II. The number, connection and purity of intermediate headers in mass exchange networks are investigated.
III. Maximisation of the use of low-quality waste in intra-plant integration with the fresh resource to prioritise the transfer of higher-quality waste for Total Site Integration.
IV. Maximum total annual economic profit of the identified mass integrated designs, considering various purification options and their purification capabilities.

4.2 An Introduced Novel Methods

Section 4.2.1 introduces the overall framework of the proposed multiple-level fresh resources Total Site Mass Integration with intermediate headers and waste recovery. The extended multiple-level fresh resources Pinch Analysis (PA-MLFR) for intra-plant integration and Total Site Mass Integration is introduced in Section 4.2.2. Section 4.2.3 introduces the optimisation procedure to identify a cost-effective and practical (technical feasibility) design

of the waste purification and regeneration process. The developed multiple-level fresh resources Pinch Analysis with intermediate headers (PA-MLFR-IH) for intra-plant integration and Total Site Mass Integration is introduced in Section 4.2.4.

4.2.1 Overall Integration Procedure of Total Site Mass Integration

This study developed a method combining multiple-level fresh resources Pinch Analysis with intermediate headers and waste regeneration to reduce the fresh resource usage and waste discharge. The method is extended to the Total Site level, considering fresh resources of various quality levels. The detailed procedure of the proposed multiple-level fresh resources Total Site Mass Integration with intermediate headers and waste recovery is shown in Figure 17.

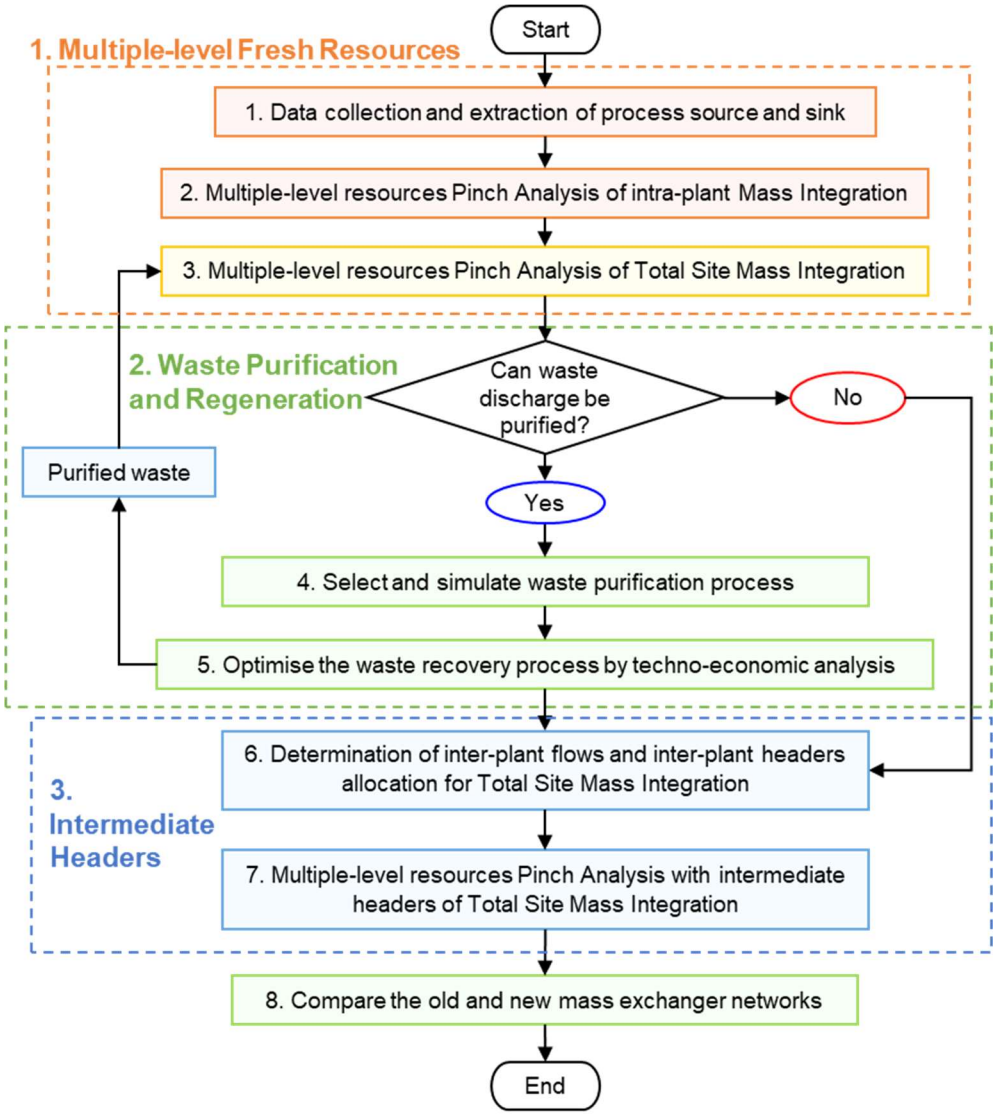

Figure 17. The procedure of the proposed multiple-level fresh resources Total Site Mass Integration with intermediate headers and waste recovery

The procedure is performed for three main contexts: multiple-level fresh resources at process-level and Total Site level, waste purification and regeneration, and intermediate headers at process-level and Total Site level.

1) Multiple-level fresh resources
   a. Mass Integration is performed on the intra-plant mass exchange networks with fresh resources at different quality levels. Please refer to the procedure of steps 1-2 in Figure 17. Refer to Section 4.2.2 (I) for detailed steps.
   b. Total Site Mass Integration is implemented to use inter-plant mass exchange networks as a degree of freedom in minimising fresh resources and waste discharge, i.e. the procedure of step 3 in Figure 17. Refer to Section 4.2.2 (II) for detailed steps.

      The potential of waste recovery can be further explored by Total Site Integration of inter-plant mass exchange network after intra-plant Mass Integration. The integration of inter-plant mass exchange network is referred to as Total Site Mass Integration, and the proposed concept is shown in Figure 18. High-quality waste discharged from some plants can be provided to other plants for further use, thus reducing both waste emission and fresh resource consumption.

2) Waste purification and regeneration after the Total Site Mass Integration is regenerated to enhance the purity for further recovery, i.e. the procedure of steps 4-5 in Figure 17. Refer to Section 4.2.3 for detailed steps.

There is still waste discharge after Total Site Mass Integration. A Total Site Mass Integration with multiple-level fresh resources and waste regeneration is proposed in this study, as shown in Figure 18. Various waste reuse/recycling and regeneration schemes may be implemented to reduce waste discharge, as shown in the light green box in Figure 18. The waste regeneration process is selected and designed by techno-economic analysis considering the advantages and application range of different purification technologies.

The waste purification process is optimised, taking total annual profit as objective. For example, waste hydrogen can be enriched to high-quality hydrogen for reuse by the waste hydrogen purification process. The hydrogen concentration of less than 30 % is not considered due to economic infeasibility. The purified hydrogen is returned to the inter-plant hydrogen network, further reducing fresh hydrogen consumption in refineries.

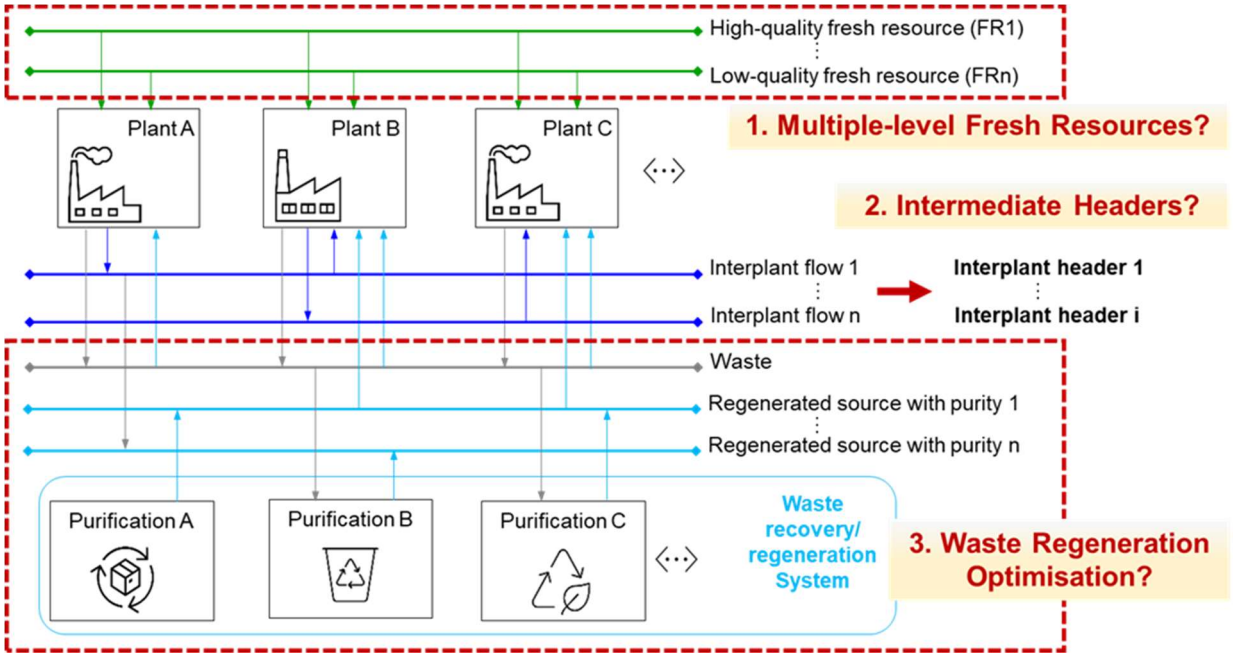

Figure 18. Multiple-level fresh resources Total Site Mass Integration with intermediate headers and waste recovery

3) Intermediate purity headers
   a. After waste purification and regeneration, the Pinch Analysis method of multiple-level fresh resources and intermediate headers and waste recovery for intra-plant Mass Integration is performed. Please refer to the procedure of step 6 in Figure 17. Refer to Section 4.2.4 (I) for detailed steps.
   b. Pinch analysis of multiple-level fresh resources and intermediate headers for Total Site Mass Integration with waste recovery is performed. Please refer to the procedure of step 7 in Figure 17. Refer to Section 4.2.4 (II) for detailed steps.
4) The final optimisation scheme is analysed and compared, i.e. the procedure of step 8 in Figure 17.

The final optimisation solution of Total Site Mass Integration with multiple-level fresh resources and waste regeneration is analysed and compared to the intra-plant Mass Integration.

4.2.2 Multiple-level Fresh Resources Pinch Analysis (PA-MLFR)

Multiple-level fresh resources Pinch Analysis (PA-MLFR) is extended at both intra-plant level and Total Site Integration of inter-plant mass exchange networks.

I. Multiple-level Fresh Resources Pinch Analysis of Intra-Plant Mass Integration – Plant Alone

In a mass exchange network, there are many impurities in material sources. Most impurities are no maximum purity, but some sensitive impurities do have very strict limits. For these special sensitive impurities, there are usually pre-treatment units in refineries, e.g. desulfurization units. Sources are supplied to sinks after the pre-treatment units, and all impurities can be considered as "inert impurities". The multiple-contaminant mass integration is simplified to a single impurity in this study. The characteristics of sources and sinks in a multiple-level fresh resources mass exchange network with a single impurity can be represented on the impurity load versus flowrate diagram as previously introduced by (Wan Alwi and Manan, 2007) for Water Pinch Analysis. The fresh resources (FR) are sorted by concentration from high to low: FR1 (highest-quality fresh resource) > FR2 > … > FRn (lowest-quality fresh resource). The principle of priority utilisation of the low-quality fresh resource is followed. If a low-quality fresh resource cannot meet the requirements, then use a high-quality fresh resource. This is because the lower-quality fresh resource is generally easier to obtain and cheaper. Therefore, the order of utilisation of fresh resources is FRn, FRn-1, ..., FR2, FR1. The sinks higher than low-quality fresh resource can only use a high-quality fresh resource to meet, so the performed order of the Pinch points is FR1, FR2, ..., FRn.

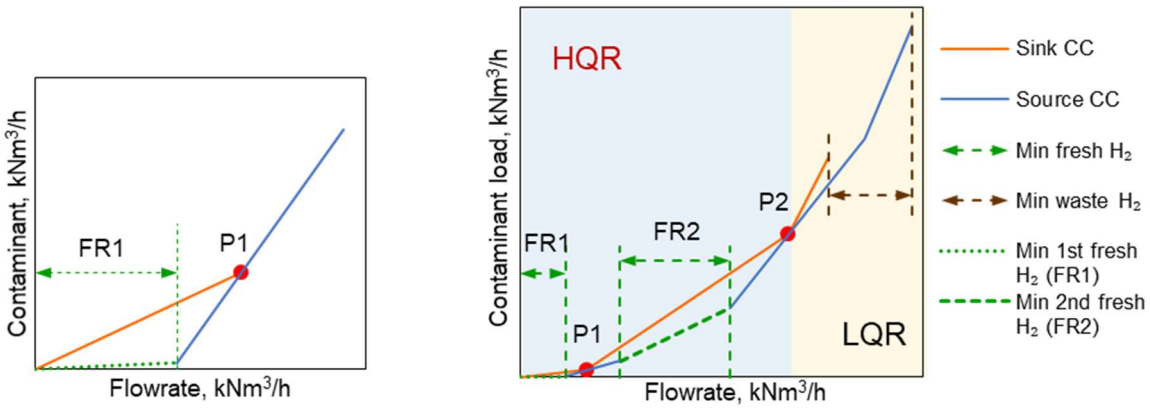

(a) High-Quality Pinch determination (b) Low-Quality Pinch determination

Figure 19. Multiple-level fresh resources Pinch Analysis of intra-plant Mass Integration

The detailed steps of multiple-level fresh resources Pinch Analysis are as follows:

1) Pinch Analysis is performed on the sources and sinks with a concentration higher than FR2 as it can be only fulfilled by FR1. The minimum requirement of the highest-quality fresh resource FR1 is determined, forming the First Pinch Point, denoted as the Highest-Quality Pinch Point (P1) (Figure 19a).

2) The sources and sinks with a concentration higher than FR3 and lower than FR2 are added (stacked) for Pinch Analysis to determine the minimum requirement of secondary-quality fresh reource FR2 forming the Second Pinch Point (P2) (Figure 19b). This sequencing (Step 1 → Step 2) with the formation of two Pinch Points could ensure the FR2 being utilised as much as possible before utilising FR1, which has a higher quality and value.
3) The rest can be done in the same manner. Finally, sources and sinks with a concentration no higher than FRn are stacked for Pinch Analysis to determine the minimum lowest-quality fresh resource (FRn) and Lowest-Quality Pinch (Pn).

Figure 19 shows the construction of mass integration curves for a problem having two fresh resources with different quality by Pinch Analysis (El-Halwagi et al., 2003). The light-blue curve is the Source Composite Curve (CC), and the orange curve is the Sink Composite Curve (CC). The slope of the line (Contaminant load/ Flowrate) represents the impurity of the stream. All sources and sinks located to the left of the lowest-quality Pinch (Pn) are called the High-Quality Region (HQR), as shown on the light blue background in Figure 19b. All sources and sinks located to the right of the lowest-quality Pinch (Pn) are called the Low-Quality Region (LQR), as shown on the light-yellow background in Figure 19b.

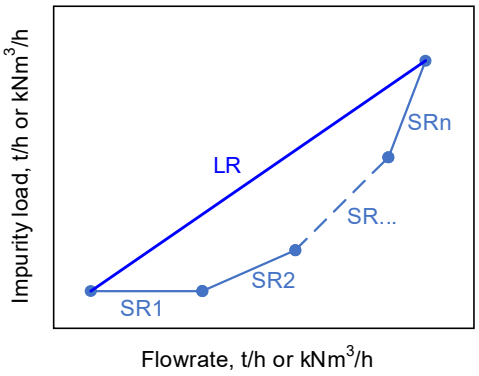

Figure 20. Triangle rule for Pinch Analysis in Mass Integration

In Pinch Analysis, both the source and sink can be represented by a straight line. The corresponding x-axis coordinate length of a line represents quantity, and the corresponding y-axis coordinate length represents quality. For example, in heat integration, the x-axis represents heat, and the y-axis represents temperature. In mass integration, the x-axis length of a line represents the flowrate of the stream, the y-axis length represents the impurity flowrate, and the line slope represents the purity of the stream. In Pinch Analysis of mass integration, each

mass source and sink can move horizontally or vertically without changing physical properties. Different sources (or sinks) are connected head to tail, and the line formed by the connection represents the mixed source (or sink). As shown in Figure 20, the line LR formed by connecting sources SR1 - SRn from the starting point to the end is formed the mixed source LR. Where the flowrate of mixed source LR is the sum of the flowrate of all sources, that is, the length of the corresponding x-axis. The impurity load of mixed source LR is the sum of the impurity load of all sources, that is, the corresponding Y-axis length. The slope of line LR represents the purity of the mixing source. The same goes for process sinks. This is the triangle rule for Pinch Analysis in Mass Integration.

II. Multiple-level Fresh Resources Pinch Analysis of Total Site Mass Integration

Total Site Mass Integration follows a similar principle as intra-plant Mass Integration with the multiple-level fresh resources (Section 4.2.2 (I)). However, a different procedure has to be used. The reason is that within each individual plant of the site, using the procedure from Section 4.2.2 (I) directly would result in extracting for site-level integration only the poorest-quality source. The higher-quality source is used internally by sinks. That procedure needs an amendment for the cases when the placement of the sources and sinks can be exchanged within each plant. It would be preferable to use a lower-quality source inside the plants in order to extract a higher quality source for site-level integration. This would make the site-level integration more efficient and will result in minimising fresh resource use at the site level.

The modified procedure starts with Intra-Process Integration. It has three major steps. Step 1 aims to provide the lower bound - the minimum fresh resource usage and waste discharge - that the integration can achieve. This approach has been previously performed by (Chew et al., 2010a) for Total Site Water Integration with a single fresh resource in identifying the targets for further design tuning. The target identified in Step 1 is deemed as the ideal target (lower bound), representing the aim to be achieved by the integration. However, in most cases, the integration design/allocation suggested in Step 1 would not be feasible, as it does not consider the intra-plant integration before Total Site Mass Integration. A large number of inter-plant integration options may incur an unnecessary cost (e.g. for infrastructure and safety of longer piping). By setting the identified targets in Step 1 as an ideal goal, Step 2 and Step 3 are performed to minimise the need for inter-plant integration and integrate only the valuable streams. Step 3 is used to calculate the flowrate of inter-plant streams. The final identified solution of Total Site Mass Integration is achieved after the completion of Step 3.

The specific steps of Total Site Mass Integration with the multiple-level fresh resources are described below, supported by Figure 21 and Figure 22 for illustration. Figure 21 and Figure 22 represent two different scenarios with different sets of sources and sinks, where step 2c is not required to perform for the scenario presented in Figure 22.

Step 1: Identify the ideal target value (lower bound of fresh resource use and waste discharge) for Total Site Mass Integration with a minimum requirement of fresh resources and minimum waste discharge. The identified targets in this step represent only a goal that cannot be exceeded.

i. All sources and sinks are included in the Composite Curves using the multiple-level fresh resources Pinch Analysis in Section 2.1, as shown in Figure 21a and Figure 22a. The length of the green dotted double-headed arrow represents the minimum flowrate of Fresh resource 1 (FR1) and Fresh resource 2 (FR2), and the grey dotted line represents the minimum waste flowrate.
ii. This targeting step produces the estimates for minimum fresh resources supply that cannot be improved upon and, in some cases, may be achieved.

Step 2: Identify inter-plant streams by revising the waste discharge to meet the ideal target in Step 1. Maximise the use of lower-quality sources at the plant level to substitute higher-quality sources and to export those higher-quality sources to the site level.

a) Intra-Plant Integration
   i. Multiple-level fresh resources Pinch Analysis is used to determine the minimum requirement of fresh resource and minimum waste discharge within each plant, as shown in Figure 21bc and Figure 22bc.
   ii. All the source streams above the Lowest-Quality Pinch-causing source of each intra-plant integration are shifted in parallel to the line of Lowest-Quality Pinch-causing sources (red dotted arrow in Figure 21b,c and Figure 22b,c) until the shifted Source Curve meets the Sink Curve, as shown in Figure 21de and Figure 22de.
   iii. Step 2a identifies the initial approximation of the minimum amount of fresh resource for Total Site Integration or combustion. In general, it could not guarantee that the identified waste source for utilisation in another plant combustion is of a higher quality. For example, by referring to Figure 21b, the quality of R12 and R13 source is sufficient to fulfil the purity requirement of sink K13. Maximising the use of waste at a lower quality (R12 and R13) inside the plant and transferring the waste at a higher quality (e.g., R11) to the site level can potentially maximise the use of

waste discharge. Step 2b is performed for this purpose.

b) Maximise the use of low-quality sources above the lowest-quality Pinch in intra-plant integration to transfer the higher-quality source for Total Site Mass Integration.
   i. Determine the limit data in Total Site Mass Integration. These sources and sinks data are extracted from the streams of high-quality regional (all streams in the light-blue area in Figure 21d,e and Figure 22d,e) and the waste discharge from low-quality regional (all the streams represented by the grey dotted lines in Figure 21d,e and Figure 22d,e) of each intra-plant integration. These sources and sinks are integrated with multiple-level fresh resources to obtain the minimum requirement of fresh resource and minimum waste discharge in this case, as shown in Figure 21f and Figure 22f.
   ii. If the identified target value (a requirement for fresh resource and waste discharge) in Step 2b is equal to the target identified in Step 1, as shown in Figure 22, it means that the ideal goal can be achieved. In this case, Step 2c becomes unnecessary and is omitted.
   iii. Otherwise, the identified target in Step 2b is higher than Step 1. It means that the ideal target cannot be met by using the current waste discharge. Waste discharge needs to be further adjusted to meet the ideal target of Step 1 and minimise inter-plant stream exchanges, making it necessary to perform Step 2c.

c) Further, revise the waste discharge by inter-plant flow, as shown in (Figure 21).
   i. If the Lowest-Quality Pinch of an intra-plant integration in Step 2b is higher than the Lowest-Quality Pinch of Step 1 (R11), then this Higher-Quality Pinch-causing source (R22, blue line) above the Pinch is used as higher-quality waste discharge (W2 of Figure 21h) for Total Site Mass Integration.
   ii. Additional source is required to supplement the insufficient flowrate of higher-quality Pinch-causing source stream (R22) in this intra-plant integration. The source stream of the Lowest-Quality Pinch of Step 1 (R11, solid grey line in Figure 21a) is used as the additional/ supplement source (R11, Figure 21h). It should not be greater than the distribution flowrate of higher-quality waste discharge (W2 of Figure 21d). The waste discharge in Step 2b is revised to further increase the higher-quality waste discharge by the inside plant flow.

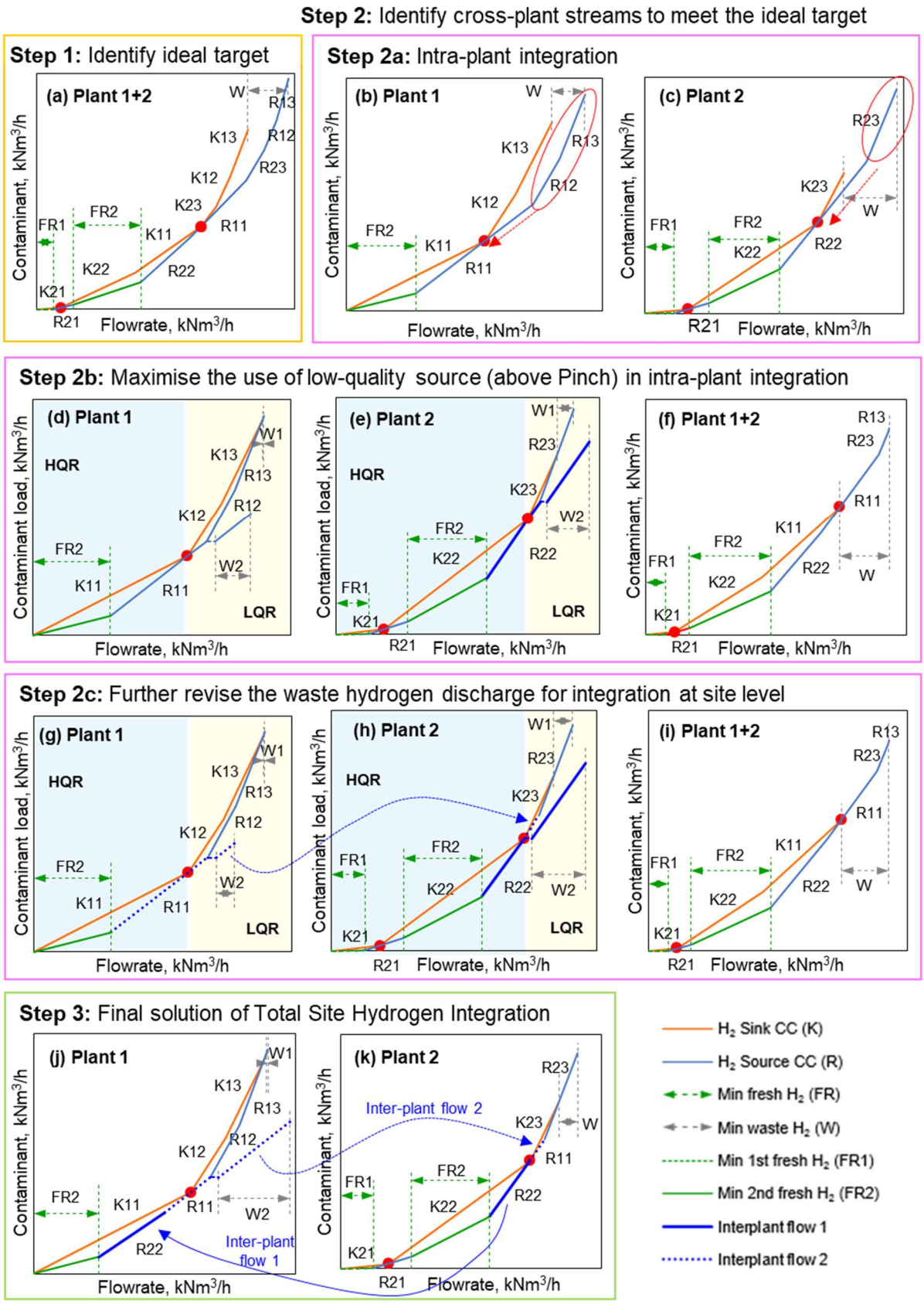

Figure 21. Pinch Analysis targeting steps for TSI with multiple-level fresh resources (Scenario 1.1)

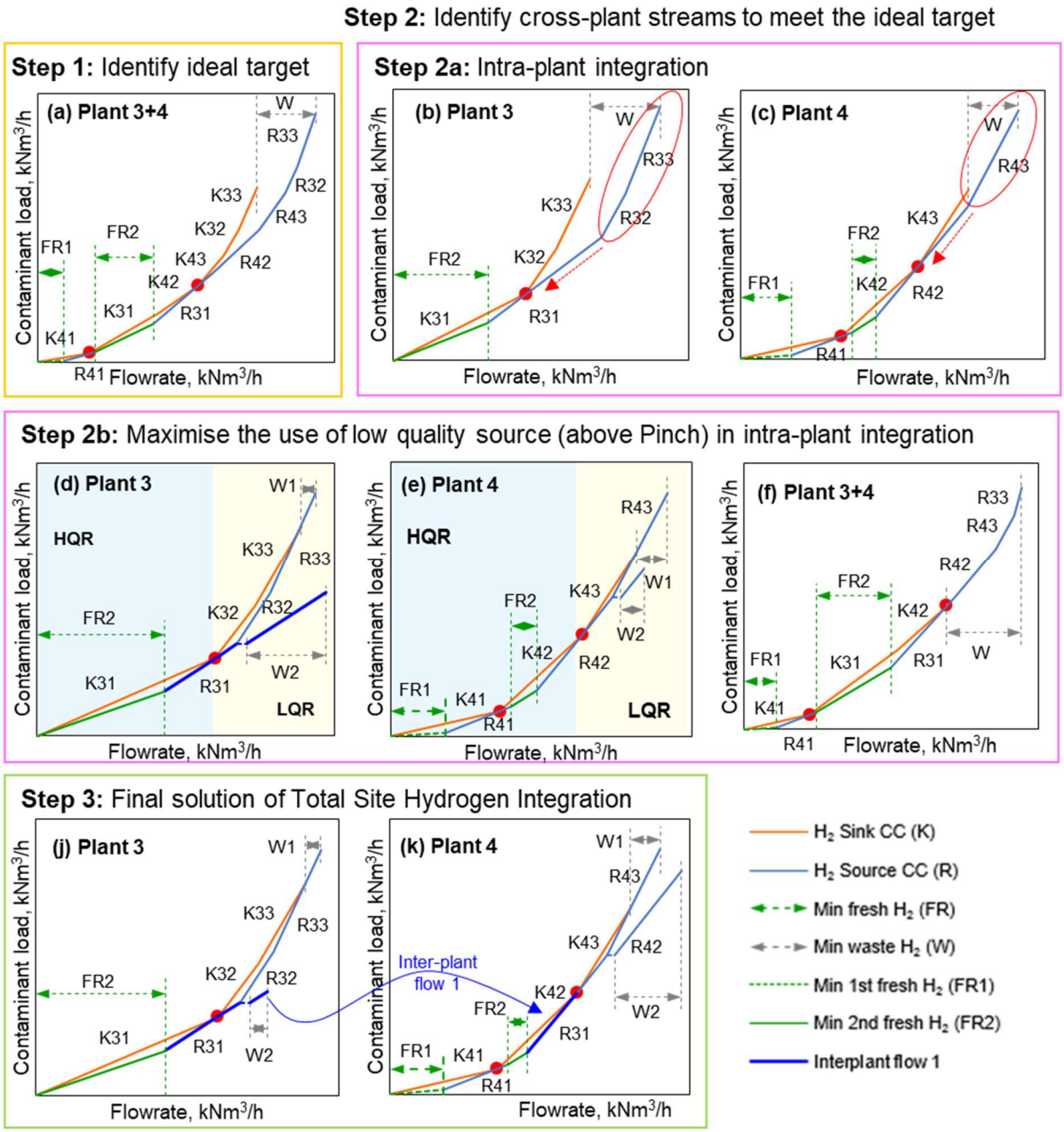

Figure 22. Pinch Analysis targeting steps for TSI with multiple-level fresh resources (Scenario 1.2)

iii. Multiple-level fresh resources integration is performed to determine the minimum flowrate target by extracting the streams of HQR (all streams on light blue background in Figure 21gh) and the waste discharge from LQR (all sources represented by a grey dotted line in Figure 21gh) of each intra-plant integration, as shown in Figure 21i. If the revised target value in this case (Step 2c) is the same as the ideal target in Step 1, then the next step can be taken to Step 3. Otherwise, continue to Step 2c until both targets are the same.

Step 3: The final solution (Figure 21jk and Figure 22jk) is achieved by minimum inter-plant flow allocation - identify the Total Site Mass Integration (both outside and inside plant design) with a minimum requirement of fresh resource and minimum inside plant flow.

i. All waste streams in LQR (light-yellow background) are potential streams to exchange between the plants. The identified higher-quality waste discharge (W2, Figure 21 and Figure 22) in Step 2 is further assessed to determine the interplant flow.
ii. Identify the distribution of inter-plant flow. The interplant flow (e.g. from Plant 1 to Plant 2 or Plant 2 to Plant 1) is determined by the lowest-quality Pinch (Pn), where the plant with a higher Pn will transfer the waste discharge (e.g. W1 or W2) to the plant with a lower Pn. For example, the residual source W2 (R31) in Plant 3 (Figure 22d) will be transferred to Plant 4 (Figure 22e) as the Pn of Plant 3 is higher. This could reduce the requirement for fresh resources in Plant 4. W2 would be given a higher priority than W1 in allocating across the plant.
iii. Sources W1 and W2, remaining after the Total Site Integration, will be transferred to the processing facilities (purification or disposal by combustion).

The above procedure obtains the final result of Total Site Mass Integration with a multi-fresh resource. This has to be done by both curves and quantitatively on some examples. The described procedure is demonstrated in Section 4.2. This method is suitable for two or more fresh resources (multiple-level fresh sources), although two fresh resources are taken as examples (Figure 21 and Figure 22).

4.2.3 Optimisation of Waste Purification and Regeneration Process

This section takes the optimisation of waste hydrogen purification and regeneration process purification as an example to demonstrate. The waste hydrogen remaining after the Total Site Mass Integration (Section 4.2.2 (II)) is necessary to purify and regenerate, to reuse waste hydrogen. It can further reduce the waste hydrogen discharge and fresh hydrogen consumption if the low-concentration waste hydrogen is purified into a high-concentration hydrogen source that can be utilised by a hydrogen sink. The purification techniques of waste hydrogen mainly include cryogenic (Aasadnia et al., 2021), PSA (Zhang et al., 2021), and membrane separation (Li et al., 2015). Different hydrogen purification technologies have different performance properties (e.g. operating conditions, separation efficiency and investment cost) due to the different separation principles. The purification performance and

efficiency will also change for the same purification technology when the operating conditions of waste hydrogen feed are changed. It is necessary to design and optimise the purification process of waste hydrogen. Various processes of waste hydrogen purification can be simulated using a process simulator. In the current work, Aspen HYSYS V11 (*Aspen HYSYS V11*, 2019) has been used.

The techno-economic performance of the waste hydrogen purification process is investigated in this study. A techno-economic index is important to measure the advantages and disadvantages of process simulation. It can directly guide actual production and determine whether a process is implemented or not. The optimisation problem formulation of waste hydrogen purification is presented. Maximum total annual economic profit is used as an objective in this study. The objective function is shown in Eq. (7). Total annual profit (TAP) is the total product value (TPV), deducting the total annual capital cost (TCC) and the total operating cost (TOC).

$$max(TAP) = TPV - TCC - TOC \tag{7}$$

Total product value (TPV) is the product value after purification, including the regenerated hydrogen product ($F_R \cdot x_{R,H_2} \cdot C_R$) and the final waste hydrogen discharged as fuel ($F_W \cdot C_W$), Eq. (8). F denote stream flowrate. C is the cost/price per unit of product.

$$TPV = F_R \cdot x_{R,H_2} \cdot C_R + F_W \cdot C_W \tag{8}$$

The calculation of the total annual capital cost (TCC) is given in Eq. (9). The subscript k represents the equipment units in the hydrogen purification process. Where CC_k is the capital cost of equipment k, as shown in Eq. (11) - (15). AF_k is annualisation factor for a capital cost of equipment k, as shown in Eq. (10). r_k is the interest rate. y_k is equipment lifetime. Z_k represents the binary variable (0, 1) of whether equipment k exists.

$$TCC = \sum_k CC_k \cdot AF_k \cdot Z_k \tag{9}$$

$$AF_k = \frac{r_k \cdot (1 + r_k)^{y_k}}{(1 + r_k)^{y_k} - 1} \tag{10}$$

The general capital cost formulation of equipment k is shown in (11), which is a linear function of a variable f_k. Where a_k and b_k are capital cost coefficients. Equipment for waste

hydrogen purification may include purifiers (e.g. membrane separation Eq. (12) and PSA Eq. (13)), compressor (Eq. (14)), and pipeline Eq. (15). Where A_{mem} is membrane area. F_{PSA} is feed flowrate of PSA. Pw_{com} is the power consumption of compressor. F_{pip} is flowrate of stream in the pipeline. P_{pip} is the maximum pressure of the pipeline. L is the distance between supplier and receiver.

$$CC_k = a_k + b_k \cdot f_k \tag{11}$$

$$CC_{mem} = a_{mem} + b_{mem} \cdot A_{mem} \tag{12}$$

$$CC_{PSA} = a_{PSA} + b_{PSA} \cdot F_{PSA} \tag{13}$$

$$CC_{com} = a_{com} + b_{com} \cdot Pw_{com} \tag{14}$$

$$CC_{pip} = \left(a_{pip} + b_{pip} \cdot \frac{F_{pip}}{P_{pip}}\right) \cdot L \tag{15}$$

The total operating cost mainly includes the cost of feed materials ($F_F \cdot C_F$) and utilities ($F_U \cdot C_U$) to maintain the operation of the purification process unit, Eq. (16). The feed materials cost is the value of the feed waste hydrogen used as fuel before purification ($F_F \cdot P_F$),

$$TOC = F_F \cdot C_F + F_U \cdot C_U \tag{16}$$

Constraints mainly include mass balance, energy balance and other upper and lower bounds. The mass balance is shown in Eq. (17) - (22). The feed waste hydrogen (F_F) of the purification process is purified and separated to obtain the regenerated hydrogen (F_R) and the final waste hydrogen (F_W) as fuel. The total flowrate is balance Eq. (17), so is the flowrate of component i, Eq. (18). Where $x_{F,i}$, $x_{R,i}$ and $x_{W,i}$ are the molar fraction of component i in feed waste hydrogen, regenerated hydrogen product and final waste hydrogen discharged as fuel. The total molar fractions of all components in each stream are 1, Eq. (19) - (21).

$$F_F = F_R + F_W \tag{17}$$

$$x_{F,i} \cdot F_F = x_{R,i} \cdot F_R + x_{W,i} \cdot F_W \tag{18}$$

$$\sum_i x_{F,i} = 1 \tag{19}$$

$$\sum_i x_{R,i} = 1 \tag{20}$$

$$\sum_i x_{W,i} = 1 \tag{21}$$

The hydrogen recovery ratio (φ_{H_2}) of the purification process is calculated as Eq. (22). Where, x_{R,H_2} and x_{F,H_2} are the hydrogen concentration in regenerated hydrogen and feed waste hydrogen.

$$\varphi_{H_2} = \frac{F_R \cdot x_{R,H_2}}{F_F \cdot x_{F,H_2}} \tag{22}$$

The energy balance is that the total inlet materials enthalpy ($\sum_k E_{input,k}$) and the total external input enthalpy ($\sum_k E_{external,k}$) is equal to the total outlet material enthalpy ($\sum_k E_{output,k}$) of equipment k in the purification unit, Eq. (23).

$$\sum_k E_{input,k} + \sum_k E_{external,k} = \sum_k E_{output,k} \tag{23}$$

The bounds mainly include the upper and lower bound of flowrate (F_k) and pressure (P_k) of streams, as shown in Eq. (24) - (25).

$$F_k^{low} \leq F_k \leq F_k^{up} \tag{24}$$

$$P_k^{low} \leq P_k \leq P_k^{up} \tag{25}$$

The payback period of the waste hydrogen purification process is also assessed. The calculation of the payback period (PT) is given in Eq. (26).

$$PT = \frac{TCC}{TAP} \tag{26}$$

The flowrate and purity of regenerated hydrogen are determined by the purification process, the feed waste hydrogen, and operating conditions. The waste hydrogen purification process is established and simulated in Aspen HYSYS V11 (*Aspen HYSYS V11*, 2019). The results are optimised using the proposed techno-economic analysis. The optimal total annual profit, the optimal purification process and operating conditions are finally determined. The

optimal regenerated hydrogen is then returned to the multiple-level fresh resources Total Site Hydrogen Integration to further reduce the minimum fresh hydrogen usage in the refineries. However, installation cost and other indirect costs (e.g. engineering and supervision, construction costs, legal and contractor, project contingency) are not considered.

4.2.4 Multiple-level Fresh Resources Pinch Analysis with Intermediate Headers (PA-MLFR-IH)

A multiple-level fresh resources Pinch Analysis with intermediate headers (extended from multiple-level fresh resources Pinch Analysis, Section 4.2.2) is presented for Total Site Mass Integration considering intermediate purity headers and multiple-level fresh resources. The concept diagram of multi-level fresh resource Total Site Mass Integration with intermediate purity headers is shown in Figure 23, where both intra-process and Total Site scopes are considered.

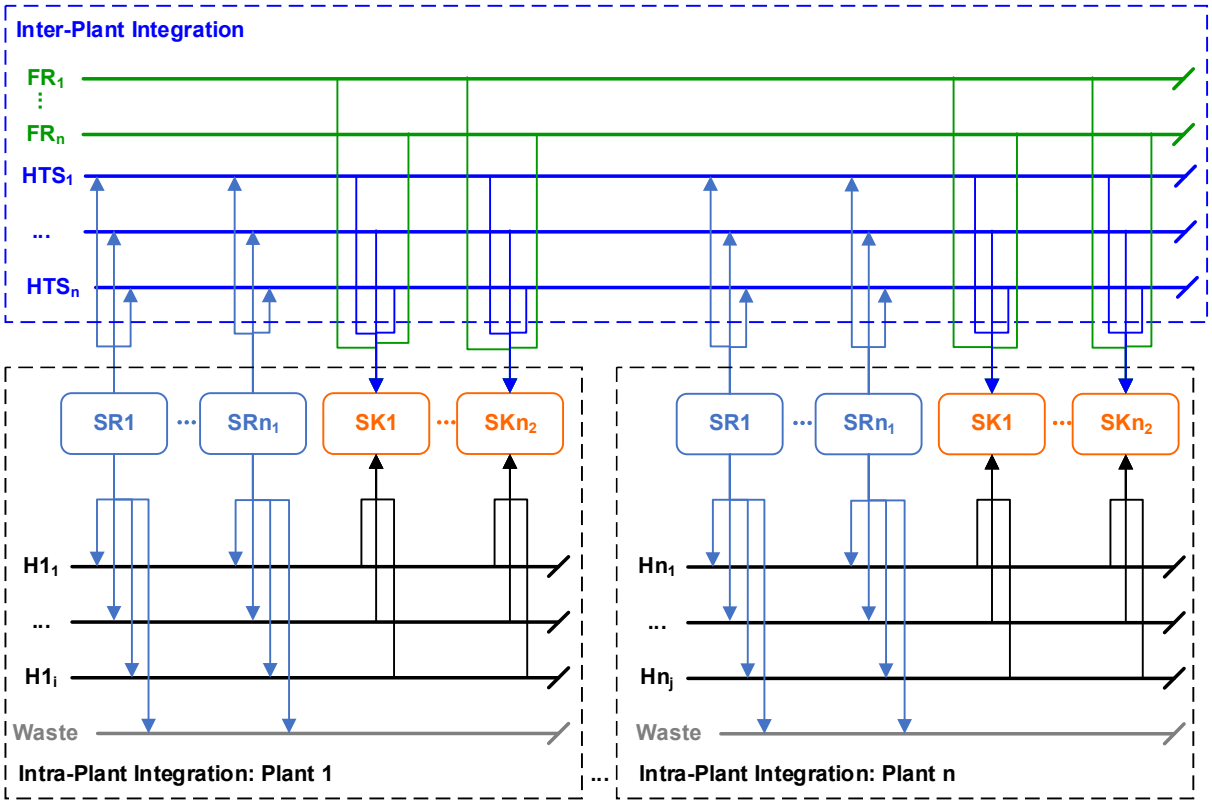

Figure 23. Multiple-level fresh resources Total Site Mass Integration with intermediate purity headers

The process sources are the units/streams of resource generation denoted by SR_1 to SR_{n1}, shown as light blue in Figure 23. SK_1 to SK_{n2} are the process sinks - units/streams that

consume resources in a process denoted by SK_1 to SK_{n2} in orange colour. $H1_1$ – $H1_i$ and Hn_1 – Hn_j are the intermediate headers of intra-plant in black lines. HTS_1 – HTS_n are the intermediate headers of inter-plant in blue lines. FR_1 – FR_n is a multiple-level fresh resource in green lines. In this work, multiple-level fresh resources mean the fresh resource with various quality levels, e.g. freshwater with different quality (contaminants) in water allocation networks, fresh hydrogen resource with different purity in hydrogen networks, etc. The sources (SR_1 to SR_{n1}) of intra-plant are mixed to several suitable intermediate purity headers ($H1_1$ – $H1_i$ and Hn_1 – Hn_j). The sources can be supplied to different sinks (SK_1 to SK_{n2}) through the headers to reduce the number of direct source-to-sink connections. At the same time, the surplus sources of intra-plant and the fresh sources provided by the outside are sent to other plants in need by inter-plant headers (HTS_1 – HTS_n) in order to minimise fresh resources consumption and waste discharge. The streams in the header are assumed to be well-mixed in this work. The intermediate purity headers allocation (number and purity of headers) and inter-plant flow are optimised to target minimum fresh resource consumption and minimum waste discharge.

Section 4.2.3 (I) proposes the Pinch Analysis method of multiple-level fresh resources and intermediate headers for intra-plant Mass Integration. In Section 4.2.3 (II), a pinch analysis method of multiple-level fresh resources and intermediate headers for Total Site Mass Integration is presented.

I. Multiple-level Fresh Resources Pinch Analysis with Intermediate Headers for Intra-plant Mass Integration

The integration of mass exchange network with headers of intermediate purity and multiple-level fresh resources (FR_1 to FR_{n1}) is investigated to reduce the consumption of expensive higher-quality fresh resources and simplify the configuration of mass exchange network in intra-plant. The concept diagram of multi-level resource Mass Integration with intermediate headers is as shown by the intra-plant mass integration in Figure 23. The sources (SR_1 to SR_{n1}) are mixed into several suitable intermediate purity headers ($H1_1$ – $H1_i$ or Hn_1 – Hn_j). The sources are supplied to different sinks (SK_1 to SK_{n2}) through the headers to reduce the number of direct source-to-sink connections. The intermediate purity headers allocation (number, connection, and purity of headers) is optimised to target minimum fresh resources consumption and minimum waste discharge.

An extended Pinch Analysis with multiple-level fresh resources and intermediate headers is proposed for the integration of the mass exchange network. The Pinch Analysis with

multiple-level fresh resources and intermediate headers for intra-plant Mass Integration is presented in the following.

Step 1: Perform multiple-level fresh resources Pinch Analysis for all sources and sinks at the intra-plant level.

Among fresh resources, those with lower quality are given higher priority because the lower-quality fresh resource is more readily available and usually cheaper. Higher-quality fresh resources should be used for the sinks, which cannot be satisfied by lower-quality resources. Multiple-level fresh resources Pinch Analysis (Gai et al., 2021a) is performed for all process sources and sinks of intra-plant integration. Take the example of two fresh resources (FR1 and FR2) with different qualities as an example, as shown in Figure 24a. The Pinch Analysis results in two Pinch points (P1 and P2), which divide the Composite Curves (CC) into three parts (or three regions). Higher-quality fresh resource (first fresh resource FR1) is required only below the first Pinch (P1). Lower-quality fresh resource (second fresh resource FR2) is required only between the first Pinch (P1) and the second Pinch (P2). Above the second Pinch (P2), the excess sources are discharged as waste and no fresh resources are needed.

Step 2: Determine the purity and a minimum number of headers with minimum fresh resources requirement and minimum waste discharge.

a) A header includes one or more sources. The excess sources are removed as waste. The remaining sources are connected head to tail from top to bottom using the triangle rule until the connecting line intersects the Sink Composite Curve. The sources before the intersecting can be merged into a header. The source that started the intersection is continued to mix the following sources in sequence, repeating the same procedure to determine the second header. Above the second Pinch (P2): sources SR8 (after waste discharge is removed) and SR7 are connected to form a straight line L1(SR7+SR8) from head to tail after removing the excess source discharged as waste, as shown in Figure 24b. The line L1 and the Sink Composite Curve (orange curve) have no intersection points. There is no intersection point between the straight line and the Sink Composite curve. Source SR6 continues to be mixed; that is, the head and tail of source SR8 and SR6 are connected to a straight line L2 (Figure 24b), which still does not intersect the Sink Composite Curve. Source SR5 above the second Pinch (P2) is continued to be merged/mixed. The top end of SR8 is connected to P2 (i.e. line L3,

Figure 24b), and the line intersects the Sink Composite Curve. The sources SR8 after waste discharge is removed, SR7 and SR6 can be mixed into one header H1 (in Figure 24e-f). The second Pinch-causing source (SR5) is separately into another header, H2 (in Figure 24e-f). It will be separated according to ratio and feed to two different sinks SK3 and SK4.

b) If a Pinch point is encountered, the Pinch-causing source is separated into a header when the tail end of a header is a Pinch, and the header intersects with the Sink Composite Curve. Below the Pinch, the source below the Pinch-causing source is begun to mix with the other following sources (SR4-SR1) in sequence to determine the next header. Between the first Pinch (P1) and the second Pinch (P2): source SR4 below the second Pinch-causing source (SR5) starts to mix with the other following sources (SR4-SR1) (Figure 24c-d). The head and tail of sources SR4 and SR3 are connected into a straight line L4, which has no intersection point with Sink Composite Curve. Source SR2 is continued to mix (i.e. line L5, Figure 24c) and still does not intersect the Sink Composite Curve.

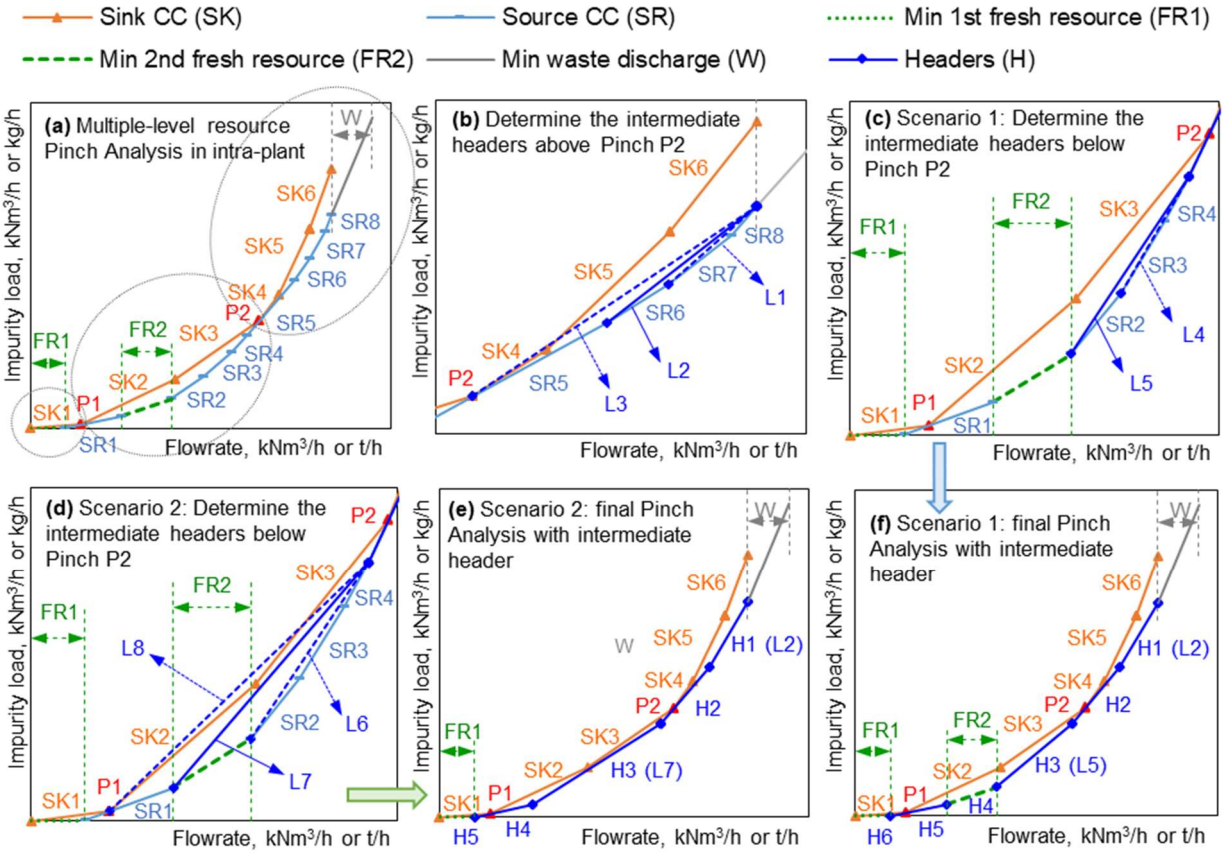

Figure 24. Pinch Analysis with multiple-level fresh resources and intermediate headers for intra-plant Mass Integration

Step 3: Determine the final integration design/allocation with intermediate headers. There are two scenarios: fresh resources can or cannot be mixed with other sources.

a) Scenario 1.1: If fresh resources do not mix with other sources, each fresh resource is used as an individual header (Figure 24c and Figure 24f).

The fresh resources that are not at the Pinch need to be moved to the corresponding Pinch, and the other sources need to be merged/mixed, as shown in Figure 24c. The first fresh resource (FR1) and the first Pinch-causing source (SR1) are separated into the header because there are only FR1 and SR1 below the first Pinch (P1). The final integration design/allocation with an intermediate header is shown in Figure 24f. FR1, SR1, FR2 and SR5 form headers H1, H2, H3 and H5. SR2, SR3 and SR4 are mixed to form a header H4. SR6, SR7 and SR8 are mixed into another header, H6.

b) Scenario 1.2: If fresh resources can be mixed with other sources to form a header, the fresh resources are treated as normal sources, as shown in Figure 24d and Figure 24e.

The sources SR4, SR3, and SR2 are continued to mix with the second fresh resource (FR2), see Figure 24d. The line L7 (Figure 24d) formed by their connection and the Sink Composite Curve still has no intersection point. The source SR1 above the first Pinch (P1) continues to mix. The endpoint of SR4 is connected with Pinch P1 to form a straight line L8 (Figure 24d), which intersects the Sink Composite Curve. Therefore, sources SR4, SR3, SR2 and FR2 are merged into one header, H3. The first Pinch-causing source (SR1) is separately formed into another header, H2. Below the first Pinch (P1), only the first fresh resource (FR1) is left to form a separate header H1. The final integration design/allocation with an intermediate header is shown in Figure 24e.

c) Steps 2(a-d) are performed until the beginning of the first source. The number of headers is the number of the minimum header with minimum fresh resources requirement and minimum waste discharge. The length of the corresponding line for each header is the flowrate of a header, and the slope represents the impurity concentration in the header. The two final headers distributions of fresh resources that can or cannot be mixed with other sources are respectively shown in Figure 24e and Figure 24f.

II. Multiple-level Fresh Resources Pinch Analysis with Intermediate Headers for Total Site Mass Integration

The summary procedure flowchart of the presented Total Site Mass Integration with intermediate headers and multiple-level fresh resources is shown in Figure 25.

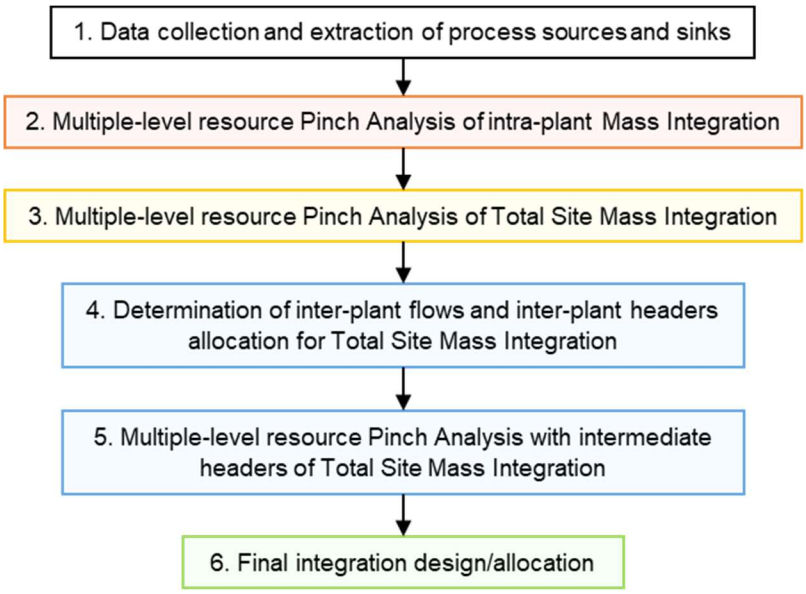

Figure 25. Procedure flowchart of Total Site Mass Integration with intermediate headers and multiple-level fresh resources

The detailed steps of the proposed Pinch Analysis with multiple-level fresh resources and intermediate headers for Total Site Mass Integration are as follows.

Step 1: Data collection and extraction of all process sources and sinks.

Step 2: Perform multiple-level fresh resources Pinch Analysis of intra-plant Mass Integration for all process sources and sinks. This step is detailed, as shown in Step 1 in Section I.

Step 3: Perform multiple-level fresh resources Pinch Analysis of Total Site Mass Integration.

The ideal target of minimum fresh resources requirement and minimum waste discharge is identified by Pinch Analysis using process sources and sinks in all plants. This study adopts the multiple-level fresh resources Pinch Analysis of Total Site Mass Integration proposed by Gai et al. (2021a). The Pinch Analysis at total site level is performed according to multiple-level fresh resources Pinch Analysis of Total Site Mass Integration until to get the ideal target by revising the sources of waste discharge.

Step 4: Determine the inter-plant flows and inter-plant headers allocation of Total Site Mass Integration.

The Pinch-causing sources could be moved to higher-quality waste discharged by using the lower-quality waste sources in individual plants before Total Site Integration. When integrated at the Total Site level, the Pinch-causing sources (higher-quality waste discharged) can be used as inter-plant streams to other plants to minimising fresh resource consumption. Therefore, the Pinch-causing sources could be inter-plant flow streams. Each inter-plant header is an individual header that could be formed by Pinch-causing sources or fresh resources.

Step 5: Perform multiple-level fresh resources Pinch Analysis with intermediate headers of Total Site Mass Integration.

The sources of intra-plant are mixed to determine the headers distribution in the individual plant, according to the Pinch Analysis with multiple-level fresh resources and intermediate headers for intra-plant Mass Integration proposed in Section I.

Step 6: Determine the final integration design/allocation of Total Site Mass Integration with intermediate headers and multiple-level fresh resources.

4.3 Case Studies

The proposed method can be flexibly applied to various scenarios (e.g. water allocation network, hydrogen network) of Total Site Mass Integration with multiple-level fresh resources and intermediate headers. The most common mass integrations are water integration and hydrogen integration. The case studies of this section are demonstrated by the integration of the water allocation network and the integration of the hydrogen network. The implementation plans are performed to minimise fresh resources consumption and waste discharge by optimising the intermediate purity headers and waste regeneration process with multiple-level fresh resources. The solutions, results and significance (e.g. reduction of fresh resource consumption and waste discharge, cost-benefits) are discussed.

4.3.1 Multiple-level Fresh Resources Pinch Analysis (PA-MLFR) of Mass Integration

Total Site Hydrogen Integration in refineries of a petrochemical industrial park is selected as a case study in demonstrating the proposed method. It is of high importance for refineries to reduce hydrogen consumption, waste hydrogen discharge and production cost to integrate and optimise inter-plant hydrogen networks. The considered site consisted of three plants – A, B and C. The flowrate and concentration of hydrogen sources and sinks are shown in Table

8. There are two fresh hydrogen sources with different quality levels. The first fresh hydrogen source (FR1-99.9 %) is a 99.9 % high-quality fresh hydrogen source. The second fresh hydrogen source (FR2-95 %) has a lower concentration of 95.0 %.

Table 8. Hydrogen sources and sinks of hydrogen network in refineries (Lou et al., 2019)

H_2 network	Source/Supply	Purity, vol% H_2	Flowrate, kNm^3/h	Sink/Demand	Purity, vol% H_2	Flowrate, kNm^3/h
Plant A	SRA1	80.0	17.30	SKA1	86.7	93.31
	SRA2	80.0	60.68	SKA2	83.6	82.66
	SRA3	75.0	55.28	SKA3	82.6	39.16
	SRA4	75.0	25.87	SKA4	74.9	12.47
	SRA5	70.0	8.00	SKA5	72.7	5.73
	SRA6	65.0	3.84			
Plant B	SRB1	93.0	50.30	SKB1	80.6	201.2
	SRB2	80.0	33.53	SKB2	78.9	14.53
	SRB3	75.0	145.3	SKB3	77.6	44.71
	SRB4	75.0	11.12	SKB4	75.1	58.12
	SRB5	73.0	27.94			
	SRB6	70.0	36.89			
Plant C	SRC1	98.3	3.23	SKC1	99.9	9.68
	SRC2	98.3	6.45	SKC2	98.6	2.24
	SRC3	97.5	6.45	SKC3	97.5	11.29
	SRC4	96.0	2.30	SKC4	97.0	8.06
	SRC5	95.0	6.45	SKC5	90.0	12.10
	SRC6	90.0	9.68			
	SRC7	85.0	6.05			

The baseline Scenario for this study is without Total Site Hydrogen Integration, i.e. intra-plant Hydrogen Integration with a multiple-level resource.

I. Intra-Plant Hydrogen Integration with Multiple-level Fresh Resources – Baseline Scenario

The multiple-level fresh resources Pinch Analysis, described in Section 4.2.2 (I), has been applied. The contaminant load and flowrate of intra-plant Hydrogen integration are plotted by using multiple-level fresh resources Pinch Analysis, as shown in Figure 26. The second fresh hydrogen source with a low concentration is cheaper and preferred. The cleaner and more expensive fresh hydrogen source is used if the second fresh hydrogen source cannot meet the requirements (Section 4.2.2 (I)). The highest hydrogen concentration of the sinks in both Plants A and B is lower than that of the second fresh hydrogen source, so Plant A and B only need a second fresh hydrogen source. The highest concentration sink of Plant C is not less than the

concentration of the first fresh hydrogen source, so Plant C needs the first fresh hydrogen source. The hydrogen source concentration at the lowest-quality Pinch Point of Plant A, B and C is 75.0 %, 70.0 % and 95.0 %. Before Total Site Hydrogen Integration, the total flowrate of the minimum first fresh hydrogen source (FR1) of the three plants (A, B and C) is 1.7 % of the total hydrogen sinks (10.10 kNm^3/h). The total flowrate of the minimum second fresh hydrogen source is 18.0 % of the total hydrogen sinks (107.10 kNm^3/h), and the total flowrate of minimum waste hydrogen discharge is 6.2 % relative to the total hydrogen sources (38.68 kNm^3/h).

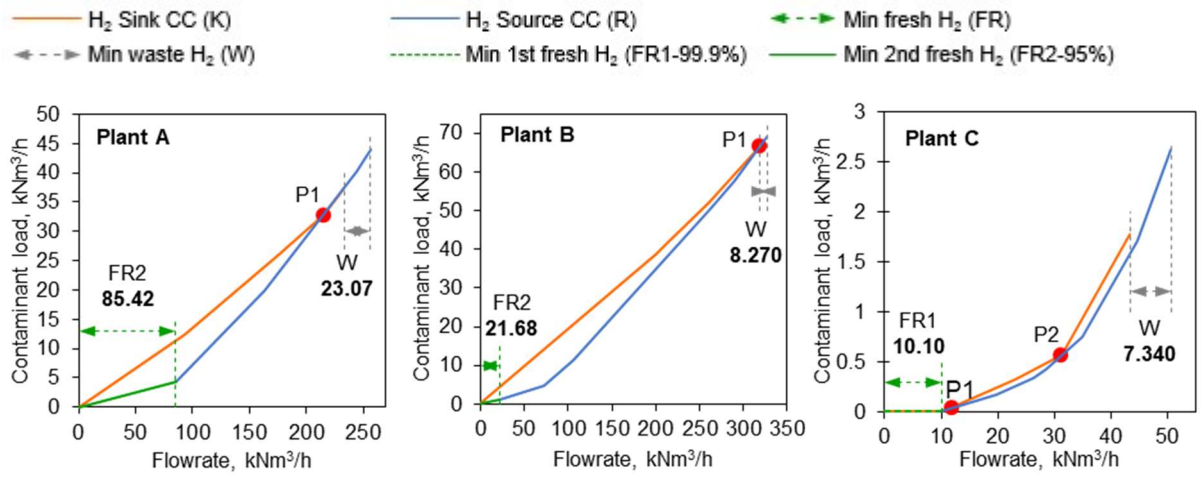

(a) (b) (c)

Figure 26. Multiple-level fresh resources Pinch Analysis of each plant Hydrogen Integration before waste hydrogen recovery (Baseline Scenario) for (a) Plant A, (b) Plant B, (c) Plant C

II. Multiple-level Fresh Resources Total Site Hydrogen Integration

The multiple-level fresh resources Pinch Analysis for Total Site Hydrogen Integration described in Section 4.2.2(II) has been applied. To further reduce waste hydrogen emissions, Total Site Hydrogen Integration between plants is implemented. First, assuming that all the hydrogen sources and sinks of Plant A, B and C are in a hydrogen network, the ideal target of Total Site Hydrogen Integration is obtained using multi-resource Pinch Analysis (as described in Step 1 of Section 4.2.2(II), Figure 21a and Figure 22a). The ideal goal for Total Site Hydrogen Integration is shown in Figure 27.

Identify the Total Site Hydrogen Integration with minimum inter-flow to meet the ideal targets in Step 1 (Figure 27) of Section 4.2.2(II). Maximise the use of low-quality source above the lowest-quality Pinch in intra-plant integration to transfer the higher quality source for Total

Site Hydrogen Integration (see Figure 21d,e and Figure 22d,e as described in Step 2 of Section 4.2.2(II)). The modified hydrogen network matching of Plant A/B/C is shown in Figure 28. For Plant A, the hydrogen source with a concentration below 75.0 % is moved along the 75.0 % Hydrogen Pinch-causing source until it touches Hydrogen Sink CC, as shown in Figure 28a. For Plant B, because the Pinch-causing source is the lowest concentration hydrogen source, it has reached the limit and does not need to be moved further. For Plant C, the hydrogen source with a concentration below 95.0 % is moved along the hydrogen source with 95.0 % Pinch until it touches Hydrogen Sink CC, as shown in Figure 28c. The waste hydrogen discharge of the three plants after adjustment are summarised in Appendix Table S6.

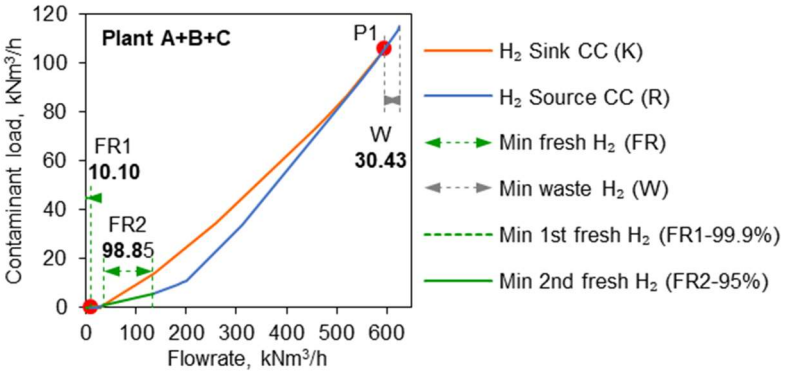

Figure 27. The lowest boundary of Total Site Hydrogen Integration

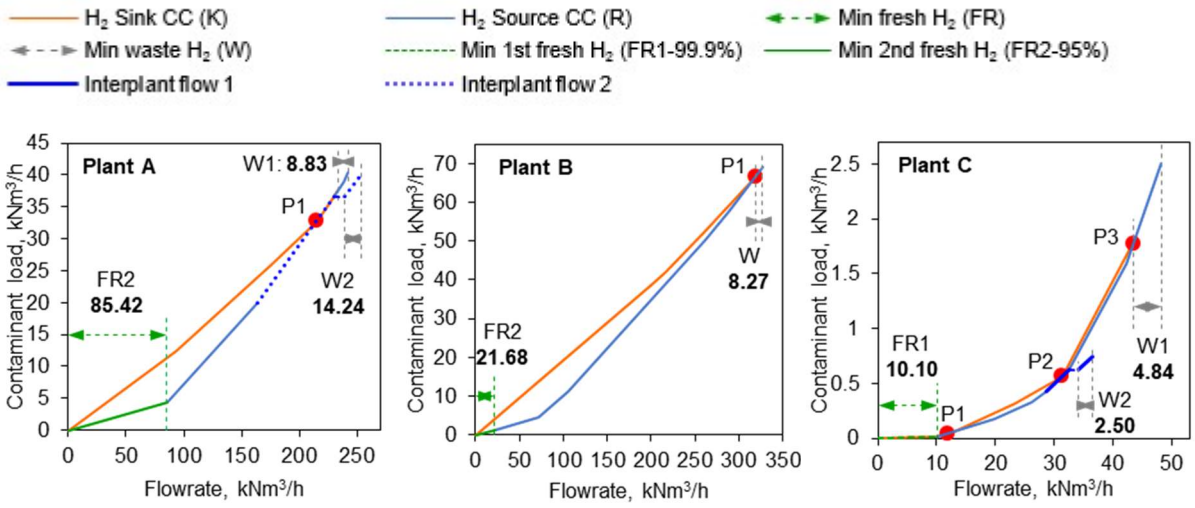

(a) (b) (c)

Figure 28. Identify inter-plant streams by revising the waste hydrogen discharge see Step 2b of Section 4.2.2(II): (a) Plant A, (b) Plant B, (c) Plant C

The waste hydrogen discharge of the three plants after adjustment and hydrogen sources

and sinks in High-Quality Region (HQR) is integrated with multiple-level fresh resources Pinch Analysis (as described in Step 2b of Section 4.2.2(II)). The results are shown in Figure 29. This target value is compared to the ideal target in Step 1 (Figure 27). These two targets are equal in this case, so this is unassisted integration, and step 2c in Section 4.2.2(II) can be skipped.

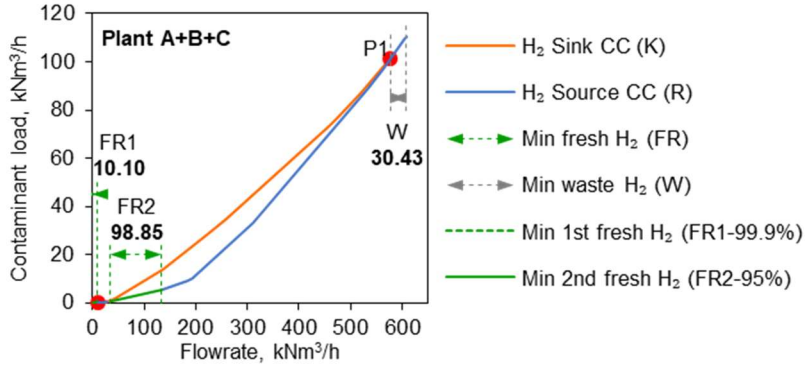

Figure 29. Identified target after the revision of waste hydrogen discharge

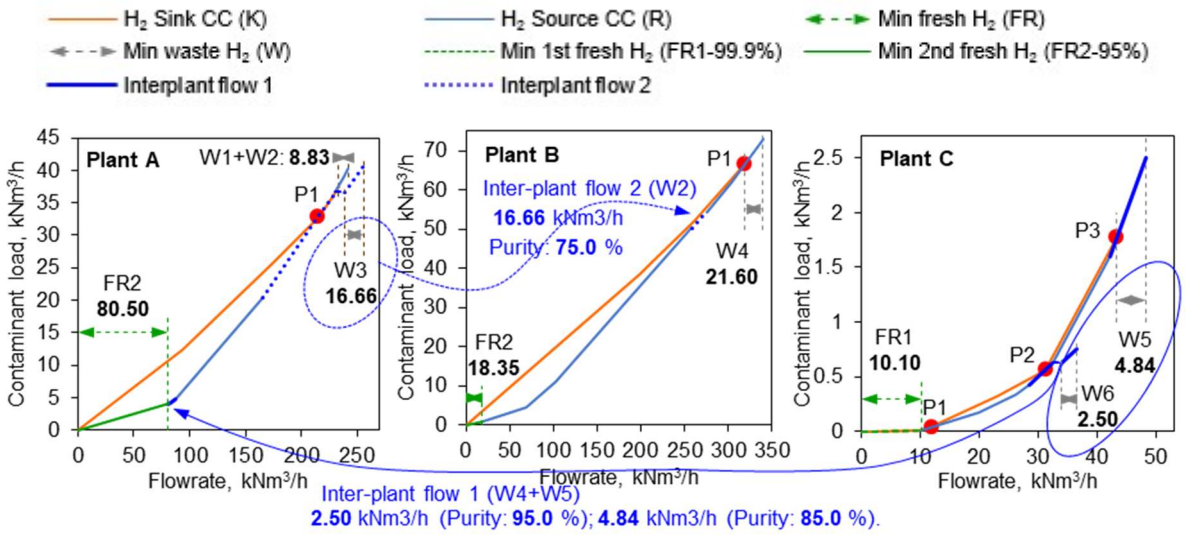

(a) (b) (c)

Figure 30. The final solution of Total Site Hydrogen Integration before waste hydrogen recovery for (a) Plant A, (b) Plant B, (c) Plant C

Finally, the optimal inter-plant flow allocation is determined to get the identified solution of Total Site Hydrogen Integration (as described in Step 3 of Section 4.2. (II)). The lowest-quality Pinch of the three plants are ordered from large to small: Plant C 95.0 % > Plant A 75.0 % > Plant B 70.0 %. According to Pinch Analysis, the waste hydrogen of Plant C with high purity can be all

used by Plant A. It reduces the fresh hydrogen sources consumption and waste hydrogen discharge of Plant A. Further integration can be performed where 65.0 % (16.66 kNm^3/h with a 75.0 % purity) of the waste hydrogen in Plant A can be utilised in Plant B. Plant A has a waste hydrogen recovery rate of 65.0 % from the Total Site Integration between Plant A and B. After inter-plant integration, the waste hydrogen discharge of Plant B is 3.5 % (21.60 kNm^3/h) relative to the total hydrogen sources. The final optimal solution of multiple-level fresh resources Pinch Analysis of Total Site Hydrogen Integration is shown in Figure 30. The hydrogen networks of Plant A, Plant B and Plant C after Total Site Integration are shown in Figure 30a, Figure 30b, and Figure 30c.

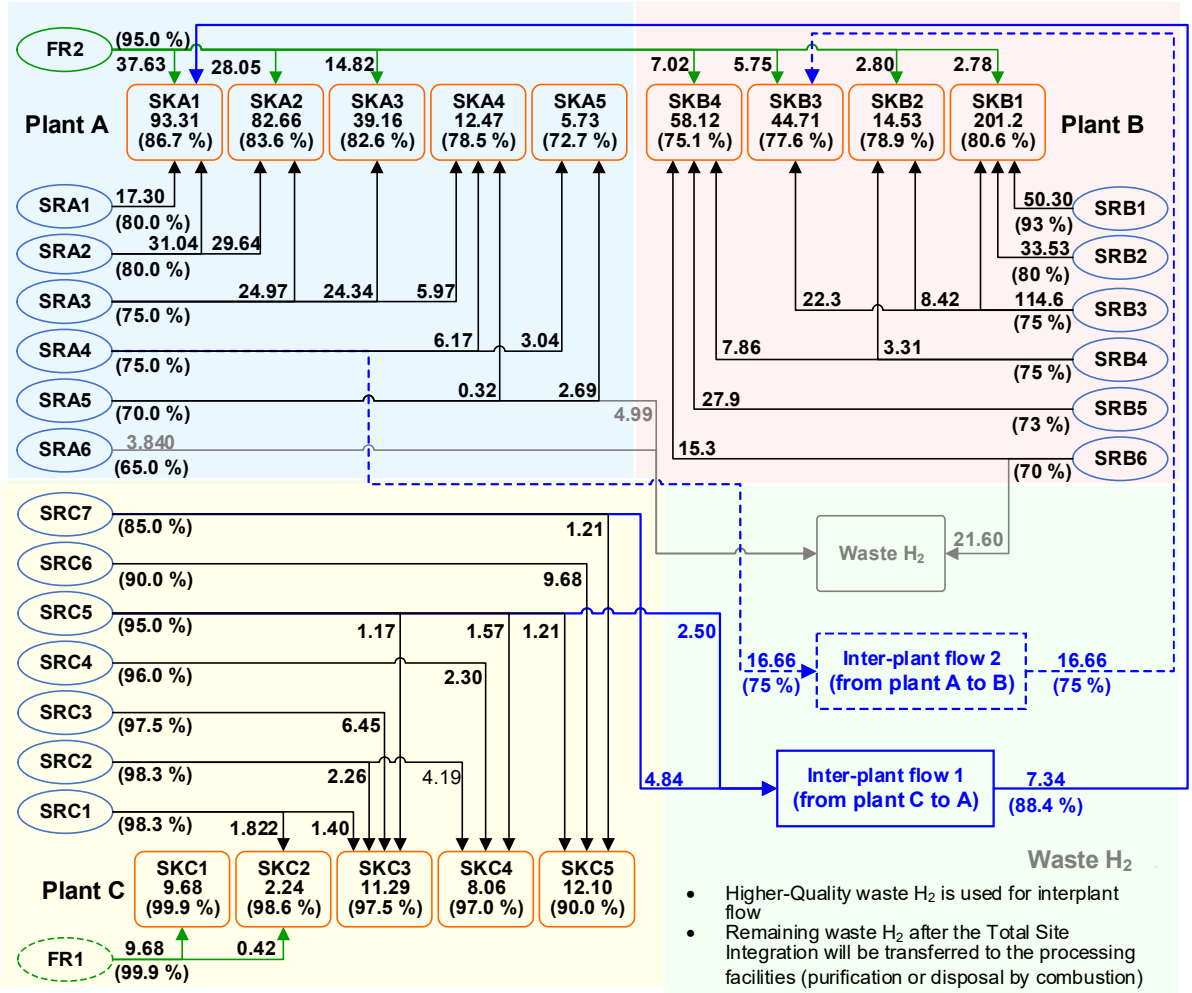

Figure 31. Identified solution of multiple-level fresh resources Total Site Hydrogen Integration before waste hydrogen regeneration. SR = source, SK = sink. A1 represents the hydrogen stream (sink or source) in Plant A. Same interpretation is applied to Bn and Cn.

The detailed hydrogen network allocation of multiple-level resource Total Site

Hydrogen Integration before waste hydrogen regeneration is shown in Figure 31. The streams in the light-blue ellipse represent hydrogen sources, and in the orange frame represent hydrogen sinks, see Figure 31. The green dash ellipse at the top represents the second fresh hydrogen source (FR2). The green dash ellipse at the bottom represents the first fresh hydrogen source (FR1). The light blue background area represents the hydrogen network allocation of Plant A. The light pink background area represents the hydrogen network allocation of Plant B. The area with a light-yellow background is a hydrogen network allocation of Plant C. The light green background area is globally integrated inter-plant flow and waste hydrogen discharge of Total Site Hydrogen Integration. The allocation of all hydrogen streams is represented by arrowed lines marked with flowrate (values without parentheses) and hydrogen concentration (values in parentheses). The arrow direction represents the direction of hydrogen streamflow. The black arrowed lines are the hydrogen streams of intra-plant flow. The blue arrowed lines represent hydrogen streams of inter-plant flow. The green arrowed lines are fresh hydrogen allocation. The grey arrowed lines are waste hydrogen discharge.

Table 9. Fresh hydrogen consumption and waste hydrogen discharge after Total Site Hydrogen Integration

Plant	Minimum fresh hydrogen sources				Minimum waste hydrogen			
	Streams	Purity, vol% H_2	Flowrate, kNm^3/h	FR/(total sinks), %	Streams	Purity, vol% H_2	Flowrate, kNm^3/h	waste/(total sources), %
A	FR2	95.0	80.50	13.5	WH1	70.0	4.99	0.8
					WH2	65.0	3.84	0.6
B	FR2	95.0	18.35	3.1	WH4	70.0	21.60	3.5
C	FR1	99.9	10.10	1.7		-	-	
Total	FR1		10.10	1.7	WH		30.43	4.9
	FR2		98.85	16.6				

The detailed minimum fresh hydrogen consumption and waste hydrogen discharge by the three plants are shown in Table 9. FR/(total sinks) is the flowrate of minimum fresh resource required relative to the total hydrogen sinks of three plants (A, B and C). Waste/(total sources) is the flowrate of minimum waste hydrogen discharge relative to the total hydrogen sources of three plants (A, B and C). This solution ensures that the targets are the same as the ideal goals in Step 1 while minimising the inter-plant flow. The Total Site Hydrogen Integration reduced the second fresh hydrogen consumption by 7.7 % (8.25 kNm^3/h) and the waste hydrogen emission by 21.3 % (8.25 kNm^3/h) compared with only intra-plant integration. However, Total Site Hydrogen

Integration requires additional equipment, e.g. pipelines, pumps or compressors. The safety issues need to be further explored to enhance the practicability of Total Site Hydrogen Integration design. It is assumed that the piping distance between each plant is 500 m with high pressure of 4.0 MPa in this study. The considered capital cost is limited to piping, which is 0.90 M€.

4.3.2 Optimisation of Waste Hydrogen Regeneration

The common waste hydrogen purification technologies and comparison are shown in. PSA can achieve a higher regeneration purity (> 99 %) than the membrane approach with 90-98 % purity. However, the higher purity of regenerated hydrogen is not always better in the purification process of waste hydrogen. Higher purity of regenerated hydrogen requires higher investment cost. In most cases, the purity of waste hydrogen is low (< 80 %). Membrane separation features a higher hydrogen recovery ratio and lower capital cost. The waste hydrogen is firstly purified and enriched by membrane separation considering the investment and hydrogen recovery ratio. Regenerated hydrogen could be returned to Total Site Hydrogen Integration to replace the required fresh hydrogen sources follows the requirement (purity and demand). If it fails to reach the recovery requirement, the appropriate purification process will be used again. The key to waste hydrogen purification is membrane separation.

Table 10. Comparison of waste hydrogen purification technology in a refinery

Projects	Cryogenic (Aasadnia et al., 2021)	PSA (Golmakani et al., 2017)	Membrane (Bernardo et al., 2020)
Purity of recovered H_2, mol%	90-96	> 99	90-98
H_2 recovery ratio, %	90-98	65-90	85-95
Feed H_2 concentration, mol%	15-75	75-90	15-90
Feed gas pressure, MPa	0.5-7.5	1-4	1-16
Product H_2 pressure, MPa	Feed pressure	Feed pressure	<< Feed pressure
Pretreatment requirement	Very few	None	Remove CO_2, H_2S, etc
Capital cost	High	Medium	Low
Degree of easy expansion	Low	Medium	High
Operational reliability	Low	Medium	High
Equipment floor space	High	Medium	Low

The main issue of membrane separation lies in the selection and calculation of membrane separation. It includes the key parameters and selection of membrane. Membrane separation coefficient ($\alpha_{i,j}$) and the permeability rate (J) are the key parameters to evaluate membrane separation performance (selectivity and permeability) (Huang et al., 2014). The

separation coefficient ($\alpha_{i,j}$) of gas membrane separation is defined as the ratio of the permeability rate (J) of the gas component i and component j, Eq. (27). Different gases permeate the membrane at different permeation rates. The permeability rate (J_i) is the permeable gas flowrate ($F_{perm,i}$) of component i after the feed gas through the separation membrane with per membrane area (A), per unit driving force (ΔP_i) as shown in Eq. (28). The pressure difference is used as the driving force in gas membrane separation. The gas separation membrane is divided into a glassy membrane and rubbery hydrogen membrane (Ruan et al., 2019). The performance parameters of the two membranes are shown in Appendix Table S5. The glassy membrane has a higher selective permeability to hydrogen, which is more suitable for waste hydrogen purification. The hydrogen penetration rate (J_{H_2}) of the glassy membrane is 200 GPU (Gas Permeation Unit) (Ruan et al., 2020). Where 1 GPU = 10^{-6} cm·s^{-1}·(cm Hg)$^{-1}$.

$$\alpha_{i,j} = \frac{J_i}{J_j} \tag{27}$$

$$J_i = \frac{F_{perm,i}}{\Delta P_i \cdot A_{mem}} \tag{28}$$

The mathematical model of gas membrane separation is established. The gas membrane separation computing unit adopted in this work is a simulation algorithm as developed by (Li et al., 2016). The model is based on the following assumptions: (a) the overall flow and permeation of the fluid are both counter-current; (b) the flow resistance of permeation side and feed side and the resistance of support layer are ignored; (c) the influence of pressure and concentration changes on the membrane performance is ignored.

The permeability equation (Eq. (29)) of the gas separation membrane is derived from Eq. (28). Where, $x_{R,i}$ is the molar fraction of component i of regenerated hydrogen product. F_R is the flowrate of regenerated hydrogen product. ΔP_i is the driving force of component i for gas membrane separation. A is the membrane area for waste hydrogen purification. The other general mass balance equations (Eq. (17) - (22)) of waste hydrogen purification is also applicable to gas membrane separation.

$$x_{R,i} \cdot F_R = J_i \cdot \Delta P_i \cdot A_{mem} \tag{29}$$

The logarithmic average of the partial pressure difference of the component i on both sides of the membrane is taken as the driving force (ΔP_i) of membrane separation. It is

calculated using Eq. (30). P_F, P_R and P_W are the pressure levels of feed waste hydrogen, regenerated hydrogen product and final waste hydrogen discharged as fuel.

$$\Delta P_i = \frac{(x_{F,i} \cdot P_F - x_{R,i} \cdot P_R) - (x_{W,i} \cdot P_W - x_{W,i} \cdot P_W)}{ln\left(\frac{x_{F,i} \cdot P_F - x_{R,i} \cdot P_R}{x_{R,i} \cdot P_R - x_{W,i} \cdot P_W}\right)} \quad (30)$$

Based on the established mathematical model, a membrane separation model is designed by combining Component Splitter, Spreadsheet and Adjust function unit in Aspen HYSYS V11 (*Aspen HYSYS V11*, 2019). The above equations are used to simulate the membrane separation. The separation model simulates the membrane component by taking the split fractions of the key component as the regulating value. The membrane area is automatically adjusted with the change of the flow rate of the feed stream to achieve the required separation purpose. The model could provide effective results for the simulation optimisation of membrane separation, which has been applied by (Li et al., 2016).

The optimisation of the waste hydrogen regeneration process described in Section 4.3.2 has been applied. It can further reduce the minimum fuel gas emission and the minimum fresh hydrogen sources if the low-concentration waste hydrogen is purified into a high-concentration hydrogen source utilised by a hydrogen sink. The operating conditions of the waste hydrogen discharge after Total Site Hydrogen Integration are shown in Table 11. The pressure of regenerated hydrogen is required to be 2.0 MPa.

Table 11. Main operating conditions of waste hydrogen discharge

Waste H_2 streams	WH1, A	WH2, A	WH4, B
Flowrate, kNm^3/h	4.99	3.84	21.60
Pressure, MPa	2.41	1.38	2.41
Temperature, °C	50	40	55
Components, vol%			
H_2	70	65	70
C1	7.1	11	16
C2	6.7	6.4	3.8
C2=	-	-	1.2
C3	6.9	4.4	2.0
C3=	-	-	0.8
C4+	9.3	11	6.2
N_2	-	2.2	-

It is necessary to separate and purify the discharged waste hydrogen to make full use of waste hydrogen after Total Site Hydrogen Integration and minimise the waste of hydrogen resources. The waste hydrogen purification process model is established in the Aspen HYSYS V11 (*Aspen HYSYS V11*, 2019), and the process is simulated and optimised, as shown in Figure 32.

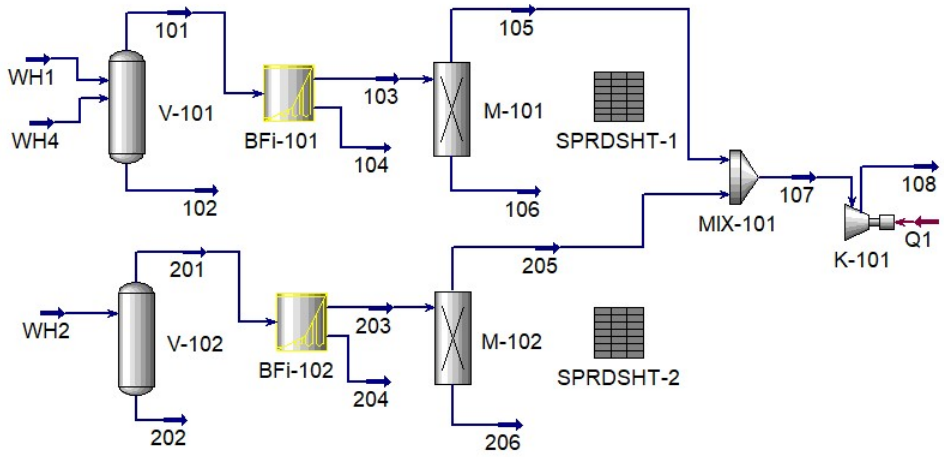

Figure 32. Flowsheet of waste hydrogen purification process by membrane separation

Table 12. Parameter data for calculating capital cost, operating cost and product value

Projects	Data	Reference
a_{com}	95.45 k€	(Hallale and Liu, 2001)
a_{mem}	41.50 k€	(Shehata, 2016)
a_{pip}	0.35 k€/m	(Shehata, 2016)
b_{com}	1.585 k€/kW	(Hallale and Liu, 2001)
b_{mem}	0.332 k€/m^2	(Shehata, 2016)
b_{pip}	0.026 k€·MPa·h/(m·kNm^3)	(Shehata, 2016)
C_F	0.13 €/m^3	("Statistical Review of World Energy | Energy economics")
C_R (99.9 % H_2)	3.427 k€/t	(Li et al., 2017)
C_R (95-99.9 % H_2)	2.730 k€/t	(Li et al., 2017)
C_U (Power)	0.104 €/(kW·h)	(Fan et al., 2020)
C_W	0.13 €/m^3	("Statistical Review of World Energy | Energy economics")
r_k	5 %	(Shehata, 2016)
y_k	8,000 h/y	(Shehata, 2016)

The parameter data for calculating capital cost, operating cost and product value is shown in Table 12. In this work, mainly membrane separators and compressors are used in the

process design. According to the actual operation situation of the membrane separation and purification in hydrogen recovery, the economic benefit analysis was carried out according to the following parameters. The lifetime of the hydrogen membrane is 5 y. The economic performance parameters of the compressor are estimated according to the suggestion of the manufacturer. The compressor price is estimated according to motor power. The equipment lifetime of compressor, piping, and others (filters, etc.) is 10 y. The membrane separator and compressor all take a 10.0 % spare capacity (Hallale and Liu, 2001). It is assumed that the piping distance between the purification unit and each plant is 500 m with high pressure of 4.0 MPa (Shehata, 2016). The annual operating time is 8,000 h. The main utility consumption is power and circulating water.

A pressure difference is a driving force in the hydrogen membrane separation process. Under different pressure, different gases pass through the membrane at different permeation rates. Feed pressure is the key factor affecting separation performance and membrane area, as shown in a - higher pressure, higher energy demand. It is necessary to optimise the feed pressure. The influence of feed pressure on an annual economic benefit is shown in Figure 33b. The points in Figure 33 showing the optimal operating conditions. The purity of regenerated hydrogen is 97.1 %. The total hydrogen recovery ratio of the waste hydrogen purification process is 95.2 %. The hydrogen recovery rates of membrane separators M-101 and M-102 are 96.3 % and 85.6 %.

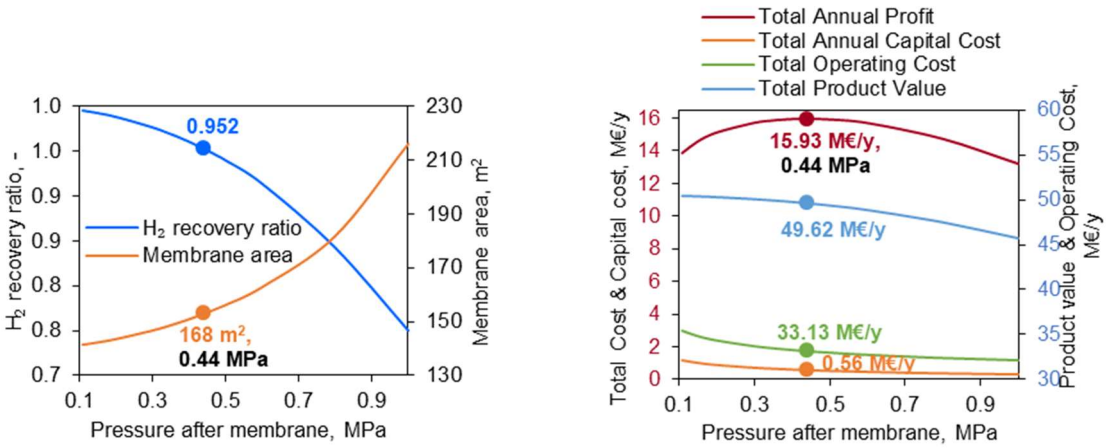

(a) pressure vs membrane separation (b) pressure vs annual economic benefit

Figure 33. The influence of pressure on the waste hydrogen regeneration process

The detailed economic benefits at the optimal point are shown in Table 13. It can be seen that the purification process proposed has significant economic benefits and a short payback

period (3.2 months). The recovery period of waste hydrogen purification by membrane separation is generally relatively shorter compared with PSA (Shehata, 2016). The payback period for waste hydrogen purification by membrane separation is generally relatively short. After the separation and purification optimisation of the hydrogen network, the minimum second fresh hydrogen source (95 %) required is 77.83 kNm^3/h, a 21.3 % reduction. The minimum waste hydrogen emission decreased by 67.6 % to 9.85 kNm^3/h. It can be seen that the separation and purification of the underutilised hydrogen source and waste hydrogen greatly reduced the emission of waste hydrogen and purchased fresh hydrogen sources. The low-quality waste hydrogen is turned into a useful secondary raw material, which significantly reduces the waste of hydrogen resources and realises waste hydrogen recycling.

Table 13. Price list of the products, utilities and equipment

Projects		Load		Costs	
Product Profit	Regenerated H_2	1.81	t/h	39.51	M€/y
	Final waste H_2	9.72	kNm^3/h	10.11	M€/y
	Total Product Value			49.62	M€/y
Capital Cost	H_2 membrane	168	m^2	0.14	M€
	Compressor	1.97	MW	3.21	M€
	Piping			0.90	M€
	Total Capital Cost			4.25	M€
	Total Annual Capital Cost			0.56	M€/y
Operating Cost	A feed of purification process	30.4	kNm^3/h	31.65	M€/y
	Power consumption	1.97	MW	1.49	M€/y
	Total Operating Cost			33.13	M€/y
Total Annual Profit				15.93	M€/y

4.3.3 Multiple-level Fresh Resources Pinch Analysis with Intermediate Headers (PA-MLFR-IH) in Mass Integration

The case study of this section is demonstrated by the integration of the water allocation network and the integration of the hydrogen network.

I. Pinch Analysis with Intermediate Headers

A case study from the literature (Deng et al., 2014) was used to verify the extended Pinch Analysis with intermediate headers. The data of sources and sinks in a mass exchange network is shown in Table 14.

Table 14. Data of sources and sinks (Deng et al., 2014)

Sources	Purity, mol%	Flowrate, mol/s	Sinks	Purity, mol%	Flowrate, mol/s
SR1	93	623.8	SK1	80.61	2,495.0
SR2	80	415.8	SK2	78.85	180.2
SR3	75	1,801.9	SK3	75.14	720.7
SR4	75	138.6	SK4	77.57	554.4
SR5	70	457.4			
SR6	73	346.5			
FR	95				

Calculations are performed using the extended Pinch Analysis. The results of the Pinch Analysis with and without intermediate headers are shown in Figure 34a and Figure 34b. The results show that the optimal number of intermediate headers is 2 with the target of minimum fresh resource consumption and waste discharge, see Figure 34b. The first intermediate header (H1) is mixed by the first fresh resource (FR1) and source SR1. Therefore, the first intermediate header H1's flowrate and purity are 892.6 mol/s and 93.6 % after synthesis. The second intermediate header (H2) is synthesised by sources SR2, SR3, SR4, SR5 and SR6, see Figure 34b. The flowrate and purity of the second intermediate header (H2) are 3,057.7 mol/s and 74.9 %. The obtained result of the presented method in this work is identical to the mathematical programming method in literature (Deng et al., 2014). This proves that the extended Pinch Analysis with intermediate headers is feasible and effective. The advantages of the extended Pinch Analysis are visualised and simple, clear physical meaning and easy to understand.

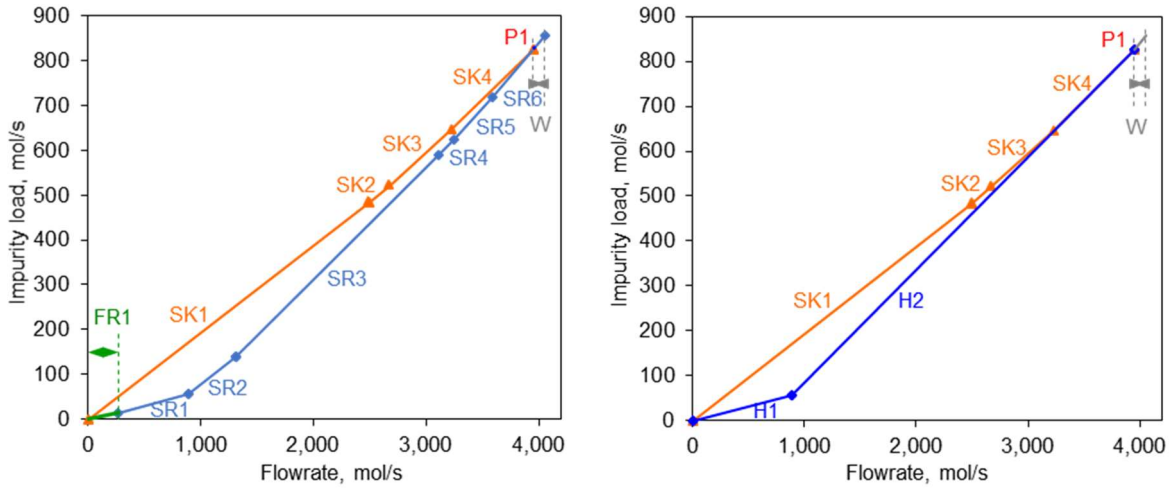

(a) PA without headers (b) PA with intermediate headers

Figure 34. Pinch Analysis of a mass exchange network

II. Intra-plant Mass Integration with Intermediate Headers and Multiple-level Fresh Resources – Hydrogen Network

A mass exchange network (hydrogen network) with multiple-level fresh resources and intermediate headers in a refinery is selected as a case study in demonstrating the proposed method. The data of sources and sinks of the hydrogen network is shown in Table 15. In a hydrogen network, two fresh resources of different qualities are available. The purity and cost of these two fresh resources are shown in Table 16. The annual operating time is assumed 8,000 h. Three scenarios are considered in this case study.

Table 15. Hydrogen sources and sinks in a refinery (Kang et al., 2018)

Sources	Purity, mol%	Flowrate, mol/s	Sinks	Purity, vol%	Flowrate, mol/s
SR1	98.5	657.2	SK1	98.0	582.8
SR2	95.6	1699.0	SK2	97.0	1176.0
SR3	95.0	189.7	SK3	96.0	1071.2
SR4	93.0	322.4	SK4	94.0	334.8
SR5	84.0	186.9	SK5	92.0	135.9
SR6	74.0	49.2	SK6	92.0	171.1
SR7	51.0	175.5	SK7	80.0	401.5
SR8	46.0	135.4			
SR9	29.0	111.6			

Table 16. Data of fresh resources of different qualities (Kang et al., 2018)

Fresh resources	Purity, mol%	Cost, EUR/mol
First fresh resource (FR1)	99.5	3.9×10^{-3}
Second fresh resource (FR2)	95.0	1.9×10^{-3}

- *Scenario 2.1: Pinch Analysis considering only a single fresh resource.*

The results of Pinch Analysis with only the first fresh resource (FR1) are shown in Figure 35a. The minimum first fresh resource (FR1) consumption is 662.7 mol/s, and the minimum waste discharge is 316.3 mol/s. The fresh resource (utility) cost is 20.68 kEUR/y.

- *Scenario 2.2: Pinch Analysis considering multiple-level fresh resources.*

Multi-resource Pinch Analysis is applied for the hydrogen network with two fresh resources of different qualities. The results are shown in Figure 35b. The minimum first fresh resource (FR1) consumption is 411.6 mol/s, minimum second fresh resource (FR2) consumption

is 276.8 mol/s, and minimum waste discharge is 341.9 mol/s. The total cost of fresh resources (utilities) is 17.05 kEUR/y. The cost of fresh resources (utilities) is reduced by 17.5 % compared to Scenario 2.1. It can be seen that the cost of total fresh resources consumption (i.e., utilities) can be reduced by using a lower-quality fresh resource (second fresh resource FR2).

- *Scenario 2.3: Pinch Analysis considering multiple-level fresh resources and intermediate headers*

For the hydrogen network considering two fresh resources of different qualities and intermediate headers, Pinch Analysis with multiple-level fresh resources and intermediate headers is used. The results are shown in Figure 35c. The minimum first fresh resource (FR1) consumption is 411.6 mol/s, minimum second fresh resource (FR2) consumption is 276.8 mol/s, and minimum waste discharge is 341.9 mol/s. Hydrogen network allocation is simplified by setting and optimising intermediate headers. In this case, the optimal number of intermediate headers is 4.

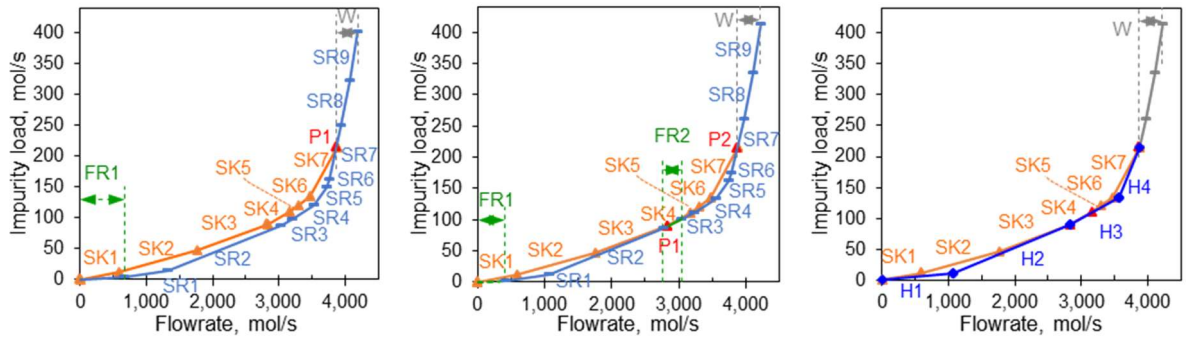

(a) Scenario 2.1 (b) Scenario 2.2 (c) Scenario 2.3

Figure 35. Mass Integration in three different scenarios

The final hydrogen network allocation is shown in Figure 36. Scenario 2.2 (without intermediate headers) is shown in Figure 36a, and Scenario 2.3 (with intermediate headers) is shown in Figure 36b. In Figure 36, the labels starting with SR denote sources shown in light-blue, the labels starting with SK denote sinks shown in orange, the labels starting with FR denote fresh resources shown in green. The labels starting with H (H1 to H4) denote the intermediate headers shown in blue, and the waste discharge is shown in grey. The allocation of all hydrogen streams is represented by arrows marked with flowrate (values without parentheses) and purity (values in parentheses).

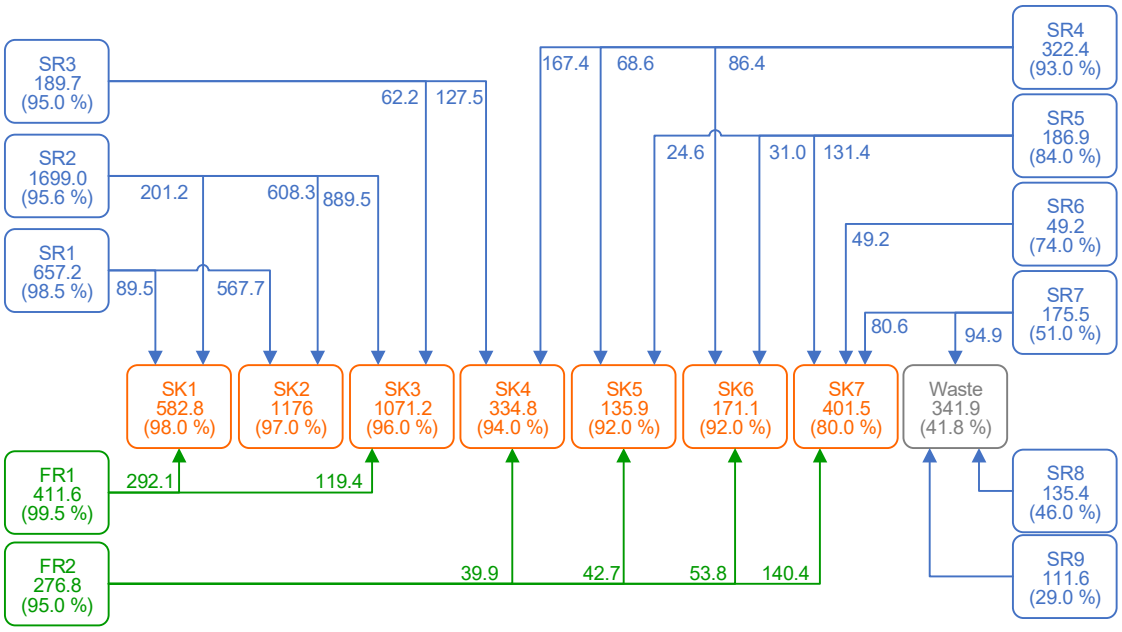

(a) Hydrogen network allocation with multiple-level fresh resources but without intermediate headers

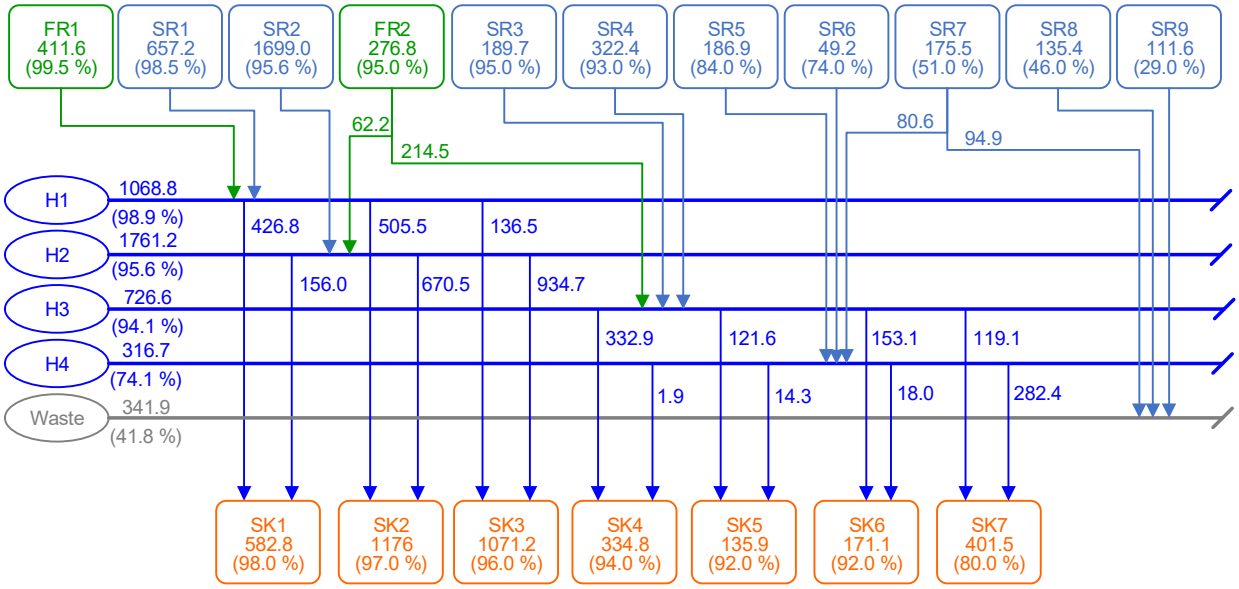

(b) Hydrogen network allocation with multiple-level fresh resources and intermediate headers

Figure 36. Detailed hydrogen network allocation

The minimum fresh resources consumption and minimum waste discharge are all the same in Scenario 2.2 and Scenario 2.3. However, in Scenario 2.2, the number of all connections between suppliers (e.g. fresh resource, source, and header) and receivers (e.g. header, and sink) is 24. The operating parameters of seven sources SR1-SR7 need to be controlled in Scenario 2.2, Figure 36a. In Scenario 2.3, the optimal number of intermediate headers is 4, and the number of

all connections between suppliers (e.g. fresh resource, source, header) and receivers (e.g. header, sink) is 27. The operating parameters of four intermediate headers, H1-H4, need to be controlled in Scenario 2.3, Figure 36b. It can be seen that by setting up and optimising the intermediate headers, the network configuration is simplified, and the scalability and flexibility of the hydrogen network are enhanced.

III. Total Site Mass Integration with Intermediate Headers and Multiple-level Fresh Resources – Water Network

The proposed method of Total Site Mass Integration with intermediate purity headers is demonstrated by mass exchange networks in an industrial park. An inter-plant water integration is considered as a case study. The data of sources and sinks of water networks in three plants is amended from (Chew et al., 2010b), as shown in Table 17.

Table 17. Water sources and sinks

Plant	Sources	C_{SR}, mg/L	F_{SR}, t/h	Sinks	C_{SK}, mg/L	F_{SK}, t/h
Plant A	SRA1	80	66.67	SKA1	0	20
	SRA2	100	20	SKA2	50	66.67
	SRA3	100	100	SKA3	50	100
	SRA4	800	41.67	SKA4	80	41.67
	SRA5	800	10	SKA5	400	10
Plant B	SRB1	80	66.7	SKB1	0	20
	SRB2	100	20	SKB2	50	66.7
	SRB3	400	15.63	SKB3	80	15.63
	SRB4	800	42.86	SKB4	100	42.86
	SRB5	1000	6.67	SKB5	400	6.67
Plant C	SRC1	50	80	SKC1	0	20
	SRC2	100	20	SKC2	25	80
	SRC3	125	50	SKC3	25	50
	SRC4	150	300	SKC4	50	40
	SRC5	800	40	SKC5	100	300

Two scenarios are considered in this case study. Scenario 3.1 is the Total Site Water Integration considering multiple-level freshwater resources but without intermediate headers. Scenario 3.2 is the Total Site Water Integration considering both multiple-level freshwater resources and intermediate headers. The freshwater resource with two different qualities is available, as shown in Table 18. The first freshwater resource (FR1) is clean water at a high price. The second freshwater resource (FR2) is the higher-impurity freshwater with a low price. The

annual operating time is 8,000 h. The presented method in this work is applied to inter-plant water integration.

Table 18. Data of freshwater of different qualities (Foo, 2012)

Freshwater	Purity, mol%	Cost, EUR/t
First freshwater (FR1)	0	0.85
Second freshwater (FR2)	80	0.17

- *Scenario 3.1: Total Site Water Integration considering multiple-level freshwater resources, but without intermediate headers*

The results of Pinch Analysis for Scenario 3.1 are shown in Figure 37. The sources in blue lines (R2 and R3 in Plant A, R4 in Plant C) not touching the Sink Composite Curve are waste discharged with higher-quality by individual plants before Total Site Integration. When integrated at the Total Site level, the higher-quality waste discharged in blue lines can be used as an inter-plant stream to other plants to minimising fresh resource consumption. The blue line with the arrow represents inter-plant flow.

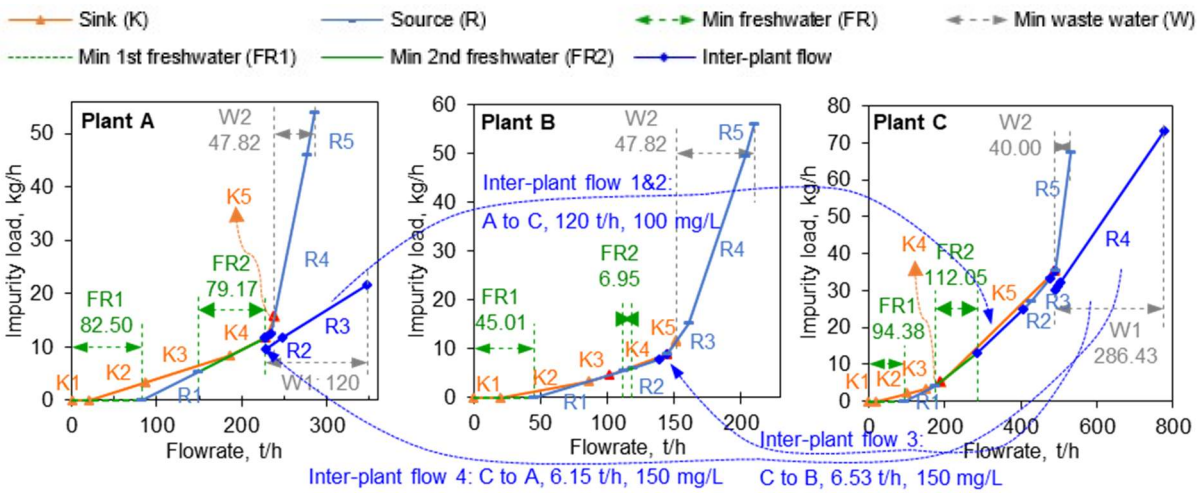

Figure 37. Final Pinch Analysis of Total Site Water Integration with multiple-level freshwater resources, but without intermediate headers (Scenario 3.1)

It can be seen that there are four inter-plant streams for Total Site Water Integration in Figure 37. The source R2 of Plant A is used as inter-plant flow 1 (20 t/h) to the Plant C. Inter-plant flow 2 (100 t/h) is the source R3 of Plant A to the Plant C. Inter-plant flow 3 (6.53 t/h) is the part of source R4 of Plant C to the Plant B. Inter-plant flow 4 (6.15 t/h) is the part of source R4 of

Plant C to the Plant A. The minimum first freshwater resource (FR1) consumption is 221.89 t/h, and the cost is 1.51 MEUR/y. The minimum second freshwater resource (FR2) consumption is 198.17 t/h, and the cost is 0.27 MEUR/y. The minimum wastewater discharge is 420.05 t/h. The total cost of freshwater resources (utility) is 1.78 MEUR/y. When only single freshwater is considered as the literature (Chew et al., 2010b), the minimum first freshwater resource (FR1) consumption is 314.35 t/h, and the minimum wastewater discharge is 314.35 t/h. Compared with the literature results, the minimum first freshwater resource (FR1) consumption is reduced by 29.41 % (92.46 t/h), and the cost is reduced by 0.63 MEUR/y. The minimum second freshwater resource (FR2) consumption is increased by 198.17 t/h, and the cost has increased by 0.27 MEUR/y. The total cost of freshwater resources (utility) is reduced by 16.8 % (0.36 MEUR/y), despite an increase of 105.71 t/h in total freshwater consumption compared to the literature. This is due to the using of cheap secondary freshwater (FR2) with higher impurity.

- *Scenario 3.2: Total Site Water Integration considering both multiple-level freshwater resources and intermediate headers*

The configuration of water networks is simplified by setting and optimising intra-plant headers and inter-plant headers under the target of minimum freshwater consumption and minimum wastewater discharge. The results of Pinch Analysis for Scenario 3.2 are shown in Figure 38. The target of minimum freshwater consumption and wastewater discharge in Scenario 3.2 should achieve the target of Scenario 3.1, which is equal/same. The minimum first freshwater resource (FR1) consumption (221.89 t/h), minimum second freshwater resource (FR2) consumption (198.17 t/h) and minimum wastewater discharge (420.05 t/h) are the same as in Scenario 3.1. The cost of minimum first freshwater resource (FR1) consumption and minimum second freshwater resource (FR2) consumption are 1.51 MEUR/y and 0.27 MEUR/y. The total cost of freshwater resources (utility) is 1.78 MEUR/y. However, the water network allocations are different. It can be seen that the optimal number of intra-plant headers of Plant A is simplified to 3, including a wastewater header. The optimal number of intra-plant headers of Plant B is simplified to 4 (including a wastewater header). The optimal number of intra-plant headers of plant C is simplified to 3 (including a wastewater header). The headers in blue lines (HTS1 in Plant A, HTS2 in Plant C) not touching the Sink Composite Curve are waste discharged with higher-quality by individual plants before Total Site Integration. When integrated at the Total Site level, the higher-quality waste discharged in blue lines can be used as inter-plant headers to other plants to minimising fresh resource consumption. The blue line with the arrow represents the direction of inter-plant flow. It can be seen that there are two inter-plant headers for Total Site

Water Integration in Figure 38. The inter-plant header HTS1 of Plant A is transferred to Plant C. The inter-plant header HTS2 of Plant C is transferred to Plant B and Plant A.

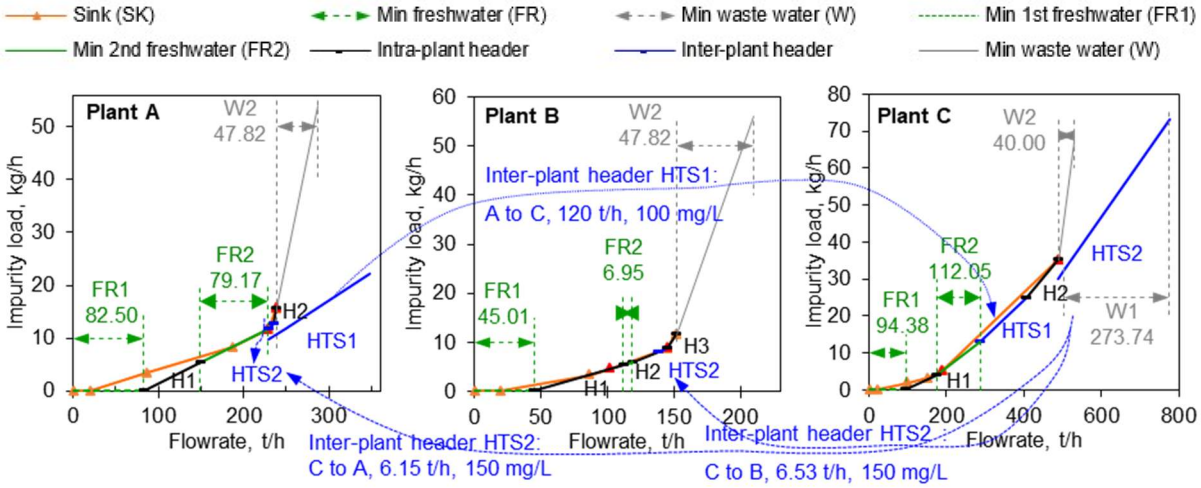

Figure 38. Final results of Total Site Water Integration with both multiple-level freshwater resources and intermediate headers (Scenario 3.2)

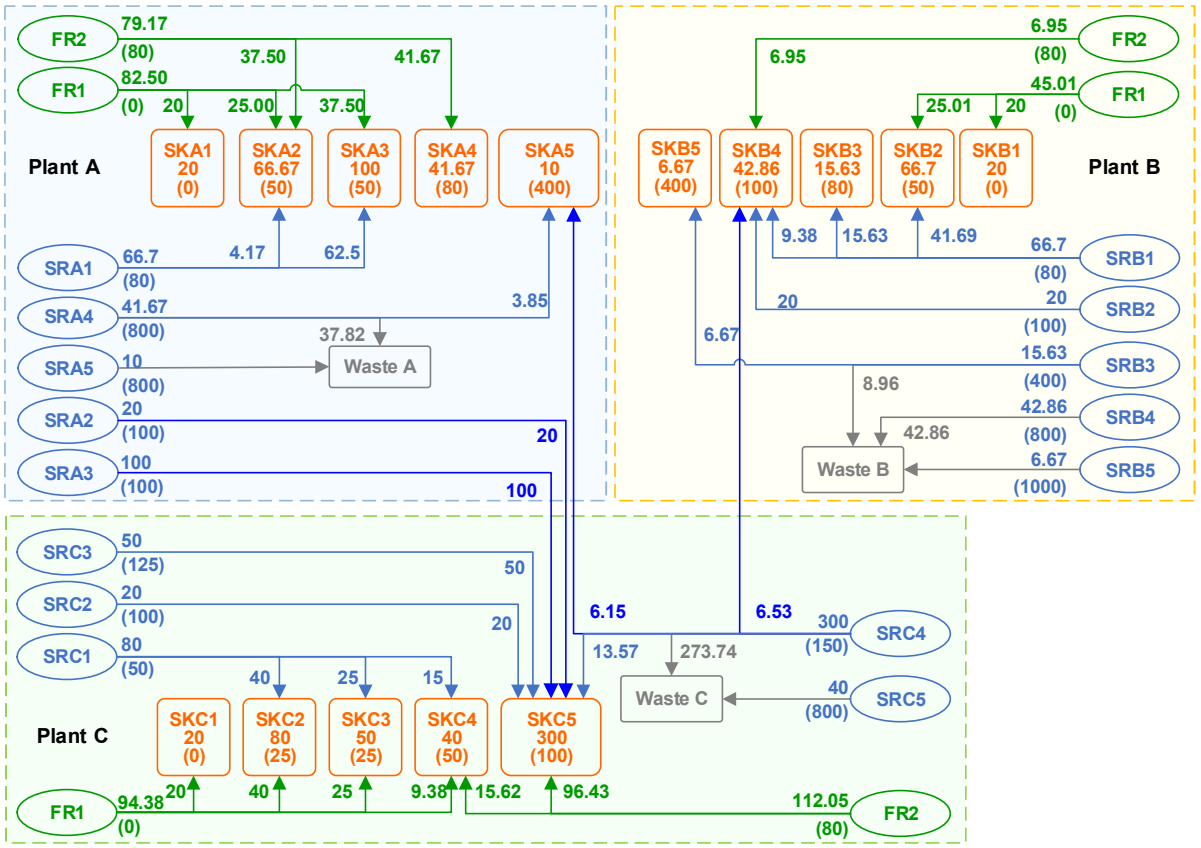

Figure 39. Detailed water network allocation with the multiple-level freshwater resources before setting intermediate headers (Scenario 3.1)

The detailed water network allocations with multiple-level freshwater resources before and after setting intermediate headers are respectively shown in Figure 39 (Scenario 3.1) and Figure 40 (Scenario 3.2). SRA, SRB, and SRC represent the sources of plants A, B, and C shown in light blue. SKA, SKB, and SKC represent the sinks of plants A, B, and C shown in orange. FR1 and FR2 are the first and second freshwater resources shown in green. HA, HB, and HC are the intra-plant headers of plants A, B, and C shown in black colour. Waste discharge is shown in grey. The allocation of all water streams is represented by arrowed lines marked with flowrate (values without parentheses) and impurity (values in parentheses). The blue arrow line in Figure 39 represents the direction of inter-plant flow. There are four inter-plant streams for Total Site Water Integration. Inter-plant flow 1-4 are source R2 of Plant A to the Plant C (20 t/h, 100 mg/L), source R3 of Plant A to the Plant C (100 t/h, 100 mg/L), partly source R4 of Plant C to the Plant B (6.53 t/h, 150 mg/L), partly source R4 of Plant C to the Plant A (6.53 t/h, 150 mg/L), respectively.

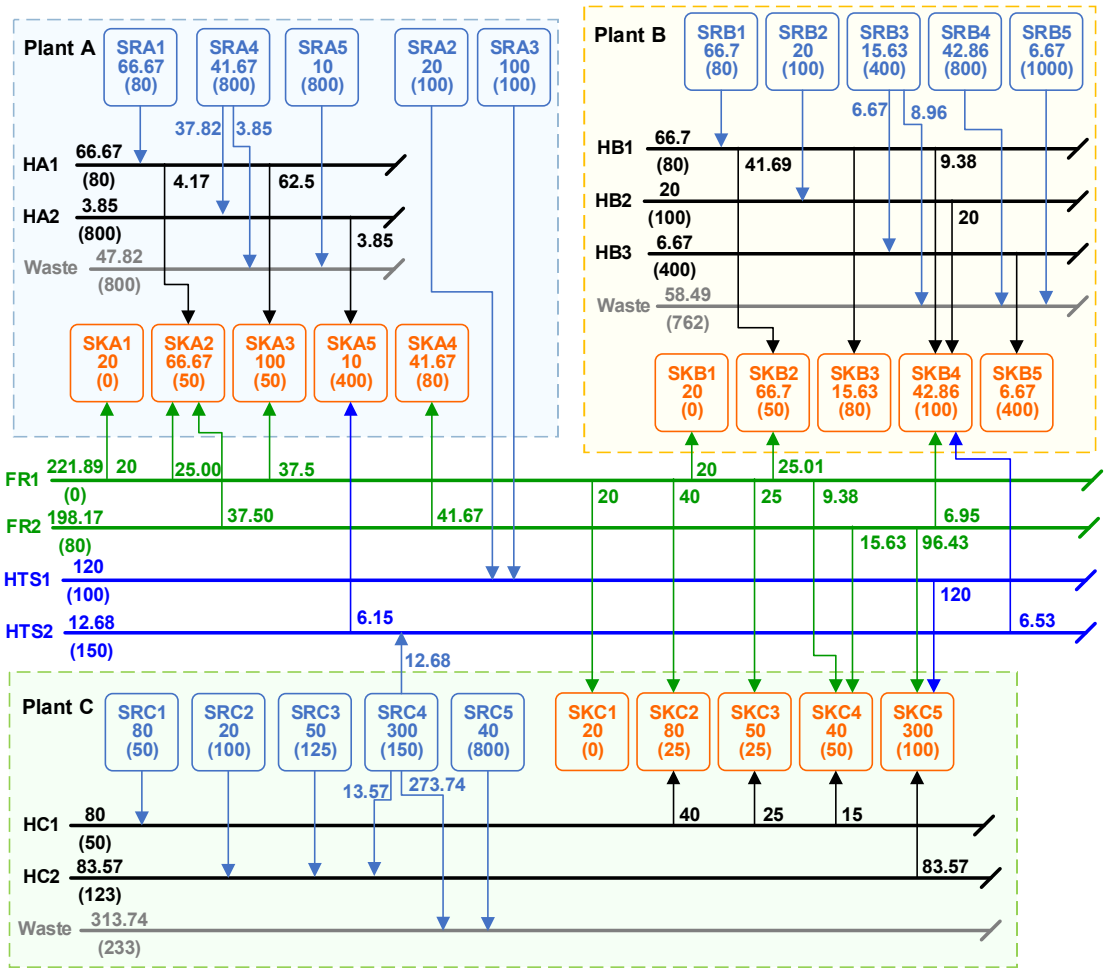

Figure 40. Detailed water network allocation with multiple-level freshwater resources after setting and optimising intermediate headers (Scenario 3.2)

The minimum freshwater consumption and minimum wastewater discharge are the same

in Scenario 3.1 and Scenario 3.2. However, the water network allocations, number of connections, pipes and headers are different. In Figure 40, HTS is the inter-plant header shown in blue, and the blue arrow line represents the direction of inter-plant flow. It can be seen that there are two inter-plant headers (HTS1, HTS2) for Total Site Water Integration. The inter-plant header HTS1 (120 t/h, 100 mg/L) is transferred to Plant C. The inter-plant header HTS2 (12.68 t/h, 150 mg/L) is transferred to the Plant B (6.53 t/h, 150 mg/L) and Plant A (6.53 t/h, 150 mg/L).

Table 19. Results of minimum freshwater consumption, minimum wastewater discharge and intermediate headers

Case study	Terms	Plant A	Plant B	Plant C	Total
Baseline (Ref. (Chew et al., 2010b))	FR1, t/h	98.33	167.78	48.24	314.35
	Wastewater, t/h	47.82	208.05	58.48	314.35
Scenario 3.1	FR1, t/h	82.50	45.01	94.38	221.89
	FR2, t/h	79.17	6.95	112.05	198.17
	Wastewater, t/h	47.82	58.49	313.74	420.05
	No. of connections	11	12	16	39
	No. of inter-plant pipes, -				6
Scenario 3.2	FR1, t/h	82.50	45.01	94.38	221.89
	FR2, t/h	79.17	6.95	112.05	198.17
	Wastewater, t/h	47.82	58.49	313.74	420.05
	No. of connections	15	15	18	48
	No. of intra-plant headers	3	4	3	10
	No. of inter-plant headers				4

The minimum freshwater consumption, minimum wastewater discharge, connections, the optimal number of intra-plant headers and inter-plant headers are summarised in Table 19. The water network configuration is simplified after setting up and optimising intermediate headers (i.e., Scenario 3.2), although the number of connections increased by 9 from 39 to 48. The optimal total number of intra-plant headers are simplified to 10, including 3 wastewater headers (grey lines, 1 wastewater header per plant). The optimal total number of inter-plant headers are 4, including 2 freshwater headers. It can be seen that the scalability and flexibility of the water network are enhanced by setting up and optimising the intermediate headers.

4.4 Conclusions

The integration of mass exchange networks with headers of intermediate purity and multiple-level fresh resources is investigated to reduce the consumption of expensive higher-

quality fresh resources and simplify the configuration of mass exchange networks. An extended Pinch Analysis method is developed in this study, dealing with Total Site Mass Integration and considering the supply of fresh resources of various quality levels. An extended Pinch Analysis with multiple-level fresh resources and intermediate headers is proposed. The optimal waste regeneration process is identified by a techno-economic analysis, in which the advantages and application range of different purification technologies are considered.

I. Multiple-level fresh resources Pinch Analysis (PA-MLFR) with optimising waste purification in mass integration

   The proposed method is demonstrated through a hydrogen network case study consisting of three refineries in a petrochemical industrial park. The results show that compared with only intra-plant integration (baseline scenario), minimum second fresh hydrogen (fresh hydrogen with 95.0 % purity, FR2-95%) consumption and waste hydrogen discharge are reduced by 7.7 % and 21.3 % in Total Site Hydrogen Integration without waste hydrogen purification.

   Waste hydrogen is further regenerated after Total Site Hydrogen Integration. The minimum second fresh hydrogen (FR2-95%) consumption and minimum waste hydrogen discharge are reduced by 21.3 % and 67.6 %. It suggests the overall 25.0 % and 74.5 % reduction of minimum fresh hydrogen consumption (-29.27 kNm^3/h) and waste hydrogen discharge (-28.83 kNm^3/h) can be achieved compared with the baseline scenario. The hydrogen recovery ratio is 95.2 %, the total annual profit is 15.93 M€/y, and the payback period is 3.2 months for the waste hydrogen purification process. A higher hydrogen saving is achieved by optimising the waste hydrogen purification process after Total Site Hydrogen Integration. It reduces the waste hydrogen discharge and reduces environmental pollution by transforms waste hydrogen into useful secondary raw material, reducing minimum fresh hydrogen consumption. The proposed integrated design with the hydrogen purification process offers significant economic benefits.

II. Multiple-level fresh resources Pinch Analysis with intermediate headers (PA-MLFR-IH) in Mass Integration

   Hydrogen networks in refineries and water networks are taken as case studies in demonstrating the proposed method.

   In hydrogen integration, the results show that the cost of fresh resources (utilities) is

reduced by 17.5 % in Scenario 2.2 with multiple-level fresh resources compared to Scenario 2.1, considering only a single fresh resource. The cost of total fresh resources consumption (utilities) can be reduced by using a lower-quality fresh resource. The number, connection, and purity of intermediate headers are optimised with the target of minimum fresh resources consumption and waste discharge. The optimal number of intermediate headers is 4, and the number of connections is 27 in Scenario 2.3, considering multiple-level fresh resources and intermediate headers.

In water integration, the total cost of freshwater resource (utility) is reduced by 16.8 % (0.36 MEUR/y), despite an increase of 105.71 t/h in total freshwater consumption, by using the cheap secondary freshwater (FR2) with higher impurity compared with only single freshwater. After setting up and optimising the intermediate headers, although the number of connections increased by 9 from 39 to 48. However, the optimal total number of intra-plant headers and inter-plant headers are respectively simplified to10 (including 3 wastewater headers), and 4 (including 2 freshwater headers).

The two case studies of hydrogen integration and water integration both show that: the network configurations are simplified, and the scalability and flexibility of the hydrogen network are enhanced by setting up and optimising the intermediate headers while keeping the target of minimising fresh resources consumption and waste discharge.

The extended Pinch Analysis has the advantages of visualised and simple, clear physical meaning and easy to understand and techno-economic analysis is implemented for waste purification. Total Site Mass Integration with multiple-level fresh resources based on Pinch Analysis (with/without intermediate headers) proposed in this work could make a significant contribution to resource conservation and environmental protection. However, issues such as the safety and agreement between factories for integration require further assessment. The effects of multiple-contaminants are yet to be assessed, which could challenge the Total Site Mass Integration without pre-treatment units. This will be considered by the mathematical programming method in our future work. Future work will also consider the integration of hydrogen and work exchange networks with hydrogen pressure.

CHAPTER 5 HIERARCHICAL TARGETING OF HEAT AND MASS INTEGRATION

The work presented in this chapter is based on the author's publication in Chemical Engineering Transactions entitled "Hierarchical Targeting of Hydrogen Network System and Heat Integration in a Refinery", as clarified on Page VII (Contributing publication). The author of this thesis is the first and corresponding author of this publication. The other co-authors who contributed to this publication are the supervisor (Varbanov, P.S.), co-supervisor (Klemeš, J.J.) and collaborator (Sun, L.). My original contributions are listed in the introduction.

5.1 Introduction

With the long-term rise of the energy demands, the requirements of energy-saving and emission reduction of petroleum refineries keep increasing. In the cost structure of the refining industry, energy consumption is a major item, next to crude oil purchase. It accounts for more than half of the cash operating expenses of an enterprise. Reducing energy consumption is of great significance for a refinery helping to reduce production costs, improve economic benefit and enhance competitiveness, promote environmental protection and socially sustainable development. The Pinch Methodology (Klemeš, 2013) is based on thermodynamics to analyse energy distribution along with temperature in the process to find the "bottleneck" of an energy system and remove the "bottleneck". Pinch Analysis (Klemeš et al., 2018b) is one of the bases of Heat Integration (HI) technology development. It is a method of targeting and prioritising the integration of process energy systems. The energy conservation methods of refineries have been developed from individual Process Integration (Chen et al., 2004) to Total Site Heat Integration (Klemeš et al., 1997).

Hydrogen as an important raw material in refineries has been paid more and more attention. The H_2 demand for refineries keeps increasing rapidly, and the cost of H_2 is rising too. The problem of H_2 supply shortage is becoming increasingly prominent (Lou et al., 2019). How to use H_2 reasonably and make the best use of everything has become a new problem faced by refineries. It is necessary to analyse, optimise and control H_2 network to reduce production cost and improve H_2 utilisation. It has great significance to improve the economic benefit of the refinery. H_2 Pinch is an extension of Pinch Analysis for Heat Integration. H_2 Pinch analysis is an important method for H_2 network optimisation. Since it was put forward in the late 1990s (Alves, 1999), it has made a mature and steady development (Elsherif et al., 2015) in solving the bottleneck of H_2 networks. It has the advantages of being simple and

intuitive, efficient and easy to understand. A variety of H_2 Pinch Analysis tools have been proposed, such as the H_2 Surplus Diagram (Alves, 1999), Material Recycle Pinch Diagram - MRPD (El-Halwagi et al., 2003), Average Pressure Profiles (Ding et al., 2011), Material Surplus Composite Curve (Saw et al., 2011) and H_2 network purification targeting (Zhang et al., 2016).

Following the foundational work on Total Site Heat Integration (Klemeš et al., 1997), there have been other studies, including algorithmic targeting (Liew et al., 2017) and extensions to trigeneration (Jamaluddin et al., 2019). Hydrogen Integration (Lou et al., 2019) is still considered separately. Few studies have considered both Heat Integration and H_2 optimisation in refineries. However, Heat Exchange Networks and H_2 Mass Networks coexist in most cases. Petroleum refineries are big consumers of both energy and hydrogen. It is necessary to consider both the Total Site Integration of heat and H_2 simultaneously in refineries to minimise resource consumption and emissions.

This study aims to combine H_2 and Heat Integration. The novel contributions of the presented study are: It investigates the heat exchange network and mass network by applying the Onion Model. A hierarchical targeting method of energy and H_2 is proposed by combining Onion Model and Pinch Analysis.

A petroleum refinery is taken as a case study. The energy and hydrogen consumption are analysed and optimised by using the proposed method.

5.2 Method

This section starts with refineries as the research object to study the Total Site Integration of both mass and energy. Refineries are significant consumers of energy and hydrogen. Hydrogen in the refinery not only takes part in the hydrogenation reaction, but the related streams also need heating and cooling before/after the hydrogenation. The H_2 Network (HN) and the Heat Exchanger Network (HEN) affect each other in refineries. It is necessary to consider the Total Site Integration of both heat and H_2 in refineries to minimise resource consumption and emissions. The problem of combined Mass and Heat Integration is investigated based on the Onion Model. A hierarchical targeting method of heat and hydrogen is proposed. The proposed method allows simultaneous energy-saving and emission reduction for a refinery. The procedure amends from the Onion Model (Linnhoff et al., 1994) for targeting the Hydrogen Network (HN) and HEN of a refinery, as shown in Figure 41. Hydrogen network

spans two layers of "Reactor" and "Separation & recycle". Heat Integration belongs to two layers of HEN and the utility system. H_2 flows belong to the inner layer and heat to the outer layer. H_2 and heat can be hierarchy targeted.

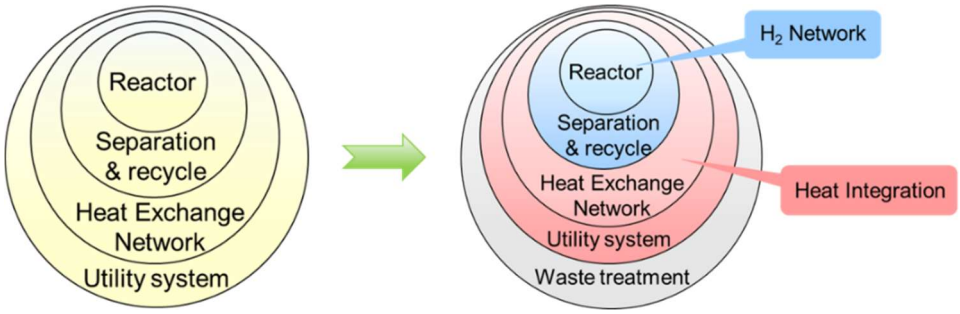

Figure 41. Onion Model of the production process, amended from (Linnhoff et al., 1994)

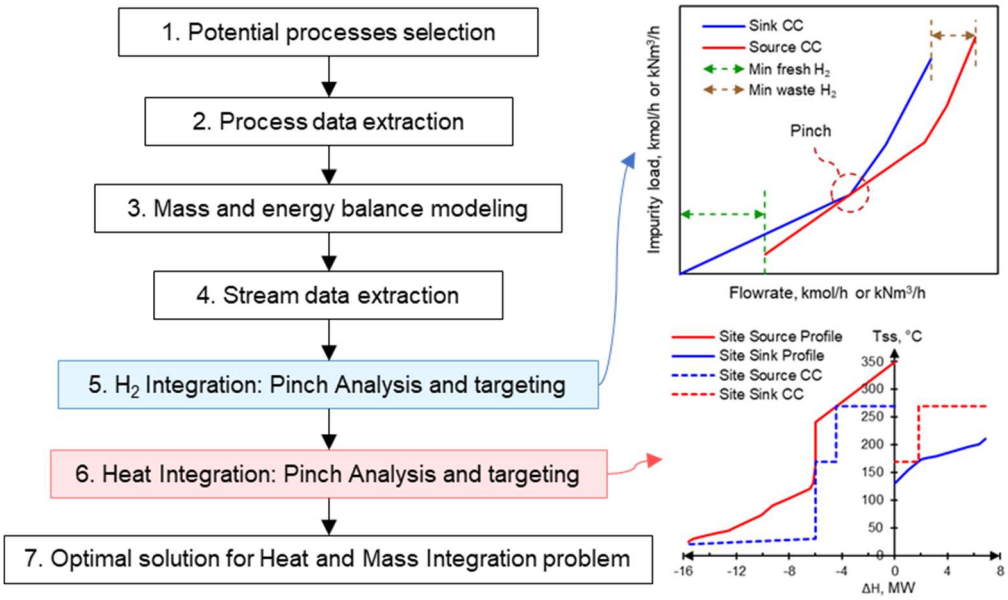

Figure 42. Procedure for Mass and Heat Integration

In the current work, the heat recovery problem is formulated from the H_2 network design. The interface between two integration phases is Data Extraction which identifies and specifies process streams for Heat Integration. At the stage of process design and targeting, the detailed information for building a model, which reflects the interactions between reactors, separators and heat recovery subsystems, is not available. This makes the feedback link from the heat recovery subsystem to the mass integration subsystem indirect. Upon performing Heat Integration, the incentive for reduction of energy demands can be evaluated, and core process

changes can be initiated based on energy analysis. The method of Mass and Heat Integration is as shown in Figure 42. The hydrogen network should be targeted first. Hydrogen Pinch was used to analyse hydrogen network bottleneck and diagnose unreasonable hydrogen use. Following with integration of the hydrogen network, HEN was targeted by Total Site Heat Integration.

5.3 Case Study

A refinery is taken for a case study. Firstly, the H_2 Network in the inner layer of the onion is targeted. The H_2 Pinch is used to target the whole H_2 Network. The H_2 source and H_2 sink streams data are shown in Table 20, based on an adaptation of (Wang, 2012). The stream SR1 with the highest purity of H_2 is considered to be the H_2 utility.

Table 20. Streams of an H_2 Network (HN) in a refinery

Stream type	Streams	H_2 concentration, vol%	Flowrate, kNm^3/h	H_2 load, kNm^3/h
H_2 source	SR1	99.9	22.75	22.73
	SR2	95.6	164.05	156.83
	SR3	92	137.05	126.09
	SR4	89	240	213.60
	SR5	88	5.07	4.46
	SR6	85	54.65	46.45
	SR7	84.3	5	4.22
H_2 sink	SK1	99.9	10	9.99
	SK2	95.1	188.2	178.98
	SK3	93.5	11.82	11.05
	SK4	92	102.08	93.91
	SK5	90.3	280	252.84
	SK6	89.2	1.73	1.54
	SK7	88.2	4.08	3.60
	SK8	85.8	64.65	55.47

According to the method in Section 5.2.2, the Cascade Table is used for calculation, and the resulting H_2 Pinch diagram is shown in Figure 43. The targets for the H_2 Pinch, the required minimum utility H_2 and the minimum waste H_2 emission of the H_2 Network are obtained. The H_2 source Composite Curve (CC) and H_2 sink CC at the Pinch is shown in Figure 43a. According to the calculation, the H_2 Pinch concentration of the H_2 network is 89 %, as shown in an enhanced plot segment (Figure 43b). At H_2 Pinch, the minimum utility H_2 required for the H_2 Network is 10.95 Nm^3/h (Figure 43c). The minimum waste H_2 discharged is 32.13

Nm^3/h (Figure 43d). It can provide guidance for the corresponding design and optimisation of the H_2 network. If the discharged waste H_2 can be recycled, it can further reduce the use of H_2 utilities.

The H_2 Pinch determines the target consumption and concentration of new and circulating H_2 in the different hydrotreating units. The H_2 streams need to be heated or cooled before or after hydrotreating. The H_2 Network Integration affects the optimisation of Heat Exchanger Network. Now comes HEN targeting. The hydrogen installations of a refinery are also big energy consumers. Hydrotreating (Robinson and Dolbear, 2006) unit is mainly the hydrotreating of distillate oil, including gasoline, diesel and kerosene. The process is roughly the same. The raw oil is mixed with circulating H_2 and heated to a certain temperature before entering the reactor for hydrotreating reaction. After the reaction product is separated from the circulating H_2, the product is removed from the unit by stripping or fractionation. The specific process flow is slightly different, but the process operating conditions are significantly different. The energy consumption structure of the unit varies greatly.

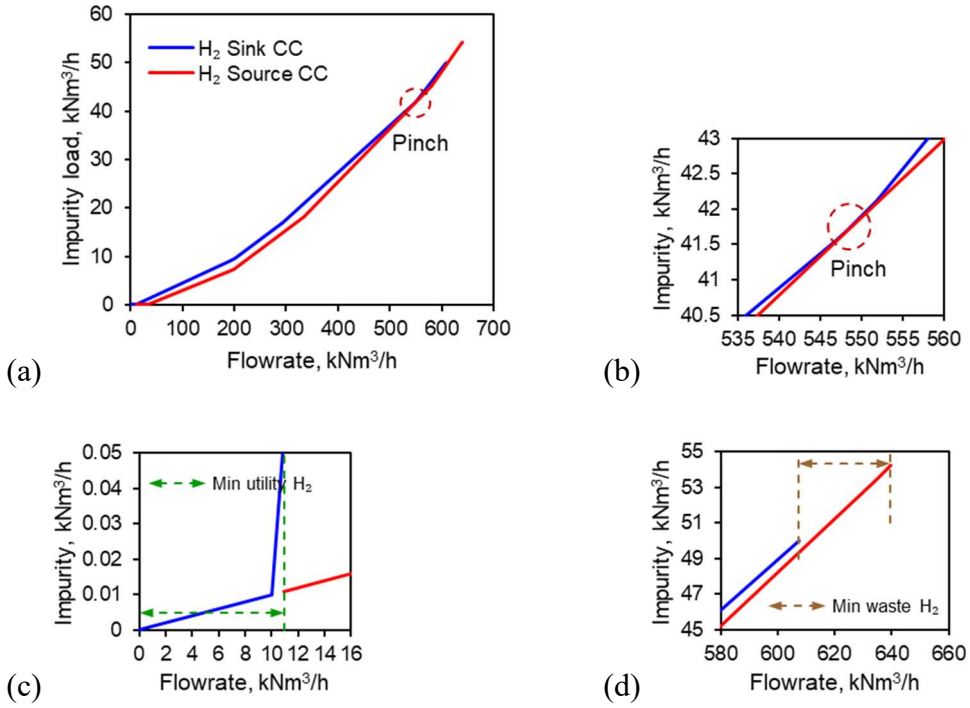

Figure 43. H_2 Network Pinch diagram for (a) the H_2 CC; (b) H_2 Pinch; (c) minimum utility H_2; (d) minimum waste H_2 discharge

In this study, the Heat Integration analysis and optimisation of three different hydrotreating processes in a refinery are studied. The process streams of three different hydrogenation units are shown in Table 21 based on an adaptation (Zhang et al., 2013). Streams Cold A2 (H_2), Cold B2 (H_2), Hot C6 (H_2) and Cold C2 (H_2) are H_2 extracted from the H_2 Network. Energy analysis is carried out in each unit according to the method described above. The GCCs of all units are given (Figure 44). It can be seen that unit A still had an 8.25 MW excess heat source after adequate heat recovery in the unit (Figure 44a). Unit B had a 2.94 MW redundant heat sink and 4.26 MW redundant heat source (Figure 44b). Unit C also had a 3.96 MW redundant heat sink and a 3.10 MW redundant heat source (Figure 44c). The Heat Integration between units has great potential for energy saving.

Table 21. Streams of three different hydrotreating processes

Stream type	Stream name	T_s, °C	T_t, °C	ΔH, MW	Flowrate, kNm^3/h
Hydrotreating Unit A					
Hot stream	Hot A1	360	35	17.91	
	Hot A2	165	40	5.23	
Cold stream	Cold A1	35	168	4.73	
	Cold A2 (H_2)	70	125	0.59	27.5
	Cold A3	40	103	1.92	
	Cold A4	103	220	7.26	
Hydrotreating Unit B					
Hot stream	Hot B1	272	207	10.3	
	Hot B2	205	36	2.33	
	Hot B3	197	40	15.04	
	Hot B4	140	42	1.94	
Cold stream	Cold B1	45	166	10.93	
	Cold B2 (H_2)	50	188	0.56	10.4
	Cold B3	164	243	15.54	
	Cold B4	36	170	1.26	
Hydrotreating Unit C					
Hot stream	Hot C1	395	220	19.12	
	Hot C2	225	95	12.67	
	Hot C3	220	50	3.31	
	Hot C4	155	40	1.47	
	Hot C5	220	50	0.4	
	Hot C6 (H_2)	395	220	8.53	125
Cold stream	Cold C1	120	370	26.1	
	Cold C2 (H_2)	73	370	20.26	175

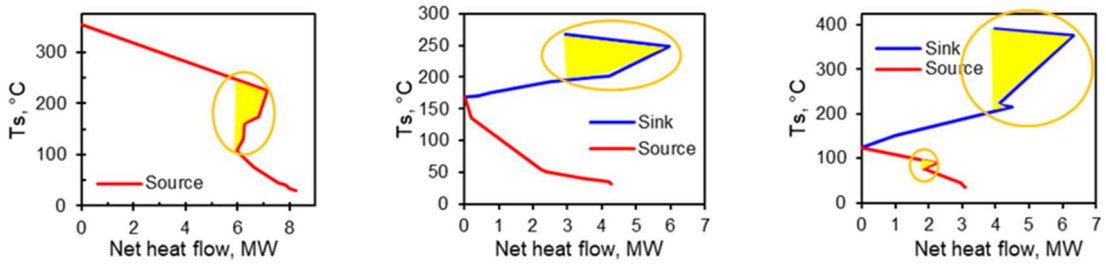

Figure 44. GCC of three different hydrogenation processes for (a) Unit A; (b) Unit B; (c) Unit C

Total Site Analysis is used to integrate the heat between the units. Total Site Profiles with utilities are shown in Figure 45. The solid red curve represents the Site Source Profile, and the solid blue curve represents the Site Sink Profile. The utility includes high-pressure (HP) steam (55 bar, 270 °C), medium-pressure (MP) steam (8 bar, 170 °C), and cooling water supplied at 20 °C and returned to the utility system at 30 °C. The blue dotted curve represents the site source CC, and the red dotted curve represents the Site Sink CC. It can be seen that the heat source can generate 4.41 MW HP steam and 1.57 MW MP steam. It also needs 9.64 MW of cooling water. The heat sink requires 5.09 MW HP steam and 1.81MW MP steam.

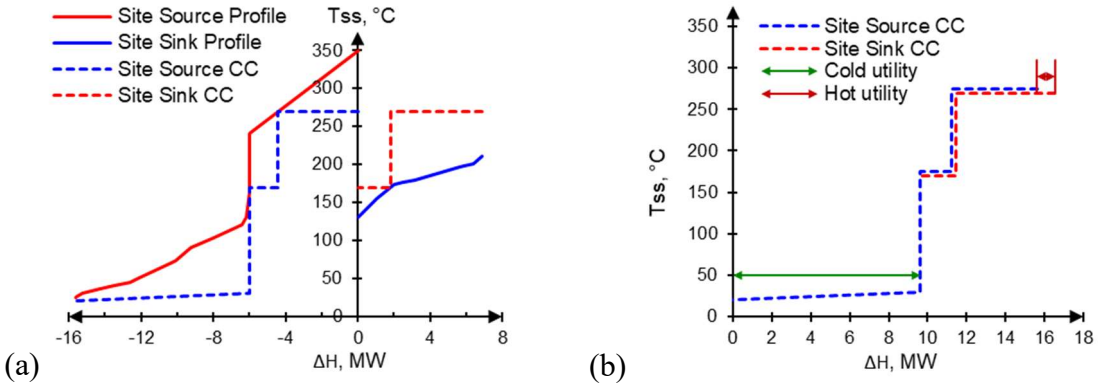

Figure 45. Total Site Composite Curves (TSCC) (a) Total Site Profiles with utilities; (b) Hot Utility Generation Composite Curve (HUGCC)

To identify the minimum cold and hot utilities for inter-unit integration, the Site Source CC and Site Sink CC were combined to obtain the Hot Utility Generation Composite Curve (Figure 45b). The minimum hot utility is 0.93 MW, and the cold utility is 9.4 MW. Before the Interplant integration, the minimum hot utility required for the three processes was 6.91 MW, and the minimum cold utility required was 15.62 MW. This shows a significant utility saving

potential – up to 86.5 % of hot utilities and 39.8 % of cold utilities. This would require further analysis and calculation of the economy (for extra Heat Exchanger (HE), piping, possible extra pressure drop, safety issues).

5.4 Conclusions

In this chapter, a hierarchical targeting procedure for combined hydrogen and heat integration in refineries is presented by applyingbased on the Onion Model for the problem of combined hydrogen and heat integration in refineries. Hydrogen Pinch is used to target the hydrogen network performance. Total Site Composite Curves are used to target the HI of the refinery. The case study results show that the H_2 network targeting can guide the optimisation of the H_2 Network, simultaneously reducing H_2 utility demands and the waste H_2 emissions. At the Total Site level, the targets show that the maximum reduction can be 86.5 % for hot utilities and 39.8 % for cold utilities. The unidirectional method, which combines the Onion Model and Pinch Analysis, is simple to use and has the advantages of graphic visualisation.

It has been demonstrated that the combined targeting of H_2 and thermal utilities for a refinery can save significant amounts of both types of resources, leading to potential environmental and economic benefits. Future steps should consider pressure drops and investments. This should include the analysis of economic benefits, piping, pressure drop, and safety issues.

CHAPTER 6 MASS AND ENERGY TRADE-OFFS

The work presented in this chapter is based on the author's publication in Resources, Conservation and Recycling entitled "Trade-offs between the Recovery, Exergy Demand and Economy in the Recycling of Multiple Resources", as clarified on Page VI (Contributing publications). The author of this thesis is the first and corresponding author of this publication. The other co-authors who contributed to this publication are the supervisor (Varbanov, P.S.), co-supervisors (Klemeš, J.J. and Fan, Y.V.) and collaborator (Romanenko, S.V.). My original contributions are listed in the introduction.

6.1 Introduction

Process optimisation should conform to the principle of Circular Economy (CE). Circular Economy is a systematic framework confined to recycling as well as accounting for the efficiency and the economy. Implementing a Circular Economy arrangement requires technology development, investment, and operating cost. Enterprises in the chain of Circular Economy should bring economic benefits along with pollution reduction to ensure sustainable development. Techno-economic analysis (Martínez et al., 2020) is needed for Process Integration. Output has to be higher than the input to be valuable. One of the ways to improve the sustainability of industrial processes is the application of Circular Economy (CE). CE minimises at a macro-scale the consumption of virgin resources and primary energy by maximising the recycling and recovery of material and energy.

The concept of CE has attracted considerable attention from scholars and practitioners. Suárez-Eiroa et al. (2019) reviewed the sources related to CE. They proposed the principle of combining the CE theoretical goal within the framework of sustainable development with the practical implementation strategy. In 2020, the European Commission adopted a new Circular Economy Action Plan (European Commission, 2020). This was one of the main blocks of the European Green Deal (European Commission, 2019) and a new agenda for sustainable development of the European Union (EU). A series of policy recommendations (Hartley et al., 2020) from the Life Cycle perspective and a set of new targets (Morseletto, 2020) was proposed to facilitate the transition to a CE. CE requires appropriate assessment tools to make progress. Many circularity indicators are available to evaluate the usefulness of circular arrangements, which is reviewed by Saidani et al. (2019). They can be applied to a multitude of contexts, ranging from multiple chemical species evaluation and up to regional or global system boundaries. Some of the indicators focus on the recovery of materials (e.g. "Circular Material

Use Rate") (Eurostat, 2018), others on energy (e.g. circularity of energy) (Zore et al., 2018) or combine both (e.g. Circularity Product Indicator) (Angioletti et al., 2017). There are also several indicators evaluating the monetary equivalents of mass or energy flows or their ratios. However, for the ECI, only the quantity of energy is considered, and the quality of energy is ignored.

Although the concept of CE is intuitively easy to understand, implementing it in practice is challenging (Kirchherr et al., 2017a) as the effectiveness of basic technical solutions is hampered (Kirchherr et al., 2018). PI is an engineering methodology for minimising resource consumption in line with the goals of CE. It can provide some of the necessary design tools for the implementation of CE. Some of the reviewed works, representative of the state-of-the-art, deal with issues relevant to the use of secondary resources via CE – emphasising the degree of circularity itself. Others model the resource recovery in terms of waste heat, wastewater, or combinations of those, as well as exergy efficiency. The Circular Integration (Walmsley et al., 2019a), extended by Fan et al. (2019) and more recently including the widely discussed plastics by (Klemeš et al., 2020), sets the thinking towards the need to consider mass and energy flow integration jointly, on the example of organic materials reuse. It has been shown in (Varbanov et al., 2020b) that material and energy flows follow different patterns, which sets them as two interacting dimensions in process efficiency evaluation. This observation indicates that the consideration of the mass and energy flows together still needs to be further improved to evaluate their interaction clearly, also accounting for the economic cost.

This work aims to extend the PI approach to target recycling and reuse of multiple resources. The multitude of properties and possible criteria can be assessed, allowing comparison, which would enable ranking the usefulness and the desirability of the options. In the recycling and reuse of waste streams as secondary resources, the trade-offs between the recycling and the supply of fresh resources determine the overall resource use and environmental impact of each process. A higher circularity generally means that more secondary products substitute the use of fresh resources (utilities). However, recycling affects both energy consumption and investment. The implementation of circularity measures also requires investment and some operating resources. For multi-resource systems, even with fixed circularity, the primary (virgin) and secondary (waste) resource supplies can be processed via different processing paths. This provides additional degrees of freedom, where energy consumption and investment may differ among the paths. Most of the previous research deals with circularity or economic benefits alone. The optimal performance of the multi-resource

system cannot be fully reflected by the degree of circularity alone. This brings up the question: How much circularity should be reached to be beneficial? Balancing and optimising these trade-offs is critical to achieving more sustainable system design and operation.

The presented study builds on the previous knowledge and formulates several new concepts for explicitly modelling the trade-offs between the mass and energy flows in Circular Integration. These concepts include a Conceptual Map for connecting secondary resources to resource demands via reuse paths, adjustment of the circularity indicators, and an evaluation model optimising the cost and energy-based criteria in relation to the degree of circularity. The novel contributions of the presented study are:

I. The Total Circularity Index (TCI) is proposed to consider both the materials and energy of a circular process system intended to close the resource cycle – connecting waste streams to resource demands. This index is formed by combining the Circular Exergy Use rate (CEU) – an extension from the "circularity of energy" in (Zore et al., 2018), and the Circular Material Use Rate (CMU) (Eurostat, 2018). TCI is essential to assess the trade-off between the degree (CMU) and quality (CEU) of circularity.
II. A novel model is proposed, linking the quantities of reused materials and energy with the use of additional resources enabling that reuse, as well as the use of resources in a linear (non-circular) way and the cost of running the system.
III. The three-way trade-off between the degree of circularity (CMU, CEU and TCI) (quantity), exergy (quality) and cost have been assessed.

The remainder of the manuscript is organised to guide the reader as follows. Section 6.2 starts with the basic concept and the scientific hypothesis. Based on those, it introduces the concept map for integration of the secondary (waste) resources. Two formulations are given that optimise the resource recycling system. As objective functions, the first uses the overall exergy input, and the second uses the total cost. In Section 6.3, a case study of a multi-resource system is provided to illustrate the discussed method. The conclusion section starts with a summary of the proposed method and the obtained results. They are then analysed, which is followed by recommendations for future work.

6.2 Method

An integration plan for multi-resource systems can be seen as a set of paths to deliver resources from supplies of secondary resources to demands for products and resources, which

compete with the delivery of products from fresh resources. Each path has different processing steps with varying complexity. These may require additional fresh resources – energy, water, other materials, to drive them. This diversity of choices defines the need for a unified framework of analytical concepts and tools.

The Concept Map of multiple resources integration is proposed, as discussed in the following sub-section. The CMU is combined with the Circular Exergy Use rate (CEU). This is an indicator extending the concept of circularity of energy use (Zore et al., 2018). The combined representation of CMU and CEU defines the Total Circularity index – TCI. TCI is used to capture the overall degree of circularity because, in the general case, product demands can be both material-based and energy-based. Their formulated concepts are integrated into a mathematical optimisation model. The model has two variations of the objective function reflecting the energy use, represented by exergy and the cost.

6.2.1 Multi-resource integration map

An energy-supply chain scheme was presented by Yan et al. (2016). Their diagram is a visual representation of the paths delivering energy from primary energy resources. A useful pattern can be noticed in that diagram, having blocks for resource supply, conversion paths (the authors call them devices), followed by a block for the energy demands. In the current work, this pattern is generalised and adapted, leading to the Multi-Resource Integration Map shown in Figure 46. The extension consists of consideration of resources and demands of both material and energy nature. The map is applied in the context of capturing waste streams as secondary raw materials and processing them into products for supplying to demands. The circular Integration diagram (see Figure 1) shows that some processes in the system take virgin resources, which are then processed and end up as products and waste. The parts of the scheme that close the cycle by processing waste streams to secondary resources are outlined with the blue dashed contours.

Within the context of the reuse of multiple resources, it is necessary to provide a clear meaning for the term “utility”. Traditionally, in the Process Design and PI literature, the term “utility” is used with the meaning of heating, cooling, or power supplied externally to the considered process system. This can be seen from the study on modelling and optimisation of utility systems (Varbanov et al., 2004) and the recent application of the Total Site concept to the Organic Rankine Cycle integration (Kamarudin et al., 2018). However, the concept is generally used in a broader context – for instance, for water-related services – freshwater

supply or wastewater management (Jiang et al., 2019), as well as for hydrogen networks (Huang and Liu, 2019). Based on this pattern, the term utility is generalised in the current work to denote the supply of materials or services based on the use of fresh resources.

The Multi-Resource Integration Map (Figure 46) includes secondary resources based on waste, demands and utilities. The secondary resource streams are denoted as **WR(1)** (Waste Resource 1) to source **WR(n1)**. These secondary resources go through various treatment paths to yield secondary products to be utilised by the demands. In this processing, some additional external energy and material inputs are needed. Footprints - such as GHG and other waste are also generated as a result of operating the secondary resource processing. Utilities are used to meet demands when the secondary products are insufficient. Common utilities include fluids for process heating (steam, hot oil or specialised heat transfer fluids) and process cooling (cooling water, chilled water, refrigerant), power, fuel for fired heaters (e.g. coal, oil, natural gas, biofuels), water (water for general use, demineralised water), compressed air, inert-gas supplies (usually nitrogen). It is expected that the resource expenditure and footprints associated with the secondary raw material processing are smaller than those resulting from the linear economy processing pattern.

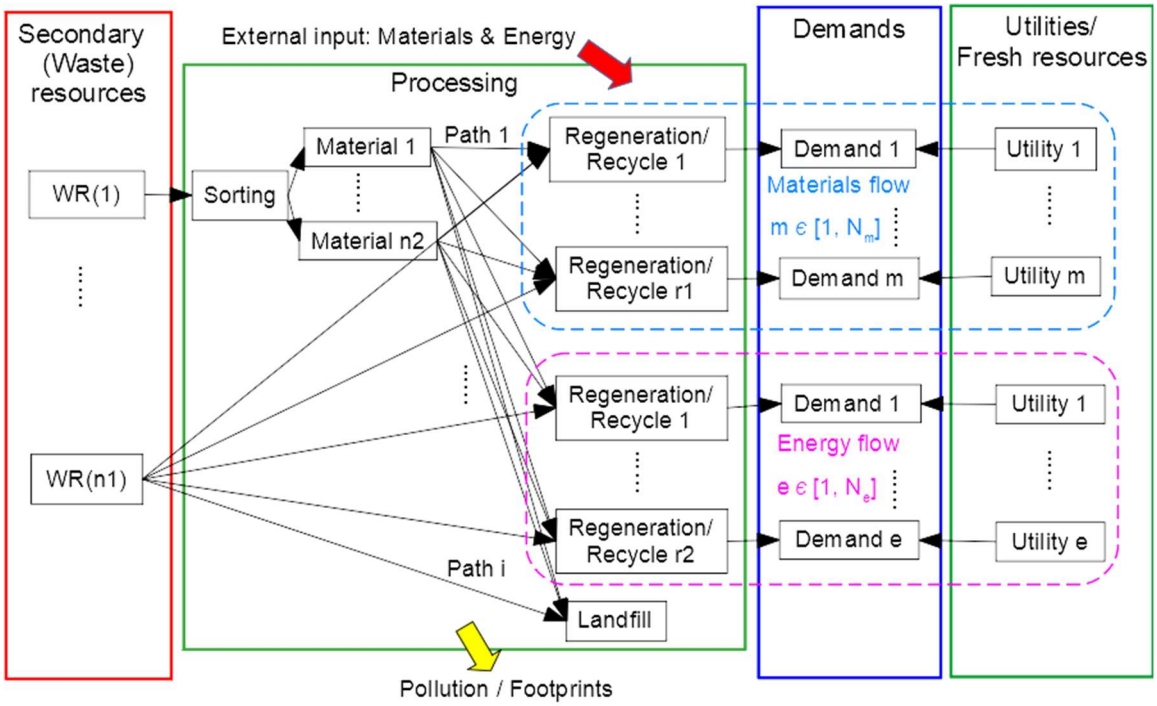

Figure 46. Multi-Resource Integration closing the loops (Multi-Resource Integration Map)

Treatment paths require external input energy and materials. Investment and operating costs are not the same, and the secondary products produced are also different. The selection of a set of treatment paths that ensures the best match between supplies and demands defines an optimisation task.

6.2.2 Degree of circularity

The degree of circularity is used to quantify the waste resources treated into secondary products and services. As analysed in the introduction, many indicators have been proposed previously. The current work focuses on the recycling of materials and energy recovery. For the materials, the Eurostat methodology (Eurostat, 2018) is used as a starting point.

1) Circular Material Use rate (CMU)

Eurostat (2018) use the CMU to measure the share of the mass of materials recycled to the overall mass flow of used materials, as shown in Eq. (31).

$$CMU = \frac{F_{recovered\ material}}{F_{total\ material}} \tag{31}$$

CMU is defined based on demands and is calculated as the fraction of the supplied secondary products to the overall demands (i.e. after the treatment paths in Figure 46b). Each demand is served by a combination of a secondary product and a utility. Each product is delivered to the demand by a single path or multiple paths. The paths and the demands are denoted as $\boldsymbol{m} \in [1, N_m]$. The CMU of a given secondary product (CMU_m) is estimated according to Eq. (32). In that, $F_{product,m}$ is the secondary material product $\boldsymbol{m}$ obtained after recovery processing; $\sum_{[m]} F_{demand,m}$ is the sum of all material requirements over all the demands. The total Circular Material Use rate (CMU_{total}) of the multi-resource system is the sum of all CMU_m values, equivalent to the ratio of the sum of all secondary material products ($\sum_{[m]} F_{product,m}$) to the total material demands, as shown in Eq. (33).

$$CMU = \frac{F_{product,m}}{\sum_{[m]} F_{demand,m}}, m \in [1, N_m] \tag{32}$$

$$CMU_{total} = \sum_{[m]} CMU_m = \frac{\sum_{[m]} F_{product,m}}{\sum_{[m]} F_{demand,m}}, m \in [1, N_m] \tag{33}$$

IV. Circular Exergy Use rate (CEU)

Since some demands in the system are for energy, the circularity of this aspect has to be considered too. The circularity of energy use is defined by Zore et al. (2018) as the fraction of the energy supplied from secondary resources within the total energy required by a given demand, as shown in Eq. (34).

$$Circularity\ of\ energy = \frac{\{Total\ energy\ reused\}}{\{Total\ energy\ demands\}} \tag{34}$$

It is clear that an energy-based indicator is needed for evaluating the process sustainability at a given value of the CMU. It has to be noted that some energy demands may be thermal – for heating or cooling, but others may require power. Similarly, some resource treatment paths may require heating, cooling or power, while other paths may release such flows. Concerning the heat flows, they are also subject to certain reference conditions, usually defined by the state of the surroundings. This leads to using the concept of exergy as the additional evaluation criterion and equivalent exergy demands are used to represent the energy demands. In this model, the CEU is defined as the fraction of the exergy supplied from treating waste resources and the overall exergy used by the process demands. The circular Exergy Use rate (CEU) is an extension of the "circularity of energy", which uses equivalent exergy demands to represent the energy demands, treating heat and power demands uniformly.

The exergy demands form a second set of entities $\boldsymbol{e} \in [1, N_e\ ]$ and are supplied by a subset of the processing paths. The relationship between the set of paths $\boldsymbol{i}$ and the two demand sets is

$$[i] = [m] \cup [e] \tag{35}$$

The CEU of a single path CEU_e in the multi-resource system is estimated according to Eq. (36), which is an adaptation of the original definition by Zore et al. (2018). In Eq. (36). $Ex_{product,e}$ is the secondary exergy product $\boldsymbol{e}$ obtained from the path with the same index. $\sum_{[e]} Ex_{demand,e}$ is the sum of all exergy requirements imposed by the product demands. The total Circular Exergy Use rate (CEU_{total}) of the multi-resource system is the sum of all CEU_eOver the domain of the exergy product demands, as shown in Eq. (37).

$$CEU = \frac{Ex_{product,e}}{\sum_{[e]} Ex_{demand,e}}, e \in [1, N_e\,] \tag{36}$$

$$CEU_{total} = \sum_{[e]} CEU_e = \frac{\sum_{[e]} Ex_{product,e}}{\sum_{[e]} Ex_{demand,e}}, e \in [1, N_e\,] \tag{37}$$

V. Total Circularity Index (TCI)

As discussed and denoted in Eq. (35), the product demands form a joint set from the sets of material and energy product demands. For gauging the degree of circularity of the overall system, it is necessary to consider both material and energy recycling. One option is to introduce weights and sum up the circularity components CMU_{total} and CEU_{total}. The weight coefficients can reflect the importance of each component (Tarne et al., 2019). The current formulation is provided in Eq. (38).

$$TCI = \omega_1 \cdot CMU_{total} + \omega_2 \cdot CEU_{total} \tag{38}$$

The reasoning for formulating the current model is that CMU_{total} has values within the range [0, 1], and CEU_{total} has values in the same numerical range, while both indicators are dimensionless. The new TCI indicator also assumes values in the range [0, 1]. The value of 0 means no circularity, and 1 means a complete circularity. These requirements imply that the sum of the weights has to amount to 1, while they are strictly non-negative:

$$\omega_1 + \omega_2 = 1;\ \omega_1 \geq 0;\ \omega_2 \geq 0 \tag{39}$$

The proposed model is agnostic of the specific situations and supports the users for setting the importance of the energy or material circularity based on their circumstances. This is why the weights in Eq. (38) have been left as user specification parameters. The supplied values are provided by the users and depend on specific cases. For instance, in an area with an abundant supply of energy, the weight coefficient of CEU would tend to assume lower values, below 0.5, leaving the coefficient for CMU to assume the remainder up to the sum of 1. This can be the case with remote locations where the need for material products would be more important. On the other hand, for highly urbanised settings, the importance of CEU would be higher.

For the current work, in the illustration case study, the weights are set equal as $\omega_1 = \omega_2 = 0.5$. It is with the assumption that different dimensions are equally important, similar to the study by ul Haq and Boz (2020) in aggregating three dimensions of sustainability. Gan et al. (2017)

reviewed methods for specifying weights, including equal weighting, statistical weighting, expert opinion weighting. Equal weighting (Nardo et al., 2005) can be used when all indicators are considered equally important or when there is no statistical or empirical evidence to support different schemes. However, the proposed TCI formulation in Eq. (38) is formulated in a way that weighting can be considered based on the preference of the stakeholder or decision-makers. For example, if environmental performance is the main priority, the weighting can be assigned based on the "eco-cost" or "environmental price" in recycling or recovering the respective secondary resources.

6.2.3 Main criteria, trade-offs and degrees of freedom

In the case of reuse, waste materials from different industries are recycled or transformed into secondary material or energy products. These processes use and supply all main forms of energy services – heating, cooling and power. Such flows are modelled with the use of exergy as the appropriate indicator because it allows the evaluation of resources with very different properties (energy, water, materials, waste), based on the second law of thermodynamics (Dincer, 2002). Exergy analysis has been widely used in various fields, e.g. to assess energy conversion technologies (Carneiro and Gomes, 2019), material conversion processes (Zhang et al., 2019), the use of renewable energy resources (Khosravi et al., 2018), environmental impact assessment (Ebrahimi-Moghadam et al., 2020), and in ecology modelling (Sciubba, 2019).

The main degrees of freedom of waste resource recovery and integration include the selection of the processing paths and the linked decisions, the selection and the rates of supply of the "utility" streams. The trade-off between recycling and fresh utilities is addressed using this setup.

6.2.4 Model formulation

The process of recovery of secondary (waste) resources requires capital investment into equipment, the supply of energy, materials and labour to run the processing and transportation units of the reuse paths. Different paths require different external inputs. Supplies may be distributed and pass through different processing paths, resulting in different energy consumption and processing costs even for the same value of TCI, as a result of the available degrees of freedom.

Higher TCI values imply a higher overall degree of circularity and mean reduction of the use of utilities (fresh resources) for the specified process demands (Figure 46). On the other hand, increased TCI value also means an increased load of any potential processing operations involved

in the reuse paths, which results in potentially higher demand for resources to run the paths. These two trends counteract each other and define a clear trade-off. As a result, a higher TCI value means better performance of the multi-resource system only to some degree. TCI alone cannot fully reflect the sustainability of the multi-resource system. Other factors or indicators also need to be considered.

In the current model, two criteria are used for the evaluation - cost and exergy. Total exergy input characterises the resource intensity of the system – balancing both the reuse paths and the utilities. Used alone, it would not account for the economic cost of the proposed solutions since what businesses spend is measured in monetary terms. It is necessary to use the system cost as a criterion. However, using the cost alone also introduces bias. The reason is that sometimes energy-intensive options may be priced low because of various market bias factors – especially subsidies. This is why it is essential to evaluate both criteria – to find out the monetary cost of attaining the exergy optimum or identify the exergy waste for attaining the cost optimum.

The objective functions defined in the model are the total annual cost and exergy with the selection of the degree of circularity and competition among the available reuse paths. The goal is to identify and evaluate the trade-off between minimum exergy or minimum total annual cost and TCI (or CMU_{total}, CEU_{total}). The model formulation is given next.

1) Objective Function

Following the reasoning on cost and exergy minimisation, two variables are used as objective functions. These are the total exergy input and total annual cost.

- *Minimisation of the supply of external exergy*

The objective function using exergy is given in Eq. (40). The exergy consumption includes the exergy of the utilities ($Ex_{utility,i}$), the external exergy inputs to processing paths "i" ($Ex_{input,i}$) and the exergy needed to dispose of the remaining waste to the landfill ($Ex_{landfill}$). In this study, the embodied exergy is adopted in the exergy of utilities, referring to the total amount of exergy spent on the product over its entire life cycle.

$$Obj\ min(Exergy) = \sum_{[i]} \left(Ex_{utility,i} + Ex_{input,i} + Ex_{landfill,i}\right),\ i \in [i] \quad (40)$$
$$= [m] \cup [e]$$

The external exergy input to the recovery process ($Ex_{input,i}$) includes the embodied

exergy of the used external materials ($Ex_{inputmass\ ,i}$) and external energy supplied with energy use ($Ex_{inputenergy,i}$) as shown in Eq. (41). The external energy input includes providing heating, cooling, power for driving equipment (e.g. pumps, compressors, fans).

$$Ex_{input,i} = Ex_{inputmass\ ,i} + Ex_{inputenergy,i},\quad i \in [i] = [m] \cup [e] \tag{41}$$

The exergy needed to dispose of the remaining waste to the landfill ($Ex_{landfill}$) is modelled in Eq. (42), where $F_{WR,i}$ denotes the flowrate of the secondary (waste) resource stream for path ***i***, used for recycling, while $F_{WR,i}^{max}$ denotes the overall waste resource availability for path ***i***. The flowrates of the directly landfilled materials are given by the difference $\left(F_{WR,i}^{max} - F_{WR,i}\right)$, which allows estimating the exergy expenditure for that part:

$$Ex_{landfill,i} = \left(F_{WR,i}^{max} - F_{WR,i}\right) \cdot ex_{landfill},\quad i \in [i] = [m] \cup [e] \tag{42}$$

- *Cost minimisation*

From the economic perspective, the Total Annual Cost (TAC) should be minimised as the objective function, Eq. (43). The TAC includes several terms. These are the annual Total Processing Cost (TPC) which includes investment, the annual Total Utilities Cost (TUC) and the annual cost of disposing of the remaining waste – Total Landfill cost (TLF), i.e., resulting from waste disposal fees, as shown in Figure 47. This is modelled from the viewpoint of a customer who has secondary resources to sell, or a customer who wants secondary resources delivered to their demands.

$$Obj\ min(TAC) = TPC + TUC + TLF \tag{43}$$

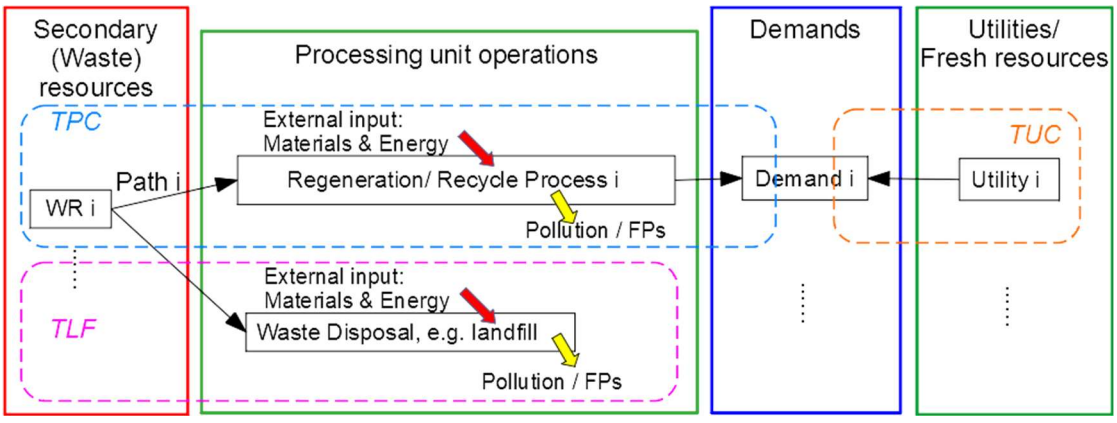

Figure 47. Representation of different costs

The TAC components from Eq. (43) are elaborated on, starting with TPC, which is given in Eq. (44). This component covers the entire processing of the "waste resource WR_i" source through the "regeneration / recycle treatment i" path to obtain secondary product i, as shown in the blue dashed box in Figure 47. TPC includes an annual capital cost (ACC_i) and annual another cost (AOC_i) – defined later in Eq. (46), as shown.

$$TPC = \sum_{[i]} (ACC_i + AOC_i), \quad i \in [i] = [m] \cup [e] \tag{44}$$

The Annual Capital Cost term (ACC_i) accounts for the purchased equipment cost and the installation costs. In this study, the annual capital cost of waste processing (ACC_i) is calculated according to (Tan et al., 2014), using a specification of the capital cost based processing charge (UCC_i) in [EUR/kg] – Eq. (7). The model also takes a specification of the annual operating time of the facilities t_i in [h/y].

$$ACC_i = UCC_i \cdot F_{WR,i} \cdot t_i, \quad i \in [i] = [m] \cup [e] \tag{45}$$

The annual other cost charges are related to the operation and maintenance of the processing facilities – including raw materials, labour, utilities supplied to the processing paths, waste treatment and disposal, replacement materials, overhead, taxes, insurance and administrative charges. The Annual Another Cost (AOC_i) is modelled, according to Tan et al. (2014), based on a specification of unit charges (UOC_i) in [EUR/kg], as shown in Eq. (46).

$$AOC_i = UOC_i \cdot F_{WR,i} \cdot t_i, \quad i \in [i] = [m] \cup [e] \tag{46}$$

As discussed in the description of the Multi-Resource Integration Map, each product demand is served by a combination of a secondary-product flow and a utility-product flow. The utilities are used as degrees of freedom to cover the demands remaining after the secondary products are supplied. The annual cost of utilities (TUC) is the sum of the cost items of all utilities provided to the demands, corresponding to the dashed orange contour in Figure 47. The calculation of the overall annual utility cost (TUC) is shown in Eq. (47), where $P_{P,i}$ is the utility price, where $[i] = [m] \cup [e]$ – see Eq. (35).

$$TUC = \sum_{[m]} \left(F_{utility,m} \cdot P_{P,m} \cdot t_m\right) + \sum_{[e]} \left(F_{utility,e} \cdot P_{P,e} \cdot t_e\right) \tag{47}$$

Waste that is not recycled for generating secondary products needs to be disposed of, such as in a sanitary landfill, which is called the cost of disposing of the remaining waste (TLF), as shown in the pink dotted box in Figure 47. The calculation of TLF is shown as Eq. (48). Where $P_{lanfillfee}$ is the landfill disposal fee. $F_{WR,i}$ is the mass flowrate of the secondary (waste) resource through the recovery process. $F_{WR,i}^{max}$ is the maximum mass flowrate of the secondary (waste) resource. The term $\left(F_{WR,i}^{max} - F_{WR,i}\right)$ represents the flowrate of materials directly landfilled.

$$TLF = \sum_{i} \left(F_{WR,i}^{max} - F_{WR,i}\right) \cdot P_{landfillfee} \cdot t_i, \quad i \in [i] = [m] \cup [e] \tag{48}$$

VI. Constraints

The constraints of the mathematical model include mass and energy balances, accounting for the net exergy demands, split fractions and bounds.

- *Mass and energy balances of resources, products and demands*

It is desired that the product demands, denoted as $F_{demand,i}$) are satisfied by the recycled resources (secondary products – $F_{product,i}$) to a maximum degree, while the rest of the demands are satisfied by the procurement of fresh resources, termed "utilities" ($F_{utility,i}$). This defines the mass and energy balance equation in Eq. (49).

$$F_{utility,i} + F_{product,i} = F_{demand,i}, \qquad i \in [i] = [m] \cup [e] \tag{49}$$

The values of variables $F_{utility,i}$ in the objective function are determined by the mass and energy balances in Eq. (49), where they are balanced with the secondary product flowrates $F_{product,i}$. The amounts of secondary products obtained through the waste processing paths can be estimated using Eq. (50), where $x_{sorting,i}$ is the sorting fraction of secondary (waste) resource, $x_{distribution,i}$ is the distribution fraction, $x_{efficiency,i}$ is the efficiency or conversion factor of different processes. That equation reflects the operations performed on the secondary (waste) resource $F_{WR,i}$ – it is first sorted to get separated materials, then the separated materials are distributed to unit operations, and the secondary products are obtained from the processing unit operations that convert the materials with the specified efficiency rates.

$$F_{product,i} = F_{WR,i} \cdot x_{sorting,i} \cdot x_{distribution,i} \cdot x_{efficiency,i}, \quad i \in [i] = [m] \cup [e] \tag{50}$$

However, Eq. (50) is a complicated equation, expressing linear relationships in a non-linear way. This logic is implemented in Eqs. (51) – sorting, (52) – distribution and (53) – conversion, which reflect the same processing stages.

$$F_{sorting,s} = F_{WR,i} \cdot x_{sorting,i}, \quad i \in [i] = [m] \cup [e] \tag{51}$$

$$F_{sorting,s} = \sum_{[i]} F_{distribution,i}, \quad i \in [i] = [m] \cup [e] \tag{52}$$

$$F_{product,i} = F_{distribution,i} \cdot x_{efficiency,i}, \quad i \in [i] = [m] \cup [e] \tag{53}$$

- *Exergy embodied in the fresh resource demands*

The specified energy demands translated to demands for exergy Ex_{demand} are first satisfied (Eq. (54)) with the recovered exergy from the waste resources ($Ex_{recovery}$), to ensure their utilisation, while the rest of the demands are satisfied by the procurement of fresh energy resources (termed "utilities"), converted to exergy ($Ex_{utility}$), as shown in Figure 48. The recovered exergy from each processing path is estimated as the difference between the exergy product flow and the external exergy that has to be supplied to that path – Eq. (55).

$$Ex_{demand,i} = Ex_{recovery,i} + Ex_{utility,i}, \qquad i \in [i] = [m] \cup [e] \tag{54}$$

$$Ex_{recovery,i} = Ex_{product,i} + Ex_{input,i}, \qquad i \in [i] = [m] \cup [e] \tag{55}$$

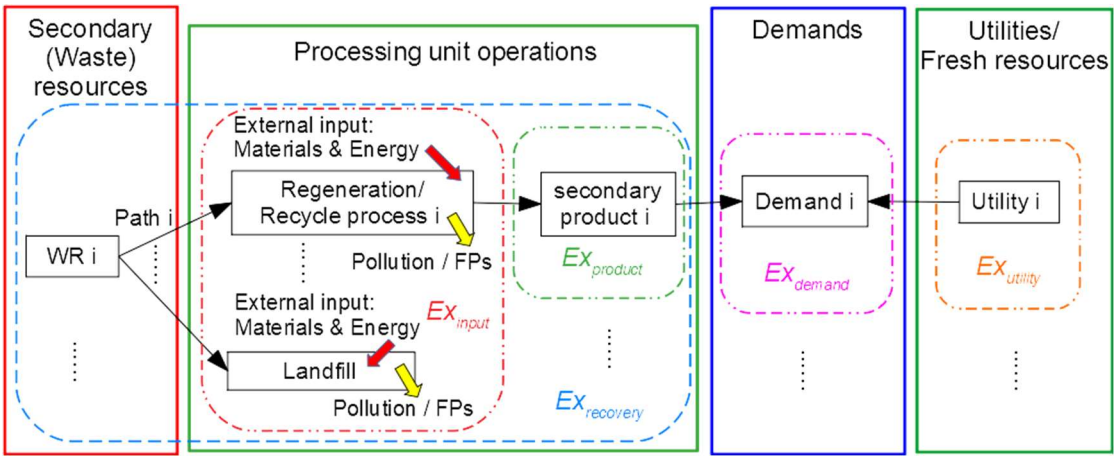

Figure 48. Representation of the various exergy flows

- *Split fraction for the secondary resources*

Although a secondary raw material may be processed via different treatment paths, the total sum of the fractions, distributed to the various paths, has to be 1, as formulated in Eq. (56). This relationship expresses the process of sorting the flow of supplied secondary raw materials (waste) to individual homogeneous fractions of materials.

$$\sum_{[i]} x_{sorting,i} = 1, i \in [i] \tag{56}$$

- *General constraints*

Some variables should also meet boundary requirements. For instance, the split fraction should be in the range [0,1], as shown in Eqs. (57) - (58). The flowrate of secondary (waste) resource $\boldsymbol{i}$ – $F_{WR,i}$, should be non-negative and less than the required maximum, as shown in Eq. (59).

$$0 \leq x_{sorting,i} \leq 1, \ \ i \in [i] \tag{57}$$

$$0 \leq x_{efficiency,i} \leq 1, \ \ i \in [i] \tag{58}$$

$$0 \leq F_{WR,i} \leq F_{WR,i}^{max}, \ \ i \in [i] \tag{59}$$

The presented model has been implemented in GAMS (2020). Two assessment cases have been performed to evaluate the variations of the important system indicators. The first case uses the minimum exergy consumption as the objective function, and the second – the minimum TAC. The exergy consumption and TAC are calculated by optimisation of the processing paths and utilities for different values of the CMU_{total}, CEU_{total} and TCI, which are obtained by varying the flowrates of recycled material and energy flows.

6.3 Case Study - integration of waste resources recovery

The method and model proposed in this chapter are demonstrated using a case study. The modelled situation is to evaluate the integration of waste resources from different sectors – residential communities and wood processing plants.

The Concept map of multi-resource integration and all the processing paths for the case study is shown in Figure 49. Synthetic Natural Gas (SNG), obtained from biogas, is available from a sewage plant of communities in the considered region. The SNG can be used to produce

hydrogen by steam methane reforming. Waste biomass (sawdust) is available from wood processing plants. The main constituent of the biomass is lignin. This material is a potential source for the production of chemicals based on bio-phenols or bio-polyols – e.g. catechol (Mabrouk et al., 2018). Catechol – $C_6H_4(OH)_2$, is widely used in the pesticide and pharmaceutical fields (Montazeri and Eckelman, 2016). Catechol is obtained from biomass in a biorefinery by biomass fractionation, lignin depolymerisation and product separation. Municipal solid waste (MSW) management methods include Landfill Gas Recovery System (LFGRS), incineration, composting, recycling and sanitary landfill. MSW is first sorted into garden waste, paper, food waste, plastic, glass, metal and textile. Secondary products (e.g. compost, recycle material and power) are then produced by various waste processing operations – composting, recycling, incineration, LFGRS. The remaining biomass and SNG are used to generate electricity by thermal power generation. The rest of the solid waste is disposed of in landfills.

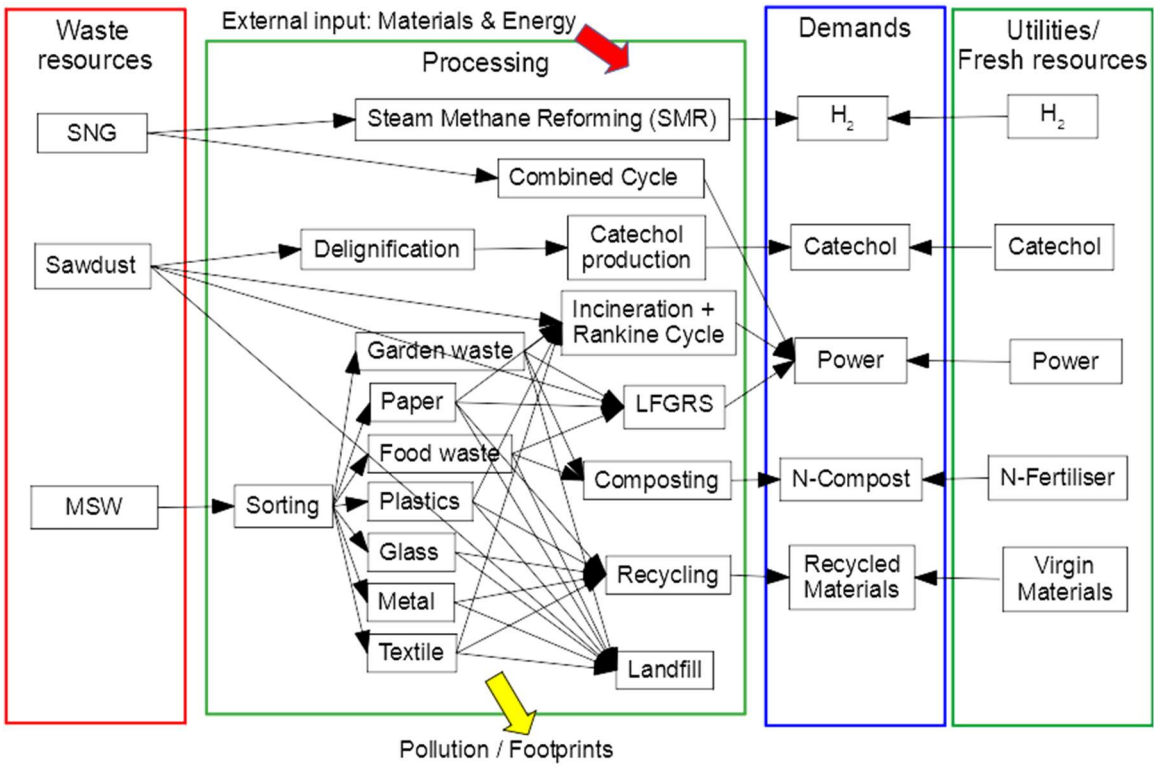

Figure 49. Concept Map of Multi-Resource Integration for the case study

The maximum flowrates of the waste resources are shown in Table 22. The data for the resource and product demands are shown in Table 23. The supplies are treated with different processes to produce secondary products that can be reused, e.g. catechol, hydrogen, compost,

corresponding recycled materials and power. For the processing of the secondary raw materials, additional external materials and energy input is required. Some examples of those are water, solvents, automotive fuels for transportation, and power. Secondary and residual waste is also generated – e.g. ashes after incineration and solid waste after landfill. The demands in this case (Figure 49) include catechol, H_2, compost, recycled materials (plastics, metals, glass, textile), and power. The secondary products are provided to the demands, while utilities or fresh resources cover the residual demands.

Table 22. Maximum flowrates of supplies

Supplies	Maximum flowrate, kg/h	LHV, MJ/kg
SNG	0.07	48.35
Sawdust (Biomass)	0.15	13.22
MSW	137.00	Details in Table 24

Table 23. The data for the demands

Demands	Unit	Value
H_2	kg/h	0.020
Catechol	kg/h	0.001
N-Compost	kg/h	38
Paper	kg/h	27
Plastic	kg/h	29
Glass	kg/h	6
Metal	kg/h	5
Textile	kg/h	10
Power	kW	60

The generated power is calculated according to the Low Heating Value (LHV) of the feed combined with the efficiencies and conversion factors of treatment units. The MSW in this study is classified and collected MSW, which may contain some impurities, such as sand and small stones. The impurity content is very few and can be ignored. The composition, the LHV, the carbon content and the fraction of the degradable organic carbon (DOC_F) of MSW are shown in Table 24. In this case study, only power is required, and the SNG-based Combined Cycle, biomass/waste incineration and LFGRS are assumed to meet part of that demand. The efficiency and conversion factors of processing units are shown in Table 25. The efficiency of a sanitary landfill is zero because no secondary products are produced in this treatment.

Table 24. Data on composition (Tan et al., 2014), LHV (Tan et al., 2014), carbon content (Tan et al., 2014) and DOC_F (Lee et al., 2017) of MSW

Sorting	Composition, %	LHV, MJ/kg	Carbon Content, %	DOC_F, %
Garden waste	2.5	0.48	41.47	23
Paper	20.9	3.08	37.37	37
Food waste	41.1	5.26	42.61	64
Plastic	22.2	5.38	60.93	0
Glass	3.6	0.00	0.00	0
Metal	2.0	0.00	0.00	0
Textile	7.7	2.48	60.42	0

Table 25. Efficiencies and conversion factors of different processes

Processes	$x_{efficiency,i}$, %	Reference
SNG to H_2 (mass)	26.32	(Khojasteh Salkuyeh et al., 2017)
Biomass to catechol (mass)	0.51	(Mabrouk et al., 2018)
SNG based Combined Cycle power generation (energy)	50	(Rao, 2012)
LFGRS (energy)	8.16	(Lee et al., 2017)
Waste Incineration to power	30	(Trindade et al., 2018)
Composting (mass)	60	(Fan et al., 2020)
Recycling (mass)	70	(Expósito and Velasco, 2018)

The task in the case study is to identify and evaluate the trade-offs between the degree of circularity (CMU_{total}, CEU_{total} and TCI) and exergy and between the degree of circularity and cost. The flowrates of waste resources used for obtaining secondary products are optimisation variables. The analysis has been performed in two stages. First, the minimum required exergy input is evaluated for a range of circularity levels. The circularity level of the system is represented by the defined indicators – CMU_{total}, CEU_{total} and TCI. For each of these indicators, the evaluation is performed by:

(1) Specifying a series of values in the LP model
(2) Running the model, for minimisation of the overall exergy input, according to Eq. (40).

The second type of analysis is the TAC minimisation. It follows the same pattern of specifying a series of values for the base indicators CMU_{total}, CEU_{total} and TCI.

6.3.1 Variation of exergy input with circularity

The exergy inputs to the recycling paths for operating processes are specified in Table 26.

The secondary (waste) resource provided with the SNG to produce H_2 contains mainly CH_4. Some part of it is used as a fuel – for instance, to heat the reactor. The remainder of the SNG is used as a reagent. The conversion factor of SNG to H_2 is sufficient, and there is no need for external exergy input to the reactor. This process only needs to provide power for running the compressors and other mechanically driven equipment. For the process of SNG based Combined Cycle to power, the external input of exergy is set to zero because any power used to drive the process here is generated internally. The materials recycling process is exergy-intensive, mainly because of the operations such as transportation, shredding, sorting, extrusion and granulation. The values for embodied exergy of the utilities used for the product demands are specified in Table 27.

Table 26. Exergy inputs for operating the recycling paths

Process	Exergy inputs to the recycling paths, MJ/kg Feed	Reference
SNG to H_2	0.10	(Khojasteh Salkuyeh et al., 2017)
Biomass to catechol	169.12	(Mabrouk et al., 2018)
SNG based Combined Cycle to power	0.00	
LFGRS	0.34	(Varbanov et al., 2020a)
Incineration	1.20	
Materials Recycling	10.44	
Composting	0.21	(Lim et al., 2019)
Landfill	0.20	

Table 27. The embodied exergy of the utilities

Utility streams	Unit	Embodied exergy	Reference
H_2	MJ/kg	180	(Kruse et al., 2002)
Catechol	MJ/kg	1,050	(Mabrouk et al., 2018)
Fertiliser	MJ/kg	6	(Embodied Energy Coefficients)
Paper	MJ/kg	25	
Plastic	MJ/kg	78	
Glass	MJ/kg	11	
Metal	MJ/kg	22	
Textile	MJ/kg	100	
Power	MJ/(kWh)	8.64	(Lou et al., 2015)

The minimum exergy consumption has been calculated by minimising the exergy objective function from Eq. (40), for a series of values of CMU_{total}, CEU_{total} and TCI. Among all

the paths processing waste resources, some require less exergy and provide exergy excess, resulting in exergy surplus. In some paths, the reaction process requires significant exergy, while the generated product has a little exergy, so there will be an exergy liability. The obtained minimum exergy values for varying the CMU_{total}, CEU_{total} and TCI are shown in Figure 50a, Figure 50b, and Figure 51a. In these figures, the black curve represents the minimum total exergy consumption. The green curve represents the exergy of utilities. The red curve represents the external input exergy for the processing. The yellow curve represents the exergy needed to dispose of the remaining waste to the landfill.

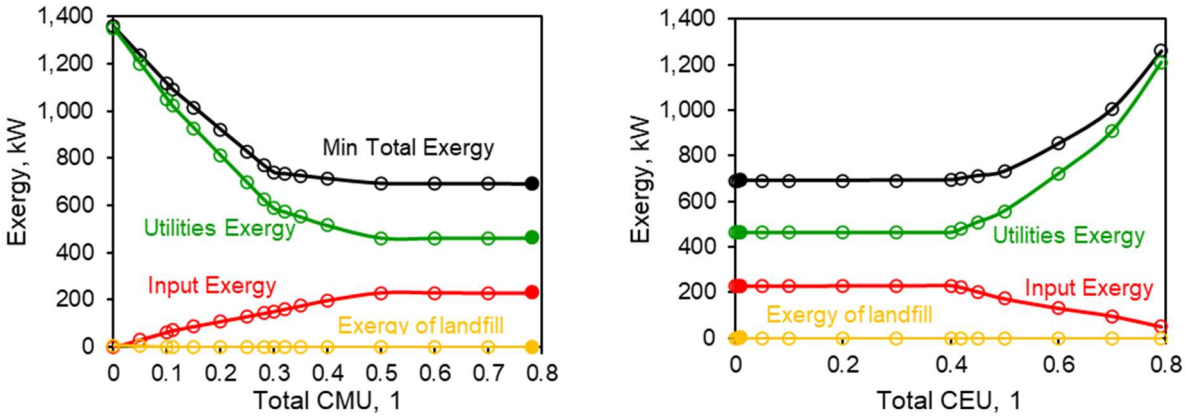

(a) Total Circular Material Use Rate (b) Total Circular Exergy Use Rate

Figure 50. Minimum total exergy under different (a) total CMU; (b) total CEU

If the emphasis is put on the recycling of materials, the plot in Figure 50a is obtained. The minimum total exergy decreases with the increase of CMU_{total} and reaches a minimum at CMU_{total} = 0.782 at the end of the evaluation. The minimum exergy required at that point is 670 kW. In Figure 50a, when CMU_{total} starts from 0, all product demands are served entirely by utilities. With the gradual increase of CMU_{total}, more secondary resources begin to be reused and converted into secondary products. That results in an increase in the exergy input required for the process and a decrease in the exergy used for landfilling. At the same time, the required utilities decrease rapidly, and the embodied exergy inflow with the utilities decreases too. The exergy input for serving the landfill is of an order of magnitude lower than the other two components and can be neglected, which can be seen from the plot. The decrease of the embodied exergy input with the utilities is faster than the increase of exergy input to the processing paths, resulting in the steep decrease of the minimum total exergy.

When CMU_{total} reaches 0.11, all secondary resources are allocated to the generation of

secondary products, and the exergy of the landfill is minimised. As the specified value of CMU_{total} is increased further (0.11 - 0.5), the distribution of the waste resources changes. An increasing share of the secondary raw materials is allocated to the generation of material products (compost, recycled paper, recycled plastics, recycled glass, recycled metals, recycled textile) at the expense of power generation. This leads to the increase of the exergy input to the processing paths and the decrease of CEU_{total}. The supply of material utility decreases, and the supply of energy utilities increases. Since the embodied exergy of material utilities is higher than that of energy utilities, the total utility exergy decreases.

As CMU_{total} continues to increase (0.5 - 0.782), food waste of secondary resources is redirected from generating power to producing compost. This leads to a further decrease in CEU_{total}. Although the exergy input required for material recycling increases, the auxiliary exergy input to the power generation from the MSW fractions decreases a little faster, according to the specifications in Table 26, resulting in a very small decrease of the recycling exergy input and the overall exergy input after CMU_{total}= 0.5. The minimum total exergy consumption reaches the minimum for CMU_{total} is 0.782, at which point the capacity for recycling waste resources is exhausted.

Changing the goal of satisfying energy demands with priority over the materials is better tracked using the CEU_{total} indicator, which results in the plot in Figure 50b. The optimal point in this variation takes place at CEU_{total} = 0.011, with total exergy (input, plus embedded) of 690 kW. This indicates that the scope for Waste-to-Energy (WtE) alone in the current case study is very limited (practically none). Instead, the WtE is efficient as part of the material circularity increase. The reasons for this can be traced to the very small capacity for efficient power generation provided by the available waste resources. The SNG and the biomass waste, even assuming their full commitment to power generation, can barely cover just under 1 kW of the overall 60 kW power demand. The available MSW has a larger capacity nominally, but its processing paths ending with power generation compete with the more exergy-efficient paths for material recycling, resulting in limiting the capacity for Waste-to-Energy.

Another reason for this trend is that, after the optimal point at CEU_{total} = 0.011, the embodied exergy contribution of the utilities – mainly materials, monotonically increases with the increasing of the CEU_{total} value. As one can see from the trend in Figure 50b, this component dominates the share of exergy supply, exceeding the input to the recycling paths about twice. At first sight, it seems contradictory that increased energy circularity causes utility exergy to grow.

However, it should be remembered that the total exergy input to the system with the utilities includes both power and other flows – including materials. The embodied exergy of most of those materials is significantly higher than that of the potential substitutes from the collected MSW.

If a combined material and energy recycling is desired, the plot in Figure 51 is obtained. Figure 51a shows the envelope of the possible solutions and illustrates the size of the solution space. For each of the sampled values of TCI, the highest and the lowest values of total exergy input varies between the maximum and the minimum and the formulated model is run to obtain the minimum total exergy input. As can be seen from the figure, the minimum exergy first decreases, reaching a minimum of 690 kW at TCI = 0.396, and then grows sharply with the TCI increase. That overall minimum is lower than the minimum total exergy consumption at the highest possible circularity of TCI = 0.463 (1,028 kW) by 338 kW, constituting nearly 33 % difference.

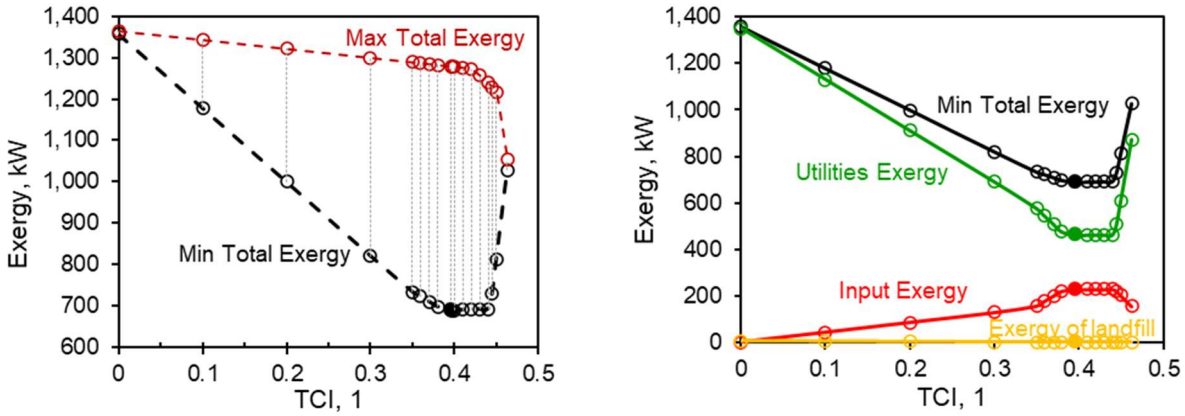

(a) Total exergy (b) Trend and breakdown by components

Figure 51. Total exergy under different TCI

The trend of the variation can be analysed on the plot in Figure 51b, which shows plots for the overall exergy and its components. At the start of the curve (TCI = 0), all waste resources are sent to the landfill (wasted). No material or energy is recovered, and this is the point of highest total exergy consumption. With the gradual increase of TCI (0 to 0.35), some waste resources are used to generate secondary products. Both CMU_{total} and CEU_{total} increase. As more secondary products are produced, the required external exergy input for the processing grows. The exergy input to the landfill is insignificant but drops. At the same time, the required utilities decrease together with their embodied exergy input. The minimum total exergy decreases rapidly because the decrease in the utility exergy is faster than the increase of the external input exergy by the

processing. As TCI continues to increase (0.35 to 0.396), CMU_{total} keeps increase while CEU_{total} gradually decreases because of the redistribution of waste resources for generating secondary material products taking priority over the power generation, while the exergy input to the treatment paths increases. The reduction of the utility exergy is still greater than the increase of the external exergy input, so the minimum total exergy consumption continues to decrease slowly. When TCI reaches 0.396, all secondary resources are allocated to generating secondary products, and the total exergy consumption is reduced to the minimum. When TCI increases from 0.396 to the maximum of 0.463, CMU_{total} gradually decreases while CEU_{total} gradually increases, indicating reallocation of waste resources from material recovery to power generation. Because of the discussed proportions of the exergy expenditure shares, this shift drives the sharp increase in the needed total exergy supply in Figure 51b.

Coming back to the optimal TCI value of 0.396, the optimal combination of paths selected for the minimum total exergy input is shown in Figure 52. The Combined Cycle power generation uses SNG. The wood and paper waste are used to generate power in a steam cycle after incineration. After the MSW is sorted, the garden waste and food waste are composted, the paper, plastics, glass, metals and textile are recycled. In summary, the optimal configuration is related to power generation, composting and materials recycling. These paths feature a lower specific embodied exergy than the utilities satisfying the corresponding demands.

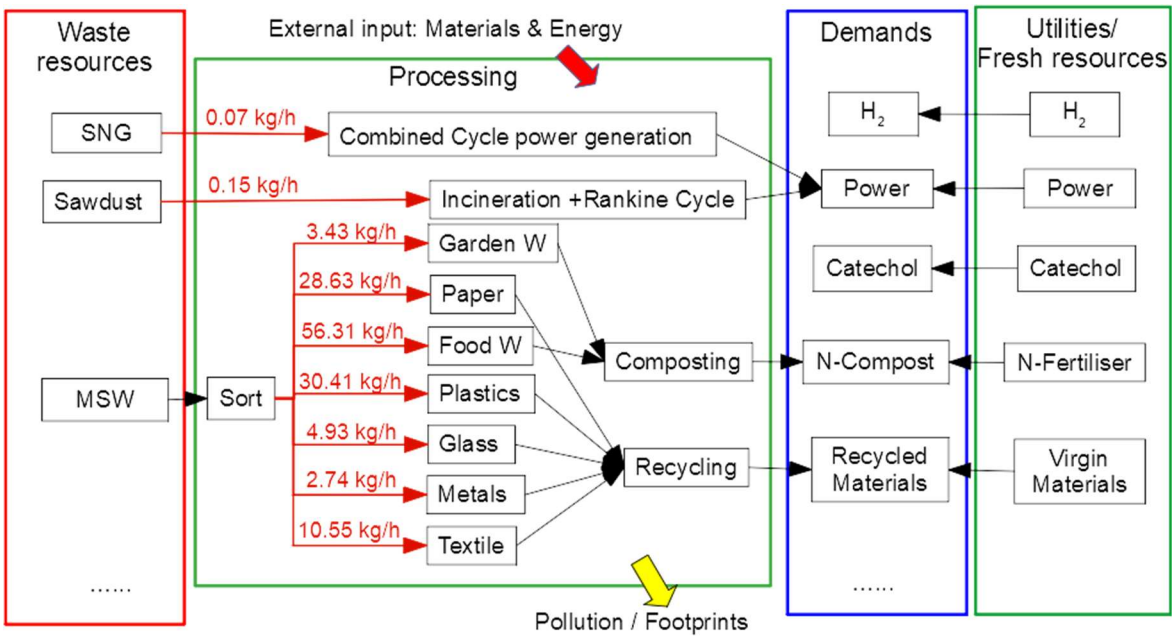

Figure 52. The optimal exergy consumption path at TCI is 0.396

Considering the exergy input as an evaluation criterion produces a configuration that requires the least amount of exergy. However, although some paths produce less exergy with more exergy consumption, their products can be of high added monetary value. While exergy and energy consumption are important indicators, using them alone introduces a bias since investment and operation decisions are made based on profit and cost, which is evaluated in the next section.

6.3.2 A trade-off between economy and circularity

The cost data of the involved processes is shown in Table 28 and the utility prices – in Table 29.

Table 28. Cost data of involved processes

Processes	UCC_i, EUR/kg	UOC_i, EUR/kg	Operating time, h/y	Reference
SNG to H_2	0.011	0.110	8,760	(Khojasteh Salkuyeh et al., 2017)
Biomass to catechol	0.052	0.281	8,000	(Mabrouk et al., 2018)
Combustion	0.021	0.008	8,640	Cost (Rizwan et al., 2018); Operation time (Tan et al., 2014); Plant Lifetime (Guo et al., 2018)
LFGRS	0.001	0.027	8,640	
Incineration	0.020	0.026	7,008	
Composting	0.005	0.010	7,008	
Recycling	0.002	0.030	7,008	
Landfill	0.005	0.106[a]	8,640	(Zhou et al., 2015), (Cewep, 2020)

[a]: The annual another cost (UOC_i) of the landfill process includes an operational cost of 5.73 EUR/t (Zhou et al., 2015) and a landfill tax of 100 EUR/t (Cewep, 2020).

Table 29. Price list of utilities

Utilities	Price	Units	Reference
H_2	1.810	EUR/kg	(Eggeman, 2004)
Catechol	1.740	EUR/kg	(Mabrouk et al., 2018)
Fertiliser	0.133	EUR/kg	(Tan et al., 2014)
Paper	0.033	EUR/kg	(Tan et al., 2014)
Plastic	0.178	EUR/kg	(Tan et al., 2014)
Glass	0.039	EUR/kg	(Tan et al., 2014)
Metal	0.199	EUR/kg	(Tan et al., 2014)
Textile	0.039	EUR/kg	(Tan et al., 2014)
Power	0.052	EUR/kWh	(Arsalis et al., 2018)

The TAC assessment follows the same procedure as for the exergy assessment case – by

varying the base indicators (CMU_{total}, CEU_{total} and TCI) and evaluating the resulting optimal TAC by optimisation at every sampling point. For fixed CMU_{total}, CEU_{total} and TCI, different processing paths can be chosen with different TAC. The charts of minimum TAC for varying the CMU_{total}, CEU_{total} and TCI values are shown in Figure 53a, Figure 53b, and Figure 54. In these figures, the black curve represents the minimum TAC. The green curve represents the annual utility cost (TUC). The red curve represents the annual processing cost (TPC). The yellow curve represents the cost of disposing of the remaining waste to a landfill (TLT).

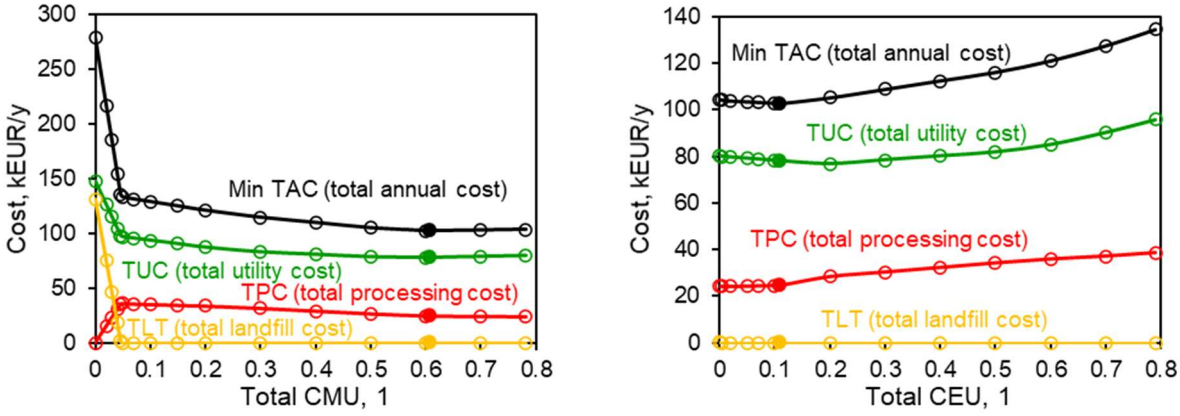

(a) Total Circular Material Use rate (b) Total Circular Exergy Use rate

Figure 53. Minimum cost under different (a) total CMU; (b) total CEU

First, the materials-based circularity is evaluated, as illustrated in Figure 53a. The minimum TAC features a minimum at CMU_{total} = 0.608, with TAC = 102.7 kEUR/y. At CMU_{total} = 0, all demands are served entirely by utilities and the waste resources are not used. With the increase of CMU_{total}, the waste resources are converted to secondary products, which reduces the required utilities and the related cost. That decrease, combined with the drop in the landfill cost, outweighs the increase of the waste resource processing cost, so TAC decreases. When the CMU_{total} reaches 0.05, all secondary resources are allocated to producing secondary products. The process investment cost increases to the maximum, and the landfill stays at the achieved minimum.

Increasing CMU_{total} further (0.05 - 0.781 max) keeps the landfill cost minimised, and the process investment cost slightly drops. The trend of the TAC mainly depends on the utility cost. With the increase of CMU_{total} from 0.05 to 0.608, the CEU_{total} drops as a result of routing waste resources more to material products (composting, recycled plastics, recycled textile) instead of power generation. This reduces the need for material utilities needed and increases the need for power utility. The trend is driven by the price of power utilities being lower than the price of

material utilities (compost, plastics, and textile). As a result, the utility cost is gradually decreased, and the minimum TAC follows the trend. When CMU_{total} increases to 0.608, the minimum TAC decreases to the overall optimum.

When CMU_{total} is increased further – from 0.608 to its maximum of 0.782, CEU_{total} is also further reduced, caused by the increased diversion of the waste resources from power generation to secondary material products (recycled paper), keeping the allocation of the waste resources at the maximum. The supply of the material utility paper is reduced, and the supply of power utility is increased. Because the price of power is higher than the price of the paper utility, the utility cost is gradually increased, and the minimum TAC follows that trend.

Similarly, the trend of the minimum TAC with the variation of CEU_{total} is shown in Figure 53b. Except for the point of $CEU_{total} = 0$, the landfill cost is of an order of magnitude lower than the other two components and can be neglected. The waste processing cost changes very little within the range 20 - 40 kEUR.y. As a result, the trend in TAC mainly depends on the utility cost. Within the range of CEU_{total} from 0 to 0.11, the price of material utility paper is lower than the price of the power utility. The utility cost slightly drops, and the minimum TAC follows the trend. When CEU_{total} is 0.11, CMU_{total} is 0.608 and TCI is 0.359, and the minimum TAC = 102.7 kEUR/y is optimal. After that point, the minimum TAC increases as the CEU_{total} increases. With the increase of CEU_{total}, the CMU_{total} behaves in a monotonic manner, with opposite trends. More and more of the waste resources are diverted from secondary material products to power generation, increasing the demand for material and reducing the demand for the power utility. With the increase of CEU_{total} from 0.11 to 0.791, the price of material utilities (recycled textile, composting, recycled plastics) is higher than the price of the power utility. This results in an increase in the utility cost and the minimum TAC.

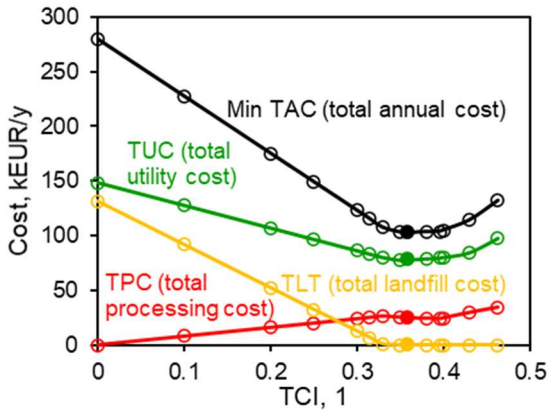

Figure 54. TAC under different TCI values

The minimum TAC trend with the variation of TCI is shown in Figure 54. The optimal TAC = 102.7 kEUR/y at TCI = 0.359, which is by 29.4 kEUR/y lower compared to the TAC = 132.1 kEUR/y at the highest value of TCI = 0.463, constituting 22 % difference. Figure 55 shows the flow distribution within the system for the minimum TAC at TCI = 0.359.

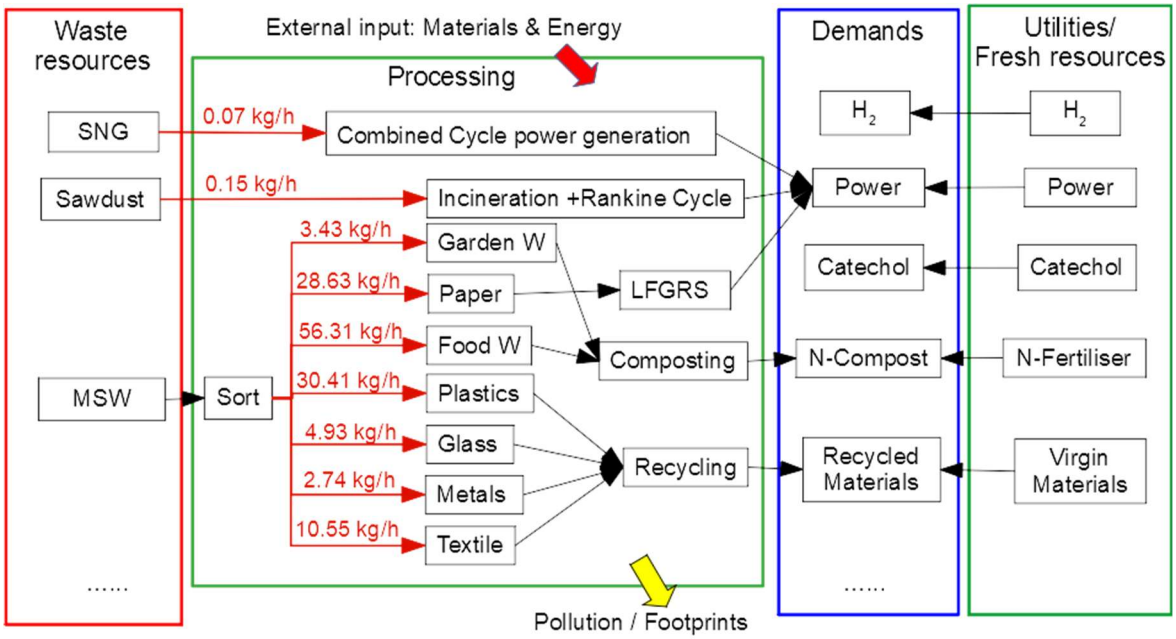

Figure 55. The optimal TAC path at TCI is 0.359

Looking at the trends in Figure 54, with the increase of TCI, the minimum TAC gradually decreases to the optimal at TCI = 0.359 and then increases. At TCI = 0, all waste resources are landfilled, and the minimum TAC is the highest. With the gradual increase of TCI (0 to 0.33), both CMU_{total} and CEU_{total} increase as a result of the utilisation of the waste resources. When TCI reaches 0.33, the waste resources are fully allocated to the recycling of secondary products. With the further increase of TCI (0.33 to 0.359), CMU_{total} gradually increases while CEU_{total} gradually decreases, reflecting that material products are generated with priority over the power. When TCI reaches 0.359, the minimum TAC decreases to the optimum. When TCI increased from 0.359 to the maximum of 0.463, the waste processing cost increases slightly, and the utility cost grows too, defining the increase of TAC. This is because, in this segment, more waste resources are diverted to generate secondary energy products at the expense of secondary material products (recycled paper). The price of material utilities (recycled paper) is lower than the price of the power utility. The utility cost is gradually increased, and the minimum TAC follows the trend. Then, as the TCI

is pushed to increase further, more secondary resources are directed to generate secondary material products (composting, recycled plastics) at the expense of reducing power generation. The price of material utilities (composting, recycled plastics) is higher than the price of power utilities. The utility cost is keeping increased, and the minimum TAC follows the trend.

6.3.3 Comparison of exergy and cost optima

A comparison of the minimum total exergy consumption curve and the minimum TAC curve against TCI is shown in Figure 56. It can be seen that the minimum total exergy consumption and the minimum TAC follow the same trends, with some displacement. The minimum of the TAC curve takes place at a lower TCI value than the exergy curve. The minimum total exergy consumption is optimal (690 kW) when TCI is 0.396, CMU_{total} is 0.782, and CEU_{total} is 0.011. The minimum TAC has the lowest value (102.7 kEUR/y) when TCI is 0.359, CMU_{total} is 0.608, and CEU_{total} is 0.11.

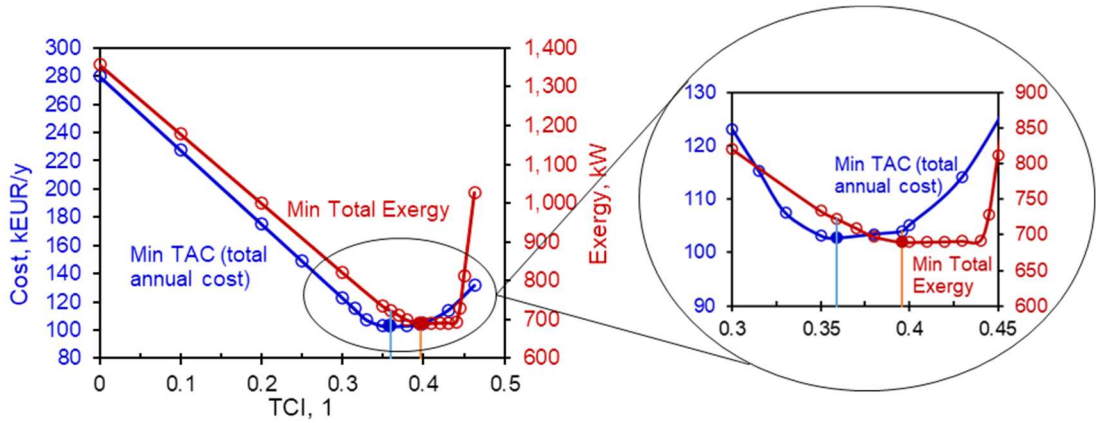

Figure 56. Minimum total exergy and TAC under different TCI

At the optimal total exergy point (TCI = 0.396), the minimum TAC is 103.9 kEUR/y, which is 1.2 kEUR/y (1.2 %) higher than the optimal TAC. At the optimal TAC point (TCI = 0.359), the minimum total exergy consumption is 723 kW, which is 33 kW (4.8 %) higher than the optimal exergy. This indicates that the exergy-related cost, in general, dominates the cost structure. This is because the utilities of textile and paper are more exergy intensive but having a lower cost. The fertiliser utility is less exergy intensive but having a higher cost.

6.4 Conclusions

This study presents an approach to the improvement of the sustainability modelling and

evaluation of multi-resource systems. This is achieved by using proposing the concept of the Multi-Resource Integration Map. This visual representation clearly outlines the key trade-off of recycling systems – between the resources dedicated to the recycling processes and the resources dedicated to the supply of fresh resources. It links the degree of circularity to the cost and to the exergy input, evaluating the trade-off.

To account for the degree of circularity, the CMU_{total} and the CEU_{total} indicators have been combined to form a TCI. The TCI is adopted as the overall circularity metric for multi-resource systems. The optimisation goal is selected in two variants to evaluate the variations of the important system indicators – exergy and TAC. The evaluation is made as a function of the degree of circularity, accounting for the competition among the available reuse paths.

The method is applied to a case study. The evaluation shows that the total annual cost for the cost-optimal degree of circularity is 22 % lower than the cost for the maximum circularity. The difference for the exergy criterion between the optimal and the highest circularity is 33 %. These results illustrate the usefulness of the proposed model. Additionally, the marginal monetary cost of attaining the exergy optimum compared to the cost optimum is 1.2 %, and the exergy penalty of attaining the cost optimum compared to the exergy one is 4.8 %, indicating that some exergy-intensive options carry a low cost. The nature of this discrepancy needs further investigation and points to one of the directions for future work.

A key advantage of the defined indicators has become apparent from the case study. The comparison of the system performance against CMU and CEU reveals the internal trade-offs between the potential uses of the waste resources for one type of products or another. This is illustrated using an example of material-based secondary products and the potential power generation from waste resources.

Based on the conclusions, the main suggestions for future work directions can include further development of the base indicators – starting from the coherent treatment of the energy and material flows. The weights of the CMU and CEU indicators should be paid further attention to for providing decision-makers with guidelines on selecting their values. For a more detailed evaluation of the economic performance and the trade-off with the use of resources, the investment cost model needs to be detailed further. Another key issue is to link the resource flows with the resulting environmental impacts – including those from the recycling and from the fresh resource supplies. This direction may involve linking the exergy expenditure and the use of other materials to GHG, Water, Nitrogen and particulate matter (PM) footprints. Lastly,

the system model can be made more detailed and linked to the relevant Process Systems software – such as chemical process simulators, for automating the data acquisition and estimation.

CHAPTER 7 CONCLUSIONS AND RECOMMENDATIONS FOR FUTURE RESEARCH

The novel methods proposed in this thesis combine into a framework methodology facilitating the combination of Circular Economy and Process Integration. The framework has emphasised the Total Site Integration decision support tools to aid in minimising energy and material consumption in a multi-resource system implementing Circular Economy in a sustainable way. Their effectiveness in solving the problems was demonstrated through a number of case studies (See Chapters 3-6). The novel graphical-based methods are superior in providing process understanding, compared with mathematical programming, and offer a wide potential for practical implementation. Some other advantages are:

(i) The performance and integration of heat pumps with various industrial processes, especially the emerging Joule-Cycle heat pump, is investigated by an extended Pinch Analysis for low-grade heat recovery.

(ii) A method combining Pinch Analysis and waste materials recovery is proposed. Pinch Analysis is extended considering multiple-level fresh resources and intermediate headers in Total Site Mass Integration. Waste material regeneration is optimised with a techno-economic objective to further reduce fresh resource consumption.

(iii) A graphical-based method considering both mass and energy quality is extended. The interactions between mass and energy exchange networks are explored.

(iv) A concept map and a model of multi-resource integration are proposed. This is a visual representation of multi-resource system integration tracing the processing paths of the secondary raw materials to useful products and services. The three-way trade-off between the degree of circularity (quantity), exergy (quality) and the cost is assessed.

The key insights identified in each of the case studies are summarised as follows. A comparative evaluation is presented for the performance of the Heat Integration scenarios of different HP types and processes by extended Pinch Analysis. The results show that for processes with larger source and sink slopes on the T–H profiles, JCHP is more suitable. For processes with a relatively smaller slope of the source and sink, VCHP is more suitable. The scope of application of TCHP is small. For processes with a relatively low source T-H slope and a relatively large sink T-H slope, it is appropriate to select TCHP. By improving the waste heat quality of the process, the HPs can save 15 to 78% of the hot utility. The COP of the VCHP decreased (from 13.07 to 4.44) with the increase of ΔT_{in} (from 1.5 °C to 11.84 °C) between

source and sink. However, the COP of JCHP decreased less with the increase of $\Delta T_{in(Sink-Source)}$. It is shown that if an inappropriate HP is selected to integrate with the process, the COP of the HP will decrease, which may lead to an investment increase. In extreme cases, the differences between the most and the least suitable integration mappings can be of the order of 100% and up to tenfold. For the different scenarios of Heat Integration with HPs, this study can provide guidance and suggestions for the selection of HPs.

An extended multiple-level fresh resources Pinch Analysis (PA-MLFR) and an extended PA-MLFR with intermediate headers (PA-MLFR-IH) are developed for Total Site Mass Integration considering fresh resources of various quality levels and simplify the configuration of mass exchange networks. The waste hydrogen recovery process is identified by a techno-economic analysis, where the advantages and application range of different purification technologies are taken into account. Hydrogen networks in refineries and water networks are taken as case studies in demonstrating the proposed methods. The results show that compared with only intra-plant integration, the overall 25.0 % (-29.27 kNm^3/h) reduction of minimum fresh hydrogen consumption and 74.5 % (-28.83 kNm^3/h) reduction of waste hydrogen discharge can be achieved for Total Site Hydrogen Integration with waste hydrogen purification. The hydrogen recovery ratio is 95.2 %, and the payback period is 3.2 months for the waste hydrogen purification process. By transforming waste hydrogen into useful secondary raw material reduces fresh hydrogen consumption and waste hydrogen discharge, and has significant economic benefits. In water integration, the optimal total number of intra-plant headers and inter-plant headers are respectively simplified to10 (including 3 wastewater headers), and 4 (including 2 freshwater headers). The scalability and flexibility of the mass exchange networks are enhanced by setting up and optimising the intermediate headers while keeping the target of minimising fresh resources consumption and waste discharge.

A hierarchical targeting method is developed by combining Onion Model and Pinch Analysis for hydrogen and Heat Integration in refineries. The case study results show that Hydrogen Pinch targeting can guide the hydrogen network optimisation and reducing hydrogen utility demands and waste hydrogen emissions. At the Total Site level, the targets show that the maximum reduction could be 86.5 % for hot utilities and 39.8 % for cold utilities. The unidirectional method is simple to use and has the advantages of graphic visualisation. It has been demonstrated that the combined targeting of hydrogen and thermal utilities for a refinery can save significant amounts of both types of resources.

A multi-resource integration concept map and an evaluation model are proposed to improve the sustainability of recycling systems. This visual representation clearly outlines the key trade-off between the resources dedicated to the recycling processes and the fresh resources supply. It links and evaluates the trade-offs between the degree of circularity (Total Circularity Index, TCI), energy consumption, and economic benefit. The optimisation goal is selected in two variants: exergy and Total Annual Cost (TAC). The evaluation is made as a function of TCI, accounting for the competition among the available reuse paths. The method is illustrated using an example of material-based secondary products and the potential power generation from waste resources. The evaluation shows that TAC for the cost-optimal degree of circularity is 22 % lower than the cost for the maximum circularity. The difference for the exergy criterion between the optimal and the highest circularity is 33 %. These results illustrate the usefulness of the proposed model. The marginal monetary cost of attaining the exergy optimum compared to the cost optimum is 1.2 %, and the exergy penalty of attaining the cost optimum compared to the exergy one is 4.8 %, indicating that some exergy-intensive options carry a low cost. The comparison of the system performance against CMU and CEU reveals the internal trade-offs between the potential uses of the waste resources for one type of product or another.

Based on the results of the thesis, the main suggestions for future work directions are as follows. The Pinch-based methods for targeting and designing Mass and Heat Integration systems should be combined with Mathematical Programming for larger-scale problems to exploit the advantages of both approaches. This type of combination has been applied successfully for Heat Integration as well as in Water-Heat Integration and is likely to be successful in the field of combined Mass and Energy Integration too.

The evaluation of environmental footprints (e.g. GHG, Water, Nitrogen and particulate matter footprints) can be further embedded into the Process Integration methods. The current methodology focuses on the minimisation of waste and intake of the targeted resources – energy, hydrogen, water. While this implicitly reduces the environmental footprints, the results from Chapter 6 indicate that the energy intensity varies with the circularity rate in the systems closing the circles in Circular Economy implementations. By implication, the related environmental footprints will also vary with the circularity rate. This indication suggests that the environmental footprints have to be explicitly evaluated when the methods for resource integration are applied, and this is a potentially fruitful direction of future research.

Nomenclature

Abbreviation

CCS	Carbon Capture and Storage
CE	Circular Economy
CMAHEN	Combined Mass And Heat Exchange Network
COP	Coefficient of Performance
CP	Specific Heat Capacity
ECI	Energy Circularity Indicator
EU	European Union
GCC	Grand Composite Curve
GWP	global warming potential
HEN	Heat Exchanger Network
HI	Heat Integration
HN	Hydrogen Network
HP	heat pump
HX	heat exchanger
JCHP	Joule cycle heat pump
LIES	Locally Integrated Energy Sectors
LP	Linear Programming
MCA	Material Cascade Analysis
MEN	Mass Exchange Network
MILP	Mixed-Integer Linear Programming
MINLP	Mixed-Integer Nonlinear Programming
MP	Mathematical Programming
MRPD	Material Recovery Pinch Diagram
NLP	Nonlinear Programming
PA	Pinch Analysis
PI	Process Integration
PSA	Pressure Swing Adsorption
RCN	Resource Conservation Network
TCHP	Transcritical Heat Pump
T–H	temperature–enthalpy
T-S	temperature–entropy
TSHI	Total Site Heat Integration
TSI	Total Site Integration
TSMI	Total Site Mass Integration
VCHP	Vapour Compression Heat Pump
VLV	let-down valve
WAHEN	Water and Heat Exchange Network
WPA	Water Pinch Analysis

Sets

$[m]$	Set of paths for secondary resources to secondary material products
$[e]$	Set of paths for secondary resources to secondary energy products
$[i]$	Set of all processing paths

Nomenclature

A_{mem}	Membrane area, m^2;
a_{com}	Capital cost coefficient of compressor, k€;
a_k	Capital cost coefficient of equipment k, k€;
a_{mem}	Capital cost coefficient of membrane separation, k€;
a_{PSA}	Capital cost coefficient of PSA, k€;
a_{pip}	Capital cost coefficient of pipeline, k€;
ACC	Annual Capital Cost, EUR/y;
AF_k	Annualisation factor for the capital cost of equipment k, -;
AOC	Annual operating and maintenance cost of processing treatment, EUR/y;
b_{com}	Capital cost coefficient of compressor, k€/kW;
b_k	Capital cost coefficient of equipment k
b_{mem}	Capital cost coefficient of membrane separation, k€/m^3;
b_{PSA}	Capital cost coefficient of PSA, k€/m^3 or k€/t;
b_{pip}	Capital cost coefficient of pipeline, k€/m;
C_F	Cost/price per unit of feed material of purification process, k€/m^3 or k€/t;
C_R	Cost/price per unit of regenerated hydrogen product, k€/m^3 or k€/t;
C_U	Cost/price per unit of utility, k€/(kW·h) or k€/t;
C_W	Cost/price per unit of final waste hydrogen, k€/m^3 or k€/t;
CC_{com}	Capital cost of compressor, k€;
CC_{mem}	Capital cost of membrane separation, k€;
CC_k	Capital cost of equipment k, k€;
CC_{PSA}	Capital cost of PSA, k€;
CC_{pip}	Capital cost of pipeline, k€;
CEU	Circular Exergy Use rate, -;
CEU_{total}	Total Circular Exergy Use rate, -;
CMU	Circular Material Use rate, -;
CMU_{total}	Total Circular Material Use rate, -;
$E_{external,k}$	External input enthalpy of equipment k, kW;
$E_{input,k}$	Inlet materials enthalpy of equipment k, kW;
$E_{output,k}$	Outlet material enthalpy of equipment k, kW;
E_{reused}	Energy supplied from secondary raw materials, kW;
E_{total}	Total energy supplied to a given demand, kW;
Ex_{demand}	Exergy of demand, kW;

Ex_{input}	External exergy input for the recovery processes, kW;
$Ex_{inputenergy}$	Exergy of external energy, kW;
$Ex_{inputmass}$	Exergy of external materials, kW;
$Ex_{landfill}$	Exergy of landfill, kW;
$Ex_{product}$	Exergy of a secondary product, kW;
$Ex_{recovery}$	Recovered exergy, kW;
$Ex_{utility}$	Exergy of utility, kW;
F_{demand}	Flowrate of the demand, kg/h or kW;
$F_{distribution}$	Mass flowrate distributed to different processes, kg/h;
F_F	Feed flowrate of a waste hydrogen purification process, kNm^3/h or t/h;
F_k^{low}	Lower bound of flowrate (F_k), kNm^3/h or t/h;
F_k^{up}	Upper bound of flowrate (F_k), kNm^3/h or t/h;
F_{PSA}	Feed flowrate of PSA, kNm^3/h or t/h;
$F_{perm,i}$	Permeable gas flowrate of component i, kmol/h;
F_{pip}	Flowrate of stream in the pipeline, kNm^3/h or t/h;
$F_{product}$	Flowrate of the secondary product, kg/h or kW;
F_R	Flowrate of regenerated hydrogen, kNm^3/h or t/h;
$F_{sorting}$	Mass flowrate after secondary product sorting, kg/h;
F_U	Compression power or Flowrate of utility, kW or t/h;
$F_{utility}$	Mass flowrate of the utility, kg/h or kW;
F_W	Flowrate of the final waste hydrogen discharged, kNm^3/h or t/h;
F_{WR}	Flowrates of the secondary (waste) resource streams used for recycling, kg/h;
F_{WR}^{max}	Mass flowrate of the overall waste resource availability, kg/h;
J_i	Permeability rate of component i, kmol/(h·m^2·kPa) or GPU;
J_j	Permeability rate of component j, kmol/(h·m^2·kPa) or GPU;
L	Distance between supplier and receiver, m;
P_2	Outlet pressure of the compressor in the HP cycle, MPa;
P_5	Outlet pressure of the expander or expansion valve in the HP cycle, MPa;
P_F,	Pressure of feed waste hydrogen, MPa;
P_k^{low}	Lower bound of pressure (P_k), MPa;
P_k^{up}	Upper bound of pressure (P_k), MPa;
$P_{landfillfee}$	Landfill disposal fee of per ton feed, EUR/t;
P_P	Utility price, EUR/t or EUR/kWh;
P_{pip}	Maximum pressure of the pipeline, MPa;
P_R	Pressure of regenerated hydrogen product, MPa;
PT	Payback period, y;
P_W	Pressure of final waste hydrogen discharged as fuel, MPa;

Pw_{com}	Power consumption of compressor, kW;
Q_h	Heat output of the heat pump, kW;
R	The compression ratio of the compressor, -
r_k	Interest rate, -;
T	Payback period, y;
t	Annual operating time, h/y;
T_5	The outlet temperature of the expansion valve in the HP cycle, °C;
T_s	supply temperature, °C;
$T_{sink\text{-}out}$	The outlet temperature of the sink, °C;
T_t	Target temperature, °C;
TAC	Total Annual Cost, EUR/y;
TAP	Total annual profit, M€/y
TCC	Total annual capital cost, M€/y
TCI	Total Circularity Index, 1;
TLF	Annual cost of disposing of the remaining waste, EUR/y;
TOC	Total operating cost, M€/y
TPC	Annual processing cost, EUR/y;
TPV	Total product value, M€/y
TUC	Annual utilities cost, EUR/y;
UCC	Capital cost of per ton feed, EUR/kg;
UOC	Annual operating and maintenance cost of per ton feed for processing treatment, EUR/kg;
W	Electrical or power consumption of the heat pump, kW;
$x_{distribution}$	Distribution fraction, 1;
$x_{efficiency}$	Efficiency or conversion factor of different processes, 1;
x_{F,H_2}	Hydrogen fraction in feed waste hydrogen, -;
$x_{F,i}$,	Molar fraction of component i in feed waste hydrogen, -;
x_{R,H_2}	Hydrogen fraction in regenerated hydrogen, -;
$x_{R,i}$	Molar fraction of component i in regenerated hydrogen, -;
$x_{sorting}$	Sorting fraction of secondary (waste) resource, 1;
$x_{W,i}$	Molar fraction of component i in final waste hydrogen discharged, -;
y_k	Equipment lifetime, y;
Z_k	Binary variable (0, 1) of whether equipment k exists, -;
$\alpha_{i,j}$	Selection coefficient of the membrane, -;
φ_{H_2}	Hydrogen recovery ratio, %;
ΔP_i	Pressure difference of the component i on both sides of membrane, kPa;
ΔP	The pressure difference, MPa;
ΔT	temperature difference, °C;
ΔT_1	The difference between the inlet temperature of the sink and the outlet

	temperature of the source, °C;
ΔT_2	The difference between the outlet temperature of the sink and the inlet temperature of the source, °C;
ΔT_{in}	The inlet temperature difference of the source and sink, °C;
ΔT_{min}	minimum approach temperature, °C;
ΔT_{out}	The outlet temperature difference of the source and sink, °C;
ω_1	Weight factor of CEU_{total}, 1;
ω_2	Weight factor of CMU_{total}, 1;

REFERENCES

Aasadnia, M., Mehrpooya, M., Ghorbani, B., 2021. A novel integrated structure for hydrogen purification using the cryogenic method. J. Clean. Prod. 278, 123872. doi:10.1016/j.jclepro.2020.123872

Abadías Llamas, A., Bartie, N.J., Heibeck, M., Stelter, M., Reuter, M.A., 2020. Simulation-Based Exergy Analysis of Large Circular Economy Systems: Zinc Production Coupled to CdTe Photovoltaic Module Life Cycle. J. Sustain. Metall. 6, 34–67. doi:10.1007/s40831-019-00255-5

Abdolmohammadi, H.R., Kazemi, A., 2013. A Benders decomposition approach for a combined heat and power economic dispatch. Energy Convers. Manag. 71, 21–31. doi:10.1016/j.enconman.2013.03.013

Adhikari, S., Fernando, S., 2006. Hydrogen Membrane Separation Techniques. Ind. Eng. Chem. Res. 45, 875–881. doi:10.1021/ie0506441

Adler, B., Mauthner, R., 2017. Rotation Heat Pump (RHP). Presented at the 12th IEA Heat Pump Conference 2017, Rotterdam, The Netherlands, p. O351.

Afshari, H., Tosarkani, B.M., Jaber, M.Y., Searcy, C., 2020. The effect of environmental and social value objectives on optimal design in industrial energy symbiosis: A multi-objective approach. Resour. Conserv. Recycl. 158, 104825. doi:10.1016/j.resconrec.2020.104825

Ahmad Fadzil, A.F., Wan Alwi, S.R., Manan, Z.A., Klemeš, J.J., 2018. Maximizing Total Site Water Reuse via a Two-Way Centralized Water Header. ACS Sustain. Chem. Eng. 6, 2563–2573. doi:10.1021/acssuschemeng.7b04050

Ahmetović, E., Ibrić, N., Kravanja, Z., Grossmann, I.E., 2015. Water and energy integration: A comprehensive literature review of non-isothermal water network synthesis. Comput. Chem. Eng. 82, 144–171. doi:10.1016/j.compchemeng.2015.06.011

Ahmetović, E., Kravanja, Z., 2013. Simultaneous synthesis of process water and heat exchanger networks. Energy 57, 236–250. doi:10.1016/j.energy.2013.02.061

Almeida, S.T. de, Borsato, M., Lie Ugaya, C.M., 2017. Application of exergy-based approach for implementing design for reuse: The case of microwave oven. J. Clean. Prod. 168, 876–892. doi:10.1016/j.jclepro.2017.09.034

Almutlaq, A.M., Kazantzi, V., El-Halwagi, M.M., 2005. An algebraic approach to targeting waste discharge and impure fresh usage via material recycle/reuse networks. Clean Technol. Environ. Policy 7, 294–305. doi:10.1007/s10098-005-0005-8

Alves, J., 1999. Analysis and design of refinery hydrogen distribution systems (PhD). UMIST, Manchester, UK, Manchester, UK.

Alves, J.J., Towler, G.P., 2002. Analysis of Refinery Hydrogen Distribution Systems. Ind. Eng. Chem. Res. 41, 5759–5769. doi:10.1021/ie010558v

Angioletti, C.M., Despeisse, M., Rocca, R., 2017a. Product Circularity Assessment Methodology, in: Lödding, H., Riedel, R., Thoben, K.-D., von Cieminski, G., Kiritsis, D. (Eds.), Advances in Production Management Systems. The Path to Intelligent, Collaborative and Sustainable Manufacturing, IFIP Advances in Information and Communication Technology. Springer International Publishing, Cham, pp. 411–418. doi:10.1007/978-3-319-66926-7_47

Angioletti, C.M., Despeisse, M., Rocca, R., 2017b. Product Circularity Assessment Methodology, in: Lödding, H., Riedel, R., Thoben, K.-D., von Cieminski, G., Kiritsis, D. (Eds.), Advances in Production Management Systems. The Path to Intelligent, Collaborative and Sustainable Manufacturing. Springer International Publishing, Cham, pp. 411–418. doi:10.1007/978-3-319-66926-7_47

Arsalis, A., Alexandrou, A.N., Georghiou, G.E., 2018. Thermoeconomic modeling of a small-scale gas turbine-photovoltaic-electrolyzer combined-cooling-heating-and-power system for distributed energy applications. J. Clean. Prod. 188, 443–455. doi:10.1016/j.jclepro.2018.04.001

Aspen HYSYS V11, 2019. Aspen Technology, Inc., Bedford, MA, USA.

Ataei, A., Tahouni, N., Haji Seyedi, S.M., Hashemian, S.M., Yoo, C., Panjeshahi, M.H., 2014. A novel approach to hot oil system design for energy conservation. Appl. Therm. Eng. 66, 423–434. doi:10.1016/j.applthermaleng.2014.01.044

Atkins, M.J., Walmsley, M.R.W., Neale, J.R., 2011. Integrating heat recovery from milk powder spray dryer exhausts in the dairy industry. Appl. Therm. Eng. 31, 2101–2106. doi:10.1016/j.applthermaleng.2011.03.006

Azevedo, S.G., Godina, R., Matias, J.C. de O., 2017. Proposal of a Sustainable Circular Index for Manufacturing Companies. Resources 6, 63. doi:10.3390/resources6040063

Bandyopadhyay, S., Sahu, G.C., Foo, D.C.Y., Tan, R.R., 2010. Segregated targeting for multiple resource networks using decomposition algorithm. AIChE J. 56, 1235–1248. doi:10.1002/aic.12050

Beangstrom, S.G., Majozi, T., 2016. Steam system network synthesis with hot liquid reuse: II. Incorporating shaft work and optimum steam levels. Comput. Chem. Eng. 85, 202–209. doi:10.1016/j.compchemeng.2015.10.016

Bernardo, G., Araújo, T., da Silva Lopes, T., Sousa, J., Mendes, A., 2020. Recent advances in membrane technologies for hydrogen purification. Int. J. Hydrog. Energy, Hydrogen separation/purification via membrane technology 45, 7313–7338. doi:10.1016/j.ijhydene.2019.06.162

Boldyryev, S., Varbanov, P.S., 2015. Low potential heat utilization of bromine plant via integration on process and Total Site levels. Energy 90, 47–55. doi:10.1016/j.energy.2015.05.071

Cai, Y.P., Huang, G.H., Yang, Z.F., Tan, Q., 2009. Identification of optimal strategies for energy management systems planning under multiple uncertainties. Appl. Energy 86, 480–495. doi:10.1016/j.apenergy.2008.09.025

Cao, D., Feng, X., Duan, X., 2004. Design of Water Network with Internal Mains for Multi-contaminant Wastewater Regeneration Recycle. Chem. Eng. Res. Des. 82, 1331–1336. doi:10.1205/cerd.82.10.1331.46732

Carnot, S., 1986. Reflexions on the Motive Power of Fire: A Critical Edition with the Surviving Scientific Manuscripts. Manchester University Press, UK.

Cewep, 2020. Landfill taxes and bans overview. URL https://www.cewep.eu/wp-content/uploads/2017/12/Landfill-taxes-and-bans-overview.pdf (accessed 30.07.2020).

Chang, C., Wang, Y., Feng, X., 2015. Indirect heat integration across plants using hot water circles. Chin. J. Chem. Eng. 23, 992–997. doi:10.1016/j.cjche.2015.01.010

Chen, C.-L., Hung, S.-W., Lee, J.-Y., 2010. Design of inter-plant water network with central and decentralized water mains. Comput. Chem. Eng., Selected papers from the 7th International Conference on the Foundations of Computer-Aided Process Design (FOCAPD, 2009, Breckenridge, Colorado, USA. 34, 1522–1531. doi:10.1016/j.compchemeng.2010.02.024

Chen, Q.L., Yin, Q.H., Wang, S.P., Hua, B., 2004. Energy-use analysis and improvement for delayed coking units. Energy, Efficiency, Costs, Optimization, Simulation and Environmental Impact of Energy Systems 29, 2225–2237. doi:10.1016/j.energy.2004.03.021

Chen, Z., Hou, Y., Li, X., Wang, J., 2014. Simultaneous optimization of water and heat exchange networks. Korean J. Chem. Eng. 31, 558–567. doi:10.1007/s11814-013-0236-z

Cheung, K.-Y., Hui, C.-W., 2004. Total-site scheduling for better energy utilization. J. Clean. Prod., Advances in cleaner production technologies 12, 171–184. doi:10.1016/S0959-6526(02)00193-2

Chew, I.M.L., Foo, D.C.Y., Ng, D.K.S., Tan, R.R., 2010a. Flowrate Targeting Algorithm for Interplant Resource Conservation Network. Part 1: Unassisted Integration Scheme. Ind. Eng. Chem. Res. 49, 6439–6455. doi:10.1021/ie901802m

Chew, I.M.L., Foo, D.C.Y., Tan, R.R., 2010b. Flowrate Targeting Algorithm for Interplant Resource Conservation Network. Part 2: Assisted Integration Scheme. Ind. Eng. Chem. Res. 49, 6456–6468. doi:10.1021/ie901804z

Chew, K.H., Klemeš, J.J., Wan Alwi, S.R., Manan, Z.A., Reverberi, A.P., 2015. Total site heat integration considering pressure drops. Energies 8, 1114–1137. doi:10.3390/en8021114

Chin, H.H., Jia, X., Varbanov, P.S., Klemeš, J.J., Liu, Z.-Y., 2021a. Internal and Total Site Water Network Design with Water Mains Using Pinch-Based and Optimization Approaches. ACS Sustain. Chem. Eng. 9, 6639–6658. doi:10.1021/acssuschemeng.1c00183

Chin, H.H., Varbanov, P.S., Klemeš, J.J., Liew, P.Y., 2021b. Enhanced Cascade Table Analysis to target and design multi-constraint resource conservation networks. Comput. Chem. Eng. 148, 107262. doi:10.1016/j.compchemeng.2021.107262

Chin, H.H., Varbanov, P.S., Klemeš, J.J., Wan Alwi, S.R., 2021c. Total Site Material Recycling Network Design and Headers Targeting Framework with Minimal Cross-Plant Source Transfer. Comput. Chem. Eng. 107364. doi:10.1016/j.compchemeng.2021.107364

Chin, H.H., Varbanov, P.S., Liew, P.Y., Klemeš, J.J., 2021d. Pinch-based targeting methodology for multi-contaminant material recycle/reuse. Chem. Eng. Sci. 230, 116129. doi:10.1016/j.ces.2020.116129

Chin, H.H., Wang, B., Varbanov, P.S., Klemeš, J.J., Zeng, M., Wang, Q.-W., 2020. Long-term investment and maintenance planning for heat exchanger network retrofit. Appl. Energy 279, 115713. doi:10.1016/j.apenergy.2020.115713

Cube, H.L.V., Steimle, F., 2013. Heat Pump Technology. Elsevier, Armsterdam, Netherland.

Cui, C., Sun, J., Li, X., 2017. A hybrid design combining double-effect thermal integration and heat pump to the methanol distillation process for improving energy efficiency. Chem.

Eng. Process. Process Intensif. 119, 81–92. doi:10.1016/j.cep.2017.06.003

Cullen, J.M., 2017. Circular Economy: Theoretical Benchmark or Perpetual Motion Machine? J. Ind. Ecol. 21, 483–486. doi:10.1111/jiec.12599

Dai, W., Shen, R., Zhang, D., Liu, G., 2017. The integration based method for identifying the variation trend of fresh hydrogen consumption and optimal purification feed. Energy 119, 732–743. doi:10.1016/j.energy.2016.11.031

Deng, C., Pan, H., Lee, J.-Y., Foo, D.C.Y., Feng, X., 2014. Synthesis of hydrogen network with hydrogen header of intermediate purity. Int. J. Hydrog. Energy 39, 13049–13062. doi:10.1016/j.ijhydene.2014.06.129

Deng, C., Zhou, Y., Feng, X., 2015. Flowrate Targeting for Hydrogen Network with Intermediate Header. Chem. Eng. Trans. 45, 43–48. doi:10.3303/CET1545008

Deng, C., Zhou, Y., Jiang, W., Feng, X., 2017a. Optimal design of inter-plant hydrogen network with purification reuse/recycle. Int. J. Hydrog. Energy 42, 19984–20002. doi:10.1016/j.ijhydene.2017.06.199

Deng, C., Zhou, Y., Zhu, M., Feng, X., 2017b. Optimal design of hydrogen network with intermediate header and minimum compressor work, in: 2017 6th International Symposium on Advanced Control of Industrial Processes (AdCONIP). Presented at the 2017 6th International Symposium on Advanced Control of Industrial Processes (AdCONIP), pp. 61–66. doi:10.1109/ADCONIP.2017.7983756

Dhole, V.R., Linnhoff, B., 1993. Total site targets for fuel, co-generation, emissions, and cooling. Comput. Chem. Eng., European Symposium on Computer Aided Process Engineering—2 17, S101–S109. doi:10.1016/0098-1354(93)80214-8

Di Maio, F., Rem, P.C., Baldé, K., Polder, M., 2017. Measuring resource efficiency and circular economy: A market value approach. Resour. Conserv. Recycl. 122, 163–171. doi:10.1016/j.resconrec.2017.02.009

Ding, Y., Feng, X., Chu, K.H., 2011. Optimization of hydrogen distribution systems with pressure constraints. J. Clean. Prod. 19, 204–211. doi:10.1016/j.jclepro.2010.09.013

Domenech, T., Bleischwitz, R., Doranova, A., Panayotopoulos, D., Roman, L., 2019. Mapping Industrial Symbiosis Development in Europe_ typologies of networks, characteristics, performance and contribution to the Circular Economy. Resour. Conserv. Recycl. 141, 76–98. doi:10.1016/j.resconrec.2018.09.016

Eggeman, T., 2004. Boundary analysis for H2 production by fermentation (No. Subcontract Report NREL/SR-560-36129). NREL National Renewal Energy Laboratory.

El-Halwagi, M.M., 2017. Sustainable Design Through Process Integration: Fundamentals and Applications to Industrial Pollution Prevention, Resource Conservation, and Profitability Enhancement. Butterworth-Heinemann.

El-Halwagi, M.M., Gabriel, F., Harell, D., 2003. Rigorous Graphical Targeting for Resource Conservation via Material Recycle/Reuse Networks. Ind. Eng. Chem. Res. 42, 4319–4328. doi:10.1021/ie030318a

El-Halwagi, M.M., Manousiouthakis, V., 1989. Synthesis of mass exchange networks. AIChE J. 35, 1233–1244. doi:10.1002/aic.690350802

Elsherif, M., Manan, Z.A., Kamsah, M.Z., 2015. State-of-the-art of hydrogen management in refinery and industrial process plants. J. Nat. Gas Sci. Eng. 24, 346–356.

doi:10.1016/j.jngse.2015.03.046

Embodied Energy Coefficients, URL https://www.wgtn.ac.nz/architecture/centres/cbpr/resources/pdfs/ee-coefficients.pdf (accessed 01.09.2020).

European Commission, 2020. New Circular Economy Action Plan. Interreg Eur. URL https://www.interregeurope.eu/plasteco/news/news-article/8056/new-circular-economy-action-plan/ , (accessed 08.08.2020).

European Commission, 2019. A European Green Deal | European Commission. URL https://ec.europa.eu/info/node/123797 , (accessed 08.08.2020).

Eurostat, 2018. Circular material use rate: calculation method : 2018 edition. Publications Office of the European Union, Luxembourg.

Expósito, A., Velasco, F., 2018. Municipal solid-waste recycling market and the European 2020 Horizon Strategy: A regional efficiency analysis in Spain. J. Clean. Prod. 172, 938–948. doi:10.1016/j.jclepro.2017.10.221

Fadzil, A.F.A., Wan Alwi, S.R., Manan, Z., Klemeš, J.J., 2018. Industrial site water minimisation via one-way centralised water reuse header. J. Clean. Prod. 200, 174–187. doi:10.1016/j.jclepro.2018.07.193

Fan, Y.V., Klemeš, J.J., Walmsley, T.G., Bertók, B., 2020. Implementing Circular Economy in municipal solid waste treatment system using P-graph. Sci. Total Environ. 701. doi:10.1016/j.scitotenv.2019.134652

Fan, Y.V., Lee, C.T., Lim, J.S., Klemeš, J.J., Le, P.T.K., 2019. Cross-disciplinary approaches towards smart, resilient and sustainable circular economy. J. Clean. Prod. 232, 1482–1491. doi:10.1016/j.jclepro.2019.05.266

Farhat, A., Zoughaib, A., El Khoury, K., 2015. A new methodology combining total site analysis with exergy analysis. Comput. Chem. Eng. 82, 216–227. doi:10.1016/j.compchemeng.2015.07.010

Feng, X., Seider, W.D., 2001. New Structure and Design Methodology for Water Networks. Ind. Eng. Chem. Res. 40, 6140–6146. doi:10.1021/ie000835i

Fogarassy, C., Kovács, A., Horváth, B., Borocz, M., 2017. The development of a circular evaluation (CEV) tool-case study for the 2024 Budapest Olympics. Hung. Agric. Eng. 10–20. doi:10.17676/HAE.2017.31.10

Foo, D.C.Y., 2012. Process Integration for Resource Conservation. CRC Press, USA.

Foo, D.C.Y., 2010. Automated Targeting Technique for Batch Process Integration. Ind. Eng. Chem. Res. 49, 9899–9916. doi:10.1021/ie100146n

Foo, D.C.Y., 2009. State-of-the-Art Review of Pinch Analysis Techniques for Water Network Synthesis. Ind. Eng. Chem. Res. 48, 5125–5159. doi:10.1021/ie801264c

Fu, C., Gundersen, T., 2016. A Novel Sensible Heat Pump Scheme for Industrial Heat Recovery. Ind. Eng. Chem. Res. 55, 967–977. doi:10.1021/acs.iecr.5b02417

Gai, L., Varbanov, P.S., Fan, Y.V., Klemeš, J.J., Nižetić, S., 2021a. Total Site Hydrogen Integration with fresh hydrogen of multiple quality and waste hydrogen recovery in refineries. Int. J. Hydrog. Energy. doi:10.1016/j.ijhydene.2021.06.154

Gai, L., Varbanov, P.S., Fan, Y.V., Klemeš, J.J., Romanenko, S.V., 2021b. Trade-offs between

the recovery, exergy demand and economy in the recycling of multiple resources. Resour. Conserv. Recycl. 167, 105428. doi:10.1016/j.resconrec.2021.105428

Gai, L., Varbanov, P.S., Walmsley, T.G., Klemeš, J.J., 2020a. Critical analysis of process integration options for joule-cycle and conventional heat pumps. Energies 13. doi:10.3390/en13030635

Gai, L., Varbanov, P.S., Klemeš, J.J., Sun, L., 2020b. Hierarchical Targeting of Hydrogen Network System and Heat Integration in a Refinery. Chem. Eng. Trans. 81, 217–222. doi:10.3303/CET2081037

Gai, L., Varbanov, P.S., Walmsley, T.G., Klemeš, J.J., 2019. Process Integration Using a Joule Cycle Heat Pump. Chem. Eng. Trans. 76, 415–420. doi:10.3303/CET1976070

GAMS, 2020. General Algebraic Modeling System. https://www.gams.com. accessed 25/ 09/2020.

Geng, Y., Fu, J., Sarkis, J., Xue, B., 2012. Towards a national circular economy indicator system in China: an evaluation and critical analysis. J. Clean. Prod. 23, 216–224. doi:10.1016/j.jclepro.2011.07.005

Golmakani, A., Fatemi, S., Tamnanloo, J., 2017. Investigating PSA, VSA, and TSA methods in SMR unit of refineries for hydrogen production with fuel cell specification. Sep. Purif. Technol. 176, 73–91. doi:10.1016/j.seppur.2016.11.030

Goumba, A., Chiche, S., Guo, X., Colombert, M., Bonneau, P., 2017. Recov'Heat: An estimation tool of urban waste heat recovery potential in sustainable cities. AIP Conference Proceedings, pp. 020038-1-020038–9. doi:10.1063/1.4976257

Gouws, J.F., Majozi, T., Foo, D.C.Y., Chen, C.-L., Lee, J.-Y., 2010. Water Minimization Techniques for Batch Processes. Ind. Eng. Chem. Res. 49, 8877–8893. doi:10.1021/ie100130a

Guo, Y., Glad, T., Zhong, Z., He, R., Tian, J., Chen, L., 2018. Environmental life-cycle assessment of municipal solid waste incineration stocks in Chinese industrial parks. Resour. Conserv. Recycl. 139, 387–395. doi:10.1016/j.resconrec.2018.05.018

Hackl, R., Andersson, E., Harvey, S., 2011. Targeting for energy efficiency and improved energy collaboration between different companies using total site analysis (TSA). Energy, PRES 2010 36, 4609–4615. doi:10.1016/j.energy.2011.03.023

Haghrah, A., Nazari-Heris, M., Mohammadi-ivatloo, B., 2016. Solving combined heat and power economic dispatch problem using real coded genetic algorithm with improved Mühlenbein mutation. Appl. Therm. Eng. 99, 465–475. doi:10.1016/j.applthermaleng.2015.12.136

Hallale, N., Liu, F., 2001. Refinery hydrogen management for clean fuels production. Adv. Environ. Res. 6, 81–98. doi:10.1016/S1093-0191(01)00112-5

Han, R., Kang, L., Jiang, Y., Wang, J., Liu, Y., 2020. Optimization of an Inter-Plant Hydrogen Network: A Simultaneous Approach to Solving Multi-Period Optimization Problems. Processes 8, 1548. doi:10.3390/pr8121548

Hartley, K., van Santen, R., Kirchherr, J., 2020. Policies for transitioning towards a circular economy: Expectations from the European Union (EU). Resour. Conserv. Recycl. 155, 104634. doi:10.1016/j.resconrec.2019.104634

Haupt, M., Vadenbo, C., Hellweg, S., 2017. Do We Have the Right Performance Indicators for

the Circular Economy?: Insight into the Swiss Waste Management System. J. Ind. Ecol. 21, 615–627. doi:10.1111/jiec.12506

Herold, K.E., Radermacher, R., Klein, S.A., 2016. Absorption Chillers and Heat Pumps, Second edition. ed. CRC Press, Taylor & Francis Group, Boca Raton, USA.

Hohmann E.C., 1971. Optimum Networks for Heat Exchange. (Ph. D thesis). Univ. of Southern California.

Huang, Y., Merkel, T.C., Baker, R.W., 2014. Pressure ratio and its impact on membrane gas separation processes. J. Membr. Sci. 463, 33–40. doi:10.1016/j.memsci.2014.03.016

Huysman, S., De Schaepmeester, J., Ragaert, K., Dewulf, J., De Meester, S., 2017. Performance indicators for a circular economy: A case study on post-industrial plastic waste. Resour. Conserv. Recycl. 120, 46–54. doi:10.1016/j.resconrec.2017.01.013

Ibrić, N., Ahmetović, E., Kravanja, Z., Grossmann, I.E., 2021. Simultaneous optimisation of large-scale problems of heat-integrated water networks. Energy 235, 121354. doi:10.1016/j.energy.2021.121354

Jagannath, A., Elkamel, A., Karimi, I. A., 2012. Optimization of multi-refinery hydrogen networks, in: Karimi, Iftekhar A., Srinivasan, R. (Eds.), Computer Aided Chemical Engineering, 11 International Symposium on Process Systems Engineering. Elsevier, pp. 1331–1335. doi:10.1016/B978-0-444-59506-5.50097-3

Jamaluddin, K., Wan Alwi, S.R., Abdul Manan, Z., Hamzah, K., Klemeš, J.J., 2019. A Process Integration Method for Total Site Cooling, Heating and Power Optimisation with Trigeneration Systems. Energies 12, 1030. doi:10.3390/en12061030

Jia, N., Zhang, N., 2011. Multi-component optimisation for refinery hydrogen networks. Energy, PRES 2010 36, 4663–4670. doi:10.1016/j.energy.2011.03.040

Jia, X., Li, Z., Wang, F., Foo, D.C.Y., Qian, Y., 2015. A new graphical representation of water footprint pinch analysis for chemical processes. Clean Technol. Environ. Policy 17, 1987–1995. doi:10.1007/s10098-015-0921-1

Jia, X., Varbanov, P., Wan Alwi, S.R., Klemeš, J., 2020. Total Site Water Main Concentration Selection: A Case Study. Chem. Eng. Trans. 81, 259–264. doi:10.3303/CET2081044

Kamat, S., Bandyopadhyay, S., 2021a. Bi-objective Pinch Analysis of heat integrated water conservation networks. J. Clean. Prod. 312, 127676. doi:10.1016/j.jclepro.2021.127676

Kamat, S., Bandyopadhyay, S., 2021b. A hybrid approach for heat integration in water conservation networks through non-isothermal mixing. Energy 233, 121143. doi:10.1016/j.energy.2021.121143

Kang, L., Liang, X., Liu, Y., 2018. Optimal design of inter-plant hydrogen networks with intermediate headers of purity and pressure. Int. J. Hydrog. Energy 43, 16638–16651. doi:10.1016/j.ijhydene.2018.07.044

Kazantzi, V., El-Halwagi, M.M., 2005. Targeting Material Reuse via Property Integration. Chem. Eng. Prog. N. Y. 101, 28–37.

KBC, 2016. Petro-SIM, KBC Advanced Technologies. London, UK.

Kemp, I.C., 2007. Pinch analysis and process integration: a user guide on process integration for the efficient use of energy, 2nd ed. ed. Butterworth-Heinemann, Amsterdam ; Boston.

Khojasteh Salkuyeh, Y., Saville, B.A., MacLean, H.L., 2017. Techno-economic analysis and life cycle assessment of hydrogen production from natural gas using current and emerging technologies. Int. J. Hydrog. Energy 42, 18894–18909. doi:10.1016/j.ijhydene.2017.05.219

Kim, H.J., Ahn, J.M., Cho, S.O., Cho, K.R., 2008. Numerical simulation on scroll expander–compressor unit for CO2 trans-critical cycles. Appl. Therm. Eng. 28, 1654–1661. doi:10.1016/j.applthermaleng.2007.11.002

Kirchherr, J., Piscicelli, L., Bour, R., Kostense-Smit, E., Muller, J., Huibrechtse-Truijens, A., Hekkert, M., 2018. Barriers to the Circular Economy: Evidence from the European Union (EU). Ecol. Econ. 150, 264–272. doi:10.1016/j.ecolecon.2018.04.028

Kirchherr, J., Reike, D., Hekkert, M., 2017a. Conceptualizing the circular economy: An analysis of 114 definitions. Resour. Conserv. Recycl. 127, 221–232. doi:10.1016/j.resconrec.2017.09.005

Kirchherr, J., Reike, D., Hekkert, M., 2017b. Conceptualizing the circular economy: An analysis of 114 definitions. Resour. Conserv. Recycl. 127, 221–232. doi:10.1016/j.resconrec.2017.09.005

Klemeš, J., Dhole, V.R., Raissi, K., Perry, S.J., Puigjaner, L., 1997. Targeting and design methodology for reduction of fuel, power and CO2 on total sites. Appl. Therm. Eng. 17, 993–1003. doi:10.1016/S1359-4311(96)00087-7

Klemeš, J.J., 2015. Assessing and Measuring Environmental Impact and Sustainability. Butterworth-Heinemann/Elsevier, Oxford, UK ; Waltham, MA, USA.

Klemeš, J.J. (ed), 2013. Handbook of Process Integration (PI): Minimisation of Energy and Water Use, Waste and Emissions. Woodhead Publishing/Elsevier, Cambridge, UK.

Klemeš, Jiří Jaromír, Fan, Y.V., Jiang, P., 2020. Plastics: friends or foes? The circularity and plastic waste footprint. Energy Sources Part Recovery Util. Environ. Eff. 0, 1–17. doi:10.1080/15567036.2020.1801906

Klemeš, J.J., Friedler, F., Bulatov, I., Varbanov, P.S., 2011. Sustainability in the Process Industry: Integration and Optimization. McGraw-Hill Education, New York, USA.

Klemeš, J.J., Kravanja, Z., 2013. Forty years of Heat Integration: Pinch Analysis (PA) and Mathematical Programming (MP). Curr. Opin. Chem. Eng. 2, 461–474. doi:10.1016/j.coche.2013.10.003

Klemeš, J.J., Varbanov, P.S., Wan Alwi, S.R., Manan, Z.A., 2018a. Sustainable Process Integration and Intensification: Saving Energy, Water and Resources, 2nd ed. Walter de Gruyter GmbH, Berlin, Germany.

Klemeš, J.J., Varbanov, P.S., Kravanja, Z., 2013. Recent developments in Process Integration. Chem. Eng. Res. Des. 91, 2037–2053. doi:10.1016/j.cherd.2013.08.019

Klemeš, J.J., Varbanov, P.S., Walmsley, T.G., Jia, X., 2018b. New directions in the implementation of Pinch Methodology (PM). Renew. Sustain. Energy Rev. 98, 439–468. doi:10.1016/j.rser.2018.09.030

Klemeš, J.J., Wang, Q.-W., Varbanov, P.S., Zeng, M., Chin, H.H., Lal, N.S., Li, N.-Q., Wang, B., Wang, X.-C., Walmsley, T.G., 2020. Heat transfer enhancement, intensification and optimisation in heat exchanger network retrofit and operation. Renew. Sustain. Energy Rev. 120. doi:10.1016/j.rser.2019.109644

Kruse, B., Grinna, S., Buch, C., 2002. Hydrogen--Status and Possibilities. Bellona, Norway.

Kuo, W.-C.J., Smith, R., 1998. Designing for the Interactions Between Water-Use and Effluent Treatment. Chem. Eng. Res. Des., Techno-Economic Analysis 76, 287–301. doi:10.1205/026387698524938

Lee, U., Han, J., Wang, M., 2017. Evaluation of landfill gas emissions from municipal solid waste landfills for the life-cycle analysis of waste-to-energy pathways. J. Clean. Prod. 166, 335–342. doi:10.1016/j.jclepro.2017.08.016

Li, B., He, G., Jiang, X., Dai, Y., Ruan, X., 2016. Pressure swing adsorption/membrane hybrid processes for hydrogen purification with a high recovery. Front. Chem. Sci. Eng. 10, 255–264. doi:10.1007/s11705-016-1567-1

Li, H., Liao, Z., Sun, J., Jiang, B., Wang, J., Yang, Y., 2020. Simultaneous Design of Hydrogen Allocation Networks and PSA Inside Refineries. Ind. Eng. Chem. Res. 59, 4712–4720. doi:10.1021/acs.iecr.9b06955

Li, P., Wang, Z., Qiao, Z., Liu, Y., Cao, X., Li, W., Wang, J., Wang, S., 2015. Recent developments in membranes for efficient hydrogen purification. J. Membr. Sci. 495, 130–168. doi:10.1016/j.memsci.2015.08.010

Li, Y., Chen, D.W., Liu, M., Wang, R.Z., 2017. Life cycle cost and sensitivity analysis of a hydrogen system using low-price electricity in China. Int. J. Hydrog. Energy 42, 1899–1911. doi:10.1016/j.ijhydene.2016.12.149

Liao, Z., Rong, G., Wang, J., Yang, Y., 2011. Systematic Optimization of Heat-Integrated Water Allocation Networks. Ind. Eng. Chem. Res. 50, 6713–6727. doi:10.1021/ie1016392

Liew, P.Y., Lim, J.S., Wan Alwi, S.R., Abdul Manan, Z., Varbanov, P.S., Klemeš, J.J., 2014. A retrofit framework for Total Site heat recovery systems. Appl. Energy 135, 778–790. doi:10.1016/j.apenergy.2014.03.090

Liew, P.Y., Theo, W.L., Wan Alwi, S.R., Lim, J.S., Abdul Manan, Z., Klemeš, J.J., Varbanov, P.S., 2017. Total Site Heat Integration planning and design for industrial, urban and renewable systems. Renew. Sustain. Energy Rev. 68, 964–985. doi:10.1016/j.rser.2016.05.086

Liew, P.Y., Walmsley, T.G., 2016. Heat pump integration for total site waste heat recovery 52, 817–822. doi:10.3303/CET1652137

Liew, P.Y., Wan Alwi, S.R., Ho, W.S., Abdul Manan, Z., Varbanov, P.S., Klemeš, J.J., 2018. Multi-period energy targeting for Total Site and Locally Integrated Energy Sectors with cascade Pinch Analysis. Energy 155, 370–380. doi:10.1016/j.energy.2018.04.184

Liew, P.Y., Wan Alwi, S.R., Varbanov, P.S., Manan, Z.A., Klemeš, J.J., 2012. A numerical technique for Total Site sensitivity analysis. Appl. Therm. Eng. 40, 397–408. doi:10.1016/j.applthermaleng.2012.02.026

Lim, L.Y., Lee, C.T., Bong, C.P.C., Lim, J.S., Klemeš, J.J., 2019. Environmental and economic feasibility of an integrated community composting plant and organic farm in Malaysia. J. Environ. Manage. 244, 431–439. doi:10.1016/j.jenvman.2019.05.050

Linder, M., Sarasini, S., Loon, P. van, 2017. A Metric for Quantifying Product-Level Circularity. J. Ind. Ecol. 21, 545–558. doi:10.1111/jiec.12552

Linnhoff, B., Flower, J.R., 1978a. Synthesis of heat exchanger networks: I. Systematic

generation of energy optimal networks. AIChE J. 24, 633–642. doi:10.1002/aic.690240411

Linnhoff, B., Flower, J.R., 1978b. Synthesis of heat exchanger networks: II. Evolutionary generation of networks with various criteria of optimality. AIChE J. 24, 642–654. doi:10.1002/aic.690240412

Linnhoff, B., Hindmarsh, E., 1983. The pinch design method for heat exchanger networks. Chem. Eng. Sci. 38, 745–763. doi:10.1016/0009-2509(83)80185-7

Linnhoff, B., Townsend, D.W., Boland, D., Hewitt, G.F., Thomas, B.E.A., Guy, A.R., Marsland, R.H., 1994. A user guide on process integration for the efficient use of energy. Rev. 1. ed. IChemE, Rugby, UK.

Liu, H., Ren, L., Zhuo, H., Fu, S., 2019. Water Footprint and Water Pinch Analysis in Ethanol Industrial Production for Water Management. Water 11, 518. doi:10.3390/w11030518

Liu, L., Sheng, Y., Zhuang, Y., Zhang, L., Du, J., 2020. Multiobjective Optimization of Interplant Heat Exchanger Networks Considering Utility Steam Supply and Various Locations of Interplant Steam Generation/Utilization. Ind. Eng. Chem. Res. 59, 14433–14446. doi:10.1021/acs.iecr.0c02852

Liu, L., Wang, J., Song, H., Du, J., Yang, F., 2016. Synthesis of water networks for industrial parks considering inter-plant allocation. Comput. Chem. Eng., 12th International Symposium on Process Systems Engineering & 25th European Symposium of Computer Aided Process Engineering (PSE-2015/ESCAPE-25), 31 May - 4 June 2015, Copenhagen, Denmark 91, 307–317. doi:10.1016/j.compchemeng.2016.03.013

Liu, X., Liu, J., Deng, C., Lee, J.-Y., Tan, R.R., 2020. Synthesis of refinery hydrogen network integrated with hydrogen turbines for power recovery. Energy 117623. doi:10.1016/j.energy.2020.117623

LLNL Flow Charts, 2019. LLNL Energy Flow Charts. Energy Flow Charts Charting Complex Relatsh. Energy Water Carbon. URL https://flowcharts.llnl.gov/ (accessed 24.08.2020).

Lopez-Echeverry, J.S., Reif-Acherman, S., Araujo-Lopez, E., 2017. Peng-Robinson equation of state: 40 years through cubics. Fluid Phase Equilibria 447, 39–71. doi:10.1016/j.fluid.2017.05.007

Lorentzen, G., 1990. Trans-critical vapour compression cycle device. International Patent Publication WO 90/07683, WO.

Lou, B., Sun, C., Ulgiati, S., 2015. Environmental Performance of Coal Power Generation in China, in: Reddy, B.S., Ulgiati, S. (Eds.), Energy Security and Development: The Global Context and Indian Perspectives. Springer India, New Delhi, pp. 307–319. doi:10.1007/978-81-322-2065-7_20

Lou, Y., Liao, Z., Sun, J., Jiang, B., Wang, J., Yang, Y., 2019. A novel two-step method to design inter-plant hydrogen network. Int. J. Hydrog. Energy 44, 5686–5695. doi:10.1016/j.ijhydene.2019.01.099

Luo, X., Huang, X., El-Halwagi, M.M., Ponce-Ortega, J.M., Chen, Y., 2016. Simultaneous synthesis of utility system and heat exchanger network incorporating steam condensate and boiler feedwater. Energy 113, 875–893. doi:10.1016/j.energy.2016.07.109

Luo, X., Zhang, B., Chen, Y., Mo, S., 2012. Operational planning optimization of multiple interconnected steam power plants considering environmental costs. Energy, 7th

Biennial International Workshop “Advances in Energy Studies” 37, 549–561. doi:10.1016/j.energy.2011.10.049

Ma, H., Feng, X., Cao, K., 2007. A Rule-Based Design Methodology for Water Networks with Internal Water Mains. Chem. Eng. Res. Des. 85, 431–444. doi:10.1205/cherd06139

Mabrouk, A., Erdocia, X., Alriols, M.G., Labidi, J., 2018. Economic analysis of a biorefinery process for catechol production from lignin. J. Clean. Prod. 198, 133–142. doi:10.1016/j.jclepro.2018.06.294

Maia, L.O.A., Qassim, R.Y., 1997. Synthesis of utility systems with variable demands using simulated annealing. Comput. Chem. Eng. 21, 947–950. doi:10.1016/S0098-1354(96)00342-0

Maio, F.D., Rem, P.C., 2015. A Robust Indicator for Promoting Circular Economy through Recycling. J. Environ. Prot. 6, 1095–1104. doi:10.4236/jep.2015.610096

Marechal, F., Kalitventzeff, B., 2003. Targeting the integration of multi-period utility systems for site scale process integration. Appl. Therm. Eng., Process Integration, Modelling and Optimisation for Energy Saving and Pollution Reduction 23, 1763–1784. doi:10.1016/S1359-4311(03)00142-X

Martínez, J., León, E., Baena-Moreno, F.M., Rodríguez-Galán, M., Arroyo-Torralvo, F., Vilches, L.F., 2020. Techno-economic analysis of a membrane-hybrid process as a novel low-energy alternative for zero liquid discharge systems. Energy Convers. Manag. 211, 112783. doi:10.1016/j.enconman.2020.112783

Matsuda, K., 2016. Comparative study of energy saving potential for heavy chemical complex by area-wide approach. Energy, Green Strategy for Energy Generation and Saving towards Sustainable Development 116, 1397–1402. doi:10.1016/j.energy.2016.07.054

Matsuda, K., Tanaka, S., Endou, M., Iiyoshi, T., 2012. Energy saving study on a large steel plant by total site based pinch technology. Appl. Therm. Eng., Optimisation of Cogeneration and Energy Intensive Processes, Heat Transfer Enhancement, Industrial Applications – PRES 11 43, 14–19. doi:10.1016/j.applthermaleng.2011.11.043

Miah, J.H., Griffiths, A., McNeill, R., Poonaji, I., Martin, R., Leiser, A., Morse, S., Yang, A., Sadhukhan, J., 2015. Maximising the recovery of low grade heat: An integrated heat integration framework incorporating heat pump intervention for simple and complex factories. Appl. Energy 160, 172–184. doi:10.1016/j.apenergy.2015.09.032

Mohammad Rozali, N.E., Wan Alwi, S.R., Manan, Z.A., Klemeš, J.J., Hassan, M.Y., 2013. Process Integration techniques for optimal design of hybrid power systems. Appl. Therm. Eng. 61, 26–35. doi:10.1016/j.applthermaleng.2012.12.038

Moita, R.D., Matos, H.A., Fernandes, C., Nunes, C.P., Prior, J.M., 2005. Dynamic modelling and simulation of a cogeneration system integrated with a salt recrystallization process. Comput. Chem. Eng., Selected Papers Presented at the 14th European Symposium on Computer Aided Process Engineering 29, 1491–1505. doi:10.1016/j.compchemeng.2005.02.015

Montazeri, M., Eckelman, M.J., 2016. Life cycle assessment of catechols from lignin depolymerization. ACS Sustain. Chem. Eng. 4, 708–718. https://doi.org/10.1021/acssuschemeng.5b00550.

Morseletto, P., 2020. Targets for a circular economy. Resour. Conserv. Recycl. 153, 104553. doi:10.1016/j.resconrec.2019.104553

Mughees, W., Al-Ahmad, M., 2015. Application of water pinch technology in minimization of water consumption at a refinery. Comput. Chem. Eng. 73, 34–42. doi:10.1016/j.compchemeng.2014.11.004

Nabi Bidhendi, G., Shafikhani, A., 2018. Presenting a Suitable Algorithm for Optimization of Water Consumption in Water Pinch Analysis (A Case Study: Shahid Tondgooyan Oil Refining Co., Tehran). Environ. Energy Econ. Res. 2, 89–99. doi:10.22097/eeer.2018.147506.1038

Nekså, P., 2002. CO2 heat pump systems. Int. J. Refrig. 25, 421–427. doi:10.1016/S0140-7007(01)00033-0

Nekså, P., Rekstad, H., Zakeri, G.R., Schiefloe, P.A., 1998. CO2-heat pump water heater: characteristics, system design and experimental results. Int. J. Refrig. 21, 172–179. doi:10.1016/S0140-7007(98)00017-6

Nemet, A., Klemeš, J.J., Varbanov, P.S., Mantelli, V., 2015. Heat Integration retrofit analysis—an oil refinery case study by Retrofit Tracing Grid Diagram. Front. Chem. Sci. Eng. 9, 163–182. doi:10.1007/s11705-015-1520-8

Nemet, A., Kravanja, Z., Klemeš, J.J., 2012. Integration of solar thermal energy into processes with heat demand. Clean Technol. Environ. Policy 14, 453–463. doi:10.1007/s10098-012-0457-6

OECD environmental outlook to 2050: the consequences of inaction, 2012. . Int. J. Sustain. High. Educ. 13, ijshe.2012.24913caa.010. doi:10.1108/ijshe.2012.24913caa.010

Oluleye, G., Jiang, N., Smith, R., Jobson, M., 2017. A novel screening framework for waste heat utilization technologies. Energy 125, 367–381. doi:10.1016/j.energy.2017.02.119

Oluleye, G., Smith, R., Jobson, M., 2016. Modelling and screening heat pump options for the exploitation of low grade waste heat in process sites. Appl. Energy 169, 267–286. doi:10.1016/j.apenergy.2016.02.015

Ong, B.H.Y., Walmsley, T.G., Atkins, M.J., Walmsley, M.R.W., 2017. Total site mass, heat and power integration using process integration and process graph. J. Clean. Prod. 167, 32–43. doi:10.1016/j.jclepro.2017.08.035

Ooi, R.E.H., Foo, D.C.Y., Ng, D.K.S., Tan, R.R., 2013. Planning of carbon capture and storage with pinch analysis techniques. Chem. Eng. Res. Des. 91, 2721–2731. doi:10.1016/j.cherd.2013.04.007

Papalexandri, K.P., Pistikopoulos, E.N., Kalitventzeff, B., Dumont, M.N., Urmann, K., Gorschluter, J., 1996. Operation of a steam production network with variable demands modelling and optimization under uncertainty. Comput. Chem. Eng., European Symposium on Computer Aided Process Engineering-6 20, S763–S768. doi:10.1016/0098-1354(96)00135-4

Papoulias, S.A., Grossmann, I.E., 1983. A structural optimization approach in process synthesis—I: Utility systems. Comput. Chem. Eng. 7, 695–706. doi:10.1016/0098-1354(83)85022-4

Pavlas, M., Stehlík, P., Oral, J., Klemeš, J., Kim, J.-K., Firth, B., 2010. Heat integrated heat pumping for biomass gasification processing. Appl. Therm. Eng. 30, 30–35. doi:10.1016/j.applthermaleng.2009.03.013

Pérez-Uresti, S.I., Martín, M., Jiménez-Gutiérrez, A., 2019. Superstructure approach for the

design of renewable-based utility plants. Comput. Chem. Eng. 123, 371–388. doi:10.1016/j.compchemeng.2019.01.019

Perry, S., Klemeš, J., Bulatov, I., 2008. Integrating waste and renewable energy to reduce the carbon footprint of locally integrated energy sectors. Energy 33, 1489–1497. doi:10.1016/j.energy.2008.03.008

Pirmohamadi, A., Ghazi, M., Nikian, M., 2019. Optimal design of cogeneration systems in total site using exergy approach. Energy 166, 1291–1302. doi:10.1016/j.energy.2018.10.167

Radermacher, R., Hwang, Y., 2005. Vapor compression heat pumps with refrigerant mixes. Taylor & Francis, Boca Raton, FL, USA.

Rao, A.D., ed, 2012. Combined Cycle Systems for Near-Zero Emission Power Generation. Woodhead Publishing, Cambridge, UK.

Ren, X.-Y., Jia, X.-X., Varbanov, P.S., Klemeš, J.J., Liu, Z.-Y., 2018. Targeting the cogeneration potential for Total Site utility systems. J. Clean. Prod. 170, 625–635. doi:10.1016/j.jclepro.2017.09.170

Rizwan, M., Saif, Y., Almansoori, A., Elkamel, A., 2018. Optimal processing route for the utilization and conversion of municipal solid waste into energy and valuable products. J. Clean. Prod. 174, 857–867. doi:10.1016/j.jclepro.2017.10.335

Robinson, P.R., Dolbear, G.E., 2006. Hydrotreating and Hydrocracking: Fundamentals, in: Hsu, C.S., Robinson, P.R. (Eds.), Practical Advances in Petroleum Processing. Springer, New York, NY, pp. 177–218. doi:10.1007/978-0-387-25789-1_7

Ruan, X., Huo, W., Wang, J., Guo, M., Zheng, W., Zou, Y., Huang, A., Shou, J., He, G., 2020. Multi-technique integration separation frameworks after steam reforming for coal-based hydrogen generation. Chin. J. Chem. Eng. doi:10.1016/j.cjche.2020.07.052

Ruan, X., Xiao, H., Jiang, X., Yan, X., Dai, Y., He, G., 2019. Graphic synthesis method for multi-technique integration separation sequences of multi-input refinery gases. Sep. Purif. Technol., Advanced Separation and Filtration (selected papers presented at the 17th APCChE, held 23-27 August, 2017 in Hong Kong) 214, 187–195. doi:10.1016/j.seppur.2018.04.082

Saidani, M., Yannou, B., Leroy, Y., Cluzel, F., Kendall, A., 2019. A taxonomy of circular economy indicators. J. Clean. Prod. 207, 542–559. doi:10.1016/j.jclepro.2018.10.014

Sarbu, I., 2014. A review on substitution strategy of non-ecological refrigerants from vapour compression-based refrigeration, air-conditioning and heat pump systems. Int. J. Refrig. 46, 123–141. doi:10.1016/j.ijrefrig.2014.04.023

Sashirekha, A., Pasupuleti, J., Moin, N.H., Tan, C.S., 2013. Combined heat and power (CHP) economic dispatch solved using Lagrangian relaxation with surrogate subgradient multiplier updates. Int. J. Electr. Power Energy Syst. 44, 421–430. doi:10.1016/j.ijepes.2012.07.038

Saw, S.Y., Lee, L., Lim, M.H., Foo, D.C.Y., Chew, I.M.L., Tan, R.R., Klemeš, J.J., 2011. An extended graphical targeting technique for direct reuse/recycle in concentration and property-based resource conservation networks. Clean Technol. Environ. Policy 13, 347–357. doi:10.1007/s10098-010-0305-5

Scheepens, A.E., Vogtländer, J.G., Brezet, J.C., 2016. Two life cycle assessment (LCA) based

methods to analyse and design complex (regional) circular economy systems. Case: making water tourism more sustainable. J. Clean. Prod. 114, 257–268. doi:10.1016/j.jclepro.2015.05.075

Schlosser, F., Seevers, J.-P., Peesel, R.-H., Walmsley, T.G., 2019. System efficient integration of standby control and heat pump storage systems in manufacturing processes. Energy 181, 395–406. doi:10.1016/j.energy.2019.05.113

Shamsi, S., Omidkhah, M.R., 2012. Optimization of Steam Pressure Levels in a Total Site Using a Thermoeconomic Method. Energies 5, 702–717. doi:10.3390/en5030702

Shang, Z., Kokossis, A., 2004. A transhipment model for the optimisation of steam levels of total site utility system for multiperiod operation. Comput. Chem. Eng. 28, 1673–1688. doi:10.1016/j.compchemeng.2004.01.010

Shehata, W.M., 2016. Automated targeting technique for indirect inter-plant hydrogen integration. Egypt. J. Pet. 25, 539–553. doi:10.1016/j.ejpe.2015.12.002

Silva Ortiz, P.A., Maciel Filho, R., Posada, J., 2019. Mass and Heat Integration in Ethanol Production Mills for Enhanced Process Efficiency and Exergy-Based Renewability Performance. Processes 7, 670. doi:10.3390/pr7100670

Simpson, D.M., 1984. Hydrogen management in a synthetic crude refinery. Int. J. Hydrog. Energy 9, 95–99. doi:10.1016/0360-3199(84)90036-3

Skouteris, G., Ouki, S., Foo, D., Saroj, D., Altini, M., Melidis, P., Cowley, B., Ells, G., Palmer, S., O'Dell, S., 2018. Water footprint and water pinch analysis techniques for sustainable water management in the brick-manufacturing industry. J. Clean. Prod. 172, 786–794. doi:10.1016/j.jclepro.2017.10.213

Song, C., Liu, Q., Deng, S., Li, H., Kitamura, Y., 2019. Cryogenic-based CO2 capture technologies: State-of-the-art developments and current challenges. Renew. Sustain. Energy Rev. 101, 265–278. doi:10.1016/j.rser.2018.11.018

Stampfli, J.A., Atkins, M.J., Olsen, D.G., Walmsley, M.R.W., Wellig, B., 2019. Practical heat pump and storage integration into non-continuous processes: A hybrid approach utilizing insight based and nonlinear programming techniques. Energy 182, 236–253. doi:10.1016/j.energy.2019.05.218

Stampfli, J.A., Atkins, M.J., Olsen, D.G., Wellig, B., Walmsley, M.R.W., Neale, J.R., 2018. Industrial heat pump integration in non-continuous processes using thermal energy storages as utility a graphical approach. Chem. Eng. Trans. 70, 901–906. doi:10.3303/CET1870151

Statistical Review of World Energy | Energy economics | Home, BP Glob. URL https://www.bp.com/en/global/corporate/energy-economics/statistical-review-of-world-energy.html (accessed 25.01.2021).

Suárez-Eiroa, B., Fernández, E., Méndez-Martínez, G., Soto-Oñate, D., 2019. Operational principles of circular economy for sustainable development: Linking theory and practice. J. Clean. Prod. 214, 952–961. doi:10.1016/j.jclepro.2018.12.271

Sun, L., Gai, L., Smith, R., 2017. Site utility system optimization with operation adjustment under uncertainty. Appl. Energy, Sustainable Thermal Energy Management (SusTEM2015) 186, 450–456. doi:10.1016/j.apenergy.2016.05.036

Suresh, C., Saini, R.P., 2020. Thermal performance of sensible and latent heat thermal energy

storage systems. Int. J. Energy Res. 44, 4743–4758. doi:10.1002/er.5255

Tan, R.R., Foo, D.C.Y., Aviso, K.B., Ng, D.K.S., 2009. The use of graphical pinch analysis for visualizing water footprint constraints in biofuel production. Appl. Energy 86, 605–609. doi:10.1016/j.apenergy.2008.10.004

Tan, S.T., Lee, C.T., Hashim, H., Ho, W.S., Lim, J.S., 2014. Optimal process network for municipal solid waste management in Iskandar Malaysia. J. Clean. Prod., Special Volume: PSE Asia for Cleaner Production 71, 48–58. doi:10.1016/j.jclepro.2013.12.005

Tan, Y.L., Manan, Z.A., Foo, D.C.Y., 2007. Retrofit of Water Network with Regeneration Using Water Pinch Analysis. Process Saf. Environ. Prot. 85, 305–317. doi:10.1205/psep06040

Tan, Y.L., Ng, D.K.S., El-Halwagi, M.M., Foo, D.C.Y., Samyudia, Y., 2013. Synthesis of Heat Integrated Resource Conservation Networks with Varying Operating Parameters. Ind. Eng. Chem. Res. 52, 7196–7210. doi:10.1021/ie302485y

Tarighaleslami, A.H., Walmsley, T.G., Atkins, M.J., Walmsley, M.R.W., Neale, J.R., 2017. Total Site Heat Integration: Utility selection and optimisation using cost and exergy derivative analysis. Energy 141, 949–963. doi:10.1016/j.energy.2017.09.148

Tian, J.R., Zhou, P.J., Lv, B., 2008. A process integration approach to industrial water conservation: A case study for a Chinese steel plant. J. Environ. Manage. 86, 682–687. doi:10.1016/j.jenvman.2006.12.014

Towler, G.P., Mann, R., Serriere, A.J.-L., Gabaude, C.M.D., 1996. Refinery Hydrogen Management: Cost Analysis of Chemically-Integrated Facilities. Ind. Eng. Chem. Res. 35, 2378–2388. doi:10.1021/ie950359+

Trindade, A.B., Palacio, J.C.E., González, A.M., Rúa Orozco, D.J., Lora, E.E.S., Renó, M.L.G., del Olmo, O.A., 2018. Advanced exergy analysis and environmental assesment of the steam cycle of an incineration system of municipal solid waste with energy recovery. Energy Convers. Manag. 157, 195–214. doi:10.1016/j.enconman.2017.11.083

Tseng, M.-L., Tan, R.R., Chiu, A.S.F., Chien, C.-F., Kuo, T.C., 2018. Circular economy meets industry 4.0: Can big data drive industrial symbiosis? Resour. Conserv. Recycl. 131, 146–147. doi:10.1016/j.resconrec.2017.12.028

Urbanucci, L., Bruno, J.C., Testi, D., 2019. Thermodynamic and economic analysis of the integration of high-temperature heat pumps in trigeneration systems. Appl. Energy 238, 516–533. doi:10.1016/j.apenergy.2019.01.115

van de Bor, D.M., Infante Ferreira, C.A., Kiss, A.A., 2015. Low grade waste heat recovery using heat pumps and power cycles. Energy 89, 864–873. doi:10.1016/j.energy.2015.06.030

Varbanov, P., Perry, S., Klemeš, J., Smith, R., 2005. Synthesis of industrial utility systems: Cost-effective de-carbonisation. Appl. Therm. Eng. 25, 985–1001. doi:10.1016/j.applthermaleng.2004.06.023

Varbanov, P.S., Chin, H.H., Plesu Popescu, A.-E., Boldyryev, S., 2020a. Thermodynamics-Based Process Sustainability Evaluation. Energies 13, 2132. doi:10.3390/en13092132

Varbanov, P.S., Chin, H.H., Plesu Popescu, A.-E., Boldyryev, S., 2020b. Thermodynamics-Based Process Sustainability Evaluation. Energies 13, 2132. doi:10.3390/en13092132

Varbanov, P.S., Doyle, S., Smith, R., 2004. Modelling and Optimization of Utility Systems. Chem. Eng. Res. Des. 82, 561–578. doi:10.1205/026387604323142603

Varbanov, P.S., Fodor, Z., Klemeš, J.J., 2012. Total Site targeting with process specific minimum temperature difference (ΔT_{min}). Energy 44, 20–28. doi:10.1016/j.energy.2011.12.025

Varbanov, P.S., Klemeš, J.J., 2010. Total sites integrating renewables with extended heat transfer and recovery. Heat Transf. Eng. 31, 733–741. doi:10.1080/01457630903500858

Varbanov, P.S., Škorpík, J., Pospíšil, J., Klemeš, J.J., 2020c. Sustainable Utility Systems: Modelling and Optimisation. De Gruyter.

Vilardi, G., Bassano, C., Deiana, P., Verdone, N., 2020. Exergy and energy analysis of three biogas upgrading processes. Energy Convers. Manag. 224, 113323. doi:10.1016/j.enconman.2020.113323

Wallerand, A.S., Kermani, M., Kantor, I., Maréchal, F., 2018a. Optimal heat pump integration in industrial processes. Appl. Energy 219, 68–92. doi:10.1016/j.apenergy.2018.02.114

Wallerand, A.S., Kermani, M., Voillat, R., Kantor, I., Maréchal, F., 2018b. Optimal design of solar-assisted industrial processes considering heat pumping: Case study of a dairy. Renew. Energy 128, 565–585. doi:10.1016/j.renene.2017.07.027

Walmsley, T.G., 2016. A Total Site Heat Integration design method for integrated evaporation systems including vapour recompression. J. Clean. Prod. 136, 111–118. doi:10.1016/j.jclepro.2016.06.044

Walmsley, T.G., Ong, B.H.Y., Klemeš, J.J., Tan, R.R., Varbanov, P.S., 2019a. Circular Integration of processes, industries, and economies. Renew. Sustain. Energy Rev. 107, 507–515. doi:10.1016/j.rser.2019.03.039

Walmsley, T.G., Varbanov, P.S., 2017. Innovative Hybrid Heat Pump for Dryer Process Integration. Chem. Eng. Trans. 57, 1039–1044.

Walmsley, T.G., Varbanov, P.S., Aviso, K., You, F., 2019b. Energy integration and optimisation for sustainable total site, process and equipment design. Energy 186, 115896. doi:10.1016/j.energy.2019.115896

Walmsley, T.G., Varbanov, P.S., Su, R., Ong, B., Lal, N., 2018. Frontiers in process development, integration and intensification for circular life cycles and reduced emissions. J. Clean. Prod. 201, 178–191. doi:10.1016/j.jclepro.2018.08.041

Wan Alwi, S.R., Manan, Z.A., 2007. Targeting Multiple Water Utilities Using Composite Curves. Ind. Eng. Chem. Res. 46, 5968–5976. doi:10.1021/ie061238k

Wang, B., Feng, X., Chu, K.H., 2012. A novel graphical procedure based on ternary diagram for minimizing refinery consumption of fresh hydrogen. J. Clean. Prod. 37, 202–210. doi:10.1016/j.jclepro.2012.07.009

Wang, B., Feng, X., Zhang, Z., 2003. A design methodology for multiple-contaminant water networks with single internal water main. Comput. Chem. Eng. 27, 903–911. doi:10.1016/S0098-1354(02)00177-1

Wang, B., Klemeš, J.J., Varbanov, P.S., Chin, H.H., Wang, Q.-W., Zeng, M., 2020. Heat exchanger network retrofit by a shifted retrofit thermodynamic grid diagram-based model and a two-stage approach. Energy 198. doi:10.1016/j.energy.2020.117338

Wang, J.F., Brown, C., Cleland, D.J., 2018. Heat pump heat recovery options for food industry dryers. Int. J. Refrig. 86, 48–55. doi:10.1016/j.ijrefrig.2017.11.028

Wang, M., Deng, C., Wang, Y., Feng, X., Lan, X., 2018. Process integration and selection of heat pumps in industrial processes. Chem. Eng. Trans. 70, 1105–1110. doi:10.3303/CET1870185

Wang, W., 2012. Study on the optimization of hydrogen network in a refinery plant. East China University of Science and Technology, Shanghai, CN. (in Chinese).

Wang, Y., Feng, X., Chu, K.H., 2014. Trade-off between energy and distance related costs for different connection patterns in heat integration across plants. Appl. Therm. Eng. 70, 857–866. doi:10.1016/j.applthermaleng.2014.06.012

Wang, Y.P., Smith, R., 1994. Wastewater minimisation. Chem. Eng. Sci. 49, 981–1006. doi:10.1016/0009-2509(94)80006-5

Wissocq, T., Ghazouani, S., Le Bourdiec, S., 2019. A methodology for designing thermodynamic energy conversion systems in industrial mass/heat integration problems based on MILP models. Energy 185, 121–135. doi:10.1016/j.energy.2019.06.124

Yáñez, M., Relvas, F., Ortiz, A., Gorri, D., Mendes, A., Ortiz, I., 2020. PSA purification of waste hydrogen from ammonia plants to fuel cell grade. Sep. Purif. Technol. 240, 116334. doi:10.1016/j.seppur.2019.116334

Yang, Y., Wang, G., Zhang, L., Zhang, S., Lin, L., 2019. Comparison of Hydrogen Specification in National Standards for China. E3S Web Conf. 118, 03042. doi:10.1051/e3sconf/201911803042

Yoro, K.O., Sekoai, P.T., Isafiade, A.J., Daramola, M.O., 2019. A review on heat and mass integration techniques for energy and material minimization during CO2 capture. Int. J. Energy Environ. Eng. 10, 367–387. doi:10.1007/s40095-019-0304-1

Zhang, B.J., Hua, B., 2007. Effective MILP model for oil refinery-wide production planning and better energy utilization. J. Clean. Prod. 15, 439–448. doi:10.1016/j.jclepro.2005.08.004

Zhang, N., Bénard, P., Chahine, R., Yang, T., Xiao, J., 2021. Optimization of pressure swing adsorption for hydrogen purification based on Box-Behnken design method. Int. J. Hydrog. Energy 46, 5403–5417. doi:10.1016/j.ijhydene.2020.11.045

Zhang, Q., Feng, X., Liu, G., Chu, K.H., 2011. A novel graphical method for the integration of hydrogen distribution systems with purification reuse. Chem. Eng. Sci. 66, 797–809. doi:10.1016/j.ces.2010.11.044

Zhang, Q., Yang, M., Liu, G., Feng, X., 2016. Relative concentration based pinch analysis for targeting and design of hydrogen and water networks with single contaminant. J. Clean. Prod. 112, 4799–4814. doi:10.1016/j.jclepro.2015.06.019

Zhang, Q., Zhang, B., Wang, B., 2013. Application of Pinch technology for Heat Integration between plants. Energy Conserv. 7, 53-57. (in Chinese).

Zhao, H., Rong, G., Feng, Y., 2015. Effective Solution Approach for Integrated Optimization Models of Refinery Production and Utility System. Ind. Eng. Chem. Res. 54, 9238–9250. doi:10.1021/acs.iecr.5b00713

Zhao, Z., Liu, G., Feng, X., 2007. The Integration of the Hydrogen Distribution System with Multiple Impurities. Chem. Eng. Res. Des. 85, 1295–1304. doi:10.1205/cherd07014

Zhao, Z., Liu, G., Feng, X., 2006. New Graphical Method for the Integration of Hydrogen Distribution Systems. Ind. Eng. Chem. Res. 45, 6512–6517. doi:10.1021/ie0604223

Zheng, X., Feng, X., Shen, R., Seider, W.D., 2006. Design of Optimal Water-Using Networks with Internal Water Mains. Ind. Eng. Chem. Res. 45, 8413–8420. doi:10.1021/ie050911n

Zhou, C., Gong, Z., Hu, J., Cao, A., Liang, H., 2015. A cost-benefit analysis of landfill mining and material recycling in China. Waste Manag. 35, 191–198. doi:10.1016/j.wasman.2014.09.029

Zore, Ž., Čuček, L., Kravanja, Z., 2018. Synthesis of sustainable production systems using an upgraded concept of sustainability profit and circularity. J. Clean. Prod. 201, 1138–1154. doi:10.1016/j.jclepro.2018.07.150

APPENDIX: Tables

Table S1. Comparison of Circularity Indicators

Indicators	Ref	Materials	Energy	Exergy	Monetary	Comment
Circular Economy Index	(Maio and Rem, 2015)	Materials generating value			Monetary ratio	
Circular Economy Performance Indicator	(Huysman et al., 2017)	Ratio of material flows				
Circular Economic Value	(Fogarassy et al., 2017)	Included	Included			Weighted ratios
Circular Material Use Rate	(Eurostat, 2018)	Ratio of material flows				
Energy Circularity Indicator	(Angioletti et al., 2017)		Ratio of energy flows			
Material Circularity Indicator	(Angioletti et al., 2017)	Ratio of material flows				
Circularity Product Indicator	(Angioletti et al., 2017)	Ratio of material flows	Ratio of energy flows			Square root weighting
Circularity Index	(Cullen, 2017)	Ratio of material flows similar to CMU	Function of energy ratios			Product of the components
Eco-cost value ratio	(Scheepens et al., 2016)				Monetary ratio	
Product-Level Circularity Metric	(Linder et al., 2017)				Monetary ratio	
Recycling rate	(Haupt et al., 2017)	Ratios of material flows				
Sustainable Circular Index	(Azevedo et al., 2017)	Included	Included		Included	A composite index including also social indicators
Value-based resource efficiency	(Di Maio et al., 2017)				Monetary ratio	

Table S2. Stream data of a dairy process. Data from (Wallerand et al., 2018b)

Stream Name	T_s, °C	T_t, °C	ΔH, kW	Stream Name	T_s, °C	T_t, °C	ΔH, kW
Refrigeration	6.0	4.0	76.0	Concentration 10	65.9	15.0	80.8
Pasteurisation 1a	4.0	66.0	2,356.0	Condensates cooling 8	60.1	60.1	849.8
Pasteurisation 2a	66.0	86.0	676.4	Condensates cooling 11	60.1	15.0	69.7
Pasteurisation 1a	86.0	4.0	2,773.2	Yoghurt production 1	4.0	94.0	1,026.0
Pasteurisation 1a	66.0	98.0	119.7	Yoghurt production 2	94.0	10.0	957.6
Pasteurisation 1a	98.0	4.0	351.6	Desert production 1	4.0	90.0	817.0
Concentration 1	4.0	70.3	504.0	Desert production 2	90.0	70.0	190.0
Concentration 2	70.3	70.3	904.2	Hot water	15.0	55.0	167.2
Concentration 3	66.4	66.4	864.1	Cleaning in place 1a	58.7	70.0	188.6
Concentration 4	60.8	60.8	849.8	Cleaning in place 1b	65.0	15.0	104.5
Concentration 5	60.8	4.0	151.5	Cleaning in place 2a	67.5	80.0	209.5
Concentration 6	68.9	68.9	904.2	Cleaning in place 2b	75.0	15.0	125.4
Concentration 7	65.9	65.9	864.1	Fridge	5.0	5.0	300.0
Concentration 9	68.9	15.0	87.8				

Table S3. Stream data of a process of candy processing and packaging. Data from (Miah et al., 2015)

Stream Name	T_s, °C	T_t, °C	ΔH, kW
Production A			
FP-02	15.0	70.0	13.66
FP-03	15.0	70.0	16.72
FP-04	25.0	60.0	29.12
FP-05	25.0	60.0	29.12
FP-06	30.0	55.0	29.10
FP-07	30.0	55.0	29.10
FP-08	130.0	80.0	60.80
[1] FP-V	120.0	25.0	76.71
FP-08	130.0	80.0	60.80
[1] FP-V	120.0	25.0	76.71
Production B			
15 x S-S	21.0	18.0	279.00
11 x N-S	44.0	47.0	550.00
28 x S-S	44.0	47.0	1,400.00
Packaging			
AHU CFP	22	18	55.52

[1] FP-V: Water, includes latent heat.

Table S4. Stream data of a 4-column double-effect methanol distillation process. Data from (Cui et al., 2017)

Stream Name	T_s, °C	T_t, °C	ΔH, MW
Crude feed preheated	40.00	85.00	8.160
PC feed preheated	78.94	135.97	13.864
LEC reboiler	78.60	78.62	27.750
PC reboiler	136.10	136.18	114.064
AC reboiler	102.90	102.92	96.267
WC reboiler	102.20	102.22	3.544
First stage condenser	81.76	70.00	26.858
Second stage condenser	70.00	40.00	1.744
PC condenser	130.50	125.19	115.115
AC condenser	66.60	40.00	107.510
WC condenser	66.60	40.00	3.584
PC top stream to tanks	125.19	40.00	7.425

Table S5. Separation performance of two kinds of membranes (Ruan et al., 2019)

$\alpha_{i,j}$	Glassy membrane	Rubbery membrane
H_2	105	2.225
C1	1	2.9
C2=	1.27	7.15
C2	0.25	8.25
C3=	0.45	8.85
C3	0.06	10.25
C4+	0.05	17.4
N_2	1.14	1

Table S6. Waste hydrogen discharge of plants A, B and C

Plant	Purity, vol% H_2	Flowrate, kNm^3/h
A	75	14.24
	70	4.99
	65	3.84
B	70	8.27
C	95	2.50
	85	4.84

APPENDIX: List of Figures

Figure 1. Trade-offs between circularity, energy consumption, and economic benefit in Circular Economy (Gai et al., 2021b) 2

Figure 2. Estimated US energy consumption in 2019 (LLNL Flow Charts, 2019) 3

Figure 3. Total Site Heat Integration of Locally Integrated Energy Sectors, amended from (Klemeš et al., 2018b) 4

Figure 4. Total Site Mass Integration with multiple-level fresh resources and intermediate purity headers (Gai et al., 2021a) 5

Figure 5. The method procedure of heat pump and process heat integration 34

Figure 6. Simulation flowsheet of the heat pump as output from Petro-SIM: (**a**) JCHP, (**b**) VCHP and (**c**) TCHP. 36

Figure 7. Grand Composite Curve (GCC) construction of a process with an integrated heat pump: (a) JCHP, (b) VCHP and (c) TCHP. 39

Figure 8. T–H diagrams of different source and sink configurations for heat pump application. (a). Gradual slope; (b). Steep slope; (c). Medium slope. 40

Figure 9. Ideal T–S diagram of the heat pumps (a) JCHP, (b) VCHP and (c) TCHP. 40

Figure 10. COP of different heat pumps varies with ΔT_{in} and ΔT_{out}: (a) JCHP-Ar, (b) JCHP-CO_2, (c) VCHP and (d) TCHP. 43

Figure 11. COP of different heat pumps varies with ΔT_1 and ΔT_2 (a) JCHP-Ar, (b) JCHP-CO_2, (c) VCHP and (d) TCHP. 44

Figure 12. GCC of Case 1 and Process Integration using (a) JCHP-Ar, (b) JCHP-CO_2, (c) VCHP and (d) TCHP. 47

Figure 13. GCC of case 2 with integration options using (a) JCHP-Ar, (b) JCHP-CO_2, (c) VCHP and (d) TCHP. 50

Figure 14. GCC of case 3 and integration options using (a) JCHP-Ar, (b) JCHP-CO2, (c) VCHP and (d) TCHP. 52

Figure 15. GCC of case 4 and integration options using (a) JCHP-Ar, (b) JCHP-CO2, (c) VCHP and (d) TCHP. 54

Figure 16. The relationship between power consumption and COP of JCHP with a compression ratio 55

Figure 17. The procedure of the proposed multiple-level fresh resources Total Site Mass Integration with intermediate headers and waste recovery 62

Figure 18. Multiple-level fresh resources Total Site Mass Integration with intermediate headers and waste recovery 64

Figure 19. Multiple-level fresh resources Pinch Analysis of intra-plant Mass Integration 65

Figure 20. Triangle rule for Pinch Analysis in Mass Integration 66

Figure 21. Pinch Analysis targeting steps for TSI with a multiple-level fresh resources (Scenario 1.1) 70

Figure 22. Pinch Analysis targeting steps for TSI with a multiple-level fresh resources (Scenario 1.2) 71

Figure 23. Multiple-level fresh resources Total Site Mass Integration with intermediate purity headers 76

Figure 24. Pinch Analysis with multiple-level fresh resources and intermediate headers for intra-plant Mass Integration 79

Figure 25. Procedure flowchart of Total Site Mass Integration with intermediate headers and multiple-level fresh resources 81

Figure 26. Multiple-level fresh resources Pinch Analysis of each plant Hydrogen Integration before waste hydrogen recovery (Baseline Scenario) for (a) Plant A, (b) Plant B, (c) Plant C 84

Figure 27. The lowest boundary of Total Site Hydrogen Integration 85

Figure 28. Identify inter-plant streams by revising the waste hydrogen discharge see Step 2b of Section 4.2.2(II): (a) Plant A, (b) Plant B, (c) Plant C 85

Figure 29. Identified target after the revision of waste hydrogen discharge 86

Figure 30. Final solution of Total Site Hydrogen Integration before waste hydrogen recovery for (a) Plant A, (b) Plant B, (c) Plant C 86

Figure 31. Identified solution of multiple-level fresh resources Total Site Hydrogen Integration before waste hydrogen regeneration. SR = source, SK = sink. A1 represents the hydrogen stream (sink or source) in Plant A. Same interpretation is applied to Bn and Cn. 87

Figure 32. Flowsheet of waste hydrogen purification process by membrane separation 92

Figure 33. The influence of pressure on the waste hydrogen regeneration process 93

Figure 34. Pinch Analysis of a mass exchange network 95

Figure 35. Mass Integration in three different scenarios 97

Figure 36. Detailed hydrogen network allocation 98

Figure 37. Final Pinch Analysis of Total Site Water Integration with multiple-level freshwater resources, but without intermediate headers (Scenario 3.1) 100

Figure 38. Final results of Total Site Water Integration with both multiple-level freshwater resources and intermediate headers (Scenario 3.2) 102

Figure 39. Detailed water network allocation with the multiple-level freshwater resources

before setting intermediate headers (Scenario 3.1) 102

Figure 40. Detailed water network allocation with multiple-level freshwater resources after setting and optimising intermediate headers (Scenario 3.2) 103

Figure 41. Onion Model of the production process, amends from (Linnhoff et al., 1994) ... 109

Figure 42. Procedure for Mass and Heat Integration 109

Figure 43. H_2 Network Pinch diagram for (a) the H_2 CC; (b) H_2 Pinch; (c) minimum utility H_2; (d) minimum waste H_2 discharge 111

Figure 44. GCC of three different hydrogenation processes for (a) Unit A; (b) Unit B; (c) Unit C 113

Figure 45. Total Site Composite Curves (TSCC) (a) Total Site Profiles with utilities; (b) Hot Utility Generation Composite Curve (HUGCC) 113

Figure 46. Multi-Resource Integration closing the loops (Multi-Resource Integration Map) 119

Figure 47. Representation of different costs 125

Figure 48. Representation of the various exergy flows 128

Figure 49. Concept Map of Multi-Resource Integration for the case study 130

Figure 50. Minimum total exergy under different (a) total CMU; (b) total CEU 134

Figure 51. Total exergy under different TCI 136

Figure 52. The optimal exergy consumption path at TCI is 0.396 137

Figure 53. Minimum cost under different (a) total CMU; (b) total CEU 139

Figure 54. TAC under different TCI values 140

Figure 55. The optimal TAC path at TCI is 0.359 141

Figure 56. Minimum total exergy and TAC under different TCI 142

APPENDIX: List of Tables

Table 1. Settings of parameters and variables. 41

Table 2. The stream data from a spray drying process. 45

Table 3. Variation settings and optimisation results of spray drying with an integrated heat pump. 45

Table 4. Variable settings and optimisation results of a dairy product with an integrated heat pump. 48

Table 5. Variable settings and optimisation results of a process of candy processing and packaging integration heat pump. 50

Table 6. Variable settings and optimisation results of a methanol distillation with an integrated heat pump. 52

Table 7. Results of different industrial processes integrated with heat pumps. 55

Table 8. Hydrogen sources and sinks of hydrogen network in refineries (Lou et al., 2019) ...82

Table 9. Fresh hydrogen consumption and waste hydrogen discharge after Total Site Hydrogen Integration 87

Table 10. Comparison of waste hydrogen purification technology in a refinery 88

Table 11. Main operating conditions of waste hydrogen discharge 90

Table 12. Parameter data for calculating capital cost, operating cost and product value 91

Table 13. Price list of the products, utilities and equipment 93

Table 14. Data of sources and sinks (Deng et al., 2014) 94

Table 15. Hydrogen sources and sinks in a refinery (Kang et al., 2018) 95

Table 16. Data of fresh resources of different qualities (Kang et al., 2018) 95

Table 17. Water sources and sinks 98

Table 18. Data of freshwater of different qualities (Foo, 2012) 99

Table 19. Results of minimum freshwater consumption, minimum wastewater discharge and intermediate headers 103

Table 20. Streams of an H_2 Network (HN) in a refinery 109

Table 21. Streams of three different hydrotreating processes 111

Table 22. Maximum flowrates of supplies 130

Table 23. The data for the demands 130

Table 24. Data on composition (Tan et al., 2014), LHV (Tan et al., 2014), carbon content (Tan et al., 2014) and DOC_F (Lee et al., 2017) of MSW 131

Table 25. Efficiencies and conversion factors of different processes.....131
Table 26. Exergy inputs for operating the recycling paths 132
Table 27. The embodied exergy of the utilities 132
Table 28. Cost data of involved processes 137
Table 29. Price list of utilities 137
Table S1. Comparison of Circularity Indicators 170
Table S2. Stream data of a dairy process. Data from (Wallerand et al., 2018b) 171
Table S3. Stream data of a process of candy processing and packaging. Data from (Miah et al., 2015) 171
Table S4. Stream data of a 4-column double-effect methanol distillation process. Data from (Cui et al., 2017) 172
Table S5. Separation performance of two kind of membranes (Ruan et al., 2019).....172
Table S6. Waste hydrogen discharge of plant A, B and C 172